CAVITAND-BASED ANION RECEPTORS

AND SELF-ASSEMBLED (HEMI)CAPSULES

IN POLAR COMPETITIVE MEDIA

PROEFSCHRIFT

ter verkrijging van
de graad van doctor aan de Universiteit Twente,
op gezag van de rector magnificus,
prof. dr. W.H.M. Zijm,
volgens besluit van het College voor Promoties
in het openbaar te verdedigen
op donderdag 23 maart 2006 om 15.00 uur

door

Gennady Veniaminovich Oshovsky

geboren op 10 april 1974
te Kiev (Sovjet Unie, tegenwoordig Oekraïne)

Dit proefschrift is goedgekeurd door:

Promotor: Prof. Dr. Ir. D. N. Reinhoudt

Assistent-promotor: Dr. W. Verboom

In memory of

my grandmother

and parents

To Lisette

Contents

GENERAL INTRODUCTION

Supramolecular chemistry is a highly interdisciplinary field of science covering the chemical, physical, and biological features of chemical species of higher complexity, which are held together and organized by means of intermolecular (non-covalent) interactions.[1] Over the past quarter century, supramolecular chemistry has grown into a major field and has induced numerous developments at the interfaces with biology and physics.[2] Beyond molecular chemistry, based on the covalent bond, supramolecular chemistry "aims at developing highly complex chemical systems from components interacting through non-covalent intermolecular forces", as defined by J.-M. Lehn.[2]

Molecular recognition[3] is the most important phenomenon in supramolecular chemistry; it is the basis for receptors,[4] self-assemblies,[5] dynamic combinatorial libraries,[6] self-organized entities,[2] molecular devices,[7] etc. Receptor-substrate interaction[8] in solution is always strongly influenced by the medium. A variety of non-covalent interactions can take place between solvent and solute (van der Waals, electrostatic, hydrogen bonding, π-π stacking, ion-π, etc.). As a consequence, the association process of a guest with a receptor can be dramatically altered or totally changed depending on the solvation properties.[9]

Until recently, the major part of supramolecular studies in solution was focused on non-covalent interactions in apolar or polar aprotic solvents, which are weakly or moderately influencing host-guest interactions. Nowadays, the design of receptors, which can survive the competitive influence of polar media, and especially water (in the cases, where the use of the hydrophobic effect[10] is supported by a smart choice of other interactions), is in continuous development and attracts increasing attention. A constantly growing number of papers devoted to studies in polar media[11] and water is a good indication of the importance of this research area.

In supramolecular chemistry a number of scaffolds are exploited, such as cyclophanes (including cavitands and calix[4]arenes), cyclodextrins, cucurbit[n]urils, cyclotriveratrilenes, etc.[12] Cavitands are useful, rigid scaffolds, functionalization of which has provided a variety of receptors for both charged molecules and neutral species.[13] Cavitands have also found a wide application in the preparation of capsule-like self-assemblies.[14]

This thesis describes a study of molecular recognition and self-assembly to capsules, using cavitand-based receptors and building blocks, respectively, in polar competitive (a)protic media. The capsules are based on electrostatic and triple-ion interactions.

In Chapter 2, recent advances of supramolecular chemistry in water are summarized. It shows numerous investigations devoted to recognition and self-assembly in aqueous media, as well as considers approaches to increase the solubility of conventional receptor building blocks in water.

Chapters 3 deals with a study of multivalent glycocluster-containing cavitand-based (thio)urea-functionalized receptors for inorganic anions in (aqueous) acetonitrile. New mass spectrometric methods for the quantitative study of the anion complexation are introduced.

In Chapter 4, (thio)urea-functionalized cavitands as excellent receptors for the recognition of organic anions in polar media are presented.

The first example of the use of 'triple ion' interactions[15] to build supramolecular architectures is shown in Chapter 5. Evidence is described for novel [2+4] capsules, consisting of two cavitand building blocks, connected together by four pyridinium-'singly charged anion'-pyridinium interactions.

Chapter 6 deals with [2+4] capsules assembled by electrostatic interaction of two tetrakis(pyridinium)cavitands with four doubly charged linkers in polar media.

The importance to consider the electrostatic interactions of the individual capsule components in a quantitative study of [1+1] capsule formation is presented in Chapter 7.

References

1.   Lehn, J.-M. *Science* **1993**, *260*, 1762-1763.
2.   Lehn, J.-M. *Science* **2002**, *295*, 2400-2403.
3.   *Comprehensive Supramolecular Chemistry*; Vol. 1; Lehn, J.-M.; Atwood, J. L.; Davies, J. E. D.; MacNicol, D. D.; Vögtle, F.; Gokel, G. W., Eds.; Pergamon: Oxford, 1996; *Comprehensive Supramolecular Chemistry*; Vol. 2; Lehn, J.-M.; Atwood, J. L.; Davies, J. E. D.; MacNicol, D. D.; Vögtle, F., Eds.; Pergamon: Oxford, 1996; Ariga, K.; Kunitake, T., *Supramolecular Chemistry - Fundamentals and Applications;* Springer: Berlin, 2005.
4.   Trembleau, L.; Rebek, J. *Science* **2003**, *301*, 1219-1220; Martin, T.; Obst, U.; Rebek, J. *Science* **1998**, *281*, 1842-1845; Heinz, T.; Rudkevich, D. M.; Rebek, J. *Nature* **1998**, *394*, 764-766; Atwood, J. L.; Barbour, L. J.; Jerga, A. *Science* **2002**, *296*, 2367-2369.
5.   Reinhoudt, D. N.; Crego-Calama, M. *Science* **2002**, *295*, 2403-2407.
6.   Lehn, J.-M.; Eliseev, A. V. *Science* **2001**, *291*, 2331-2332; Otto, S.; Furlan, R. L. E.; Sanders, J. K. M. *Science* **2002**, *297*, 590-593.
7.   Badjic, J. D.; Balzani, V.; Credi, A.; Silvi, S.; Stoddart, J. F. *Science* **2004**, *303*, 1845-1849; Leigh, D. A.; Wong, J. K. Y.; Dehez, F.; Zerbetto, F. *Nature* **2003**, *424*, 174-179.
8.   For reviews on synthetic receptors, see: Kubik, S.; Reyheller, C.; Stuwe, S. *J. Incl. Phenom. Macrocycl. Chem.* **2005**, *52*, 137-187; *Functional Synthetic Receptors*; Schrader, T.; Hamilton, A. D., Eds.; Wiley-VCH: Weinheim, 2005; Fitzmaurice, R. J.; Kyne, G. M.; Douheret, D.; Kilburn, J. D. *J. Chem. Soc., Perkin Trans. 1* **2002**, 841-864; Hartley, J. H.; James, T. D.; Ward, C. J. *J. Chem. Soc., Perkin Trans. 1* **2000**, 3155-3184.
9.   Reichardt, C., *Solvents and Solvent Effects in Organic Chemistry;* 3rd ed.; VCH: Weinheim, 2003; Rekharsky, M.; Inoue, M., *Solvation Effects in Guest Binding. In Encyclopedia of Supramolecular Chemistry;* Atwood, J. L.; Steed, J. W., Eds.; Marcel Dekker, Inc.: New York, 2004; pp 1322-1329.
10. Widom, B.; Bhimalapuram, P.; Koga, K. *Phys. Chem. Chem. Phys.* **2003**, *5*, 3085-3093; Southall, N. T.; Dill, K. A.; Haymet, A. D. J. *J. Phys. Chem. B* **2002**, *106*, 521-533.
11. Katritzky, A. R.; Fara, D. C.; Yang, H. F.; Tamm, K.; Tamm, T.; Karelson, M. *Chem. Rev.* **2004**, *104*, 175-198.
12. Weber, E., *Classification and Nomenclature of Supramolecular Compounds. In Encyclopedia of Supramolecular Chemistry;* Atwood, J. L.; Steed, J. W., Eds.; Marcel Dekker, Inc.: New York, 2004; pp 261-273.
13. For reviews about cavitands, see: Botta, B.; Cassani, M.; D'Acquarica, I.; Subissati, D.; Zappia, G.; Delle Monache, G. *Curr. Org. Chem.* **2005**, *9*, 1167-1202; Pinalli, R.; Suman, M.; Dalcanale, E. *Eur. J. Org. Chem.* **2004**, 451-462; Sliwa, W.; Matusiak, G.; Deska, M. *Heterocycles* **2002**, *57*, 2179-2206; Verboom, W., *Cavitands. In Calixarenes 2001;* Asfari, Z.; Böhmer, V.;

Harrowfield, J.; Vicens, J., Eds.; Kluwer: Dordrecht, 2001; pp 181-198; Rudkevich, D. M.; Rebek, J. *Eur. J. Org. Chem.* **1999**, 1991-2005.

14.   For reviews on capsules and encapsulation, see: Rebek, J. *Angew. Chem., Int. Ed.* **2005**, *44*, 2068-2078; Rudkevich, D. M. *Bull. Chem. Soc. Jpn.* **2002**, *75*, 393-413; Böhmer, V.; Vysotsky, M. O. *Aust. J. Chem.* **2001**, *54*, 671-677; Conn, M. M.; Rebek, J. *Chem. Rev.* **1997**, *97*, 1647-1668.

15.   Hojo, M.; Hasegawa, H.; Morimoto, Y. *J. Phys. Chem.* **1995**, *99*, 6715-6720.

CHAPTER 2

RECENT ADVANCES OF SUPRAMOLECULAR

CHEMISTRY IN WATER

Supramolecular chemistry in water is a constantly growing research area due to the importance of non-covalent interactions in aqueous media for a better understanding of the major processes in Nature. This chapter offers an overview of recent advances in the area of water-soluble synthetic receptors, with consideration of the functionalities that are used to increase the water solubility, as well as the supramolecular interactions and approaches used for effective guest recognition in water.

2.1 Introduction

One of the goals of supramolecular chemistry is the creation of synthetic receptors that have both a high affinity and a high selectivity for guest binding in water.[1-3] Natural receptors such as enzymes and antibodies show strong and selective host-guest complexation by multiple weak, non-bonded interactions between the functional groups on the binding partners.[3] These natural systems provide the inspiration for the rational design of synthetic receptors that can be used to achieve an understanding of the binding forces that contribute to complex formation.[1,4] So far most of the synthetic receptors have been studied in organic solvents, although all the recognition events in nature take place in aqueous medium. The design of synthetic receptors, which can be used in water, represents a special challenge. First, the host needs to be soluble in water. This severely limits the type of building blocks, which can be used to construct the receptor. Second, special interactions and approaches have to be chosen to overcome the competitive influence of water. Another important feature of large water-soluble receptors is the encapsulation of several (different) guests. That allows to study molecular interactions within a confined space and to carry out chemical reactions between them in aqueous media. A cavity catalyses and directs synthesis, and protects from water. The confined space strictly controls the enclathration by steric nature and subsequent chemical transformations are sterically controlled.[5]

This Chapter gives an overview of recent (from the year 2000) synthetic water-soluble receptors. Cyclodextrins[6] and crown ethers[7] are not included due to the huge number of publications dealing with these water-soluble supramolecular platforms. The organization of the chapter is based on the structure of the receptors. It starts with relatively simple receptors containing one or several binding sites, as well as some dipodal receptors. Subsequently, tripodal receptors, appropriately functionalized cyclophanes and cucurbiturils will be discussed. Self-assembled receptors, such as capsules, organometallic receptors and cages are described in the last part of this overview, which considers not only the host-guest properties of these receptors, but also chemical reactions within the cages in aqueous media.

2.2 Relatively simple receptors containing one or several binding sites

2.2.1. Guanidinocarbonyl pyrroles, pyridines and pyrazoles

Schmuck et al. have recently reported the guanidinocarbonyl pyrroles **1**.[8,9] The combination of multiple hydrogen bonds along with electrostatic interactions allows effective binding of amino acids and peptides in aqueous solution (Chart 1).
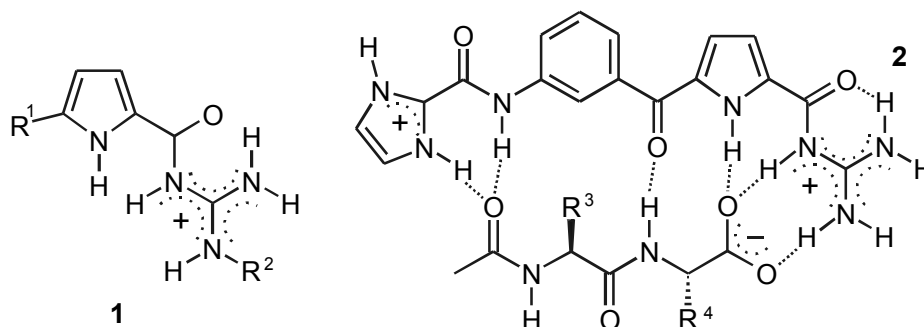
Chart 1

Addition of NH- or charged substituents to either the pyrrole or the guanidinium moiety of the guanidinocarbonyl pyrrole **1** significantly increases the affinity toward carboxylates. Compound **1** ($R^1 = R^2 = H$) binds Ac-L-Ala-O$^-$ with a K_a-value of only 130 M^{-1} (water:DMSO=2:3).[10] Attachment of a peptide at the guanidinium moiety leads to receptor **1** ($R^1 = H$, $R^2 = CH_2CH_2CO$-Val), that strongly binds carboxylates of amino acids with K_a-value $\geq 10^3$ M^{-1} in an aqueous buffer solution.[11] Functionalization of the pyrrole moiety gives receptor **1** ($R^1 = C(O)NHEt$, $R^2 = H$), which binds acetate with a K_a-value of $\sim 3 \times 10^3$ M^{-1} and *N*-acetylated amino acids with K_a-values ranging from 360 to 1700 M^{-1} (water:DMSO = 2:3).[10] Extra ionic interactions introduced by the imidazolium moiety in *de novo* designed receptor **2** allowed efficient binding of dipeptides in water[12] with binding constants up to 5.43×10^4 M^{-1}, which is almost 10 times higher than the binding affinity toward simple amino acids (Chart 1). A search for the best binding motif for Ac-Val-Val-Ile-Ala-O^{-*} in water has been carried out by screening a beads-bound combinatorial library (512 members) of structurally related tripeptide-functionalized receptors **3** for their binding properties against a fluorophore-labeled derivative of the tetrapeptide.[13] The binding constants vary from 20 M^{-1} (in H$_2$O, pH = 6.1, 10 μM bis-tris buffer) for the worst tripeptide linker sequence up to 4200 M^{-1} for the best one (Chart 2).

---

* This tetrapeptide represents the C-terminal sequence of the amyloid-*β*-peptide responsible for the formation of protein plaques within the brains of patients suffering from Alzheimer's disease.
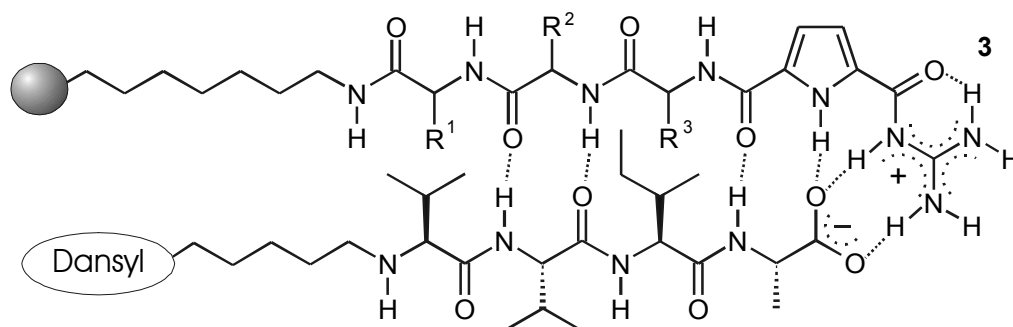
Chart 2

Receptors **4** (Chart 3), which are analogues of receptor **1**, containing a pyridine instead of a pyrrole moiety, bind dipeptides in aqueous solution much less effectively (K_a-values of 30 – 460 M^{-1} in water/[D$_6$] DMSO, 40% v/v).[9]

A combination of two aminopyrazole substituents with di- or tripeptides gives water-soluble amyloid-β-peptide-specific ligands.[14,15] For example, receptor **5** (Chart 3) binds the *KLVFF* peptide sequence in the central region of amyloid-β-peptide, which is responsible for pathogenic aggregation of the Alzheimer's peptide (K_a = 1700 M^{-1} in water).[14]
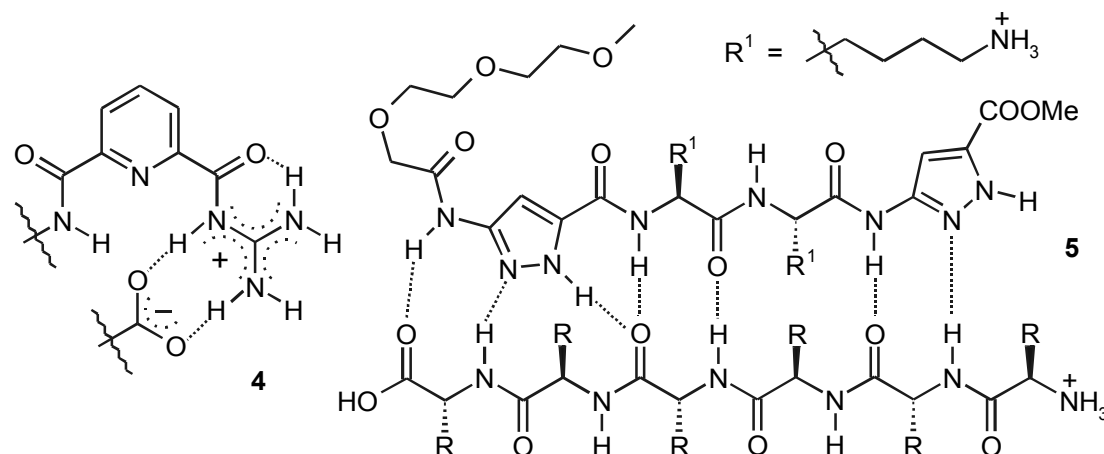
Chart 3

2.2.2 Boronic acid receptors

Aromatic boronic acids strongly interact with bifunctional substrates such as sugars, α-hydroxyacids and vicinal diols in aqueous media.[16,17] Although the first study of saccharide complexation by boronic acids in water appeared already more than half a century ago,[16] this functionality is still being used for the design of new sensitive and selective receptors.[18,19] The influence of the pKa of the boronic acid, the pH of the aqueous medium, and the influence of substituents (especially amines complexed to the boronic acids) have been studied to understand the complexation mechanism and for implementation in sensors.[19,20]

Enantioselective association events between boronic acid receptors **6** and bifunctional substrates such as *R*-hydroxycarboxylates and vicinal diols have been studied by Anslyn c.s. to develop enantioselective colorimetric and fluorescent indicator displacement assays (for example, Scheme 1).[21,22] The use of a variety of receptor-indicator pairs [K_a-values of the pairs ranging from 9.4×10^2 M^{-1} to 5.7×10^4 M^{-1} (for example: the K_a-value of **6×7** is about 3×10^4 M^{-1}) in 75% methanolic aqueous solution buffered with 10 mM HEPES at pH 7.4] provided a broad dynamic range, where these assays are effective in analyzing chiral α-hydroxyacid and diol samples. The determined *ee* values were in good agreement with the actual numbers.[21]
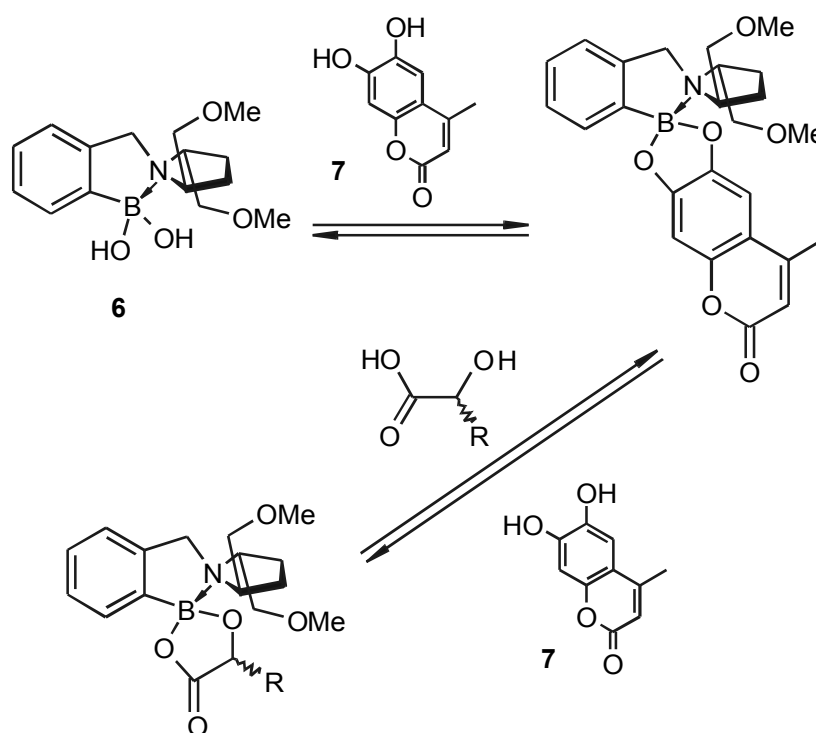
Scheme 1 Enantioselective indicator-displacement assays for the fluorescent indicator 4-methylesculetin.

James c.s. reported dipodal diboronic fluorescent[23,24] or electrochemical[25] sensors **8-10** for saccharides and sugar acids in aqueous media (Chart 4). For example, chiral fluorescent sensor **9** is highly sensitive, chemoselective, and enantioselective to sugar acids, for example: *D*- or *L*-tartaric acid (K_a-value up to 8.3×10^5 M^{-1}), *D*-glucaric acid (K_a-value up to 5.4×10^5 M^{-1}), *D*-gluconic acid (K_a-value up to 5.4×10^4 M^{-1}) in 52.1% methanol in water (pH = 5.6; 50 mM NaCl ionic buffer).[23]
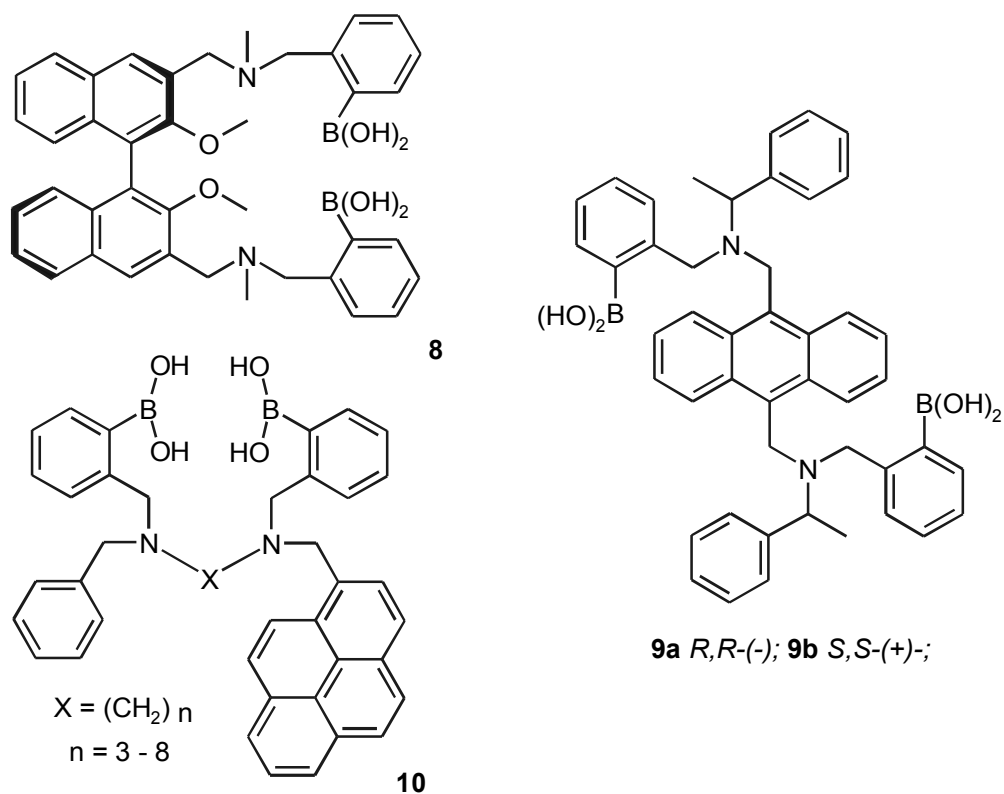
Chart 4

Efficient binding of *L*-Dopa in aqueous solution ($K_a = 1.6 \times 10^3$ M^{-1}, 0.1 M MOPS buffer, pH = 7.2) was realised by combination of a boronic acid and sulphonium groups in one receptor (Scheme 2).[26]
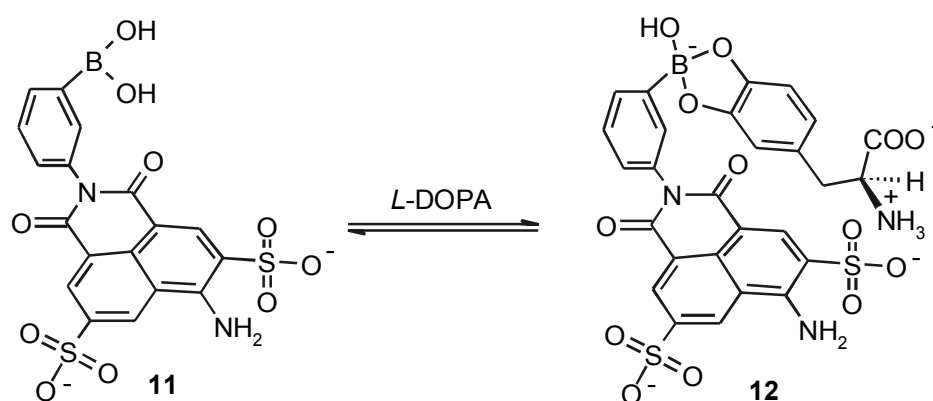
Scheme 2 Binding of *L*-Dopa.

2.2.3 Fluorescent sensor for the recognition of natural compounds

Gawley et al. reported a range of azacrowns that bind saxitoxin **13**, a potent marine toxin (Chart 5).[27] Receptor **14** showed the best binding in a 4:1 ethanol-water mixture (K_a-value of ~ 3.6×10^4 M^{-1}).
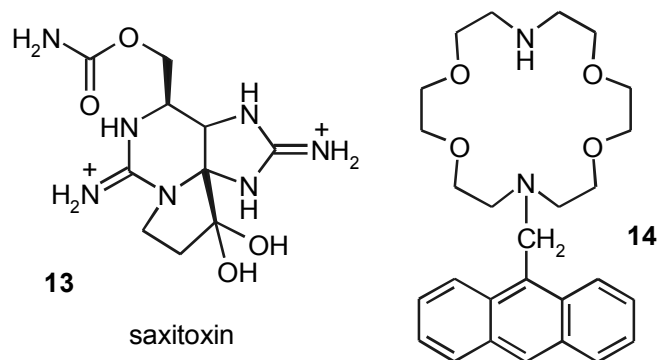
Chart 5

2.3 Tripodal receptors

Tripodal water-soluble receptors **15-17** have been prepared by functionalization of trisubstituted amine or 1,3,5-triethylbenzene platforms with amine-, pyridine-, ammonium-, and guanidinium groups or their metal complexes. Anslyn c.s. designed receptors that provide excellent shape, size, and charge complementarity to phosphate (Scheme 3) and arsenate, which allows selective binding of these anions in water at neutral pH (K_a-value of **15** with HPO_4^{2-} 1.5×10^4 M^{-1}, of **15** with $HAsO_4^{2-}$ 1.7×10^4 M^{-1}, and of **15** with other anions studied < 100 M^{-1}).[28,29] Receptor **15** has been used in an indicator-displacement assay to determine the phosphate concentrations in both horse serum and human saliva at biological pH.[29]
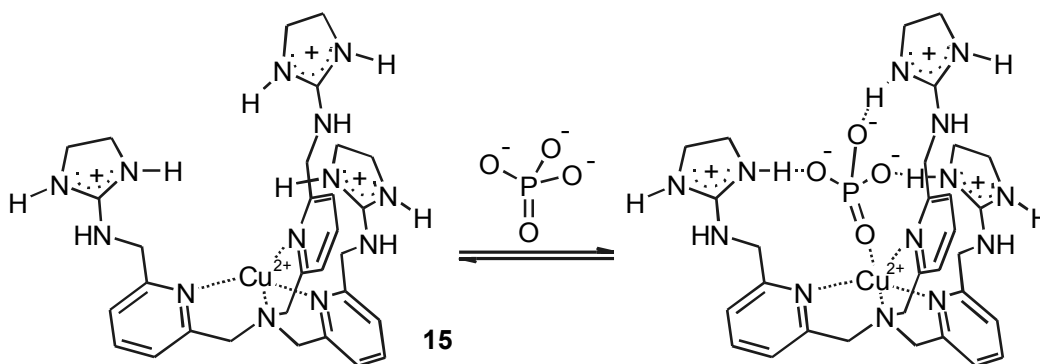
Scheme 3 Phosphate binding to receptor **15**.

Tritopic receptors such as **15-17** efficiently recognize and distinguish polyfunctional guests in water. For example, receptor **16** binds tricarballate and 1,2,3,4-butanetetracarboxylate with K_a-values of ~ 1.8×10^4 – 2.2×10^5 M^{-1} in aqueous solution (HEPES buffer, pH = 7.4), which is 1 – 3 orders of magnitude higher than the binding of glutarate and acetate (K_a-values of ~ 3×10^2 – 2×10^3 M^{-1}).[30] Anslyn c.s. also studied a variety of modified triethylbenzene receptors functionalized with guanidinium and/or boronic acid substituents (for example **17**, containing two 2-aminoimidazolium substituents and one boronic acid function

intramolecularily complexed with a nitrogen atom).[31-34] These receptors efficiently complex citrate, tartrate, and malate, with in the case of receptor **16** K_a-values of 2.0×10^5 M^{-1}, 5.5×10^4 M^{-1}, and 4.8×10^4 M^{-1} (in 75% methanol in water, $5 - 10$ mM HEPES, pH 7.4), respectively.[32] If at least one boronic acid substituent is present on the scaffold, recognition of saccharides (glucose, fructose) and aromatic polyols (gallate, 3,4-dihydroxybenzoate, catechin, etc) takes place with K_a-values of $\sim 1.4 \times 10^2 - 2.0 \times 10^4$ M^{-1} in methanol:water = 3:1 (5-10 mM HEPES, pH 7.4).[32] These receptors also allow differentiation between the structurally related tartrate and malate in aqueous methanol solution.[33] Studies in aqueous buffer solution revealed an enthropically driven aggregation of citrate with the tris-imidazolium analogue of **17**, observed upon dilution (Chart 6).[34]

Chart 6
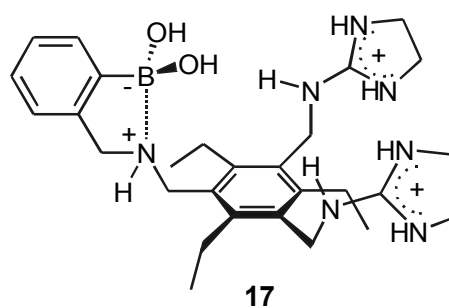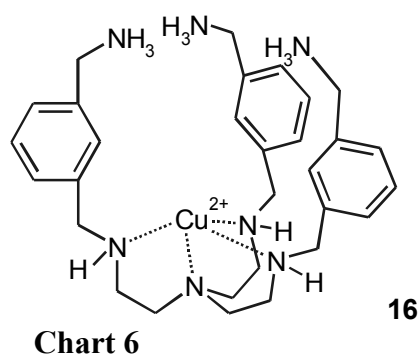
Schmuck and Schwegmann attached three pyrrologuanidinium moieties to the triethylbenzene scaffold, resulting in an excellent receptor for tricarboxylates in water: trimesic acid tricarboxylate is bound with a K_a-value of 3.4×10^5 M^{-1} (pH = 6.3), citrate with K_a-values up to 2.3×10^5 M^{-1} in pure water and 8.4×10^4 M^{-1} in bis-tris buffer solution, and Kemps triacid tricarboxylate with a K_a-value of $\sim 5.1 \times 10^4$ M^{-1} (bis-tris buffer solution).[35]

Receptor **18,** obtained by combination of two triethylbenzene scaffolds functionalized with guanidinium substituents via a Cu-pyridinium binding centre, is selective for 2,3-biphosphoglycerate (K_a-value is 8×10^8 M^{-1} in 1:1 water/methanol at pH = 4, 25 °C). The binding of phospho(enol)pyruvate, 2-phosphoglycerate, and 3-phosphoglycerate, that are analogs of 2,3-biphosphoglycerate, is more than one order of magnitude weaker (K_a-values are $4.7 \times 10^6 - 1.3 \times 10^7$ M^{-1}, the same conditions). The complexation of other types of anions, such as β-glycerophosphate ($K_a = 6 \times 10^4$ M^{-1}) and acetate ($K_a = 7 \times 10^3$ M^{-1}) is even 4-5 orders of magnitude weaker (Chart 7).[36]
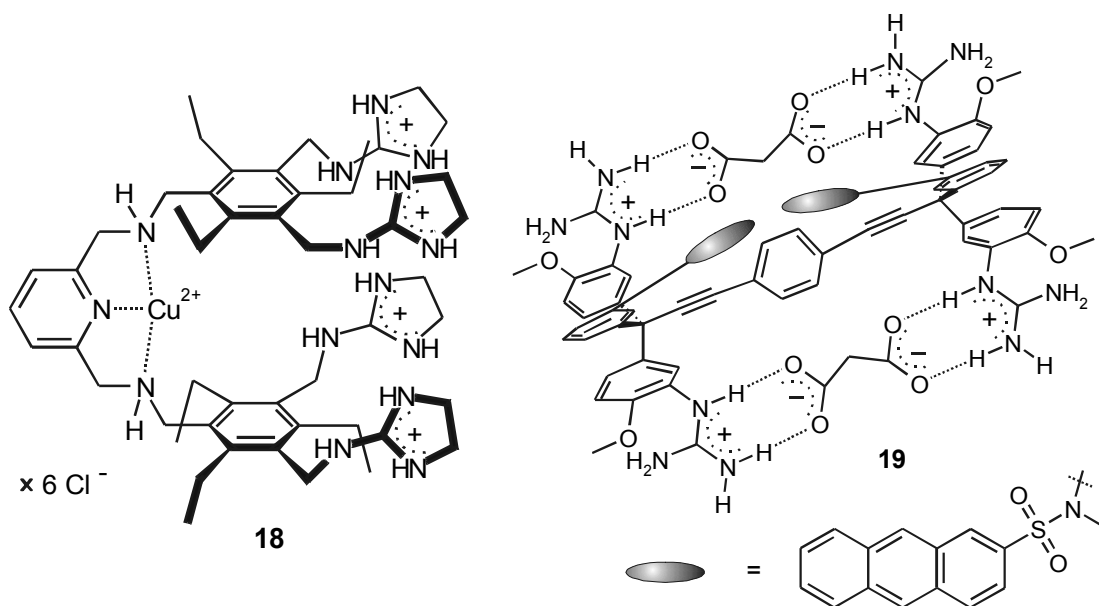
Chart 7

2.4 Pinwheel

Raker and Glass reported a cooperative pinwheel chemosensor for dicarboxylates **19** (Chart 7).[37] The sensor possesses four guanidinium recognition elements to cooperatively bind two dicarboxylates of varying size. The cooperativity effect contributes to favorable binding constants for dicarboxylates in water, as well as a high degree of selectivity over monocarboxylates. That allows sensing of dicarboxylates in the presence of a 1000-fold excess of monocarboxylates, such as acetate (for example, phthalate binding: Hill coef. = 2.0, K_a-value of 1.2×10^9 M^{-2} in 10 mM solution of sodium acetate in water).

2.5 Cyclophanes

Cyclophanes are defined as molecular assemblies that have a cavity capable of binding guests.[38] The description of the host-guest behavior of cyclophanes in water will start with molecules containing several (het)arene moieties connected by a variety of linkers. Subsequently, special examples, viz. calixarenes, and the related cavitands and carcerands, will be described.

2.5.1 Cyclophanes containing several (het)arene moieties connected by different linkers

A variety of groups have been used to solubilize cyclophane scaffolds in water, such as pyridinium,[39,40] ammonium,[41,42] carboxylic,[43] phosphonic moieties, saccharides, etc. Addition of adamantyl substituents followed by complexation with β-cyclodextrins also significantly increases the solubility of cyclophanes in water.[44]

Schneider c.s. reported that pyridinium-containing cyclophane receptors strongly bind AMP (for example, in the case of **20**, $K_a = 6.3 \times 10^5$ M^{-1}) in water. Complexation of AMP gives a significant fluorescent response (large emission increase), in contrast to GMP and UMP, complexation of which with **20** does not give rise to specific changes

20

21

22

23

24

2Br$^-$
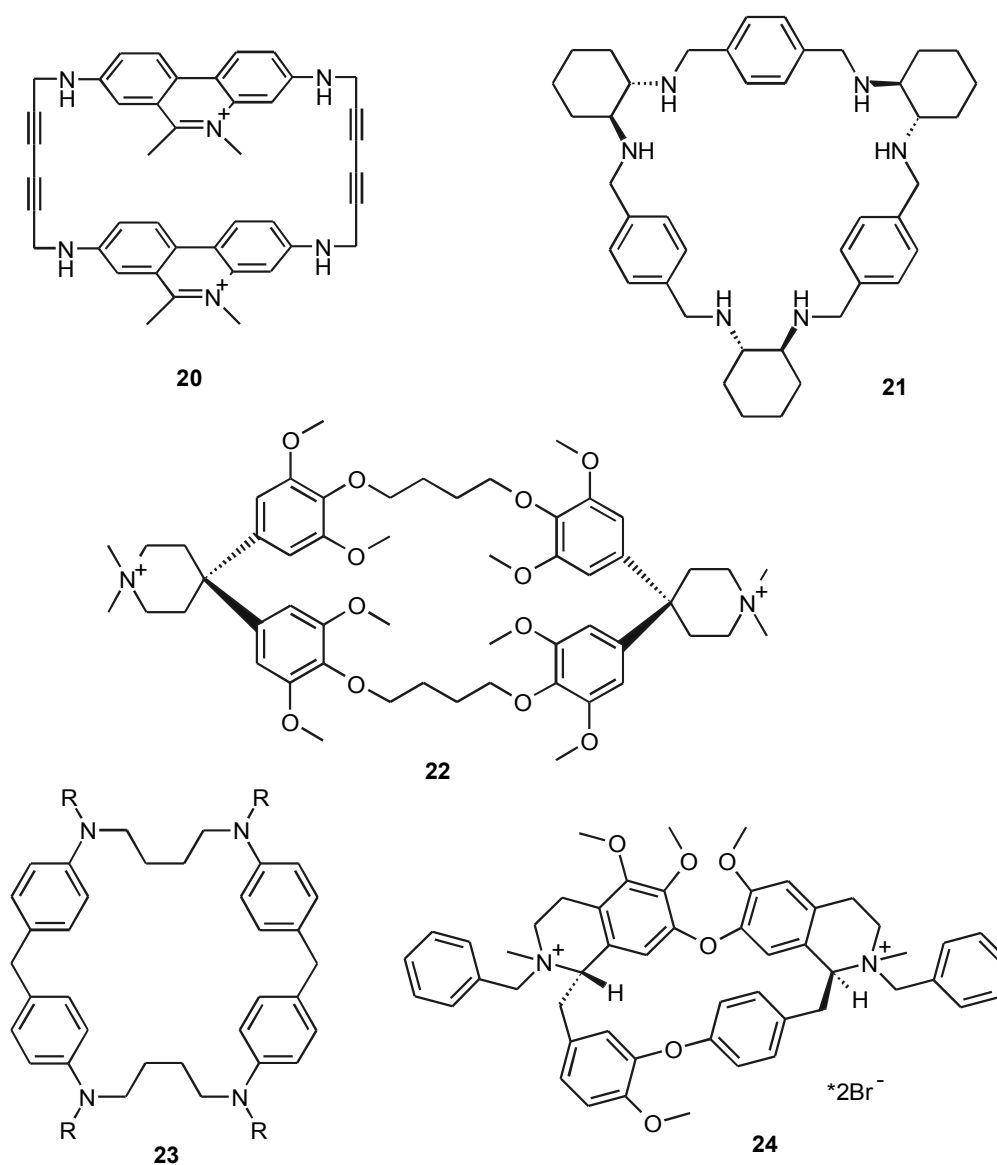
Chart 8

in the fluorescence spectra.[40] Receptor **21** efficiently recognizes benzene-tricarboxylates in water, for example, for trimesate the K_a-value is ~ $1.5 \times 10^4 - 3.9 \times 10^6$ M^{-1} (the exact value depends on the degree of protonation of **21**).[41] Cyclophane **22** has been proposed as a tool for removing chloronaphthalenes from water: photoexcitation of complexes of cyclophane **22** and 1- or 2-chloronaphthalene in aqueous solution causes rapid dechlorination of the guest (a reaction driven by electron transfer from the host to the excited guest), which leads to covalent

attachment of the naphthyl group to the host **22**.[42] Functionalized cyclophanes **23** (R = saccharide- or ammonium-containing substituents, as well as adamantane or dansyl functions solubilized by complexation with β-cyclodextrin) form strong complexes with α- and β-naphthalene sulphonate dyes (K_a-values up to 1.1×10^4 M^{-1}) or pyrene (K_a-values up to 1.1×10^5 M^{-1}) in neutral aqueous media.[44] A dicationic cyclophane-type *N,N'*-dibenzylated chiral derivative of a bisisoquinoline macrocyclic alkaloid *S,S*-(+)-tetrandrine **24** binds amino acids (stereoselectivity ≥ 10) and (di)carboxylates with K_a-values up to 135 M^{-1} in water (Chart 8).[45]

Cyclophanes **25** and **26** containing exo/endo-cyclic phosphonium and phosphinium groups are good receptors for catecholamines in aqueous medium, as has been reported by Schrader c.s.[46-48] Receptor **25** binds adrenaline, noradrenaline, and dopamine with binding constants of ~ $1.5 – 2.5 \times 10^2$ M^{-1} in methanol/water = 1:1 with a 1:1 stoichiometry.[47] Two guest molecules can be bound by cyclophane **26** in water (Chart 9). Although the binding is noncooperative, its guest affinity is higher than that of receptor **25** toward catecholamines and related structures such as β-blockers with extended aromatic π-faces (K_a-values are up to 7×10^3 M^{-1} for each single complexation step or 5×10^7 M^{-2} for both steps).[46]
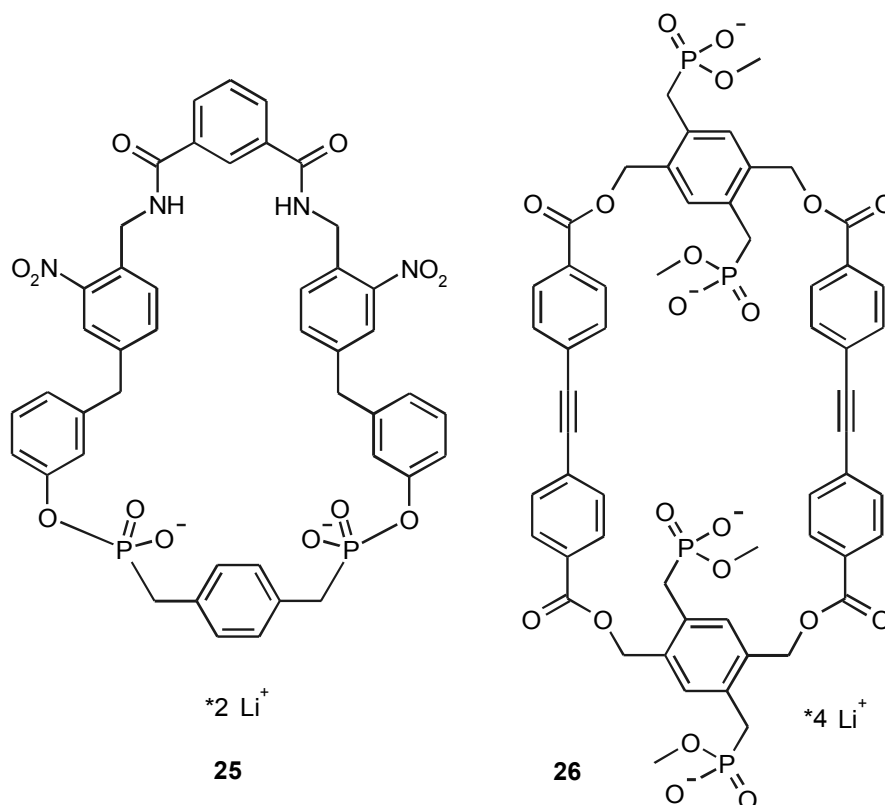
Chart 9

Pyrenophanes **27**, possessing various hydrophilic functionalities such as ammonium-, hexaammonium-, bis(diazoniacrown)-, and tetrakis(octa(oxyethylene))-ones, show a moderate solubility in pure water. The cationic pyrenophanes strongly recognize anionic arenes including nucleotides (the complexation mode is shown in Figure 1). The relative affinity toward nucleotides is triphosphate > diphosphate > monophosphate; for example, K_a (ATP) = 1.0×10^6 M^{-1}, K_a (ADP) = 5.3×10^3 M^{-1}, K_a (ADP) = 1.9×10^3 M^{-1} in water.[49]
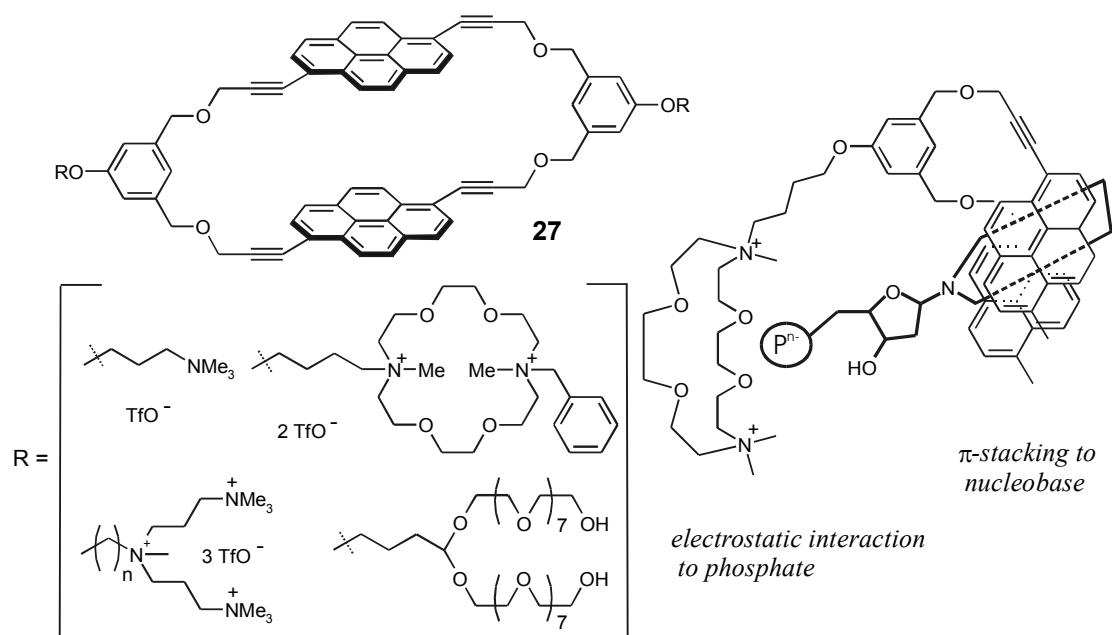
Figure 1 Nucleotide recognition by the pyrenophanes **27**.

Sanders c.s. reported a guest amplified cyclophane synthesis in water, which was realized using dynamic combinatorial libraries based on disulfide chemistry.[50-52] The mercaptanes involved form a variety of disulfides in the presence of oxygen and a small amount of base. The disulfide exchange takes place efficiently under mild conditions in the presence of catalytic amounts of thiol.[50] For example, the mixture of disulfides formed from mercaptanes **28** and **29** contains less than 10% of cyclophanes **32** and **33**, but addition of methylquinolinium iodide **30** or methylmorphinium iodide **31** leads to the formation of macrocycles **32** and **33**, respectively, in good to excellent yields (Scheme 4).[51] The hosts have a high binding affinity toward the amplifiers. For example, K_a **30@32** = 2.5×10^5 M^{-1} (ΔG = -30.8 kJ/mol, ΔH = -41.6 kJ/mol, $T\Delta S$ = -10.8 kJ/mol) and K_a **31@33** = 7.1×10^5 M^{-1} (ΔG = -33.4 kJ/mol, ΔH = -47.8 kJ/mol, $T\Delta S$ = -14.4 kJ/mol) in aqueous 10 mM borate buffer (pH = 9.0). The thermodynamic data show that binding is invariably enthalpy-driven and counteracted by entropy,

suggesting that binding is dominated by electrostatic interactions including cation-π interactions and possibly salt-bridge formation.[51]
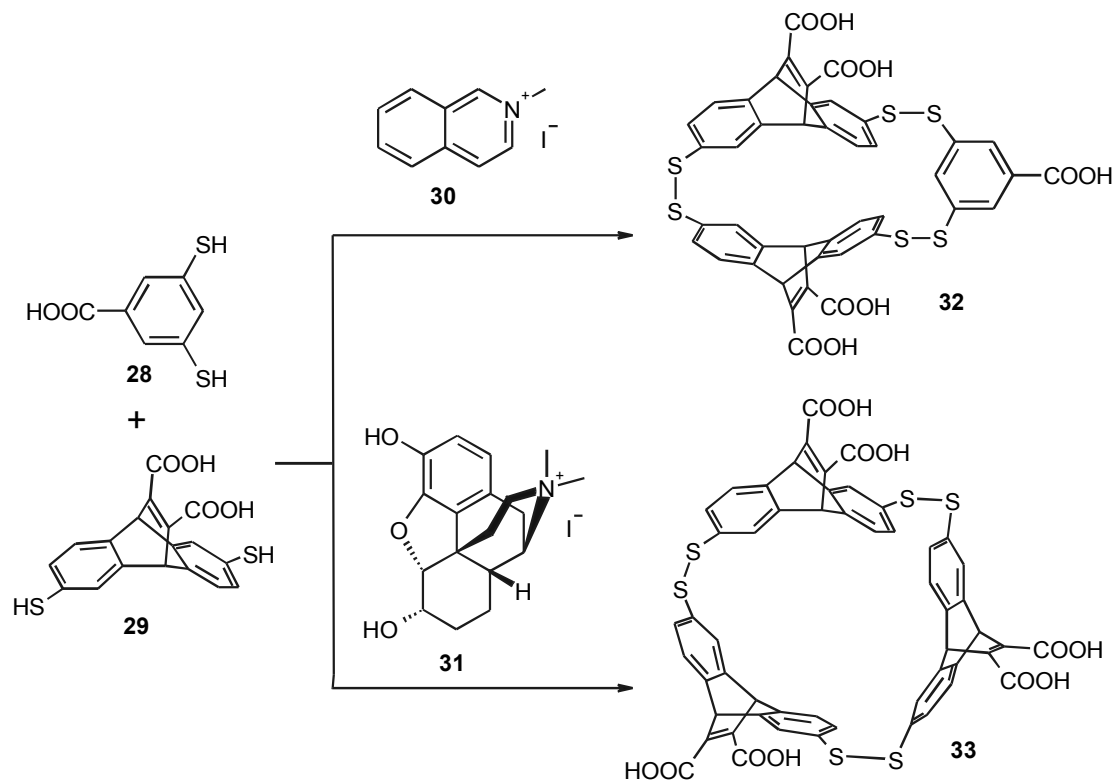
Scheme 4 Guest-amplified cyclophane synthesis.

2.5.2 Calix[n]arenes, n = 4-8

Calixarenes **34** (Chart 10) are among the most versatile and useful building blocks in supramolecular chemistry.[53,54] Water-soluble calixarenes[55] have been made by attachment of water-soluble functions such as sulfonates,[56] carboxylic acids, phosphonates, amines, guanidinium,[57] peptides,[58] and saccharides[58,59] either directly or via linkers to the upper or lower rims of calix[n]arenes. More recently, calixarenes have become attractive scaffolds to make multivalent amphiphiles useful in both biological and chemical applications.[53,60]
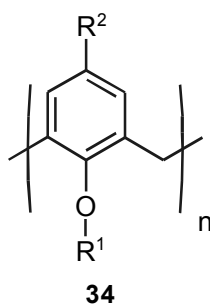
Chart 10

Calix[n]arenes with sulfonate substituents at the upper rim have a high solubility in water. They form complexes with a variety of charged and neutral guests in aqueous solution. Calix[4]arene tetrasulfonate **34** [n = 4, R^1 = H, R^2 = SO_3H] binds small neutral organic molecules such as acetonitrile, acetone, butanone, and 1-propanol ($K_a \approx 15 - 65$ M^{-1}; pD = 7.3),[61] substituted benzenes such as benzaldehyde and iodobenzene ($K_a \approx 8 - 191$ M^{-1}; pD = 7.3-7.4),[62,63] heterocycles such as 2,2'-bipyridine ($K_a \approx 10260$ M^{-1}; pH = 2.0)[64] and 4,4'-bipyridine ($K_a \approx 1185$ M^{-1}; pH = 2.0),[64] with a 1:1 stoichiometry in water. They also bind trimethylammonium cations (K_a-values of $\sim 2.5 \times 10^3 - 8 \times 10^4$ M^{-1} in D$_2$O, pD = 7.3).[65-67] The inclusion process is enthalpically favored and entropically disfavored (for example, complexation of **34** [n = 4, R^2 = SO_3H, R^1 = CH_2COOH] with tetramethylammonium chloride in water, pH = 7, 25 °C: K_a-value of $\sim 3.2 \times 10^3$ M^{-1}, ΔG = -20.1 kJ/mol, ΔH = -24.3 kJ/mol, $T\Delta S$ = -4.2 kJ/mol). The negative entropy contribution is mainly caused by stiffening of the system upon inclusion of the guest into the host cavity.[64,66,67] The complexation of aliphatic guests takes place through inclusion of the alkyl moiety of the guest into the calixarene cavity, which is accompanied by an up to 2 ppm upfield shift of the guests' Me-group protons in the ^{1}H NMR spectra.[61] In the case of substituted benzenes either the aryl moiety or the substituents can be located in the cavity.[63,65,66] Calix[5]arene pentasulfonate **34** [n = 5, R^1 = H or CH_2COO^-, R^2 = SO_3H] binds trimethyl-ammonium cations (K_a-value of $\sim 4 \times 10^3 - 1.3 \times 10^5$ M^{-1} in D$_2$O, pD = 7.3)[65] in water in such a way that the alkylammonium group is exclusively included into the cavity. Calix[6]arene hexasulfonate **34** [n = 6, R^1 = H, R^2 = SO_3H] forms complexes with 4-nitrophenol (differential scanning microcalorimetry: K_a = 192.6 M^{-1}, ΔG = -5.3 kJ/mol, ΔH = -68.2 kJ/mol, ΔS = -185 J/K×mol).[56] The calix[6]arene hexasulfonate also solubilizes C$_{60}$ fullerene in water (the stoichiometry of the complex is 1:1 and the log of the extraction constant from toluene to water is 5.48).[68] The sulfonated calixarenes exhibit neither toxicity nor immune responses, which results in an increases of its use in biopharmaceutical studies, such as drug delivery (Chart 10).[69]

Kalchenko c.s. have described water-soluble calix[4]arenes bearing one, two or four proton ionisable dihydroxyphosphoryl groups at the lower rim, and their salt formation with *L*-(-)-α-phenylethylamine and (1*S*,2*R*)-(+)-ephedrine.[70] Coleman c.s. reported a series of amphiphilic calix[4]arenes having four hydrophobic acyl chains at

the upper rim as well as two hydrophilic dihydroxyphosphoryloxy groups at the lower rim that self-assemble at the air-water interface as stable Langmuir monolayers.[71] Calix[4]arenes substituted at the upper rim by hydroxyethoxyphosphoryl groups and its self-assembly to capsules with tetracationic counterparts in polar solvents has recently been described by Schrader c.s.[72] Unfortunately, the 1:1 complexes were often insoluble in water and in some cases precipitated even from methanol. Rachon c.s. have reported the complexation of hydrochloride salts of (1*R*,2*S*)-(-)-ephedrine, (1*R*,2*S*)-(-)-norephedrine, (*R*)-(-)-noradrenaline and 2-phenylethylamine by a calix[4]arene containing four phosphonate groups at the upper rim.[73] The binding constants of 1:1 complex formation vary from 45 M^{-1} to 145 M^{-1} in 200 mM phosphate buffered D_2O. Homocalix[3]arene forms 2:1 complexes with C_{60} fullerene in water.[74]

2.5.3 Resorcinarenes

Resorcinarenes (**35**, R^1 = alkyl, R^2 = H) are macrocyclic molecules containing eight hydroxyl groups at the upper rim forming intramolecular hydrogen bonds (Chart 11).[75] Aoyama c.s. found artificial resorcinarene-based viruses that could be used for gene delivery.[76] Resorcinarenes **35** (R^1 = C_5H_{11}) containing eight saccharide moieties form small micelle-like glycocluster nanoparticles (d ~ 3 nm) in water that interact with biological saccharide receptors or are agglutinated with Na_2HPO_4 and assembled on plasmid DNA in a number-, size-, and shape-controlled manner to give artificial glycoviral particles (d ~ 50 nm) capable of transfection.[76,77]
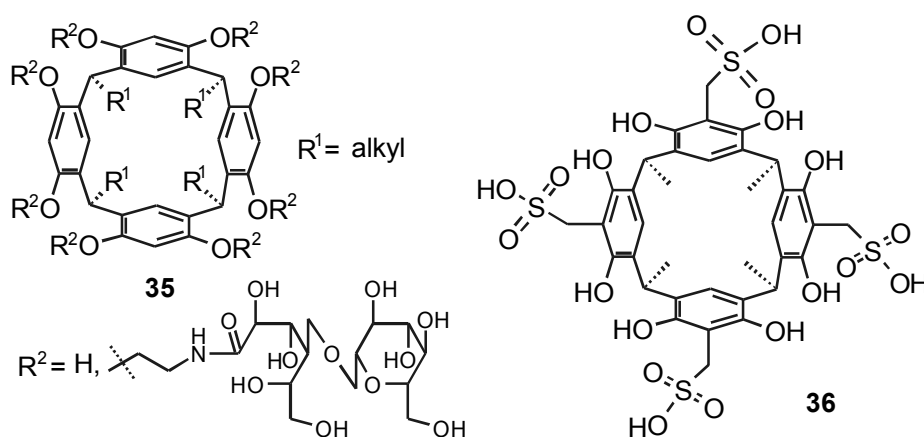
Chart 11

Kazakova c.s. reported water-soluble sulfonato-methyl resorcinarene **36** (Chart 11)[78-81] that recognizes amino acids in aqueous solution (K_a-values up to 150 M^{-1}, pD = 7.2).[78] The tetrasodium salt of **36** binds organic and inorganic ions (for example, for

methylpyridinium the K_a-value is $\sim 10^5$ M^{-1}),[79] as well as differently sized and shaped metal complexes in neutral and basic aqueous solution: for example, the K_a-values with [Co(histidine)$_2$]$^+$, [Co(ethylenediamine)$_2$C$_2$O$_4$]$^+$, or [K(18-crown-6)]$^+$ in alkaline aqueous media are $\sim 8 \times 10^5$ M^{-1}, $\sim 1.3 \times 10^5$ M^{-1}, and 1×10^4 M^{-1}, respectively.[80]

2.5.4 Cavitands

Cavitands are macrocyclic compounds, consisting of multiple aromatic rings covalently linked in a highly constrictive manner and possessing a well-formed hydrophobic cavity.[82] Parent cavitands **37** (X = CH$_2$, R^1 = alkyl, R^2 = H, alkyl) are insoluble in water. To make them soluble in aqueous media, charged groups[83-85] or dendritic oxo substituents[84,85] have been introduced to the upper- or bottom rim (Chart 12). Gui and Sherman studied the binding of simple organic molecules by water-soluble cavitand **37** [R^1 = O(CH$_2$)$_3$OPO$_3$HNH$_4$, R^2 = Me]: acetone, acetonitrile, toluene, benzene, chloroform, ethyl acetate, methyl acetate, and methyl propionate are bound with a 1:1 stoichiometry and K_a-values of $\sim 19 - 270$ M^{-1} in D$_2$O (50 mM (NH$_4$)$_2$CO$_3$, pD = 9.4).[83]

R^1 = alkyl

R^2 = any

X = CH$_2$, CH$_2$CH$_2$, CH$_2$CH$_2$CH$_2$,
o-substituted (het)arene

37
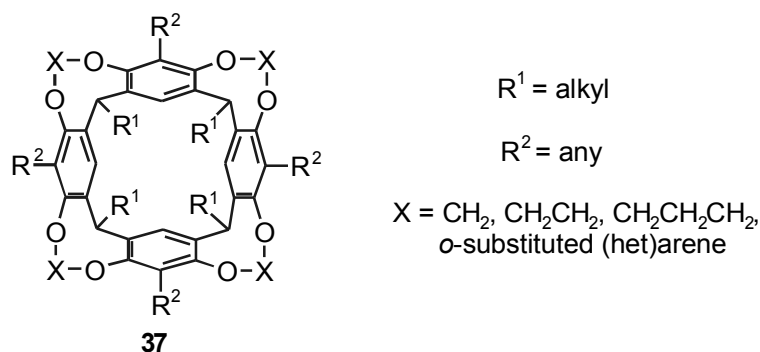
Chart 12

A systematic investigation of the solubilities and binding properties in water by cavitands upper rim functionalized with dendrimers, amines, amino-alcohols, pyridiniums or pyrazyniums has been carried out by Middel et al.[85] These cavitands show a high affinity to phenol, *p*-cresol (K_a-values up to 1.7×10^4 M^{-1}), and benzene (K_a-values up to 6.9×10^3 M^{-1}) in D$_2$O.[84,85]

The volume of the cavity of the classical cavitand **37** is much smaller than that of cucurbituril and Fujita's organometallic cages (*vide infra*). It can accommodate only one molecule of water as was proven by Paek c.s. at -50 °C in water saturated CD$_2$Cl$_2$ ($K_a \sim 70$ M^{-1}).[86]

Cavitands **37**, that have another linker (X = -CH$_2$CH$_2$- or -CHR=CHR- [usually *o*-substituted (hetero)aromatic compounds]) between the resorcinarene oxygens than CH$_2$, have a bigger cavity and, hence, show a different complexation behavior. Diederich c.s. have shown that tetraamidinium functionalized cavitand **38** is a very good receptor for benzene dicarboxylates and nucleotides in water (Chart 13).[87] 5-Nitro- and 5-methoxy-1,3-benzenedicarboxylates are bound with a 1:2 stoichiometry with binding constants of $K_{a1} = 14.8 \times 10^3$ M^{-1}, $K_{a2} = 3.8 \times 10^3$ M^{-1} and $K_{a1} = 8.6 \times 10^4$ M^{-1}, $K_{a2} = 7.7 \times 10^3$ M^{-1}, respectively. In the case of 1:2 isophthalate complexes, one of the guest molecules is included with the less polar segment of its phenyl ring into the receptor cavity, while the second guest molecule forms an ion-paired complex outside. In aqueous buffer solution, the complexation of the second isophthalate is completely suppressed, resulting in a 1:1 binding stoichiometry (K_a-values of **38** with 5-nitro- and 5-methoxy-1,3-benzenedicarboxylates are 12.2×10^3 M^{-1} and $\sim 1.2 \times 10^5$ M^{-1}, respectively; in D$_2$O containing Tris/HCl, pH = 8.3). Both in water and in aqueous buffer solution 5-methoxyisophthalate is bound about 5-10 times stronger than 5-nitroisophthalate. Among 11 nucleotides studied, AMP, ADP, and ATP form the strongest complexes with **38**. The complexation strength increases with increasing guest charge: the K_a-values increase in the series AMP < ADP < ATP ($K_a = 1 \times 10^4$ M^{-1}, 4.87×10^4 M^{-1}, and 6.6×10^5 M^{-1}, respectively; in D$_2$O containing Tris/HCl, pH 8.3; 1:1 stoichiometry was observed in all cases).

X = -CH$_2$CH$_2$-, R = (CH$_2$)$_3$(OCH$_2$CH$_2$)$_3$OMe
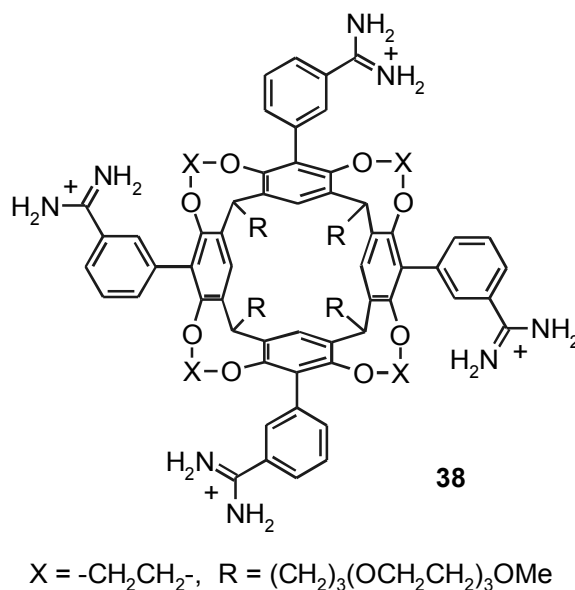
Chart 13

Rebek c.s. studied the molecular recognition in aqueous media of a variety of broad deep-cavity cavitands (e.g. **39**), that were made water-soluble by the attachment of carboxylate,[88-91] ammonium,[92] or amino[93] groups. For example, cavitand **39**, having a solubility of 5 mM in water, forms complexes with a variety of guests like *S*-nicotinium, tetramethyl-ammonium bromide, choline chloride, acetylcholine chloride, quinuclidinium (K_a-values $> 10^4$ M^{-1}).[88-90] Adamantane dissolves in an aqueous solution of **39** upon sonication; amantadine hydrochloride and rimantadine hydrochloride also form stable 1:1 complexes with **39** in water with binding constants of 1.1×10^3 and $>10^4$ M^{-1}, respectively.[89] In the complexes the hydrophobic adamantane moiety is bound deeply within the cavity, while the primary amines are directed toward the tetracarboxylate rim and the solvent.[89] Cavitand **39** forms complexes with the long alkyl chain surfactants[91] **40** and **41** so that the alkyl moieties of the guests experience spontaneous helix formation upon encapsulation (Chart 14).[88]
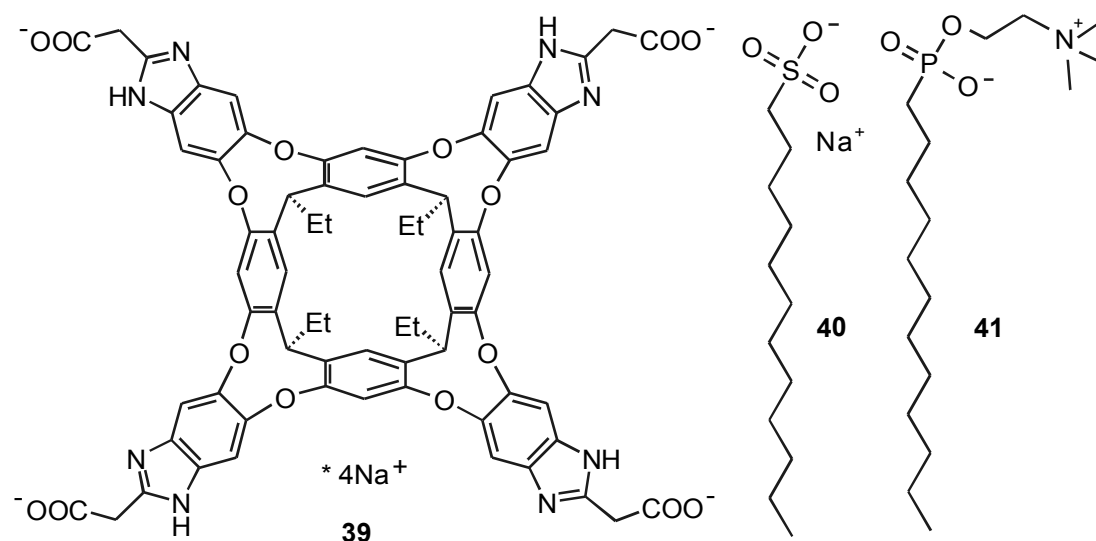
Chart 14

2.6 Cucurbit[n]urils, n = 5-8

Cucurbiturils **42** are macrocyclic compounds made by an acid-catalyzed condensation reaction of glycoluril and formaldehyde. Characteristic structural features of cucurbiturils **42** are the hydrophobic cavity and the polar carbonyl groups surrounding the portals (Chart 15).[94,95] Cucurbit[5]uril and cucurbit[7]uril are quite well soluble in water (2-3 $\times 10^{-2}$ M). Cucurbit[6]uril and cucurbit[8]uril have a very low solubility in pure water. Nevertheless, all the cucurbiturils are soluble in acidic water, as well as in an aqueous alkali metal solution, presumably due to protonation or

coordination of the metal ions to the portal carbonyl oxygens. The solubility of cucurbiturils in common organic solvents is less than 10^{-5} M. Therefore, most host-guest chemistry of cucurbiturils has been studied in aqueous media. Several modes of intermolecular interactions promote the binding of guests by cucurbiturils. First, like for cyclodextrins, a hydrophobic effect applies, i.e., a composite effect derived from the interplay between the release of "high-energy water" upon complexation of nonpolar organic residues and concomitant differential dispersion interactions inside the cavity and in bulk water. Second, ion-dipole interactions of metal cations or organic ammonium ions with any of the two ureido carbonyl rims may come into play, while hydrogen-bonding interactions prevail less frequently. As a peculiarity, the complexation of metal cations at the ureido rims (which is often required to enhance solubility) can lead to ternary supramolecular complexes composed of host, included guest, and associated metal ion. In fact, it has been suggested that the cations function as "lids" to seal the portal and promote binding.[95]

n = 5 - 8

42
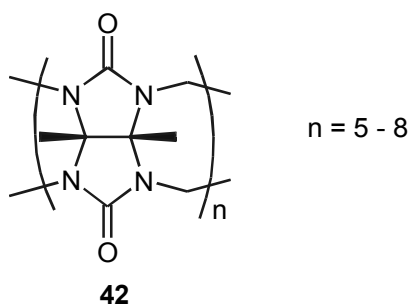
Chart 15

Variation of the cavity and portal sizes leads to a variety of cucurbiturils with different molecular recognition properties. In the bigger ones even encapsulation of several (different) guests is possible and hence chemical reactions of the guests within the cavity. Electrochemically-induced reversible substitution of the guests from the cavity was used for the 'construction' of molecular machines.[95,96]

2.6.1 Cucurbit[5]uril

The smallest homologue, cucurbit[5]uril can encapsulate small molecules, such as N_2, O_2, or Ar in the cavity and binds Pb^{2+} in water/formic acid = 1:1 or in water ($K_{a1} > 10^9$ M^{-1}, $K_{a1} \times K_{a2} > 10^{17}$ M^{-2}) with a very high selectivity ($>10^{5.5}$) over alkali, alkaline earth, NH_4^+, and Cd^+ cations.[97] Two NH_4^+ ions can completely seal both the openings of cucurbit[5]uril.

2.6.2 Cucurbit[6]uril

Cucurbit[6]uril forms very stable complexes with protonated diaminoalkanes ($^+NH_3(CH_2)_nNH_3^+$, n = 4-7, K_a > 10^5 M^{-1}) and moderately stable complexes with protonated aromatic amines such as *p*-methylbenzylamine ($K_a \approx 3 \times 10^2$ M^{-1}) (the *o*- and *m*-isomers are not included), and protonated cyclohexylamine.[98] It also encapsulates neutral molecules such as tetrahydrofuran (K_a = 1700 M^{-1}) and atoms such as Xe ($K_a \approx 200$ M^{-1}) in an aqueous Na$_2$SO$_4$ solution.[99]

2.6.3 Cucurbit[7]uril

Due to its larger cavity cucurbit[7]uril forms 1:1 complexes with protonated adamantylamine, as well as viologen dications[100-102] ($K_a \approx 10^5$ M^{-1} in water) and 2,6-bis(4,5-dihydro-1*H*-imidazol-2-yl)naphthalene. Two types of complexation of viologen dications by cucurbit[7]uril have been found: methyl and ethyl viologen dication form *internal* complexes in which viologen is located within the cavity, but butyl (and other viologens with longer aliphatic *N*-substituents) form *external* complexes in which the viologen nucleus is not engulfed by the host.[101] Ong and Kaifer found that salts strongly influence the apparent association constant of cucurbit[7]uril with methyl viologen dication, with a more pronounced effect for solutions containing divalent Ca^{2+} cations than for solutions containing monovalent Na$^+$ cations.[102] Neutral molecules such as ferrocene, cobaltocene, and carborane are easily encapsulated in cucurbit[7]uril in aqueous solution.[103]

2.6.4 Cucurbit[8]uril

Cucurbit[8]uril encapsulates one or two methylviologen molecules. The stoichiometry of the complex is controlled by the redox chemistry of the guest.[104] The cavity of cucurbit[8]uril, which is similar to that of γ-cyclodextrin, is large enough to include two 2,6-bis(4,5-dihydro-1*H*-imidazol-2-yl)naphthalene molecules to form a 1:2 complex, or two different guest molecules such as methylviologen^{2+} and 2,6-dihydroxynaphthalene to give a 1:1:1 complex. The formation of this 1:1:1 complex is driven by the markedly enhanced charge-transfer interaction between the electron-deficient and electron-rich guest molecules inside the hydrophobic cavity of cucurbit[8]uril. A molecular loop lock, a novel redox-driven molecular machine based on this phenomenon, has been reported.[105] It can also encapsulate other macrocycles, such as cyclen and cyclam.

2.6.5 Hemicucurbit[6]uril

The solubility of hemicucurbit[6]uril **43** is very low in water, however, it increases dramatically in the presence of metal or ammonium thiocyanates[106] or iodides.[107] From solubility measurements binding constants were obtained for these anions: 200 M^{-1} (I$^-$), 220 M^{-1} (SCN$^-$), that are counterion independent.[107] In contrast with cucurbit[n]urils, surprisingly, no cation complexation has been observed by *hemi*cucurbit[6]uril (Chart 16).

43
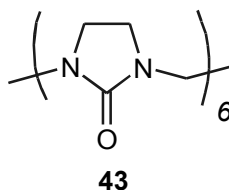
Chart 16

2.7 Self-assembled receptors

Self-assembly is the spontaneous, noncovalent association of two or more molecules under equilibrium conditions into stable, well-defined aggregates.[108] Water-soluble self-assemblies such as capsules, cyclic organometallic arrays or cages have been realized with the help of multivalent electrostatic or metal-ligand interactions.

2.7.1 Capsules

Water-soluble capsules have been prepared based on different supramolecular scaffolds, such as calix[n]arenes,[72,109-112] trisubstituted benzenes,[113] or porphyrins[114] functionalized with charged groups. The scaffolds represent hemispheres that are brought together by ion-pair interactions using sulphonate and pyridinium,[114] monoalkyl esters of phosphonic acids and ammonium, pyrazolium or imidazolium,[72,115,116] and sulphonate or carboxylate with amidinium moieties.[109-112] Schematic representations of a capsule based on two building blocks, containing four charged groups are shown in Figure 2. Two modes of interaction between the capsule components are proposed: separate contact ion pairing (Figure 2a)[110-112] and the formation of a cyclic array of anion-cation bonds (Figure 2b).[116] The water solubility of capsules is usually lower than that of the individual capsule components due to the neutralization of charges and the less effective solvation of ion pairs compared with that of the separate ions.[116] Therefore, to increase the water solubility of capsules polyethylenoxy chains have been introduced.[109-112]
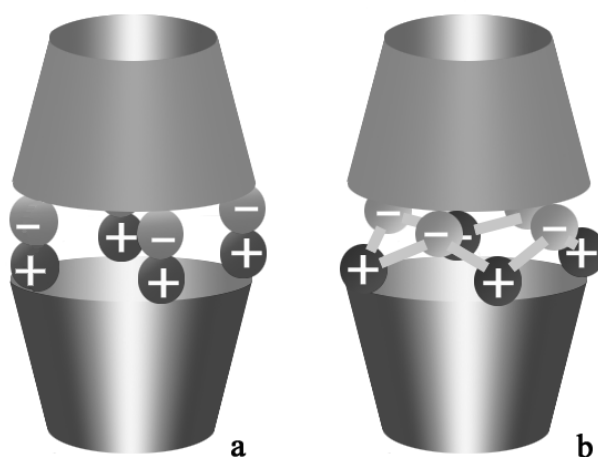
Figure 2 Two types of interaction between the capsule components: ion-pairing (a), gear-like structure (b)

In the case of three electrostatic interactions the binding constants are 1-4 $\times$ 10^3 M^{-1} in water.[113,117] The association of capsules brought together by four salt bridges is about 1-3 orders of magnitude stronger. Salts usually decrease the apparent stability constant of the capsule formation.[112]

In addition to complex formation inside [1+1] capsules, guests can also be complexed in the exterior in polar protic media.[116] In general, encapsulation of charged guests (ammonium salts, such as e.g. methylquinuclidinium) in capsules is very weak, mainly due to the competitive influence of water.[109,110] Some guests prefer complex formation with capsule components more than with the capsule itself and, therefore, may cause significant dissociation of the capsule.[116] This behavior significantly differs from that of capsules studied in apolar solvents.[118] One of the explanations of the low host-guest affinity is the decrease of the inner volume of the capsule by the solvation shell of the electrostatic walls of the capsule.[113,116]

2.7.2 Organometallic receptors

Organometallic receptors are macrocyclic assemblies or cages formed by metal ligand interactions.[119,120] The organometallic receptor complexes of Ru, Rh, Pt, Pd and Ir, with pyridine, cyclopentadiene ligands, or their analogs, are in general soluble in aqueous media, and not sensitive to air. The metal ligand interactions provide sufficiently high association constants, even in polar competitive solvents such as water.[120]

Buryak and Severin reported the use of assemblies of organometallic half-sandwich complexes **44** with a variety of dyes (for example, azophloxine **45**) as

indicator displacement assays for the detection of peptides[121] and amino acids[122] in aqueous buffer solution. The **44·45** sensing assay ($K_a \approx 3.2 \times 10^7$ M^{-1} in 100 mM aqueous phosphate buffer solution, pH = 7.0) allows differentiation of peptides that contain either His or Met residues in positions one or two from the N terminus from other types of peptides. For example, the association constant of His-Ala, His-Gly-Gly, Leu-His-Leu or Gly-Met-Gly with Rh-complex **44** is more than *three* orders of magnitude larger than that of the **44·45** complex. On the other hand, Val-Phe and Lys-Tyr are weak competitors: they form 10^4 times weaker complexes with **44** than dye **45**. It allows detection of micromolar concentrations of, for example, His-Ala in the presence of a 100-fold excess of Val-Phe in aqueous solution.[121] The pH sensitivity of the binding affinity of amino acids with assembly **44** has been used to develop a chemosensor array for the colorimetric identification of 20 natural amino acids in water (Chart 17).[122]
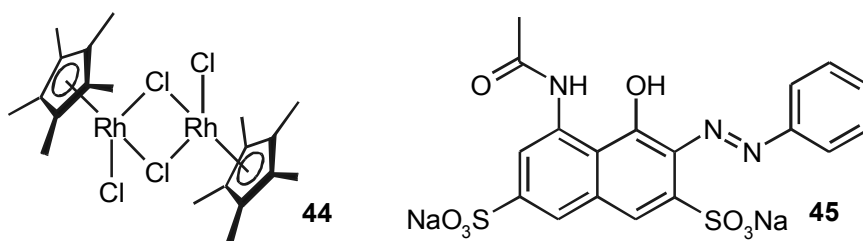
Chart 17

Macrocyclic complexes of type **46** (M = Ru, Rh and Ir, L = (un)substituted benzenes or cyclopentadienes, R = substituted aminomethanes) can be regarded as organometallic analogues of 12-crown-3. Similarly, they are able to bind lithium ions (Scheme 5), although with a much higher affinity (K_a-values are up to 5.8×10^4 M^{-1} in aqueous 100 mM phosphate buffer solution, pH = 7.0) and selectivity over sodium ($\sim 10^4$ times; complexation of K$^+$ or Cs$^+$ could not be detected at all).[119,120,123,124] Upon addition of Fe(III) salts, receptor **46** immediately decomposes to give a dark-brown solution from which a brown powder slowly precipitated. In the presence of lithium ions, when the more stable complex **47** is formed, this reaction is kinetically inhibited, and addition of FeCl$_3$ does not lead to immediate color change. This difference in reactivity allows "naked eye" detection of Li$^+$ in water in the pharmacologically relevant concentration range of 0.5 - 1.5 mM.[123] Complexes **46** also selectively extract Li$^+$ from an aqueous solution to the organic phase.[125]
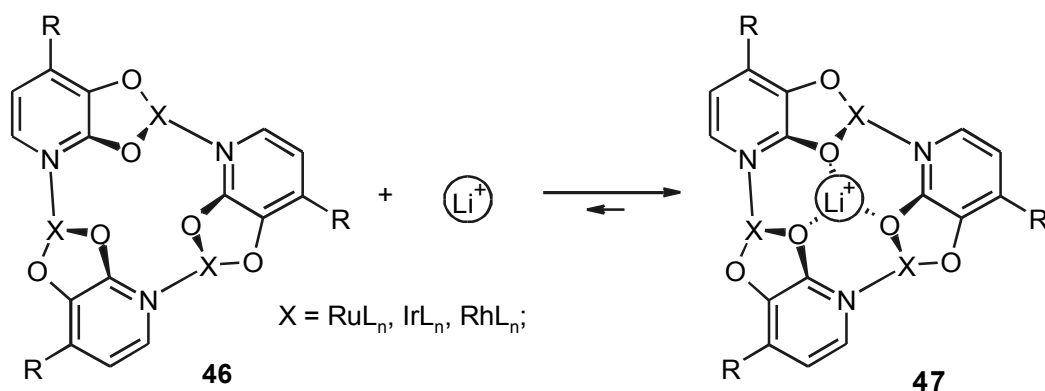
Scheme 5 Host-guest complex formation between the organometallic self-assembled receptor **46** and Li^+.

Anion recognition in water by metal-assembled bowl-shaped molecules that are structural analogues of calixarenes, such as metallacalix[n]arenes (n = 3, 4, 6), has been reported by the groups of Fujita,[126] Lippert,[127] and Navarro.[128,129] The metallacalix[n]arenes (for example Pd- or Pt-calix[3]arene **48**) are highly soluble in water and bind sulphate with a 1:1 stochiometry (apparent K_a sulphate/nitrate value of ~ 250 M^{-1});[126,127] a 1:3 stoichiometry has been observed in the case of acetate.[126] Metallacalixarenes also show preferential complex formation with adenosine 5'-monophosphate (K_a-value is up to 85 M^{-1})[129] compared with cytidine and thymidine 5'-monophosphates in aqueous (pH = 7.1) solution (Chart 18).[128,129]
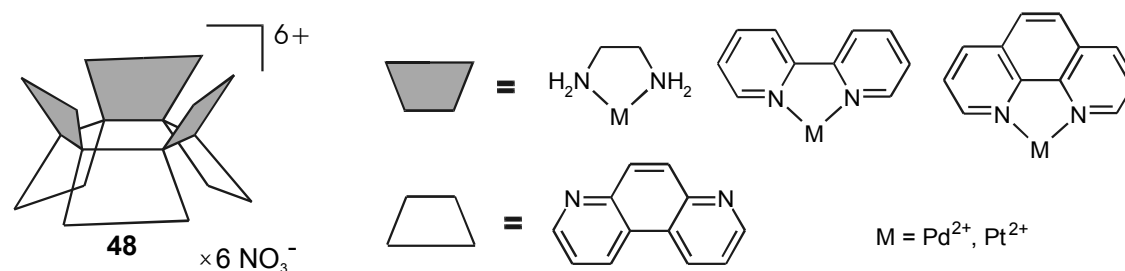
Chart 18

Fujita c.s. have reported water-soluble nanometer sized cages (for example, M_6L_4-type coordination cage **49** or organic pillared coordination cage **50**), obtained via self-assembly.[130,131] The cages have the ability to encapsulate large molecules or assemblies of molecules,[132] as well as to regulate or catalyse specific reactions in aqueous media. Depending on the size and the shape of the guests, in the case of the cage **49** three enclathration modes[133] have been observed: (i) 1:4 host-guest complexation with small ~ 6-8 Å guests like ferrocene,[134] *o*-carborane[133] or adamantane;[135] (ii) formation of 1:2 complexes with medium-sized, twisted or bended

guests like acenaphthylene,[136] diphenylmethane or 1,2-bis(4-methoxyphenyl)-1,2-ethanedione;[133,137] (iii) larger guests (tri-*tert*-butylbenzene, tetrabenzylsilane, substituted phenylsilanol trimers[137-139]) with dimensions > 8 Å give complexes with a 1:1 stoichiometry.[133] Two 1,4-naphthoquinones or two azulenes can also be encapsulated in **49**, but inclusion of the 1,4-naphthoquinone-azulene couple is preferential (so-called OR molecular recognition).[140] Perylene and *cis*-decaline can be accommodated into the cavity only together, and no complex formation was observed with either of these molecules alone (AND molecular recognition).[140] Cage **49** selectively recognizes tripeptides in water,[141] for example, the K_a-value with Ac-Trp-Trp-Ala-NH$_2$ is >10^6 M^{-1}, but no binding was observed with Ac-Trp-His-Ala-NH$_2$. Guests also template the architecture of organometallic nanostructures, such as prisms,[131,142] coordination nanotubes,[143] dimeric capsules,[144] boxes,[145] clipped aromatic sandwiches,[146] homoleptic or heteroleptic cages,[147] as well as tetragonal pyramidal or closed tetrahedron structures[148] in water or aqueous acetonitrile/DMF solution (Chart 19).
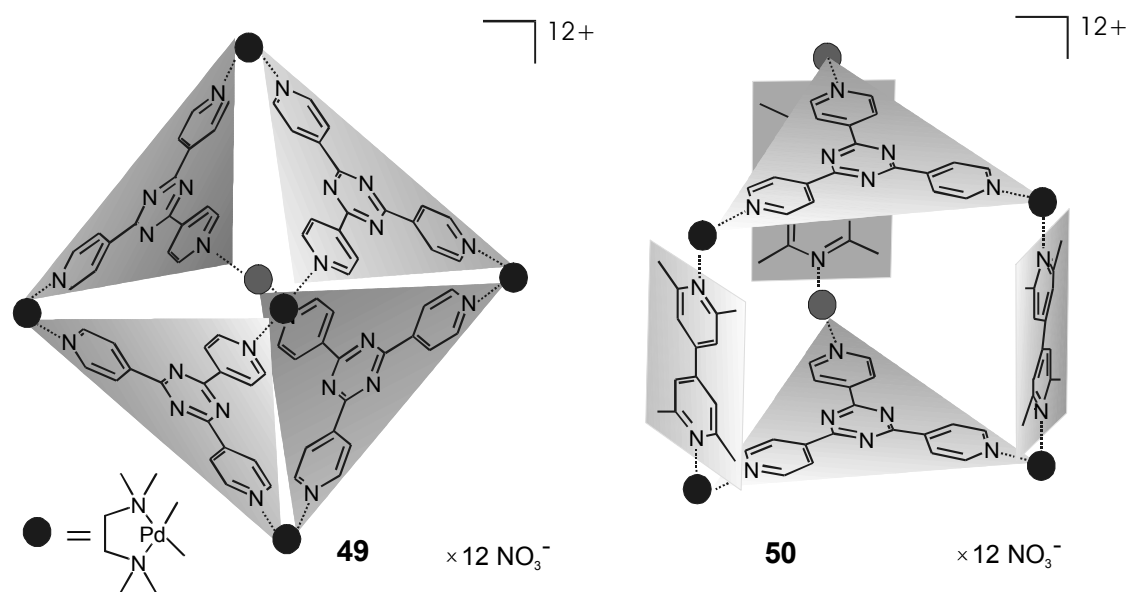
Chart 19

Within the hydrophobic cavity of cage **49**, an adamantanoid (H$_2$O)$_{10}$ cluster is formed,[149] which is termed "molecular ice", because its structure is the smallest unit of naturally occurring cubic (I$_c$-type) ice.[150] The molecular recognition by cage **49** is assumed to be entropy-driven, in which the binding of guests is compensated by the "melting" of the encapsulated molecular ice into free water molecules (Chart 19).[149]

Self-assembled cages act as molecular flasks to promote the intermolecular [2+2] photodimerization of large olefins in water in a very efficient fashion. Fujita c.s. reported the remarkably accelerated, highly stereoregulated [2+2] photodimerization of acenaphthylenes **51** within the coordination cage **49** exclusively giving *syn* isomer **52** (Scheme 6a) in aqueous medium.[136] Accommodation of two *different* olefin molecules in a pairwise selective fashion makes the selective [2 + 2] *cross*-photodimerization[151] possible or accelerates Diels-Alder reactions.[152] For example, substituted maleimide derivative **53** and dibenzosuberenone **54** undergo [2+2] cross-photodimerization to give **55** with *syn*-stereochemistry in quantitative yield (Scheme 6b).[151] The reactions are extremely efficient in terms of reaction rate, stereoselectivity, and, most importantly, pairwise selectivity. The key step of the exclusive formation of the cross-dimer begins with the selective formation of a ternary complex in water before irradiation, which is governed by the size compatibility of the guests with the restricted space of the cavity.[151] Cage **49** also efficiently promotes the photochemical oxidation of inert guests (like adamantane) in aqueous solution.[135]
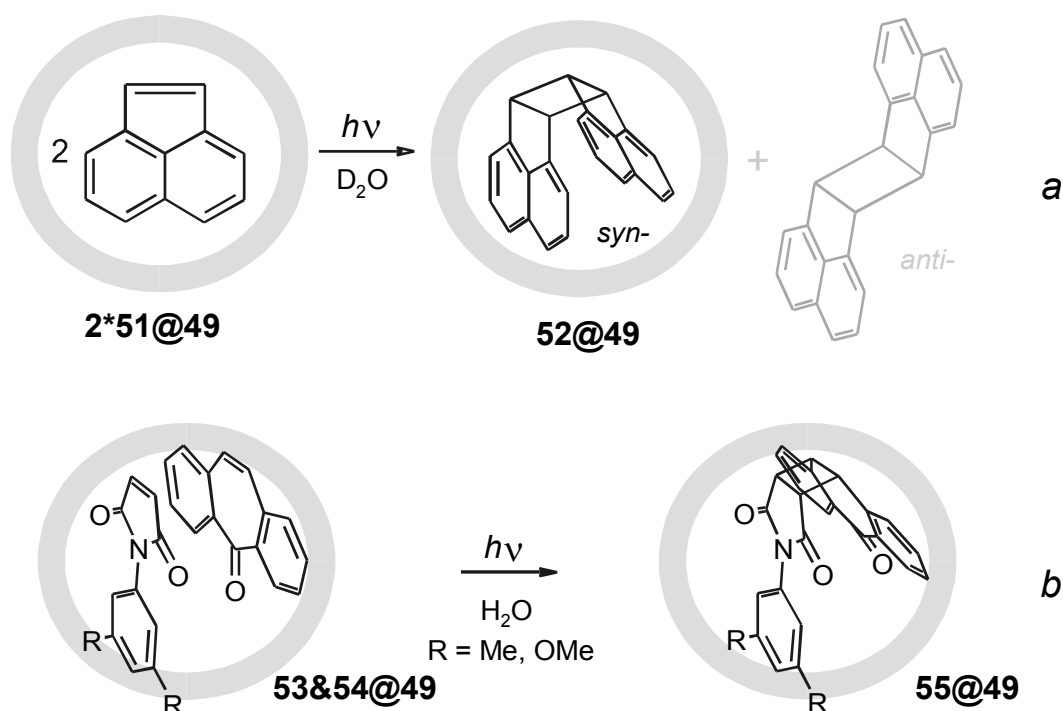
Scheme 6 Examples of [2+2] photodimerization of olefins within the self-assembled cage **49** (schematically depicted as a grey circle).

Cavity directed oligomerization of silanetriols **56** allowed the stereoselective preparation of the all-*cis* cyclic trimer **57** (Scheme 7a).[137-139] The enclathrated trimer is stable in water (at room temperature for about 1 month) and survives low pH (<1.0). However, without the cage the cyclic trimer **57** is a kinetic, short-lived compound that is rapidly converted into a thermodynamically favored cyclic tetramer and further condensed products.[138] Variation of the volume of the cavity of the self-assembled coordination cage allowed the isolation of stable enclathrated complexes of silanetriol **58** or silanol dimer **59**, which are otherwise very labile and cannot be isolated as a stable form in aqueous solution unless a stabilizing group or a sterically demanding group is attached.[139]
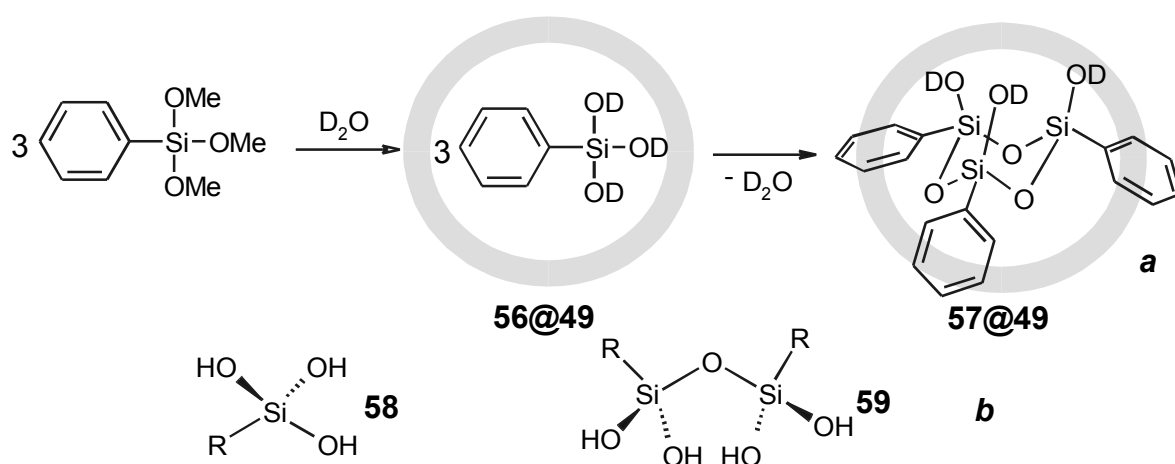
Scheme 7 a) Example of silanol formation within cage **49** (schematically depicted as a grey circle); b) Silanols prepared within the other coordination cages.

2.8 Conclusions and outlook

A variety of approaches have been used to design artificial receptors capable of selective binding of a number of guests in aqueous media. This has resulted in a wide range of water-soluble receptors based on different supramolecular scaffolds. Different host–guest interactions have been employed to stabilize the host-guest complexes in aqueous medium and varying degrees of preorganization have been used to overcome the competitive influence of water. Encapsulation of several guests allowed studying the interaction of these guests in the interior of a cage in aqueous solution. However, the role of the unique properties of water[150] in molecular recognition and self-assembly has not been completely understood, and strong

receptors for many organic guests have not been found yet. Therefore, a substantial growth of the research in the area of supramolecular chemistry in water is expected.

This thesis contributes to understanding the influence of water on molecular recognition and self-assembly driven by electrostatic interactions. Anion recognition by (thio)urea functionalized cavitands in aqueous media and the effect of saccharide substituents on the solubility of the cavitand receptors in water are described in Chapters 3 and 4. The second part of the thesis deals with the development and complexation behaviour of a new type of capsules based on 'triple ion' and electrostatic interactions.

References

1.   *Functional Synthetic Receptors;* Schrader, T.; Hamilton, A. D., Eds.; Wiley-VCH: Weinheim, 2005; p 440.
2.   Ariga, K.; Kunitake, T., *Supramolecular Chemistry - Fundamentals and Applications;* Springer: Berlin, 2005; p 200.
3.   *Highlights in Bioorganic Chemistry: Methods and Applications;* Schmuck, C.; Wennemers, H., Eds.; Wiley-VCH: Weinheim, 2004; p 600.
4.   Hartley, J. H.; James, T. D.; Ward, C. J. *J. Chem. Soc., Perkin Trans. 1* **2000**, 3155-3184; Fitzmaurice, R. J.; Kyne, G. M.; Douheret, D.; Kilburn, J. D. *J. Chem. Soc., Perkin Trans. 1* **2002**, 841-864.
5.   Vriezema, D. M.; Aragones, M. C.; Elemans, J.; Cornelissen, J.; Rowan, A. E.; Nolte, R. J. M. *Chem. Rev.* **2005**, *105*, 1445-1489.
6.   For recent reviews see: Chankvetadze, B. *Chem. Soc. Rev.* **2004**, *33*, 337-347; Douhal, A. *Chem. Rev.* **2004**, *104*, 1955-1976; Engeldinger, E.; Armspach, D.; Matt, D. *Chem. Rev.* **2003**, *103*, 4147-4173; Monti, S.; Sortino, S. *Chem. Soc. Rev.* **2002**, *31*, 287-300; Harada, A. *Acc. Chem. Res.* **2001**, *34*, 456-464; Shpigun, O. A.; Ananieva, I. A.; Budanova, N. Y.; Shapovalova, E. N. *Usp. Khim.* **2003**, *72*, 1167-1189 (Engl. Transl.: *Russ. Chem. Rev.* **2003**, 1035).
7.   For recent reviews see: Gokel, G. W.; Leevy, W. M.; Weber, M. E. *Chem. Rev.* **2004**, *104*, 2723-2750; Nesterov, S. V. *Usp. Khim.* **2000**, *69*, 840-855 (Engl. Transl.: *Russ. Chem. Rev.* **2000**, 769).
8.   Schmuck, C.; Geiger, L. *Curr. Org. Chem.* **2003**, *7*, 1485-1502.
9.   Schmuck, C.; Machon, U. *Chem. Eur. J.* **2005**, *11*, 1109-1118.
10.   Schmuck, C. *Chem. Eur. J.* **2000**, *6*, 709-718.
11.   Schmuck, C.; Bickert, V. *Org. Lett.* **2003**, *5*, 4579-4581.
12.   Schmuck, C.; Geiger, L. *J. Am. Chem. Soc.* **2004**, *126*, 8898-8899.
13.   Schmuck, C.; Heil, M. *ChemBioChem* **2003**, *4*, 1232-1238.
14.   Rzepecki, P.; Schrader, T. *J. Am. Chem. Soc.* **2005**, *127*, 3016-3025.
15.   Rzepecki, P.; Gallmeier, H.; Geib, N.; Cernovska, K.; Konig, B.; Schrader, T. *J. Org. Chem.* **2004**, *69*, 5168-5178.
16.   James, T. D.; Shinkai, S., Artificial receptors as chemosensors for carbohydrates. In *Topics in Current Chemistry. Host-Guest Chemistry*, 2002; Vol. 218, pp 159-200 and references cited therein.

17. Wang, W.; Gao, X. M.; Wang, B. H. *Curr. Org. Chem.* **2002**, *6*, 1285-1317; Striegler, S. *Curr. Org. Chem.* **2003**, *7*, 81-102; Hirata, O.; Kubo, Y.; Takeuchi, M.; Shinkai, S. *Tetrahedron* **2004**, *60*, 11211.

18. Gao, X. M.; Zhang, Y. L.; Wang, B. H. *New J. Chem.* **2005**, *29*, 579-586; Cao, H. S.; Heagy, M. D. *J. Fluoresc.* **2004**, *14*, 569-584; Fang, H.; Kaur, G.; Wang, B. H. *J. Fluoresc.* **2004**, *14*, 481-489; Sato, K.; Sone, A.; Arai, S.; Yamagishi, T. *Heterocycles* **2003**, *61*, 31-38; Kanekiyo, Y.; Tao, H. *Chem. Lett.* **2005**, *34*, 196-197.

19. Bosch, L. I.; Fyles, T. M.; James, T. D. *Tetrahedron* **2004**, *60*, 11175.

20. Ni, W. J.; Kaur, G.; Springsteen, G.; Wang, B. H.; Franzen, S. *Bioorg. Chem.* **2004**, *32*, 571-581; Wiskur, S. L.; Lavigne, J. J.; Ait-Haddou, H.; Lynch, V.; Chiu, Y. H.; Canary, J. W.; Anslyn, E. V. *Org. Lett.* **2001**, *3*, 1311-1314; Yan, J.; Springsteen, G.; Deeter, S.; Wang, B. *Tetrahedron* **2004**, *60*, 11205; Bosch, L. I.; Mahon, M. F.; James, T. D. *Tetrahedron Lett.* **2004**, *45*, 2859-2862; Mulla, H. R.; Agard, N. J.; Basu, A. *Bioorg. Med. Chem. Lett.* **2004**, *14*, 25-27; Franzen, S.; Ni, W. J.; Wang, B. H. *J. Phys. Chem. B* **2003**, *107*, 12942-12948; DiCesare, N.; Adhikari, D. P.; Heynekamp, J. J.; Heagy, M. D.; Lakowicz, J. R. *J. Fluoresc.* **2002**, *12*, 147-154.

21. Zhu, L.; Zhong, Z. L.; Anslyn, E. V. *J. Am. Chem. Soc.* **2005**, *127*, 4260-4269.

22. Zhu, L.; Anslyn, E. V. *J. Am. Chem. Soc.* **2004**, *126*, 3676-3677.

23. Zhao, J. Z.; Davidson, M. G.; Mahon, M. F.; Kociok-Kohn, G.; James, T. D. *J. Am. Chem. Soc.* **2004**, *126*, 16179-16186.

24. Phillips, M. D.; James, T. D. *J. Fluoresc.* **2004**, *14*, 549-559; Zhao, J. Z.; Fyles, T. M.; James, T. D. *Angew. Chem., Int. Ed.* **2004**, *43*, 3461-3464; Arimori, S.; Phillips, M. D.; James, T. D. *Tetrahedron Lett.* **2004**, *45*, 1539-1542; Arimori, S.; Bell, M. L.; Oh, C. S.; Frimat, K. A.; James, T. D. *J. Chem. Soc., Perkin Trans. 1* **2002**, 803-808; Arimori, S.; Consiglio, G. A.; Phillips, M. D.; James, T. D. *Tetrahedron Lett.* **2003**, *44*, 4789-4792; Arimori, S.; Bell, M. L.; Oh, C. S.; James, T. D. *Org. Lett.* **2002**, *4*, 4249-4251.

25. Arimori, S.; Ushiroda, S.; Peter, L. M.; Jenkins, A. T. A.; James, T. D. *Chem. Commun.* **2002**, 2368-2369.

26. Atilgan, S.; Akkaya, E. U. *Tetrahedron Lett.* **2004**, *45*, 9269-9271.

27. Gawley, R. E.; Pinet, S.; Cardona, C. M.; Datta, P. K.; Ren, T.; Guida, W. C.; Nydick, J.; Leblanc, R. M. *J. Am. Chem. Soc.* **2002**, *124*, 13448-13453.

28. Tobey, S. L.; Jones, B. D.; Anslyn, E. V. *J. Am. Chem. Soc.* **2003**, *125*, 4026-4027; Tobey, S. L.; Anslyn, E. V. *J. Am. Chem. Soc.* **2003**, *125*, 14807-14815; Zhang, T. Z.; Anslyn, E. V. *Tetrahedron* **2004**, *60*, 11117-11124.

29. Tobey, S. L.; Anslyn, E. V. *Org. Lett.* **2003**, *5*, 2029-2031.

30. Tobey, S. L.; Anslyn, E. V. *J. Am. Chem. Soc.* **2003**, *125*, 10963-10970.

31. Hennrich, G.; Anslyn, E. V. *Chem. Eur. J.* **2002**, *8*, 2218-2224; Niikura, K.; Anslyn, E. V. *J. Org. Chem.* **2003**, *68*, 10156-10157; Schneider, S. E.; O'Neil, S. N.; Anslyn, E. V. *J. Am. Chem. Soc.* **2000**, *122*, 542-543.

32. Wiskur, S. L.; Lavigne, J. L.; Metzger, A.; Tobey, S. L.; Lynch, V.; Anslyn, E. V. *Chem. Eur. J.* **2004**, *10*, 3792-3804.

33. Wiskur, S. L.; Floriano, P. N.; Anslyn, E. V.; McDevitt, J. T. *Angew. Chem., Int. Ed.* **2003**, *42*, 2070-2072.

34. Rekharsky, M.; Inoue, Y.; Tobey, S.; Metzger, A.; Anslyn, E. *J. Am. Chem. Soc.* **2002**, *124*, 14959-14967.

35. Schmuck, C.; Schwegmann, M. *J. Am. Chem. Soc.* **2005**, *127*, 3373-3379.

36. Zhong, Z. L.; Anslyn, E. V. *Angew. Chem., Int. Ed.* **2003**, *42*, 3005-3008.

37. Raker, J.; Glass, T. E. *J. Org. Chem.* **2002**, *67*, 6113-6116.
38. Thilgen, C.; Azov, V. A., *Cyclophanes: Definition and Scope.* In *Encyclopedia of Supramolecular Chemistry;* Atwood, J. L.; Steed, J. W., Eds.; Marcel Dekker, Inc.: New York, 2004; pp 414-423; Nishimura, J.; Nakamura, Y.; Hayashida, Y.; Kudo, T. *Acc. Chem. Res.* **2000**, *33*, 679-686.
39. Piantanida, I.; Palm, B. S.; Cudic, P.; Zinic, M.; Schneider, H. J. *Tetrahedron* **2004**, *60*, 6225-6231.
40. Piantanida, N.; Palm, B. S.; Cudic, P.; Zinic, M.; Schneider, H. J. *Tetrahedron Lett.* **2001**, *42*, 6779-6783.
41. Hodacova, J.; Chadim, M.; Zavada, J.; Aguilar, J.; Garcia-Espana, E.; Luis, S. V.; Miravet, J. F. *J. Org. Chem.* **2005**, *70*, 2042-2047.
42. Williamson, D. A.; Barenberg, A. M.; Coleman, C. A.; Benson, D. R. *Chemosphere* **2000**, *40*, 1443-1446.
43. Virues, C.; Velaquez, E. F.; Inoue, M. B.; Inoue, M. *J. Incl. Phenom. Macrocycl. Chem.* **2004**, *48*, 141-146.
44. Hayashida, O.; Hamachi, I. *J. Org. Chem.* **2004**, *69*, 3509-3516; Hayashida, O.; Hamachi, I. *Chem. Lett.* **2003**, *32*, 288-289; Hayashida, O.; Hamachi, I. *Chem. Lett.* **2004**, *33*, 548-549; Hayashida, O.; Hamachi, I. *Chem. Lett.* **2003**, *32*, 632-633.
45. Lara, K. O.; Godoy-Alcantar, C.; Eliseev, A. V.; Yatsimirsky, A. K. *Org. Biomol. Chem.* **2004**, *2*, 1712-1718; Lara, K. O.; Godoy-Alcantar, C.; Rivera, I. L.; Eliseev, A. V.; Yatsimirsky, A. K. *J. Phys. Org. Chem.* **2001**, *14*, 453-462.
46. Molt, O.; Rubeling, D.; Schafer, G.; Schrader, T. *Chem. Eur. J.* **2004**, *10*, 4225-4232.
47. Herm, M.; Molt, O.; Schrader, T. *Chem. Eur. J.* **2002**, *8*, 1485-1499; Herm, M.; Molt, O.; Schrader, T. *Angew. Chem., Int. Ed.* **2001**, *40*, 3148-3151.
48. Finocchiaro, P.; Failla, S.; Consiglio, G. A.; Wehner, M.; Grawe, T.; Schrader, T. *Phosphorus, Sulfur, Silicon Relat. Elem.* **2002**, *177*, 1633-1636; Herm, M.; Schrader, T. *Chem. Eur. J.* **2000**, *6*, 47-53.
49. Abe, H.; Mawatari, Y.; Teraoka, H.; Fujimoto, K.; Inouye, M. *J. Org. Chem.* **2004**, *69*, 495-504.
50. Otto, S.; Furlan, R. L. E.; Sanders, J. K. M. *J. Am. Chem. Soc.* **2000**, *122*, 12063-12064.
51. Otto, S.; Furlan, R. L. E.; Sanders, J. K. M. *Science* **2002**, *297*, 590-593.
52. Otto, S.; Furlan, R. L. E.; Sanders, J. K. M. *Curr. Opin. Chem. Biol.* **2002**, *6*, 321-327.
53. Agrawal, Y. K.; Bhatt, H. *Bioinorg. Chem. Appl.* **2004**, *2*, 237-274.
54. Ludwig, R.; Dzung, N. T. K. *Sensors* **2002**, *2*, 397-416.
55. Casnati, A.; Sciotto, D.; Arena, G., *Water soluble calixarenes.* In *Calixarenes 2001;* Asfari, Z.; Böhmer, V.; Harrowfield, J.; Vicens, J., Eds.; Kluwer: Dordrecht, 2001; pp 440-456.
56. Kunsagi-Mate, S.; Szabo, K.; Lemli, B.; Bitter, I.; Nagy, G.; Kollar, L. *Thermochimica Acta* **2005**, *425*, 121-126.
57. Dudic, M.; Colombo, A.; Sansone, F.; Casnati, A.; Donofrio, G.; Ungaro, R. *Tetrahedron* **2004**, *60*, 11613-11618.
58. Casnati, A.; Sansone, F.; Ungaro, R. *Acc. Chem. Res.* **2003**, *36*, 246-254.
59. Fulton, D. A.; Stoddart, J. F. *Bioconjugate Chem.* **2001**, *12*, 655-672; Sansone, F.; Chierici, E.; Casnati, A.; Ungaro, R. *Org. Biomol. Chem.* **2003**, *1*, 1802-1809.

60.   Da Silva, E.; Lazar, A. N.; Coleman, A. W. *J. Drug Deliv. Sci. Tech.* **2004**, *14*, 3-20.

61.   Arena, G.; Contino, A.; Gulino, F. G.; Magri, A.; Sciotto, D.; Ungaro, R. *Tetrahedron Lett.* **2000**, *41*, 9327-9330.

62.   Baur, M.; Frank, M.; Schatz, J.; Schildbach, F. *Tetrahedron* **2001**, *57*, 6985-6991.

63.   Kon, N.; Ki, N.; Miyano, S. *Org. Biomol. Chem.* **2003**, *1*, 751-755.

64.   Liu, Y.; Guo, D. S.; Yang, E. C.; Zhang, H. Y.; Zhao, Y. L. *Eur. J. Org. Chem.* **2005**, 162-170.

65.   Arena, G.; Gentile, S.; Gulino, F. G.; Sciotto, D.; Sgarlata, C. *Tetrahedron Lett.* **2004**, *45*, 7091-7094.

66.   Arena, G.; Casnati, A.; Contino, A.; Gulino, F. G.; Sciotto, D.; Ungaro, R. *J. Chem. Soc., Perkin Trans. 2* **2000**, 419-423.

67.   Arena, G.; Contino, A.; Fujimoto, T.; Sciotto, D.; Aoyama, Y. *Supramol. Chem.* **2000**, *11*, 279-288.

68.   Kunsagi-Mate, S.; Szabo, K.; Bitter, I.; Nagy, G.; Kollar, L. *Tetrahedron Lett.* **2004**, *45*, 1387-1390.

69.   Da Silva, E.; Shahgaldian, P.; Coleman, A. W. *Int. J. Pharm.* **2004**, *273*, 57-62; Da Silva, E.; Lazar, A.; Coleman, A. W. *Stp Pharma Sciences* **2004**, *14*, 3-20.

70.   Tairov, M. A.; Vysotsky, M. O.; Kalchenko, O. I.; Pirozhenko, V. V.; Kalchenko, V. I. *J. Chem. Soc., Perkin Trans. 1* **2002**, 1405-1411.

71.   Shahgaldian, P.; Coleman, A. W.; Kalchenko, V. I. *Tetrahedron Lett.* **2001**, *42*, 577-579.

72.   Zadmard, R.; Schrader, T.; Grawe, T.; Kraft, A. *Org. Lett.* **2002**, *4*, 1687-1690.

73.   Witt, D.; Dziemidowicz, J.; Rachon, J. *Heteroatom Chem.* **2004**, *15*, 155-161.

74.   Islam, S. D. M.; Fujitsuka, M.; Ito, O.; Ikeda, A.; Hatano, T.; Shinkai, S. *Chem. Lett.* **2000**, 78-79.

75.   Botta, B.; Cassani, M.; D'Acquarica, I.; Misiti, D.; Subissati, D.; Delle Monache, G. *Curr. Org. Chem.* **2005**, *9*, 337-355; Gibb, B. C. *Chem. Eur. J.* **2003**, *9*, 5180-5187.

76.   Aoyama, Y. *Chem. Eur. J.* **2004**, *10*, 588-593.

77.   Aoyama, Y.; Kanamori, T.; Nakai, T.; Sasaki, T.; Horiuchi, S.; Sando, S.; Niidome, T. *J. Am. Chem. Soc.* **2003**, *125*, 3455-3457; Hayashida, O.; Mizuki, K.; Akagi, K.; Matsuo, A.; Kanamori, T.; Nakai, T.; Sando, S.; Aoyama, Y. *J. Am. Chem. Soc.* **2003**, *125*, 594-601; Nakai, T.; Kanamori, T.; Sando, S.; Aoyama, Y. *J. Am. Chem. Soc.* **2003**, *125*, 8465-8475.

78.   Kazakova, E. H.; Ziganshina, A. U.; Muslinkina, L. A.; Morozova, J. E.; Makarova, N. A.; Mustafina, A. R.; Habicher, W. D. *J. Incl. Phenom. Macrocycl. Chem.* **2002**, *43*, 65-69.

79.   Mustafina, A. R.; Fedorenko, S. V.; Makarova, N. A.; Kazakova, E. K.; Bazhanova, Z. G.; Kataev, V. E.; Konovalov, A. I. *J. Incl. Phenom. Macrocycl. Chem.* **2001**, *40*, 73-76; Amirov, R. R.; Mustafina, A. R.; Nugaeva, Z. T.; Fedorenko, S. V.; Kazakova, E. K.; Konovalov, A. I.; Habicher, W. D. *J. Incl. Phenom. Macrocycl. Chem.* **2004**, *49*, 203-209.

80.   Mustafina, A. R.; Skripacheva, V. V.; Kazakova, E. K.; Markarova, N. A.; Kataev, V. E.; Ermolaeva, L. V.; Habicher, W. D. *J. Incl. Phenom. Macrocycl. Chem.* **2002**, *42*, 77-81.

81.   Amirov, R. R.; Nugaeva, Z. T.; Mustafina, A. R.; Fedorenko, S. V.; Morozov, V. I.; Kazakova, E. K.; Habicher, W. D.; Konovalov, A. I. *Colloid Surface A*

2004, *240*, 35-43; Mustafina, A. R.; Amirov, R. R.; Elistratova, Y. G.; Skripacheva, V. V.; Nugaeva, Z. T.; Kazakova, E. K. *Colloid J.* **2002**, *64*, 734-739.

82. Verboom, W., *Cavitands.* In *Calixarenes 2001;* Asfari, Z.; Böhmer, V.; Harrowfield, J.; Vicens, J., Eds.; Kluwer: Dordrecht, 2001; pp 181-198.

83. Gui, X.; Sherman, J. C. *Chem. Commun.* **2001**, 2680-2681.

84. Middel, O. Cavitand and calixarene modules for capsules and water-soluble receptors. University of Twente, Enschede, The Netherlands, 2002.

85. Middel, O.; Verboom, W.; Reinhoudt, D. N. *Eur. J. Org. Chem.* **2002**, 2587-2597.

86. Ihm, C.; In, Y.; Park, Y.; Paek, K. *Org. Lett.* **2004**, *6*, 369-372.

87. Sebo, L.; Diederich, F.; Gramlich, V. *Helv. Chim. Acta* **2000**, *83*, 93-113.

88. Trembleau, L.; Rebek, J. *Science* **2003**, *301*, 1219-1220.

89. Biros, S. M.; Ullrich, E. C.; Hof, F.; Trembleau, L.; Rebek, J. *J. Am. Chem. Soc.* **2004**, *126*, 2870-2876.

90. Hof, F.; Trembleau, L.; Ullrich, E. C.; Rebek, J. *Angew. Chem., Int. Ed.* **2003**, *42*, 3150-3153.

91. Trembleau, L.; Rebek, J. *Chem. Commun.* **2004**, 58-59.

92. Haino, T.; Rudkevich, D. M.; Shivanyuk, A.; Rissanen, K.; Rebek, J. *Chem. Eur. J.* **2000**, *6*, 3797-3805.

93. Ballester, P.; Shivanyuk, A.; Far, A. R.; Rebek, J. *J. Am. Chem. Soc.* **2002**, *124*, 14014-14016.

94. Liu, S. M.; Wu, C. T. *Progress in Chem.* **2005**, *17*, 143-150.

95. Lee, J. W.; Samal, S.; Selvapalam, N.; Kim, H. J.; Kim, K. *Acc. Chem. Res.* **2003**, *36*, 621-630.

96. Kim, K.; Selvapalam, N.; Oh, D. H. *J. Incl. Phenom. Macrocycl. Chem.* **2004**, *50*, 31-36; Gerasko, O. A.; Samsonenko, D. G.; Fedin, V. P. *Usp. Khim.* **2002**, *71*, 840-861; Kim, K. *Chem. Soc. Rev.* **2002**, *31*, 96-107.

97. Zhang, X. X.; Krakowiak, K. E.; Xue, G. P.; Bradshaw, J. S.; Izatt, R. M. *Ind. Eng. Chem. Res.* **2000**, *39*, 3516-3520; Zhao, J. Z.; Kim, H. J.; Oh, J.; Kim, S. Y.; Lee, J. W.; Sakamoto, S.; Yamaguchi, K.; Kim, K. *Angew. Chem., Int. Ed.* **2001**, *40*, 4233-4235.

98. Marquez, C.; Hudgins, R. R.; Nau, W. M. *J. Am. Chem. Soc.* **2004**, *126*, 5806-5816.

99. El Haouaj, M.; Ko, Y. H.; Luhmer, M.; Kim, K.; Bartik, K. *J. Chem. Soc., Perkin Trans. 2* **2001**, 2104-2107; El Haouaj, M.; Luhmer, M.; Ko, Y. H.; Kim, K.; Bartik, K. *J. Chem. Soc., Perkin Trans. 2* **2001**, 804-807.

100. Ong, W.; Kaifer, A. E. *Angew. Chem., Int. Ed.* **2003**, *42*, 2164-2167; Ong, W.; Gomez-Kaifer, M.; Kaifer, A. E. *Org. Lett.* **2002**, *4*, 1791-1794; Kim, H. J.; Jeon, W. S.; Ko, Y. H.; Kim, K. *Proc. Natl. Acad. Sci. U. S. A.* **2002**, *99*, 5007-5011.

101. Moon, K.; Kaifer, A. E. *Org. Lett.* **2004**, *6*, 185-188.

102. Ong, W.; Kaifer, A. E. *J. Org. Chem.* **2004**, *69*, 1383-1385.

103. Ong, W.; Kaifer, A. E. *Organometallics* **2003**, *22*, 4181-4183.

104. Jeon, W. S.; Kim, H. J.; Lee, C.; Kim, K. *Chem. Commun.* **2002**, 1828-1829.

105. Jeon, W. S.; Kim, E.; Ko, Y. H.; Hwang, I. H.; Lee, J. W.; Kim, S. Y.; Kim, H. J.; Kim, K. *Angew. Chem., Int. Ed.* **2005**, *44*, 87-91.

106. Miyahara, Y.; Goto, K.; Oka, M.; Inazu, T. *Angew. Chem., Int. Ed.* **2004**, *43*, 5019-5022.

107. Buschmann, H. J.; Cleve, E.; Schollmeyer, E. *Inorg. Chem. Commun.* **2005**, *8*, 125-127.

108. Whitesides, G. M.; Grzybowski, B. *Science* **2002**, *295*, 2418-2421.

109. Corbellini, F.; Di Costanzo, L.; Crego-Calama, M.; Geremia, S.; Reinhoudt, D. N. *J. Am. Chem. Soc.* **2003**, *125*, 9946-9947.

110. Corbellini, F.; Fiammengo, R.; Timmerman, P.; Crego-Calama, M.; Versluis, K.; Heck, A. J. R.; Luyten, I.; Reinhoudt, D. N. *J. Am. Chem. Soc.* **2002**, *124*, 6569-6575.

111. Corbellini, F.; Knegtel, R. M. A.; Grootenhuis, P. D. J.; Crego-Calama, M.; Reinhoudt, D. N. *Chem. Eur. J.* **2004**, *11*, 298-307.

112. Corbellini, F.; van Leeuwen, F. W. B.; Beijleveld, H.; Kooijman, H.; Spek, A. L.; Verboom, W.; Crego-Calama, M.; Reinhoudt, D. N. *New J. Chem.* **2005**, *29*, 243-248.

113. Grawe, T.; Schrader, T.; Zadmard, R.; Kraft, A. *J. Org. Chem.* **2002**, *67*, 3755-3763.

114. Fiammengo, R.; Timmerman, P.; Huskens, J.; Versluis, K.; Heck, A. J. R.; Reinhoudt, D. N. *Tetrahedron* **2002**, *58*, 757-764; Fiammengo, R.; Timmerman, P.; de Jong, F.; Reinhoudt, D. N. *Chem. Commun.* **2000**, 2313-2314.

115. Zadmard, R.; Schrader, T. *J. Am. Chem. Soc.* **2005**, *127*, 904-915.

116. Zadmard, R.; Junkers, M.; Schrader, T.; Grawe, T.; Kraft, A. *J. Org. Chem.* **2003**, *68*, 6511-6521.

117. Grawe, T.; Schrader, T.; Gurrath, M.; Kraft, A.; Osterod, F. *Org. Lett.* **2000**, *2*, 29-32.

118. Rebek, J. *Angew. Chem., Int. Ed.* **2005**, *44*, 2068-2078.

119. Severin, K. *Chimia* **2004**, *58*, 181-185.

120. Severin, K. *Coord. Chem. Rev.* **2003**, *245*, 3-10.

121. Buryak, A.; Severin, K. *Angew. Chem., Int. Ed.* **2004**, *43*, 4771-4774.

122. Buryak, A.; Severin, K. *J. Am. Chem. Soc.* **2005**, *127*, 3700-3701.

123. Grote, Z.; Scopelliti, R.; Severin, K. *J. Am. Chem. Soc.* **2004**, *126*, 16959-16972.

124. Grote, Z.; Lehaire, M. L.; Scopelliti, R.; Severin, K. *J. Am. Chem. Soc.* **2003**, *125*, 13638-13639; Lehaire, M. L.; Schulz, A.; Scopelliti, R.; Severin, K. *Inorg. Chem.* **2003**, *42*, 3576-3581.

125. Piotrowski, H.; Severin, K. *Proc. Natl. Acad. Sci. U. S. A.* **2002**, *99*, 4997-5000; Piotrowski, H.; Hilt, G.; Schulz, A.; Mayer, P.; Polborn, K.; Severin, K. *Chem. Eur. J.* **2001**, *7*, 3196-3208; Piotrowski, H.; Polborn, K.; Hilt, G.; Severin, K. *J. Am. Chem. Soc.* **2001**, *123*, 2699-2700.

126. Yu, S. Y.; Huang, H.; Liu, H. B.; Chen, Z. N.; Zhang, R. B.; Fujita, M. *Angew. Chem., Int. Ed.* **2003**, *42*, 686-690.

127. Schnebeck, R. D.; Freisinger, E.; Glahe, F.; Lippert, B. *J. Am. Chem. Soc.* **2000**, *122*, 1381-1390.

128. Galindo, M. A.; Galli, S.; Navarro, J. A. R.; Romero, M. A. *Dalton Trans.* **2004**, 2780-2785; Barea, E.; Navarro, J. A. R.; Salas, J. M.; Quiros, M.; Willermann, M.; Lippert, B. *Chem. Eur. J.* **2003**, *9*, 4414-4421.

129. Galindo, M. A.; Navarro, J. A. R.; Romero, M. A.; Quiros, M. *Dalton Trans.* **2004**, 1563-1566.

130. Fujita, M.; Tominaga, M.; Hori, A.; Therrien, B.; *Acc. Chem. Res.* **2005**, *38*, 369-378.

131. Yoshizawa, M.; Nakagawa, J.; Kumazawa, K.; Nagao, M.; Kawano, M.; Ozeki, T.; Fujita, M. *Angew. Chem., Int. Ed.* **2005**, *44*, 1810-1813.
132. Umemoto, K.; Tsukui, H.; Kusukawa, T.; Biradha, K.; Fujita, M. *Angew. Chem., Int. Ed.* **2001**, *40*, 2620-2622; Nakabayashi, K.; Kawano, M.; Yoshizawa, M.; Ohkoshi, S.; Fujita, M. *J. Am. Chem. Soc.* **2004**, *126*, 16694-16695.
133. Kusukawa, T.; Fujita, M. *J. Am. Chem. Soc.* **2002**, *124*, 13576-13582.
134. Sun, W. Y.; Kusukawa, T.; Fujita, M. *J. Am. Chem. Soc.* **2002**, *124*, 11570-11571.
135. Yoshizawa, M.; Miyagi, S.; Kawano, M.; Ishiguro, K.; Fujita, M. *J. Am. Chem. Soc.* **2004**, *126*, 9172-9173.
136. Yoshizawa, M.; Takeyama, Y.; Kusukawa, T.; Fujita, M. *Angew. Chem., Int. Ed.* **2002**, *41*, 1347-1349.
137. Kusukawa, T.; Yoshizawa, M.; Fujita, M. *Angew. Chem., Int. Ed.* **2001**, *40*, 1879-1884.
138. Yoshizawa, M.; Kusukawa, T.; Fujita, M.; Yamaguchi, K. *J. Am. Chem. Soc.* **2000**, *122*, 6311-6312.
139. Yoshizawa, M.; Kusukawa, T.; Fujita, M.; Sakamoto, S.; Yamaguchi, K. *J. Am. Chem. Soc.* **2001**, *123*, 10454-10459.
140. Yoshizawa, M.; Tamura, M.; Fujita, M. *J. Am. Chem. Soc.* **2004**, *126*, 6846-6847.
141. Tashiro, S.; Tominaga, M.; Kawano, M.; Therrien, B.; Ozeki, T.; Fujita, M. *J. Am. Chem. Soc.* **2005**, *127*, 4546-4547.
142. Fujita, N.; Biradha, K.; Fujita, M.; Sakamoto, S.; Yamaguchi, K. *Angew. Chem., Int. Ed.* **2001**, *40*, 1718-1721; Kumazawa, K.; Biradha, K.; Kusukawa, T.; Okano, T.; Fujita, M. *Angew. Chem., Int. Ed.* **2003**, *42*, 3909-3913.
143. Yamaguchi, T.; Tashiro, S.; Tominaga, M.; Kawano, M.; Ozeki, T.; Fujita, M. *J. Am. Chem. Soc.* **2004**, *126*, 10818-10819; Tashiro, S.; Tominaga, M.; Kusukawa, T.; Kawano, M.; Sakamoto, S.; Yamaguchi, K.; Fujita, M. *Angew. Chem., Int. Ed.* **2003**, *42*, 3267-3270.
144. Yu, S. Y.; Kusukawa, T.; Biradha, K.; Fujita, M. *J. Am. Chem. Soc.* **2000**, *122*, 2665-2666.
145. Yamanoi, Y.; Sakamoto, Y.; Kusukawa, T.; Fujita, M.; Sakamoto, S.; Yamaguchi, K. *J. Am. Chem. Soc.* **2001**, *123*, 980-981.
146. Kumazawa, K.; Yamanoi, Y.; Yoshizawa, M.; Kusukawa, T.; Fujita, M. *Angew. Chem., Int. Ed.* **2004**, *43*, 5936-5940.
147. Hiraoka, S.; Kubota, Y.; Fujita, M. *Chem. Commun.* **2000**, 1509-1510.
148. Umemoto, K.; Yamaguchi, K.; Fujita, M. *J. Am. Chem. Soc.* **2000**, *122*, 7150-7151.
149. Yoshizawa, M.; Kusukawa, T.; Kawano, M.; Ohhara, T.; Tanaka, I.; Kurihara, K.; Niimura, N.; Fujita, M. *J. Am. Chem. Soc.* **2005**, *127*, 2798-2799.
150. Ludwig, R. *Angew. Chem., Int. Ed.* **2001**, *40*, 1809-1827.
151. Yoshizawa, M.; Takeyama, Y.; Okano, T.; Fujita, M. *J. Am. Chem. Soc.* **2003**, *125*, 3243-3247.
152. Kusukawa, T.; Nakai, T.; Okano, T.; Fujita, M. *Chem. Lett.* **2003**, *32*, 284-285.

ANION COMPLEXATION BY GLYCOCLUSTER THIOUREAMETHYLCAVITANDS; NOVEL, ESI-MS-BASED METHODS FOR THE DETERMINATION OF K_a-VALUES[℘]

A series of saccharide-thiourea functionalized cavitands was prepared in good yields (72-86%) by reaction of tetrakis(aminomethyl)cavitand with the thiocyanate derivatives of acetylated glucose, galactose, and cellobiose. The anion complexation behavior of the acetylated and deacetylated glycocluster thioureamethylcavitands was studied with electrospray ionization mass spectrometry (ESI-MS) in acetonitrile and a 1:1 acetonitrile/water mixture, respectively. All compounds show a preference for Cl⁻. A linear relationship was found between the square root of the intensity and the concentration of the formed host-guest complex. Based on this relationship, novel methods have been developed for K_a-values determination, both via direct titration and competition experiments.

3.1 Introduction

Molecular recognition is the most important phenomenon in supramolecular chemistry.[1] A number of established analytical methods are used to study the strength of the host-guest interactions. The most commonly used methods include NMR and UV spectroscopy, calorimetry, and electrochemical techniques.[2]

Electrospray ionization mass spectrometry (ESI-MS) has been applied to directly determine binding constants of large biological complexes.[3] From titration experiments the intensities of both the free and the bound guest (or the free and bound host) are used to derive a Scatchard plot. The prerequisite is that host or guest and the host-guest complex are ionic, but this approach is not applicable to small ions as guests. Recently, ESI-MS has been used to determine the binding constants of crown ether alkali metal cation complexes by means of competition experiments.[4,5] Very recently, Russell et al. reported a qualitative study of the anion complexation by polydentate Lewis acids using nanoelectrospray MS.[6] However, to the best of our knowledge, ESI-MS has not been used to study anion complexation *quantitatively*.

Resorcinarene-based cavitands with proper ligating sites give rise to different types of receptors.[7] Previously, we have demonstrated that thiourea-functionalized cavitands are good receptors for halides in chloroform with a preference for chloride.[8,9] With the ultimate objective to mimic nature, the study of supramolecular interactions in aqueous media is very challenging. Several groups have reported the synthesis of cavitands with an enhanced solubility in water. This requires the introduction of either charged moieties such as quaternary ammonium,[10] amidinium,[11] pyridinium,[12] carboxylate,[13] phosphoric acid salt,[14] phenoxide,[15] etc, or neutral substituents such as peptides,[16] diethanolamine,[17] dendritic wedges,[18] and Pd-organometallic centers.[19] Saccharides have been used as water-solubilizing moieties in the cases of calix[4]arenes[20] and resorcinols,[21] and there is one example of a cavitand.[22]

In this chapter the synthesis of cavitands containing both saccharide[23] and thiourea moieties and their complexation with anions[24] in polar solvents are reported. Novel methods for the determination of the binding constants of the anion complexation using ESI-MS are described.

3.2 Results and discussion

3.2.1 Synthesis

The synthesis of the saccharide-thiourea functionalized cavitands **11-14** is summarized in Scheme 1.

Tetrakis(aminomethyl)cavitand **5** was prepared starting from the corresponding bromomethylcavitand[25] **1** by reaction with potassium phthalimide followed by deprotection of the formed phthalimidocavitand **2** with hydrazine hydrate, analogously to the synthesis of the previously reported pentyl derivative **6**.

Reaction of tetrakis(aminomethyl)cavitand **5** with the thiocyanate derivatives of acetylated glucose, galactose, and cellobiose in pyridine at room temperature afforded the acetyl-protected saccharide-thiourea functionalized cavitands **7**, **8**, and **10** in 80, 85, and 86% yield, respectively. In an analogous way cavitand **9** was prepared in 72% yield by reaction of pentyl derivative **6** with acetylated glucosyl isothiocyanate. Subsequent deacetylation of compounds **7**, **8**, **9**, and **10** with sodium methoxide in a 4:1 mixture of methanol and dichloromethane gave saccharide-thiourea functionalized cavitands **11-14** in 96, 95, 90, and 92% yield, respectively.

To study the influence of the thiourea linker between the cavitand and the saccharide moieties, cavitand **16** with SCH_2 linkers was prepared (Scheme 2). Reaction of tetrakis(bromomethyl)cavitand **1** with 2,3,4,5-tetra-O-acetyl-ß-D-glucopyranosylthiol in dichloromethane gave gluco-thiamethyl cavitand **15** in 88% yield. Subsequent deacetylation with a catalytic amount of sodium methoxide afforded cavitand **16** in 91% yield.

The formation of both the acetylated (**7-10**) and deacetylated cavitands (**11-14**) was evident from the MALDI mass spectra and satisfactory elemental analyses. Their ^{1}H NMR spectra in $CDCl_3$ and CD_3CN only exhibit broad signals. However, spectra with sharp signals were obtained using DMSO-d_6 as a solvent. Characteristic is the signal at 5.8 and 5.2 ppm of the anomeric CH of the sugars in the acetylated and deacetylated compounds, respectively.

1, 2 X=Br

3, 4 X = (phthalimide) ⎫ *a*

5, 6 X=NH$_2$ ⎫ *b*

1, 3, 5 R^1 = Me

2, 4, 6 R^1 = C$_5$H$_{11}$

7	R^1 = Me, R^2 = ·····OAc
8	R^1 = Me, R^2 = —OAc
9	R^1 = C$_5$H$_{11}$, R^2 = ·····OAc
10	R^1 = Me, R^2 = (galactose-OAc)

11	R^1 = Me, R^2 = ·····OH
12	R^1 = Me, R^2 = —OH
13	R^1 = C$_5$H$_{11}$, R^2 = ·····OH
14	R^1 = Me, R^2 = (galactose-OH)

a: potassium phthalimide, MeCN; *b*: hydrazine hydrate, MeOH
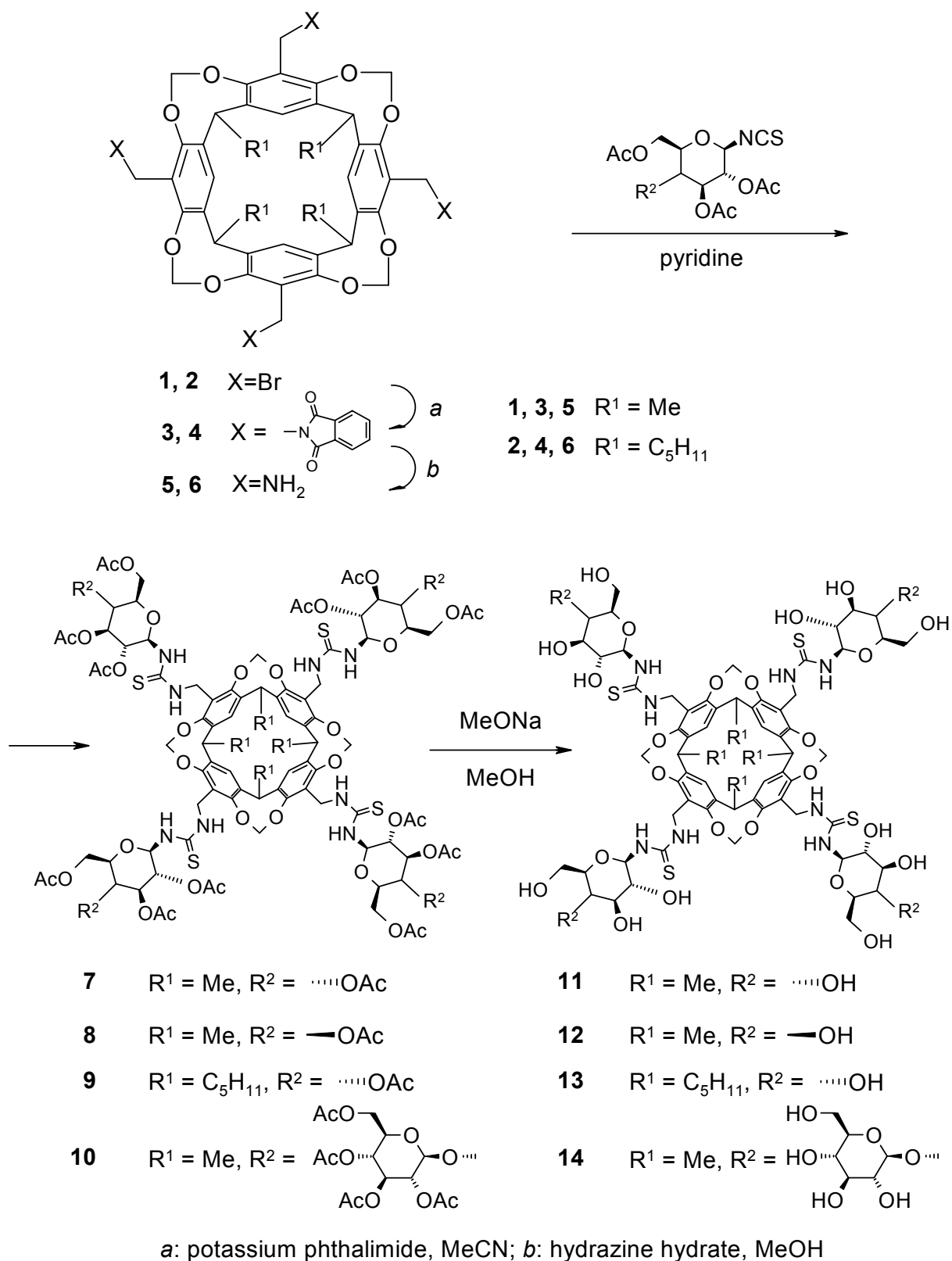
Scheme 1. Synthesis of glycocluster thioureamethylcavitands.
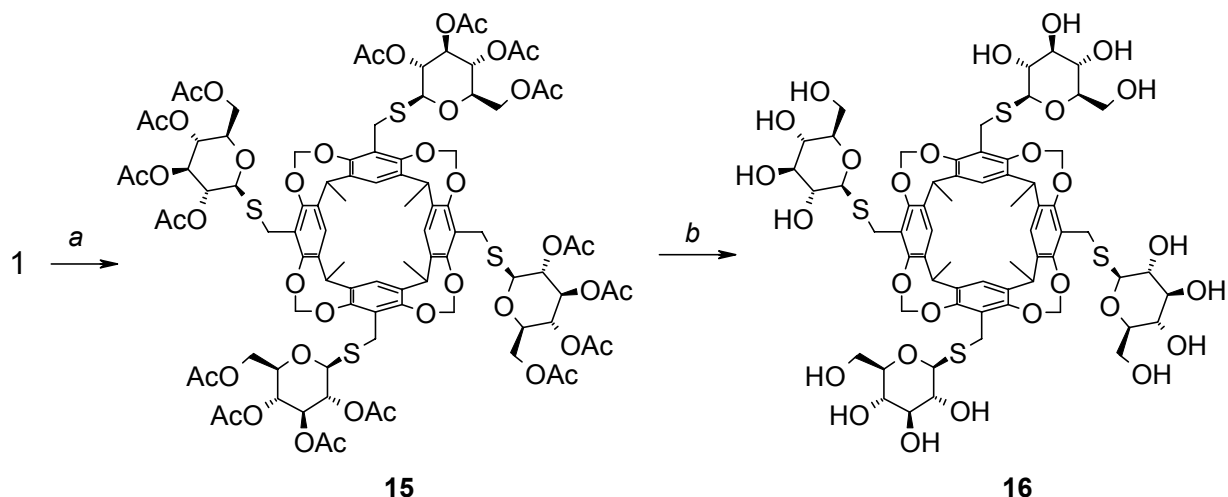
a: 2,3,4,6-tetraacetyl-1-thiaglucose, Na_2CO_3, CH_2Cl_2; b: MeONa, MeOH, CH_2Cl_2

Scheme 2. Synthesis of cavitandglycoclusters containing sulfide linkers.
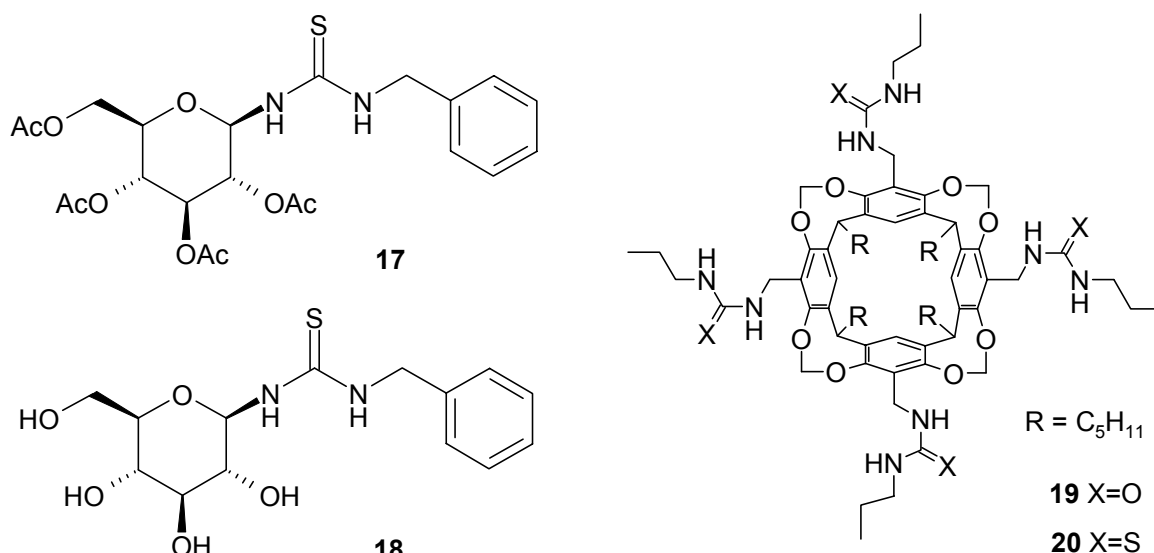
Chart 1. Reference compounds.

In acetonitrile the solubility of the acetylated glycocluster thioureacavitands **7-10** is twice as high as that of the propylthioureacavitand **20** (about 5 vs. 2.2 mM/L). The solubility of the corresponding propylureacavitand **19** in acetonitrile is 0.4 mM/L. The solubilities of glycocluster thioureacavitands **11-14** in water are 0.5, 0.6, 0.8, and > 300 mM/L, respectively, while that of compound **15** is 1 mM/L. The much higher water solubility of cavitand **14** clearly shows the influence of four disaccharide moieties. The solubility of **14** in water is even higher than that of a cavitand containing dendritic wedges with a total of 45 tetraethylene glycol chains (221 mM/L).[18]

Simpler analogs of cavitand glycoclusters, used for competitive experiments, are shown in Chart 1.

3.2.2 Anion complexation behavior studied by ESI-MS

General: The anion complexing ability of both the acetylated (**7-10**, **15**) and deacylated glycocluster thioureacavitands **11-14**, **16** was clearly followed from the signal of the 1:1 complexes in the ESI-MS negative ion mode spectra. Since in the ^{1}H NMR spectra rather broad signals were obtained, ^{1}H NMR spectroscopy was not suitable to determine K_a-values of the complexes. Therefore we investigated whether ESI-MS can be used to determine K_a-values.

In ESI-MS, charged host-guest complexes are transferred from solution via small droplets into the gas phase under relatively mild conditions.[26,27] In general, this does not give rise to fragmentation. Some parameters involve: (i) properties of the species measured e.g. ionization potential and volatility (ii) the properties of the solvent used e.g. conductivity and surface tension (iii) the co-solutes present, and (iv) the settings of the mass spectrometer such as applied voltage, temperature, gas flow, etc. However, all these parameters remain constant during a set of experiments. We investigated whether there is a relationship between the intensity of the signal of the 1:1 complex and the concentration of the complex in the solution.

As a model experiment, the chloride complexation of acetylated glucose-functionalized thioureacavitand **7** was studied in acetonitrile. Two different kinds of titrations were carried out: Bu$_4$NCl with **7** (keeping the total concentration of the chloride guest constant) and host **7** with Bu$_4$NCl (with a constant total host concentration). For both titrations the relationship between the intensity of the signal of the host-guest complex **7**@Cl$^-$ and its concentration is depicted in Figures 1a and 1b, respectively. In Figure 1a, the peak intensity increases parabolically, which is very clear from Figure 1c, depicting the square root of the peak intensity vs the concentration of the host-guest complex.[28] The relationship fits with equation 1.

$$I = A \times [HG]^2 \qquad\qquad 1$$

In this equation I is the peak intensity and A is a constant that includes the properties of the complex, the settings of the mass spectrometer, etc. (vide supra). In the case of Figure 1b, the increase of the peak intensity of the host-guest complex is

followed by a decrease. This so-called suppression[27] is caused by a co-solute (in our case the titrant) that is present in the measuring solution. A co-solute can prevent the formation of droplets of the required small size as well as decrease the volatization efficiency of the measured ions from the formed droplets, since they occupy its surface. In general, electrolytes cause a higher suppression than non-electrolytes. Figure 1d shows that the same quadratic relationship as equation 1 obeyed until suppression starts to play a role.

Direct method for K_a*-value determination by ESI-MS titration:* The relationship found (equation 1) can be used to determine association constants. When the concentration of the anion ($[G]$) is maintained constant, the concentration of the host-guest complex ($[HG]$) can be calculated at each moment from the intensity I of the signal of the complex with equation 2:

$$[HG] = [HG]_{max} \frac{\sqrt{I}}{\sqrt{I_{max}}} \qquad\qquad 2$$

$$[HG] = [G]_{tot} \frac{\sqrt{I}}{\sqrt{I_{max}}} \qquad\qquad 3$$

In equation 2 I_{max} is the intensity when $[HG] = [HG]_{max}$. Since the maximum concentration of the host-guest complex $[HG]_{max}$ is equal to the total concentration of the anionic guest $[G]_{tot}$, substitution gives a relationship between the intensity of the signal and the concentration of the host-guest complex $[HG]$ and $[G]_{tot}$ (equation 3).

Non-linear fitting of the experimental data I_{exp}, $[G]_{tot}$, and $[H]_{tot}$ with the calculated value of the intensity I_{calc} by varying $\sqrt{I_{max}}$ and K_a ultimately gives the calculated association constant K_a. An example of the calculated and the experimental ESI-MS data of a titration of acetylated galactose functionalized thiourea cavitand **8** with Bu_4NCl is presented in Figure 2.
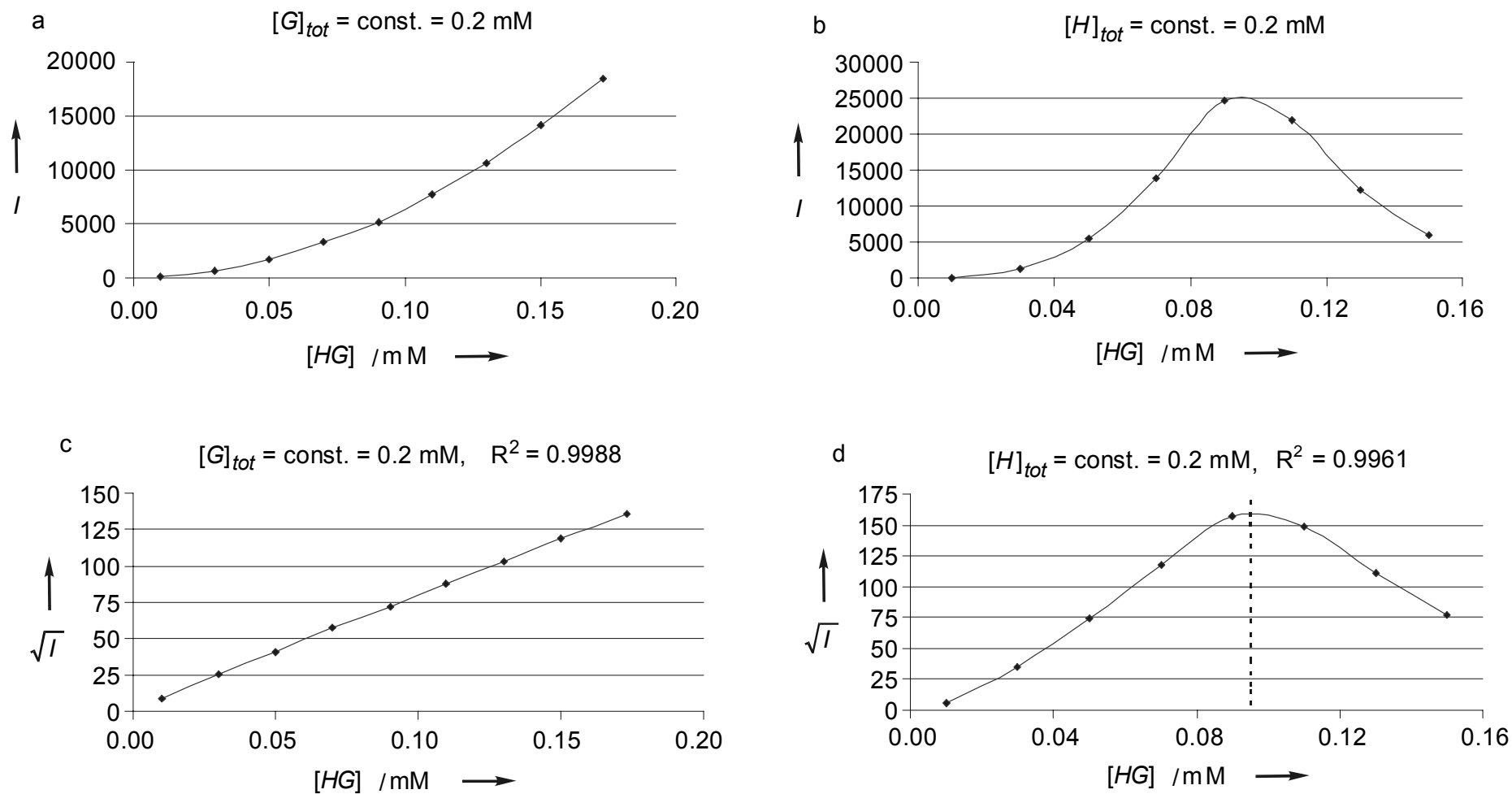
Figure 1. a, c: Titration of Bu₄NCl with **7**, a: Intensity vs concentration of **7**@Cl⁻, c. √Intensity vs concentration of **7**@Cl⁻; b, d: Titration of **7** with Bu₄NCl, b: Intensity vs concentration of **7**@Cl⁻, d: √Intensity vs concentration of **7**@Cl⁻.
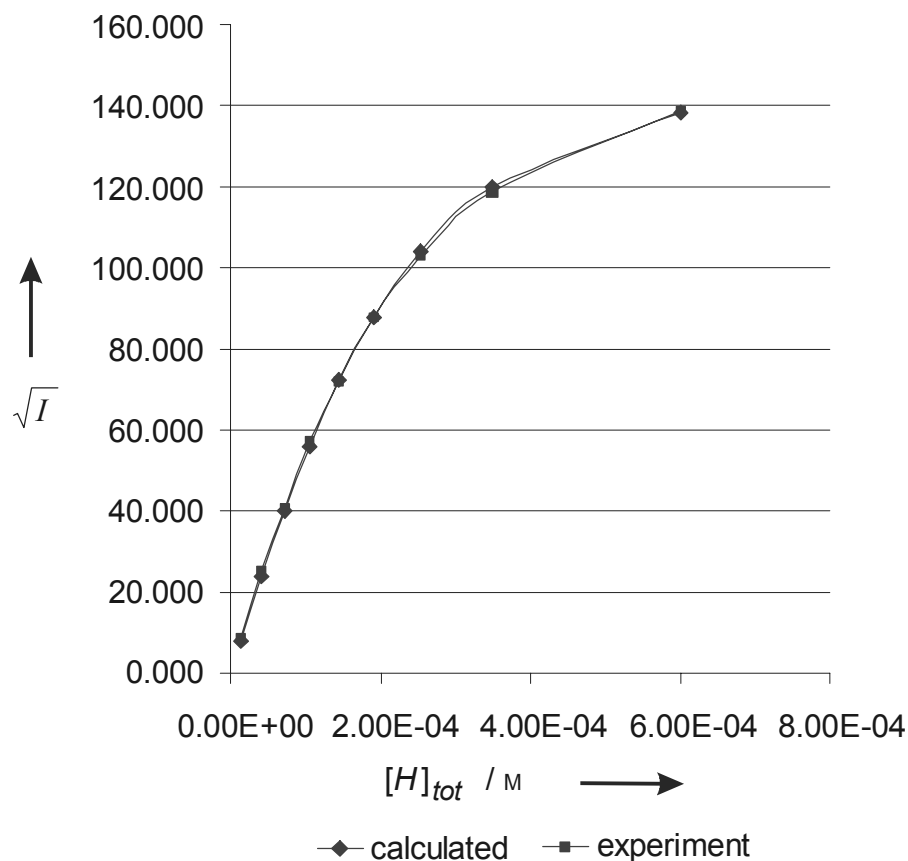
Figure 2. Nonlinear curve fitting of data of ESI-MS titration of **8** with Bu$_4$NCl. The titration data are within the Weber concentration range of 20-80% complex formation.

Table 1. ESI-MS and ITC data of the complexation of Cl$^-$
by compounds **7-9** in acetonitrile.

| Compound | ESI-MS | Isothermal microcalorimetry data | | |
	K_a, M^{-1}	K_a, M^{-1}	ΔG, kcal/mol	ΔH, kcal/mol	TΔS, kcal/mol
7	15100	15000	-5.694	-4.685	1.009
8	15000	14700	-5.685	-4.271	1.414
9	14500	14600	-5.657	-4.283	1.374

This methodology was used to study the chloride complexation of acetylated glycocluster thiourea cavitands **7-9** in acetonitrile; the K_a-values are summarized in

Table 1. In the case of lower binding constants, the larger amount of host necessary to give a sufficient amount of host-guest complex may also give rise to suppression (vide supra) of the peak intensity. Nevertheless, the K_a-values can be calculated by taking into account only the non-suppression area of the ESI-MS titration curve (compare Figure 1d). In this way a K_a-value of 720 M^{-1} (with ITC $K_a = 680$ M^{-1}) was obtained for the complexation of compound **7** with Bu$_4$NBr in acetonitrile.

In all cases the K_a-values found are in excellent agreement with those obtained with isothermal microcalorimetry (ITC) (Table 1), confirming the validity of the described ESI-MS titration method.

Calibrated competitive method: Some years ago Kempen and Brodbelt[4] reported a method for the determination of binding constants of crown ethers with cations by means of ESI-MS. The peak intensity of a reference host-guest complex with a known K_a-value was monitored before and after addition of a second host or guest. The K_a-value of the new complex is calculated on the basis of the change in intensity of the reference complex and extrapolation from a calibration curve ([*HG*] vs I_{HG}).[29] To obtain reliable results, the difference in the K_a-values involved should be within two orders of magnitude.[30]

We have used this methodology to study anion complexation by addition of a new host to an existing host-guest complex. The determination of the K_a-value of **19**@Cl$^-$ was studied in more detail. A set of solutions with different concentrations of propylthiourea cavitand **19** in acetonitrile solution containing constant initial total concentration of acetylated glucose-functionalized thiourea cavitand **7** and Bu$_4$NCl were prepared. From a calibration curve ([$H_I G$] vs $\sqrt{I_{H_1 G}}$) the changes in the intensities of **7**@Cl$^-$ were transformed to its concentration and used for the calculation of the K_a-value of **19**@Cl$^-$ (Table 2). The averaged K_a-value of entries 2-4 is 17100 ± 100 M^{-1}, in agreement with the K_a-value of 17300 M^{-1} determined with ITC. However, the K_a-value in entry 5 is much too high, originating from suppression caused by the higher competitor concentration. This also illustrates the disadvantage of this method. Several experiments must always be carried out with different competitor concentrations. When at least two of the initial K_a-values were within the experimental error, much higher K_a-values caused by suppression were excluded.

Table 2. K_a-values of **19**@Cl⁻ with the ESI-MS calibrated competitive method using **7**@Cl⁻ as the reference complex.

Entry	Concentration[a], mM		K_a (**19**@Cl⁻), M⁻¹
	19	**[7@Cl⁻]**	
1	0	0.11	-
2	0.1	0.09	17200
3	0.2	0.074	17100
4	0.3	0.062	17000
5	0.4	0.047	22400

a. Initial concentrations of Bu₄NCl and **7** are 0.2 mM and 0.191 mM, respectively.

Complex **7**@Cl⁻ was used as the reference to study the Cl⁻ complexation of compounds **9**, **10**, **15**, **17**, and **20** in acetonitrile; the K_a-values are summarized in Table 3. The choice of the reference complex has hardly any effect. Competition experiments of compounds **7**@Cl⁻ or **8**@Cl⁻ with **17** in acetonitrile gave K_a-values of 450 and 440 M⁻¹, respectively. The K_a-values are very close to that obtained with ITC, namely 430 M⁻¹. These experiments show the possibility to determine relatively low K_a-values using this methodology.

Table 3. K_a-values of Cl⁻ complexation by different hosts in acetonitrile obtained with the ESI-MS calibrated competitive method using **7**@Cl⁻ as the reference complex.

Entry	Host	K_a, M⁻¹
1	**9**	14900
2	**10**	4600
3	**15**	5200
4	**17**	450 (440[a], 430[b])
5	**20**	15400

a. **8**@Cl⁻ as the reference complex; b. ITC data.

Competition experiments of the reference complexes **7**@Cl⁻ and **8**@Cl⁻ with Br⁻, as an anionic guest, showed considerable suppression of the signal. Upon titration with Br⁻, the intensity of the reference complex dropped much more than expected, even if only small amounts of Br⁻ were added. Suppression was even observed upon addition of small amounts of the anions PF_6^- and BPh_4^-. Since anionic species cause significant suppression, this methodology cannot be used to study the complexation behavior of a host toward a variety of anions.

Competition method: On account of the above-mentioned problems, a novel, relatively simple competitive method was developed.[31] For this approach, the K_a-value of one host-guest complex has to be known, determined by the direct ESI-MS titration (vide supra) or another method. Since we are dealing with rather large hosts and relatively small guests, we assumed that the volatility of the different complexes is (almost) equal. This means that equation 4 can be derived from equation 1. Equation 4 describes the ratio of the concentration of the two *HG* complexes as the ratio of the square roots of the respective intensities.

$$\frac{[HG_1]}{[HG_2]} = \frac{\sqrt{I_1}}{\sqrt{I_2}} \qquad\qquad 4$$

Together with the mass balance equations 5-7 and the binding constants equations 8 and 9, the different unknowns in the equations can be solved giving the K_{a2}-value.

$$[HG_1] + [HG_2] + [H] = [H]_{tot} \qquad\qquad 5$$

$$[HG_1] + [G_1] = [G_1]_{tot} \qquad\qquad 6$$

$$[HG_2] + [G_2] = [G_2]_{tot} \qquad\qquad 7$$

$$K_{a1} = \frac{[HG_1]}{[H] \times [G_1]} \qquad\qquad 8$$

$$K_{a2} = \frac{[HG_2]}{[H] \times [G_2]} \qquad\qquad 9$$

This approach was used to study the complexation behavior of compounds **7** and **8** toward Br^-, I^-, ClO_4^-, HSO_4^-, and NO_3^- (in all cases Bu_4N^+ salts) in acetonitrile; the K_a-values are summarized in Table 4 and typical examples of the spectra are shown in Figure 3. The K_a-values for the complexation of Br^-, I^-, and ClO_4^- were also determined with ITC and are in excellent agreement. The data for ClO_4^- complexation clearly demonstrate the validity of this method even for very low K_a-values.

Table 4. K_a-values in acetonitrile of different complexes of compounds **7** and **8** obtained with the ESI-MS competitive method.

Complexes[a]	$K_a{}^b$, M^{-1}	Complexes[a]	$K_a{}^b$, M^{-1}
7@Br^- [c]	680 (680)	**8**@Br^- [c]	680 (670)
7@I^-	170 (175)	**8**@I^-	180 (173)
7@ClO_4^-	39 (37)	**8**@ClO_4^-	40 (35)
7@HSO_4^-	1700	**8**@HSO_4^-	1680
7@NO_3^-	870	**8**@NO_3^-	880

a. **7**@Br^- and **8**@Br^- were used as the reference complexes; b. ITC data are between brackets; c. In these cases the corresponding Cl^- complexes were used as reference complexes.

The possible influence of changing the settings of the mass spectrometer on the ratio of the peak intensities of the complexes **7**@Cl^- and **7**@Br^- (and consequently on the K_a-value) was studied. Varying the capillary voltage from 110 eV to 50 eV caused significant changes in the intensities of the complexes, but the ratio remained the same (only a variation of 5%). This means that the influence on the K_a-value is negligible.
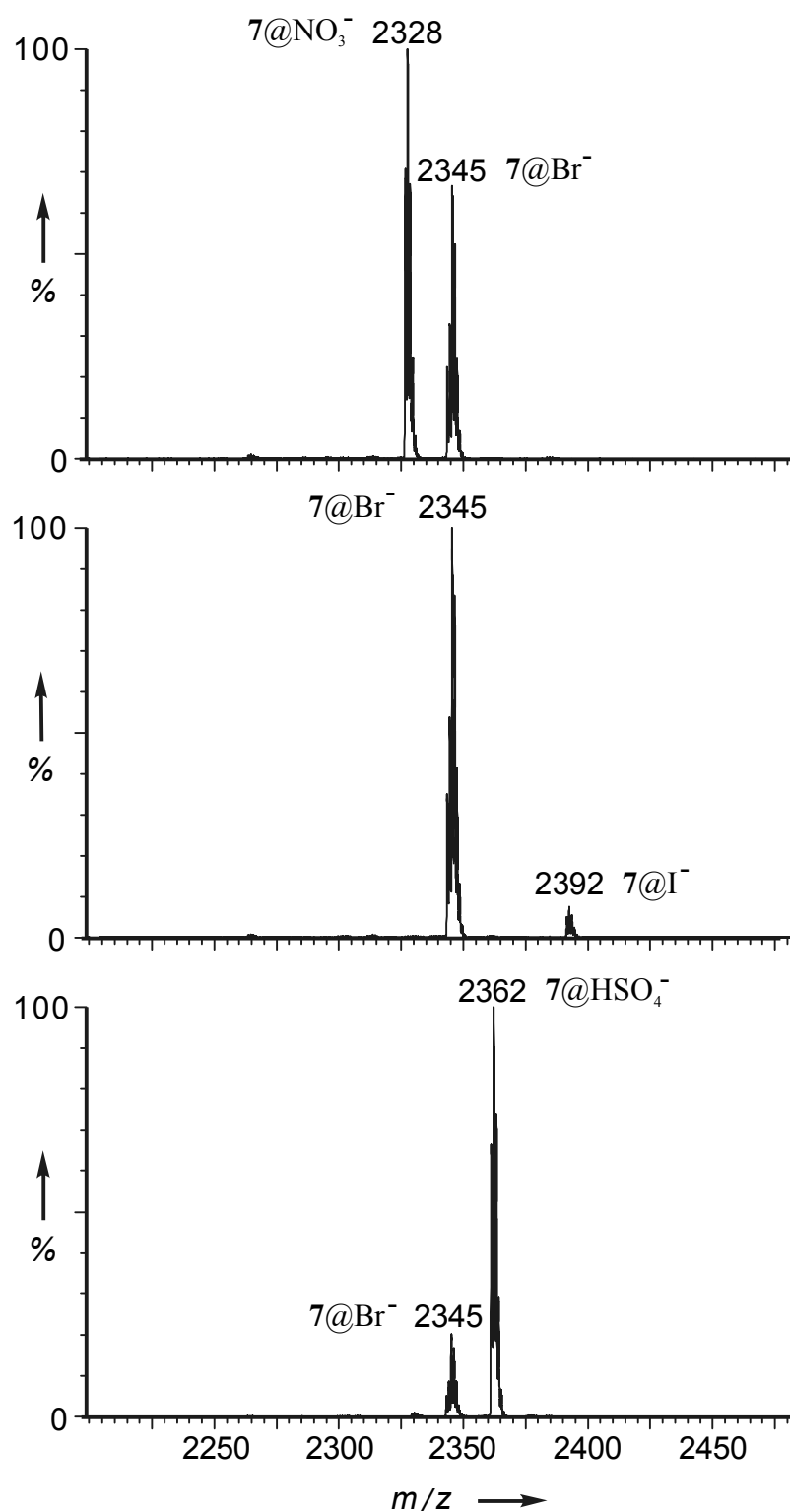
Figure 3. ESI-MS spectra in acetonitrile of mixtures of the complexes: **7**@Br⁻ with a) **7**@NO₃⁻, b) **7**@I⁻, c) **7**@HSO₄⁻. Initial concentrations: **7** (0.2 mM), Bu₄NBr (0.4 mM), Bu₄NNO₃ (0.4 mM), Bu₄NI (0.4 mM), Bu₄NHSO₄ (0.4 mM).

This method has also been validated by studying the influence of variations in the concentrations of the competing anions. The results in triplicate are summarized in Table 5 for the competitive titration of **8**@I⁻ with different concentrations of Bu$_4$NBr. Table 5 clearly shows the reproducibility within one set of experiments, but it also makes clear that changing the concentration hardly influences the K_a-value. The absolute values of the intensities in **8**@Br⁻ in entries 2 and 3 in Table 5 are almost the same, despite the larger Br⁻ concentration in entry 3. This is caused by suppression (vide supra), but since the intensity of **8**@I⁻ also drops, the ultimate K_a-value is unaffected.

Table 5. Competitive titration of **8**@I⁻ with Bu$_4$NBr.

Entry	Concentration, mM			Intensity		$\dfrac{\sqrt{I(\mathbf{8}@\,\mathrm{Br}^-)}}{\sqrt{I(\mathbf{8}@\,\mathrm{I}^-)}}$	K_a (**8**@I⁻), M⁻¹
	Bu$_4$NBr	Bu$_4$NI		**8**@Br⁻	**8**@I⁻		
1	0.2	0.4	a	60322	18287	1.8162	172.9
			b	60977	18653	1.8080	173.7
			c	61231	18562	1.8166	172.8
2	0.4	0.4	a	81919	6111	3.6613	172.7
			b	81435	6093	3.6558	173.0
			c	80289	6132	3.6185	174.8
3	0.6	0.4	a	80458	2807	5.3538	178.4
			b	81313	2803	5.3860	177.3
			c	80425	2819	5.3413	178.8

The ESI-MS competitive method has also been successfully applied to determine the K_a-values of the anion complexation behavior of the glucose- and galactose-

functionalized thioureacavitands **11** and **12** toward Br^-, I^-, HSO_4^-, and NO_3^- in a 1:1 mixture of acetonitrile and water. The results are summarized in Table 6.

Table 6. K_a-values of different complexes of compounds **11** and **12** in acetonitrile:water = 1:1 obtained with the ESI-MS competitive method.

Complexes	K_a^a, M^{-1}	Complexes	K_a^b, M^{-1}
11@Br^-	162	**12**@Br^-	157
11@I^-	83	**12**@I^-	78
11@HSO_4^-	173	**12**@HSO_4^-	176
11@NO_3^-	114	**12**@NO_3^-	109

a. Reference complex **11**@Cl^- (K_a = 260 M^{-1}, determined by ITC);

b. Reference complex **12**@Cl^- (K_a = 250 M^{-1}, determined by ITC).

3.2.3 Evaluation of the K_a-values

The complexation behavior of the acetylated cavitands **7** and **8** and their deacetylated analogues **11** and **12** toward different anions was studied. There is a selectivity for Cl^- in all cases. For compounds **7** and **8** (in acetonitrile) the binding affinities follow the order: $Cl^->HSO_4^->NO_3^->Br^->I^->ClO_4^-$ (Table 4). As expected, in a 1:1 acetonitrile:water mixture the K_a-values are much lower. For compounds **11** and **12** the K_a-values follow almost the same the order: $Cl^->HSO_4^-> Br^->NO_3^-> I^-$ (Table 6). For the Cl^- complexation of compounds **7**, **8** and **9** the thermodynamic data have been determined with ITC (Table 1). The complexation is enthalpically driven, but the entropy factor also favors the complexation. In the cases of compounds **7** and **8** there is a Cl^-/Br^- selectivity of about 22. Surprisingly, this selectivity is much more pronounced than that in the corresponding non-sugar containing thioureamethylcavitands such as **20** in $CDCl_3$. The preference for Cl^- has also been

found in other studies.[9,32] The Br^- and I^- anions are more weakly complexed because of their 'softer' nature, despite the increased size. Presumably the spherical Cl^- has a better fit within the thiourea binding pocket than the trigonal NO_3^- and tetrahedral HSO_4^-.

The presence of a glucose or a galactose moiety hardly influences the K_a-value for the Cl^- complexation (in acetonitrile). The K_a-value of propylthioureamethyl cavitand **20** is 15400 M^{-1}, compared with 14900 M^{-1} for the corresponding pentyl chain-containing acetylated glucose thioureamethylcavitand **9** (Table 3). However, probably for steric reasons, the cellobiose unit has a negative effect on the complexation. Comparing the values for the Cl^- complexation of acetylated **7** and **10** and deacetylated **11** and **14**, the K_a-values drop from 15100 to 4600 M^{-1} (in acetonitrile) and from 250 to 100 M^{-1} (in acetonitrile:water = 1:1), respectively.

Our study clearly shows the positive effect of bringing together ligating sites on a molecular platform. For instance, compound **7** binds Cl^- in acetonitrile about 33 times better than the acyclic anolgue **17** (K_a = 440 M^{-1}). The corresponding deacetylated compounds **11** and **18** give K_a-values of 250 and about 5 M^{-1} for Cl^- complexation in acetonitrile:water (1:1).

Despite the absence of a thiourea moiety, the thiamethyl linked glucose-containing cavitands **15** and **16** exhibit a reasonable complexation of Cl^-, viz. K_a-values of 5200 (acetonitrile) and about 60 M^{-1} (acetonitrile:water = 1:1), respectively. In the former case the K_a-value is only three times lower than that of the corresponding thioureacavitand **7**. Apparently, the combination of a cavitand cavity and glucose units facilitates Cl^- complexation.

3.3 Conclusions

In this study we have demonstrated the value of ESI-MS for the determination of K_a-values for anion complexation with (acetylated) glycocluster thioureamethyl-cavitands. The linear relationship found between the square root of the intensity and the concentration of the formed HG complex, allows the direct determination of the K_a-value by means of a titration experiment. However, this linearity is only observed when the suppression, the competitive influence of the titrant, is negligible. To avoid the possible influence of suppression, competitive methods were elaborated, viz. the "calibrated curve competitive method" and the "competitive method". The latter

method is not sensitive to suppression and does not require a calibration curve. It is based on the comparison of the square roots of intensities of different related HG complexes. It is an excellent method for the rapid quantitative determination of the complexation behavior of a host toward a variety of guests.

The (acetylated) glycocluster thioureamethyl cavitands show a high affinity for chloride in acetonitrile. The K_a-values for compounds **7-9** is about 1.5×10^4 M^{-1}, which is more than 20 times higher than the corresponding values for the complexation of bromide. In general, the affinity of cavitand-based anion receptors for anions is 30 times higher than that of the simple analogs **17** and **18** in both acetonitrile and acetonitrile:water (1:1).

We feel that the described ESI-MS-based methods are very valuable, new tools for K_a-value determinations. They are a useful alternative when other K_a-value determinations fail.

3.4 Experimental Section

The reagents used were purchased from Aldrich or Acros Chimica and used without further purification. All the reactions were performed under a dry argon atmosphere. All solvents were freshly distilled before use. Dry pyridine was obtained by distillation over calcium hydride. Melting points were measured using a Sanyo Gellenkamp Melting Point Apparatus and are uncorrected. Proton and carbon NMR spectra were recorded on a Varian Unity Inova (300 MHz) spectrometer. Residual solvent protons were used as internal standard and chemical shifts are given relative to tetramethylsilane (TMS). Chromatography was performed with silica gel (SiO$_2$, Merck, 0.063-0.2 mm). MALDI spectra were recorded using a Voyager-DE™ RP Biospectrometry™ Workstation by PerSeptive Biosystems, Inc (accelerating voltage 20000 V; mode of operation: reflector; polarity: positive; matrixes: dithranol and DHB). Compounds **1**,[25] **2**,[33] **4**,[33] **6**,[33] **17**,[34] **18**,[34] and **19**[35] were prepared following literature procedures.

ESI-MS: The ESI-MS experiments were carried out with a Micromass LST ESI-TOF instrument. The solutions were introduced at a flow rate of 20 µL/min for 2 min (120 scans). The standard spray conditions, unless otherwise specified are: capillary voltage 2500 V, sample cone voltage 30-110 V (optimal conditions for compounds **7-10** 80 V, and for **11-14** 30 V), desolvation gas flow 250 L/h, source temperature 100

°C, desolvation temperature 100 °C, extraction cone voltage ~0 V and flow cone gas is maintained at about 0 L/h. During a set of measurements the distance between the capillary and the cone is kept the same. Every solution was injected five times. The values of the three intensities that are the closest to one another were used for the calculations. To check the stability of the signal one of the solutions was used as a reference one; it was injected in between of the five injections of each solution. The intensity of the signal of the complex was calculated as the sum of the intensities of all the components of the isotopic pattern.

ITC: The calorimetric titration experiments were performed using a Microcal VP-ITC microcalorimeter with a cell volume of 1.4115 mL. The final curves were modeled using a nonlinear regression analysis. The fittings were done using Microcal Origin software.

Solubility measurements: A suspension of the concerning compound in water (or acetonitrile) was sonicated for 20 min at 25 °C. The solid was filtered off and the resulting solution (1-5 mL) was evaporated to dryness (in the case of water a freeze dryer was used). The experiments were repeated twice.

Calculations: The system of equations 4-9 was numerically solved with the Maple 8 program (Waterloo Maple Inc.). Calibration curve data were also treated with the Maple 8 program based on the system of equations 10-14 that include binding constant equations 10, 11 and mass balance equations 12-14 (knowns: $K_{a,ref}$ – binding constant of the reference host-guest complex; $[G_{ref}]_{tot}$, $[H]_{tot}$, $[G_{new}]_{tot}$ – total concentration of the reference guest, host, and the new guest added, respectively; $[HG_{ref}]$ – concentration of the reference host-guest complex derived from the calibration curve; unknowns: $K_{a,new}$ – binding constant of the host with new guest; $[G_{ref}]$, $[G_{new}]$, $[H]$, $[HG_{new}]$ – concentrations of the reference guest, new guest, host, and the complex of the host with the new guest, respectively):

$$K_{a,ref} = \frac{[HG_{ref}]}{[H][G_{ref}]} \qquad\qquad 10$$

$$K_{a,new} = \frac{[HG_{new}]}{[H][G_{new}]} \qquad\qquad 11$$

$$[G_{ref}]_{tot} = [HG_{ref}] + [G_{ref}] \qquad\qquad 12$$

$$[G_{new}]_{tot} = [HG_{new}] + [G_{new}] \qquad\qquad 13$$

$$[H]_{tot} = [HG_{ref}] + [HG_{new}] + [H] \qquad\qquad 14$$

Equation 15 represents the analytical solution of the system of equations 10-14, which is more convenient for the analysis of an array of data. The calculations were performed using the Microsoft Excel program.

$$K_{a,new} = \frac{K_{a,ref}([G_{ref}]_{tot} - [HG_{ref}])([H]_{tot} - [HG_{ref}]) - [HG_{ref}]}{K_{a,ref}([G_{ref}]_{tot} - [HG_{ref}])([G_{new}]_{tot} - [H]_{tot} + [HG_{ref}]) + [HG_{ref}]} \times$$
$$\times \frac{K_{a,ref}([G_{ref}]_{tot} - [HG_{ref}])}{[HG_{ref}]} \qquad\qquad 15$$

Tetrakis(phthalimidomethyl)tetramethylcavitand (3): A mixture of tetrakis-(bromomethyl)tetramethylcavitand **1** (0.96 g, 1 mmol) and potassium phthalimide (1.11 g, 6 mmol) in acetonitrile (50 mL) was refluxed for 5 days. The reaction mixture was evaporated to dryness, whereupon CH_2Cl_2 (50 mL) and 1N NaOH (25 mL) were added to the residue. After stirring for 10 min the organic layer was separated and washed with 1N NaOH (2 × 25 mL) and water (25 mL), dried over $MgSO_4$, and evaporated to dryness. The resulting solid was purified by column chromatography (eluent: CH_2Cl_2 containing 2.5% MeOH). Yield: 65%; m.p. > 350 °C (CH_2Cl_2/EtOAc); ^{1}H NMR ($CDCl_3$) δ: 7.93-7.78 (m, 8 H; Phth), 7.78-7.63 (m, 8 H; Phth), 7.20 (s, 4 H; ArH), 5.81 (d, J = 7.3 Hz, 4 H; O_2CH), 4.92 (q, J = 7.3 Hz, 4 H; Ar_2CH), 4.43 (d, J = 7.3 Hz, 4 H; O_2CH), 4.66 (s, 8 H; $ArCH_2N$), 1.68 (d, J = 7.3 Hz, 12 H; CH_3C); ^{13}C NMR (DMSO-d_6) δ: 168.0, 153.5, 138.8, 134.0, 123.4, 132.1, 121.1, 119.7, 99.6, 32.7, 31.1, 16.1; MS (MALDI) m/z (%): 1228.9 (100) [M^+]; elemental analysis calcd (%) for $C_{72}H_{52}N_4O_{16}$ (1229.2): C 70.35, H 4.26, N 4.56; found: C 70.07, H 4.18, N 4.83.

Tetrakis(aminomethyl)tetramethylcavitand (5): A mixture of tetrakis-(phthalimidomethyl)tetramethylcavitand **3** (2.9 g, 2.36 mmol) and hydrazine hydrate (2.95 g) in MeOH:CH_2Cl_2 (1:3; 200 mL) was refluxed for 26 h. The solid was filtered off, the solution was evaporated to dryness, and the crude product was triturated with diethyl ether (3 × 30 mL). Double recrystallization from EtOH/i-PrOH gave pure **5** as

a white powder. Yield: 60%; m.p. > 350 °C (EtOH/*i*-PrOH); ^{1}H NMR (DMSO-*d6*) δ: 7.61 (s, 4 H; ArH), 5.89 (d, *J* = 7.3 Hz, 4 H; O$_2$CH), 4.80 (q, *J* = 7.7 Hz, 4 H; Ar$_2$CH), 4.41 (d, *J* = 7.7 Hz, 4 H; O$_2$CH), 3.46 (s, 8 H; ArCH$_2$N), 1.79 (d, *J* = 7.7 Hz, 12 H; CH$_3$C); ^{13}C NMR (DMSO-*d6*) δ: 152.1, 138.7, 129.3, 119.6, 99.4, 35.2, 31.2, 16.1; MS (MALDI) *m/z* (%): 708.5 (100) [*M*+], 731.5 (50) [*M*+Na+]); elemental analysis calcd (%) for C$_{40}$H$_{44}$N$_4$O$_8$ (708.8): C 67.78, H 6.26, N 7.90; found: C 67.94, H 6.50, N 7.71.

General procedure for the preparation of the acetylated glycoclusters 7, 8, 9, 10: A solution of a pyranosylisothiocyanate[36-38] (1.06 mmol) and tetrakis-(aminomethyl)cavitand **5** or **6** (0.21 mmol) in pyridine (20 mL) was stirred at room temperature for 3 days. After evaporation of the solvent, the resulting solid was triturated with diethyl ether (2 × 20 mL) and subsequently recrystallized from isopropanol. The pyranosylisothiocyanates used for this synthesis (tetra-O-acetyl-β-D-glucopyranosylisothiocyanate,[36] tetra-O-acetyl-β-D-galactopyranosylisothiocyanate[37] and hepta-O-acetyl-β-D-cellobiosyl-isothiocyanate[38]) were prepared by a slightly modified procedure used for the synthesis of the glucose derivative[36] (refluxing the corresponding α-bromopyranoside with Pb(NCS)$_2$ in toluene for 4-6 h).

Tetrakis(1-tetraacetylglucosylthioureidomethyl)tetramethylcavitand (7): Yield: 80%; m.p. 230-231 °C (isopropanol); ^{1}H NMR (DMSO-*d6*) δ: 7.73 (bs, 12 H; ArH, NH), 5.91 (d, *J* = 7.0 Hz, 4 H; O$_2$CH), 5.78 (bs, 4 H; H$_1$-glu), 5.33 (t, *J* = 9.3 Hz, 4 H; H$_3$-glu), 5.0 - 4.7 (m, 12 H; H$_2$, H$_4$-glu, Ar$_2$CH), 4.43 (bs, 8 H; ArCH$_2$), 4.25 (bs, 4 H; O$_2$CH), 4.15 (dd, *J*$_{6a6b}$ = 12.0 Hz, *J*$_{6a5}$ = 4.0 Hz, 4 H; H$_{6a}$-glu), 3.95 and 3.92 (bs+s, 8 H; H$_{6b}$, H$_5$-glu), 1.97 (bs, 36 H; CH$_3$CO), 1.93 (s, 12 H; CH$_3$CO), 1.81 (d, *J* = 7.0 Hz, 12 H; CH$_3$C); ^{13}C NMR (DMSO-*d6*) δ: 183.1, 169.9, 169.4, 169.2, 152.5, 139.0, 123.3, 121.3, 99.2, 81.4, 72.7, 71.9, 70.4, 67.9, 61.6, 38.1, 31.3, 20.2, 20.2, 15.9; MS (MALDI) *m/z* (%): 2265.1 (100) [*M*+], 2288.1 (80) [*M*+Na+]; elemental analysis calcd (%) for C$_{100}$H$_{120}$N$_8$O$_{44}$S$_4$ (2266.4): C 53.00, H 5.34, N 4.94, S 5.66; found: C 52.73, H 5.59, N 4.86, S 5.62.

Tetrakis(1-tetraacetylgalactosylthioureidomethyl)tetramethylcavitand (8): Yield: 85%; m.p. 233 °C (isopropanol); ^{1}H NMR (DMSO-*d6*) δ: 7.73 (bs, 12 H; ArH, NH), 5.91 (d, *J* = 7.5 Hz, 4 H; O$_2$CH), 5.78 (t, *J* = 9.5 Hz, 4 H; H$_1$-gal), 5.38-5.18 (m, 8 H; H$_4$, H$_3$-gal), 4.93 (t, *J* = 9.2 Hz, 4 H; H$_2$-gal), 4.81 (d, *J* = 7.5 Hz, 4 H; Ar$_2$CH), 4.44 (bs, 8 H; ArCH$_2$), 4.22 (t+bs, *J* = 6.2 Hz, 8 H; O$_2$CH, H$_5$-gal), 3.98 and 3.97 (s, 8 H;

H$_{6a}$, H$_{6b}$-gal), 2.09 (s, 12 H; CH$_3$CO), 1.99 (s, 12 H; CH$_3$CO), 1.90 (s, 24 H; CH$_3$CO), 1.82 (d, *J* = 7.3 Hz, 12 H; CH$_3$C); ^{13}C NMR (DMSO-*d$_6$*) δ: 183.2, 169.9, 169.4, 169.3, 152.5, 139.0, 123.1, 121.8, 99.1, 81.4, 72.7, 71.9, 70.4, 67.9, 61.6, 37.8, 31.3, 20.2, 20.3, 15.9; MS (MALDI) *m/z* (%): 2265.0 (100) [*M$^+$*], 2288.0 (80) [*M*+Na$^+$]; elemental analysis calcd (%) for C$_{100}$H$_{120}$N$_8$O$_{44}$S$_4$ (2266.4): C 53.00, H 5.34, N 4.94, S 5.66; found: C 52.80, H 5.50, N 4.83, S 5.60.

Tetrakis(1-tetraacetylglucosylthioureidomethyl)tetraamylcavitand (9): Yield: 72%; m.p. 179-180 °C (isopropanol); ^{1}H NMR (DMSO-*d$_6$*) δ: 7.77 (bs, 8 H; NH), 7.58 (s, 4 H; ArH), 5.91 (d, *J* = 7.3 Hz, 4 H; O$_2$CH), 5.82 (bs, 4 H; H$_1$-glu), 5.34 (t, *J* = 9.4 Hz, 4 H; H$_3$-glu), 4.95-4.7 (m, 8 H; H$_2$, H$_4$-glu), 4.60 (t, *J* = 7.9 Hz, 4 H; Ar$_2$CH), 4.43 (bs, 8 H; ArCH$_2$), 4.28 (bd, 4 H; O$_2$CH), 4.15 (dd, *J*$_{6a6b}$ = 12.4 Hz, *J*$_{6a5}$ = 4.4 Hz, 4 H; H$_{6a}$-glu), 4.1-3.7 (bs+s, 8 H; H$_{6b}$, H$_5$-glu), 2.35 (bs, 8 H; C*H$_2$*CH), 1.98 and 1.97 (s, 36 H; CH$_3$CO), 1.93 (s, 12 H; CH$_3$CO), 1.45-1.2 (bm, 24 H; (CH$_2$)$_3$), 0.88 (d, *J* = 7.0 Hz, 12 H; CH$_3$C); ^{13}C NMR (DMSO-*d$_6$*) δ: 183.2, 169.9, 169.4, 169.2, 152.9, 138.0, 123.4, 121.7, 99.1, 81.4, 72.7, 71.9, 70.5, 68.0, 61.6, 38.1, 36.9, 31.4, 29.2, 27.4, 22.1, 20.2, 20.3, 13.9; MS (MALDI) *m/z* (%): 2489.1 (70) [*M$^+$*], 2512.1 (100) [*M*+Na$^+$]; elemental analysis calcd (%) for C$_{116}$H$_{152}$N$_8$O$_{44}$S$_4$ (2490.8): C 55.94, H 6.15, N 4.50, S 5.15; found: C 56.07, H 6.25, N 4.26, S 5.07.

Tetrakis(1-tetracellobiosylthioureidomethyl)tetramethylcavitand (10): Yield: 86%; m.p. 248-250 °C (isopropanol); ^{1}H NMR (DMSO-*d$_6$*) δ: 7.74 (bs, 12 H; ArH, NH), 5.91 (bs, 4 H; O$_2$CH), 5.78 (t, *J* = 8.4 Hz, 4 H; H$_1$-cel), 5.35-5.1 (m, 8 H; H$_{1'}$, H$_3$-cel), 5.0-4.7 (m, 16 H; Ar$_2$CH, H$_2$, H$_{2'}$, H$_{3'}$-cel), 4.65 (t, *J* = 9.0 Hz, 4 H; H$_{4'}$-cel), 4.42 (bs, 8 H; ArCH$_2$), 4.25 (t+bs, *J* = 10.8 Hz, 8 H, O$_2$CH, H$_4$-cel), 4.14-3.9 (m, 16 H; H$_{6a}$, H$_{6a'}$, H$_{6b}$, H$_{6b'}$-cel), 3.7-3.9 (m, 8 H; H$_5$, H$_{5'}$-cel), 2.05 (s, 12 H; CH$_3$CO), 2.02 (s, 12 H; CH$_3$CO), 2.0-1.94 (m, 48 H; CH$_3$CO), 1.92 (s, 12 H; CH$_3$CO), 1.82 (d, *J* = 6.6 Hz, 12 H; CH$_3$C); ^{13}C NMR (DMSO-*d$_6$*) δ: 183.2, 170.2, 169.9, 169.5, 169.4, 169.3, 169.1, 168.9, 152.5, 139.0, 123.3, 121.3, 99.2, 81.2, 76.2, 73.1, 72.6, 72.2, 71.0, 70.6, 70.4, 67.7, 62.2, 61.5, 38.0, 31.3, 20.6, 20.4, 20.3, 20.1, 15.9; MS (MALDI) *m/z* (%): 3438.5 (100) [*M*+Na$^+$]; elemental analysis calcd (%) for C$_{149}$H$_{186}$N$_8$O$_{75}$S$_4$ (3417.4): C 52.37, H 5.49, N 3.28, S 3.75; found: C 52.31, H 5.53, N 3.16, S 3.79.

General procedure for the preparation of the glycoclusters 11, 12, 13, 14, 16: A catalytic amount of MeONa (about 5% with respect to each AcO-substituent in the

precursor) was added to a solution of the acetylated glycoclusters **7, 8, 9, 10, 15** (0.088 mmol) in MeOH:CH$_2$Cl$_2$ (1:4; 50 mL). The reaction mixture was stirred overnight at room temperature. Water (5 mL) was added and the reaction mixture was stirred for an additional 20 min. Subsequently Amberlite IR-120 H$^+$ (washed before with methanol) was added and stirring was continued for an additional 15 min. The Amberlite was filtered off and the organic solvents were evaporated at reduced pressure (t<30 °C); the water was removed by freeze-drying. The yield of glycoclusters is almost quantitative. An additional purification by sonication with diisopropyl ether and washing with isopropanol is also possible.

Tetrakis(1-glucosylthioureidomethyl)tetramethylcavitand (11): Yield: 96%; m.p. > 350 °C; ^{1}H NMR (DMSO-d_6) δ: 7.73 (s, 4 H; ArH), 7.67 (s, 4 H; NH), 7.49 (s, 4 H; NH), 5.95 (d, $J = 6.6$ Hz, 4 H; O$_2$CH), 5.16 (bs, 4 H; H$_1$-glu), 4.81 (q, $J = 7.3$ Hz, 4 H; Ar$_2$CH), 4.43 (bs, 8 H; ArCH$_2$), 4.30 (d, $J = 6.6$ Hz, 4 H; O$_2$CH), 3.97 (bs, 16 H; OH), 3.59 (bd, $J_2 = 11.3$ Hz, 4 H, H$_{6a}$-glu), 3.42 (bd, $J_2 = 10.0$ Hz, 4 H; H$_{6b}$-glu), 3.22-2.85 (m, 16 H; H$_2$, H$_3$, H$_4$, H$_5$-glu), 1.81 (d, $J = 7.3$ Hz, 12 H; CH$_3$C); ^{13}C NMR (DMSO-d_6) δ: 183.1, 152.5, 139.0, 123.8, 121.1, 99.1, 83.6, 78.0, 77.5, 72.8, 69.7, 60.5, 37.8, 31.3, 15.9; MS (MALDI) m/z (%): 1615.8 (100) [M+Na$^+$]; elemental analysis calcd (%) for C$_{68}$H$_{88}$N$_8$O$_{28}$S$_4$ (1593.7): C 51.25, H 5.57, S 8.05; found: C 50.98, H 5.61, S 8.00.

Tetrakis(1-galactosylthioureidomethyl)tetramethylcavitand (12): Yield: 95%, m.p. > 350 °C; ^{1}H NMR (DMSO-d_6) δ: 7.23 (s, 4 H; ArH), 7.67 (s, 4 H; NH), 7.49 (s, 4 H; NH), 5.95 (d, $J = 6.6$ Hz, 4 H; O$_2$CH), 5.15 (bs, 4 H; H$_1$-gal), 4.98 (bs, 8 H; OH), 4.81 (bd, $J = 7.3$ Hz, 8 H; Ar$_2$CH, OH), 4.42 (bs, 12 H; ArCH$_2$, OH), 4.29 (d, $J = 6.6$ Hz, 4 H; O$_2$CH), 3.58 (d, $J_2 = 11.3$ Hz, 4 H; H$_{6a}$-gal), 3.5-2.8 (m, 20H; H$_2$, H$_3$, H$_4$, H$_5$, H$_{6b}$-gal), 1.81 (d, $J = 7.3$ Hz, 12 H; CH$_3$C); ^{13}C NMR (DMSO-d_6) δ: 183.0, 152.5, 139.0, 123.8, 121.1, 99.1, 83.5, 78.0, 69.7, 72.8, 77.5, 60.5, 37.8, 31.3, 15.9; MS (MALDI) m/z (%): 1615.6 (100) [M+Na$^+$]; elemental analysis calcd (%) for C$_{68}$H$_{88}$N$_8$O$_{28}$S$_4$ (1593.7): C 51.25, H 5.57, S 8.05; found: C 50.95, H 5.67, S 7.98.

Tetrakis(1-glucosylthioureidomethyl)tetraamylcavitand (13): Yield: 90%; m.p. > 350 °C; ^{1}H NMR (DMSO-d_6) δ: 7.72 (s, 4 H; NH), 7.58 (s, 4 H; ArH), 7.48 (s, 4 H; NH), 5.95 (d, $J = 6.6$ Hz, 4 H; O$_2$CH), 5.19 (bs, 4 H; H$_1$-glu), 4.96 (bs, 8 H; OH), 4.82 (bs, 4 H; OH), 4.62 (q, $J = 7.3$ Hz, 4 H; Ar$_2$CH), 4.43 (bs, 8 H; ArCH$_2$), 4.30 (d, $J = 6.6$ Hz, 4 H; O$_2$CH), 3.60 (d, $J_2 = 11.0$ Hz, 4 H; H$_{6a}$-glu), 3.46 (d, $J_2 = 10$ Hz, 4 H;

H$_{6b}$-glu), 3.4-2.9 (m, 20 H; OH, H$_2$, H$_3$, H$_4$, H$_5$-glu), 2.37 (q, J = 7.2 Hz, 8 H; CH_2CH), 1.52-1.15 (m, 24 H; (CH$_2$)$_3$), 0.89 (t, J = 7.2 Hz, 12 H; CH$_3$); ^{13}C NMR (DMSO-d_6) δ: 183.1, 152.8, 138.0, 123.8, 121.5, 99.2, 83.6, 78.0, 77.5, 72.8, 69.7, 60.5, 37.8, 36.9, 31.4, 29.2, 27.4, 22.2, 13.9; MS (MALDI) *m/z* (%): 1840.0 (100) [*M*+Na$^+$]; elemental analysis calcd (%) for C$_{84}$H$_{120}$N$_8$O$_{28}$S$_4$ (1818.2): C 55.49, H 6.65, S 7.05; found.: C 55.28, H 6.75, S 6.95.

Tetrakis(1-cellobiosylthioureidomethyl)tetramethylcavitand (14): Yield: 92%; m.p. > 350 °C; ^{1}H NMR (DMSO-d_6) δ: 7.73 (s, 8 H; ArH, NH), 7.51 (s, 4 H; NH), 5.96 (bs, 4 H; O$_2$CH), 5.21 (bs, 4 H; H$_1$-cel), 4.81 (d, J = 6.9 Hz, 8 H; Ar$_2$CH, OH), 4.6-2.9 (bs+m, 88 H+water; ArCH$_2$, O$_2$CH, OH, H$_{2\text{-}6b}$, H$_{1'\text{-}6b'}$-cel), 1.81 (d, J = 6.3 Hz, 12 H; CH$_3$C); ^{13}C NMR (DMSO-d_6) δ: 180.9, 152.5, 139.0, 123.8, 121.1, 103.0, 83.3, 79.7, 76.7, 76.4, 76.2, 75.7, 74.8, 73.3, 72.5, 70.0, 61.0, 60.2, 37.8, 31.3, 15.9; MS (MALDI) *m/z* (%): 2263.9 (100) [*M*+Na$^+$]; elemental analysis calcd (%) for C$_{92}$H$_{128}$N$_8$O$_{48}$S$_4$·10H$_2$O (2422.5): C 45.62, H 6.16, N 4.63, S 5.29; found: C 45.82, H 6.04, N 4.43, S 5.18.

Tetrakis(1-glucosylthiomethyl)tetramethylcavitand (16): Yield: 91%; m.p. > 350 °C; ^{1}H NMR (DMSO-d_6) δ: 7.63 (s, 4 H; ArH), 6.02 (d, J = 7.3 Hz, 4 H; O$_2$CH), 5.04 (bs, 8 H; OH), 4.79 (q, J = 7.3 Hz, 4 H; Ar$_2$CH), 4.70 (bs, 4 H; OH), 4.40-4.20 (m, 8 H; O$_2$CH, H$_1$-glu), 3.85-3.67 (m, 8 H; H$_{6a}$-glu, OH), 3.5-3.25 (m, 12 H; H$_{6b}$-glu, ArCH$_2$S), 3.25-3.0 (m, 12 H; H$_3$, H$_4$, H$_5$-glu), 2.93 (t, J = 9.0 Hz, 4 H; H$_2$-glu) 1.82 (d, J = 7.3 Hz, 12 H; CH$_3$C); ^{13}C NMR (DMSO-d_6) δ: 152.1, 138.8, 125.9, 120.0, 99.2, 84.3, 81.0, 78.2, 73.0, 70.2, 31.2, 21.9, 16.0; MS (MALDI) *m/z* (%): 1447.6 (100) [*M*+Na$^+$]; elemental analysis calcd (%) for C$_{64}$H$_{80}$O$_{28}$S$_4$ (1425.6): C 53.92, H 5.66, S 9.00; found: C 53.63, H 5.77, S 8.89.

Tetrakis(1-tetraacetylglucosylthiomethyl)tetramethylcavitand (15): A solution of 2,3,4,6-tetra-O-acetyl-β-glucopyranosylthiol[39] (530 mg, 1.45 mmol) in CH$_2$Cl$_2$ (5 mL) was added to a suspension of K$_2$CO$_3$ (0.95 g, 2.9 mmol) in a solution of tetrakis(bromomethyl)tetramethylcavitand **1** (289 mg, 0.29 mmol) in CH$_2$Cl$_2$ (15 mL). The reaction mixture was stirred at room temperature for 75 h, whereupon the salts were filtered off. The solution was evaporated to dryness at reduced pressure (t<40 °C). The solid was triturated with diethyl ether and recrystallized from MeOH. Yield: 88%; m.p. 176-177 °C (MeOH); ^{1}H NMR (CDCl$_3$) δ: 7.20 (s, 4 H; ArH), 5.91 (d, J = 7.3 Hz, 4 H; O$_2$CH), 5.19 (t, J = 9.2 Hz, 4 H; H$_3$-glu), 5.09 (t, J = 9.5 Hz, 4 H; H$_4$-

glu), 5.00 (t, $J = 9.9$ Hz, 4 H; H_2-glu), 4.98 (q, $J = 7.3$ Hz, 4 H, Ar_2CH), 4.55 (d, $J = 9.9$ Hz, 4 H; H_1-glu), 4.36 (d, $J = 7.3$ Hz, 4 H; O_2CH), 4.24 (dd, $J_{6a6b} = 12.5$ Hz, $J_{56b} = 4.4$ Hz, 4 H; H_{6b}-glu), 4.10 (dd, $J_{6b6a} = 12.5$ Hz, $J_{56a} = 2.4$ Hz, 4 H; H_{6a}-glu), 3.6-3.9 (m, 12 H; $ArCH_2$, H_5-glu), 2.07 (s, 12 H; CH_3CO), 2.04 (s, 12 H; CH_3CO), 2.00 (s, 12 H; CH_3CO), 1.81 (s, 12 H; CH_3CO), 1.76 (d, $J = 7.3$ Hz, 12 H; CH_3C); ^{13}C NMR (DMSO-d_6) δ: 169.9, 169.4, 169.2, 168.9, 152.2, 138.6, 124.2, 120.5, 99.5, 82.5, 74.3, 72.9, 69.6, 68.1, 61.9, 31.2, 23.5, 20.3, 20.2, 19.6, 15.9; MS (MALDI) *m/z* (%): 2119.7 (80) $[M+Na^+]$; elemental analysis calcd (%) for $C_{96}H_{112}O_{44}S_4$ (2098.2): C 54.96, H 5.38, S 6.11; found: C 54.80, H 5.38, S 6.06.

Tetrakis(propylthioureidomethyl)tetraamylcavitand (20): A solution of propyl-isothiocyanate (242 mg, 0.25 mL, 1.8 mmol) and tetrakis(aminomethyl)cavitand **6** (278 mg, 0.3 mmol) in MeOH:CH_2Cl_2 (1:3; 20 mL) was stirred at room temperature for 2 days. The solvent was evaporated to dryness. The resulting solid was triturated with hexane (2 × 20 mL) and then purified by column chromatography (CH_2Cl_2 containing 5% MeOH, $R_f = 0.17$) followed by trituration with acetonitrile (2 × 5 mL). Yield: 83%; m.p. 214-215 °C; ^1H NMR (CDCl$_3$) δ: 7.12 (s, 4 H; ArH), 6.30 (bs, 4 H; NH), 6.13 (bs, 4 H; NH), 5.99 (d, $J = 7.2$ Hz, 4 H; O_2CH), 4.73 (t, $J = 8.0$ Hz, 4 H; Ar_2CH), 4.41 (d, $J = 7.2$ Hz, 4 H; O_2CH), 4.35 (bs, 8 H; $ArCH_2N$), 3.42 (bs, 8 H; $AlkCH_2N$), 2.20 (q, $J = 7.2$ Hz, 8 H; CH_2CH), 1.76-1.60 (m, 8 H; $MeCH_2CH_2N$), 1.48-1.28 (m, 24 H; $(CH_2)_3$), 1.02-0.86 (m, 24 H; CH_3); ^{13}C NMR (CDCl$_3$) δ: 181.0, 153.1, 138.5, 122.8, 120.4, 99.9, 36.9, 32.0, 30.0, 27.6, 22.6, 22.2, 14.1, 11.5; MS (MALDI) *m/z* (%): 1336.7 (100) $[M^+]$; elemental analysis calcd (%) for $C_{72}H_{104}N_8O_8S_4$ (1337.9): C 64.64, H 7.83, N 8.38, S 9.59; found: C 64.67, H 7.82, N 8.29, S 9.64.

References and notes

1.   *Comprehensive Supramolecular Chemistry;* Vol. 1; Lehn, J.-M.; Atwood, J. L.; Davies, J. E. D.; MacNicol, D. D.; Vögtle, F.; Gokel, G. W., Eds.; Pergamon: Oxford, 1996; *Comprehensive Supramolecular Chemistry;* Vol. 2; Lehn, J.-M.; Atwood, J. L.; Davies, J. E. D.; MacNicol, D. D.; Vögtle, F., Eds.; Pergamon: Oxford, 1996; Zhang, X. X.; Bradshaw, J. S.; Izatt, R. M. *Chem. Rev.* **1997**, *97*, 3313-3361.

2.   Connors, K. A., *Binding Constants: The Measurement of Molecular Complex Stability;* Wiley-Interscience: New York, 1987; Fielding, L. *Tetrahedron* **2000**, *56*, 6151-6170; Hirose, K. *J. Incl. Phenom. Macro.* **2001**, *39*, 193-209.

3.   For reviews on the application of mass spectrometry for studying supramolecular interactions, see: Loo, J. A. *Mass Spectrom. Rev.* **1997**, *16*, 1-23; Schalley, C. A. *Int. J. Mass. Spec.* **2000**, *194*, 11-39; Brodbelt, J. S. *Int. J. Mass. Spec.* **2000**, *200*, 57-69; Schalley, C. A. *Mass Spectrom. Rev.* **2001**, *20*, 253-309; Vincenti, M.; Irico, A. *Int. J. Mass. Spec.* **2002**, *214*, 23-36; Daniel, J. M.; Friess, S. D.; Rajagopalan, S.; Wendt, S.; Zenobi, R. *Int. J. Mass. Spec.* **2002**, *216*, 1-27; Ganem, B.; Henion, J. D. *Bioorg. Med. Chem.* **2003**, *11*, 311-314.

4.   Kempen, E. C.; Brodbelt, J. S. *Anal. Chem.* **2000**, *72*, 5411-5416.

5.   Nakamura, M.; Fujioka, T.; Sakamoto, H.; Kimura, K. *New J. Chem.* **2002**, *26*, 554-559.

6.   Koomen, J. A.; Lucas, J. E.; Haneline, M. R.; King, J. D. B.; Gabbai, F.; Russell, D. H. *Int. J. Mass. Spec.* **2003**, *225*, 225-231.

7.   Timmerman, P.; Verboom, W.; Reinhoudt, D. N. *Tetrahedron* **1996**, *52*, 2663-2704; Jasat, A.; Sherman, J. C. *Chem. Rev.* **1999**, *99*, 931-967; Verboom, W., *Cavitands.* In *Calixarenes 2001;* Asfari, Z.; Böhmer, V.; Harrowfield, J.; Vicens, J., Eds.; Kluwer: Dordrecht, 2001; pp 181-198; Sherman, J. *Chem. Commun.* **2003**, 1617-1623.

8.   Nissink, J. W. M.; Boerrigter, H.; Verboom, W.; Reinhoudt, D. N.; van der Maas, J. H. *J. Chem. Soc., Perkin Trans. 2* **1998**, 2541-2546; Nissink, J. W. M.; Boerrigter, H.; Verboom, W.; Reinhoudt, D. N.; van der Maas, J. H. *J. Chem. Soc., Perkin Trans. 2* **1998**, 2623-2630.

9.   Boerrigter, H.; Grave, L.; Nissink, J. W. M.; Chrisstoffels, L. A. J.; van der Maas, J. H.; Verboom, W.; de Jong, F.; Reinhoudt, D. N. *J. Org. Chem.* **1998**, *63*, 4174-4180.

10. Ahn, D. R.; Kim, T. W.; Hong, J. I. *Tetrahedron Lett.* **1999**, *40*, 6045-6048; Haino, T.; Rudkevich, D. M.; Shivanyuk, A.; Rissanen, K.; Rebek, J. *Chem. Eur. J.* **2000**, *6*, 3797-3805.

11. Sebo, L.; Diederich, F.; Gramlich, V. *Helv. Chim. Acta* **2000**, *83*, 93-113.

12. Grote Gansey, M. H. B.; Bakker, F. K. G.; Feiters, M. C.; Geurts, H. P. M.; Verboom, W.; Reinhoudt, D. N. *Tetrahedron Lett.* **1998**, *39*, 5447-5450.

13. Piatnitski, E. L.; Flowers II, R. A.; Deshayes, K. *Chem. Eur. J.* **2000**, *6*, 999-1006; Fox, O. D.; Leung, J. F. Y.; Hunter, J. M.; Dalley, N. K.; Harrison, R. G. *Inorg. Chem.* **2000**, *39*, 783-790; Park, S. J.; Hong, J. I. *Tetrahedron Lett.* **2000**, *41*, 8311-8315.

14. Gui, X.; Sherman, J. C. *Chem. Commun.* **2001**, 2680-2681.

15. Fraser, J. R.; Borecka, B.; Trotter, J.; Sherman, J. C. *J. Org. Chem.* **1995**, *60*, 1207-1213.

16. Mezo, A. R.; Sherman, J. C. *J. Org. Chem.* **1998**, *63*, 6824-6829; Mezo, A. R.; Sherman, J. C. *J. Am. Chem. Soc.* **1999**, *121*, 8983-8994.

17. Pellet-Rostaing, S.; Nicod, L.; Chitry, F.; Lemaire, M. *Tetrahedron Lett.* **1999**, *40*, 8793-8796.

18. Middel, O.; Verboom, W.; Reinhoudt, D. N. *Eur. J. Org. Chem.* **2002**, 2587-2597.

19. Lim, C. W.; Hong, J. I. *Tetrahedron Lett.* **2000**, *41*, 3113-3117; Park, S. J.; Shin, D. M.; Sakamoto, S.; Yamaguchi, K.; Chung, Y. K.; Lah, M. S.; Hong, J. I. *Chem. Commun.* **2003**, 998-999.

20. Sansone, F.; Chierici, E.; Casnati, A.; Ungaro, R. *Org. Biomol. Chem.* **2003**, *1*, 1802-1809; For a recent review, see: Casnati, A.; Sansone, F.; Ungaro, R. *Acc. Chem. Res.* **2003**, *36*, 246-254.

21. For a recent example, see: Aoyama, Y.; Kanamori, T.; Nakai, T.; Sasaki, T.; Horiuchi, S.; Sando, S.; Niidome, T. *J. Am. Chem. Soc.* **2003**, *125*, 3455-3457, and references cited therein.

22. Hayashida, O.; Nishiyama, K.; Matsuda, Y.; Aoyama, Y. *Tetrahedron Lett.* **1999**, *40*, 3407-3410.

23. For recent reviews on carbohydrate clusters, see: Fulton, D. A.; Stoddart, J. F. *Bioconjugate Chem.* **2001**, *12*, 655-672; Ortiz Mellet, C.; Defaye, J.; Garcia Fernandez, J. M. *Chem. Eur. J.* **2002**, *8*, 1982-1990.

24. For reviews on anion recognition, see: Antonisse, M. M. G.; Reinhoudt, D. N. *Chem. Commun.* **1998**, 443-448; Beer, P. D.; Gale, P. A. *Angew. Chem., Int. Ed.* **2001**, *40*, 486-516; Gale, P. A. *Coord. Chem. Rev.* **2003**, *240*, 191-221, and other reviews in this issue.

25. Sorrell, T. N.; Pigge, F. C. *J. Org. Chem.* **1993**, *58*, 784-785.

26. In ESI-MS, a dilute analyte solution is pumped through a needle to which a high voltage is applied. A Taylor cone with an excess of negative or positive charge on its surface forms as a result of the electric field gradient between the ESI needle and the counter electrode. Charged droplets, formed at the tip of the Taylor cone, move towards the entrance of the mass spectrometer to produce free, charged analyte molecules by mechanisms that involve dividing large droplets into smaller and smaller ones (coulomb fission mechanism) and a release of ions from the droplet surface (ion evaporation mechanism). For reviews on the mechanisms involved in ESI-MS, see: Kebarle, P.; Tang, L. *Anal. Chem.* **1993**, *65*, A972-A986; Kebarle, P. *J. Mass. Spec.* **2000**, *35*, 804-817.

27. Cech, N. B.; Enke, C. G. *Mass Spectrom. Rev.* **2001**, *20*, 362-387.

28. In the case of ESI-MS studies of simple analyte solutions a linear response to changes in the concentration is usually monitored. However, the presence of co-solvents and additional species such as salts cause rather large decreases in the observed signal intensity (Sherman, C. L.; Brodbelt, J. S. *Anal. Chem.* **2003**, *75*, 1828-1836). We found that in a titration experiment the systematic signal intensity decrease is excellently fitted with a parabolic function within the non-suppressed area.

29. In ref. 4 the authors found a linear calibration curve, since they only selected a relatively narrow concentration range to enhance the accuracy of their K_a-value determination.

30.   Advantages and disadvantages of competitive experiments are thoroughly evaluated in a recent paper on the rapid screening of binding constants by calibrated competitive ^{1}H NMR spectroscopy: Heath, R. E.; Dykes, G. M.; Fish, H.; Smith, D. K. *Chem. Eur. J.* **2003**, *9*, 850-855.

31.   For evaluations of *relative* binding affinities of different host-guest complexes based on relative intensities of signals in mass spectrometry see, for example: Brady, P. A.; Sanders, J. K. M. *New J. Chem.* **1998**, *22*, 411-417; Irico, A.; Vincenti, M.; Dalcanale, E. *Chem. Eur. J.* **2001**, *7*, 2034-2042.

32.   For instance: Jagessar, R. C.; Burns, D. H. *Chem. Commun.* **1997**, 1685-1686.

33.   Boerrigter, H.; Verboom, W.; Reinhoudt, D. N. *J. Org. Chem.* **1997**, *62*, 7148-7155.

34.   Tashpulatov, A. A.; Rakhmatullaev, I.; Afanas'ev, V. A.; Ismailov, N. *Zh. Org. Khim.* **1988**, *24*, 1893-1897, *J. Org. Chem. USSR (Engl. Transl.)* **1988**, *24*, 1707-1710.

35.   Nissink, J. W. M.; Wink, T.; van der Maas, J. H. *J. Mol. Struct.* **1999**, *479*, 65-73.

36.   Yamamoto, I.; Fukui, K.; Yamamoto, S.; Ohta, K.; Matsuzaki, K. *Synthesis* **1985**, 686-688.

37.   Selkti, M.; Kassab, R.; Lopez, H. P.; Villain, F.; de Rango, C. *J. Carbohydr. Chem.* **1999**, *18*, 1019-1032.

38.   Ogura, H.; Takahashi, H. *Heterocycles* **1982**, 87-90.

39.   Peerlings, H. W. I.; Nepogodiev, S. A.; Stoddart, J. F.; Meijer, E. W. *Eur. J. Org. Chem.* **1998**, 1879-1886.

(THIO)UREA-FUNCTIONALIZED CAVITANDS AS EXCELLENT RECEPTORS FOR ORGANIC ANIONS IN POLAR MEDIA[℘]

*Ureidocavitand **1** and thioureidocavitand **2** bind in acetonitrile organic anions such as acetate, propionate, butyrate, etc. with K_a-values of $2\text{-}8 \times 10^5 \ M^{-1}$ and $2\text{-}9 \times 10^6 \ M^{-1}$, respectively, as was determined with isothermal microcalorimetry (ITC). Bringing together four (thio)urea binding sites on a molecular platform gives rise to about 2000 times higher binding constants, compared with those of the corresponding single binding sites. Glucose- and galactose-containing thioureidocavitands **5** and **6** bind acetate in 1:1 acetonitrile/water with a K_a-value of $2.15 \times 10^3 \ M^{-1}$.*

4.1 Introduction

Recognition of anions by synthetic receptors, which mimics non-covalent interactions in nature, represents an important area in supramolecular chemistry.[1] Urea and thiourea moieties are well known binding sites for anions.[2] To enhance the sensitivity and the selectivity for the recognition of organic anions,[3] they have been attached to a variety of scaffolds, viz. calixarenes,[4,5] azamacrocycles,[6] saccharides,[7] organometallic complexes,[8] crown ethers,[9] and heterocycles,[10] as well as incorporated in cyclophanes[11] or dendritic wedges.[12] For instance, acetate recognition has been reported for mono- and bis(thio)urea-appended calixarenes. Stibor et al. found that a 1,3-alternate calix[4]arene urea receptor binds acetate ($K_a \sim 4000$ M^{-1} in CDCl$_3$:acetonitrile-d_3 = 4:1) with a profound allosteric effect.[13] The groups of Beer[14] and Ungaro[5] published ditopic calix[4]arene receptors in which an acetate counter-ion is bound by (a) (thio)urea moiety(ies).

Recently, Boerrigter et al. reported that cavitand-based anion receptors, having four thiourea moieties, complex inorganic anions with a preference for chloride.[15] In Chapter 3 the complexation behavior of the corresponding glycocluster-containing cavitands was described.[16] This chapter deals with the excellent complexation behavior of cavitand (thio)urea receptors toward a variety of organic anions.

4.2 Results and discussion

Self-association of the hosts. (Thio)ureidocavitands **1** and **2** undergo 1:1 self-association similarly to that of the corresponding tetraurea calixarenes derivatives.[17] The nanoelectrospray ionization (nanoESI) mass spectra showed distinct peaks for 1:1 capsules+Na$^+$. The formation of higher aggregates could not be detected. In addition, the formation of unspecific dimers can be excluded, since the ^{1}H NMR spectra show C_4 symmetry. ^{1}H NMR dilution experiments gave for **2@2** a K_a-value of 7.0 ± 0.2×10^4 M^{-1} in acetonitrile-d_3; changing the concentration from 1.5 mM to 0.01 mM, the NH shifted from 6.47 to 6.95 ppm and the ArCH$_2$ from 4.31 to 4.47 ppm. ITC dilution experiments showed that the association is a strongly entropy-driven exothermic process (K_{diss} = 1.46 ± 0.05×10^{-5} mol l^{-1}; K_a = 6.85 ± 0.2×10^4 M^{-1}, ΔG = -6.59 kcal mol^{-1}, ΔH = -2.90 kcal mol^{-1}, ΔS = 12.4 cal mol^{-1} K^{-1}). Ureidocavitand **1** has a less pronounced tendency to self-assemble (K_a = 4600 M^{-1} in acetonitrile-d_3).[18]
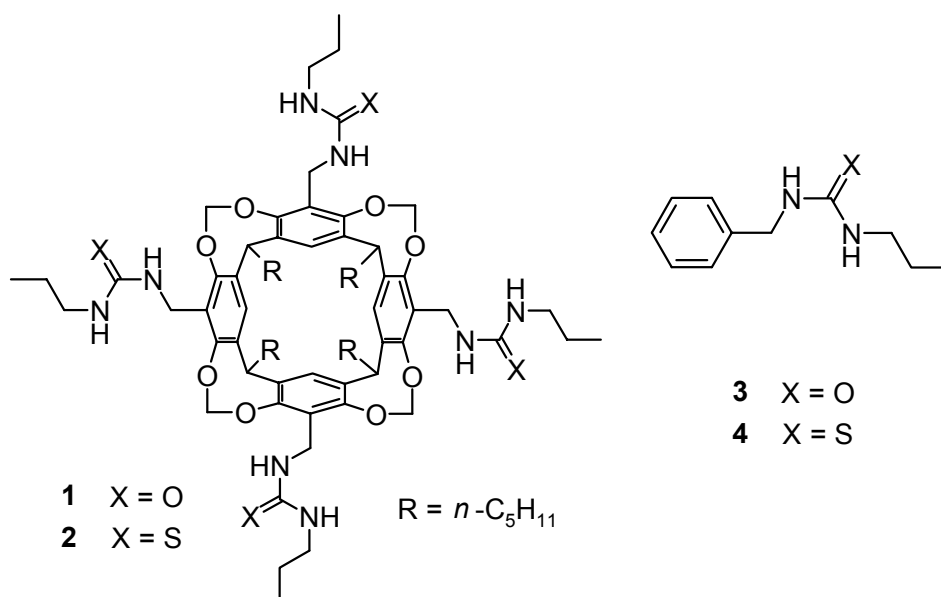
Chart 1. (Thio)ureidocavitands and reference compounds.

Complexation studies. The complexation behavior of (thio)ureidocavitands **1** and **2** towards formate, acetate, propionate, butyrate, valerate, benzoate, and lactate (tetrabutylammonium salts) in acetonitrile (or acetonitrile-d_3) was studied. In all cases, 1:1 complexation was clearly observed in the electrospray ionization (ESI) negative-ion mode mass spectra. Peaks of complexes of the 1:1 self-assembled capsules with an anion were not present. The formation of 1:1 capsules containing two anions (overall 2:2 stoichiometry) can be excluded, since in the ESI-MS spectra the corresponding doubly charged species were not detected.

^{1}H NMR spectroscopy evidently showed the formation of host-guest complexes. In a few cases, pronounced shifts of the guest hydrogens are observed (Table 1). Both dilution and titration experiments in the cases of acetate and propionate and hosts **1** and **2** did not give rise to chemical shift changes of the encapsulated guests, indicating a slow process on the ^{1}H NMR time scale. In addition, upon dilution the ratio of the intensities of signals of the host and bound guest did not change, which indicates a strong binding.

The four convergent (thio)urea binding sites can provide eight NH-protons. The complexation of thioureidocavitand **2** with acetate was studied with molecular modeling (Quanta 97, CHARMm 24.0), which showed that all eight NH-protons are involved in the complexation of the carboxylate forming hydrogen bonds,[19] and the methyl group pointing into the cavitand. The included anion can adopt two

orientations depending on the size of the substituent attached to the carboxylate function. In principle, it can point outside (*out*-isomer) or inside (*in*-isomer) the cavity. From the large negative chemical shift values in the cases of acetate and propionate (Table 1), it is clear that they prefer the formation of *in*-isomers. Apparently, the alkyl chains fit well in the cavity of the cavitand, which is, due to the anisotropy effect, reflected in large upfield shifts (for acetate $\Delta\delta$ is ~ 3.7 ppm). Butyrate cannot be efficiently accommodated in the cavity anymore; therefore, it appears as very broad signals.[20] Increasing the alkyl chain to valerate gives rise to the formation of an *out*-isomer. The C_4-valerate chain is too large for the cavitand cavity. In the ^{1}H NMR spectrum, there is only a small shift from 0.86 to 0.81 ppm for the terminal methyl group upon complexation. NOESY ^{1}H NMR spectra of the acetate and propionate complexes of hosts **1** and **2** reveal cross-peaks between the guest and the cavitand (Ar*H*, O_2CH^i*H*) and the presence of small cross-peaks between the *in*- and *out*-isomers (Fig. 1). Unfortunately, the signal of the *out*-isomer (δ ~ 1.95 ppm) is hidden under that of CHD_2CN. However, based on the integrals of the peaks of the *in*-isomer and those of a few signals of the hosts in 1:1 complexes, the amount of out-isomer in both cases is only 5-7 %. A corresponding experiment in $CDCl_3$ showed the same behavior and the presence of a small peak for the *out*-isomer at δ 2.05 ppm (in-isomer: -2.04 ppm, free acetate: 1.97 ppm). In both solvents the chemical shift of the acetate out-isomer is at lower field than that of the unbound acetate, which is probably due to the more electron-withdrawing environment upon complexation.

Table 1. ^{1}H NMR data of the CH_3 protons of free and complexed carboxylates

(tetrabutylammonium salts) in hosts **1** and **2** in acetonitrile-d_3.

Entry	Guest	^{1}H NMR chemical shifts, ppm		
		CH_3 of free guest	**1**@guest	**2**@guest
1	Acetate	1.65	- 2.14	- 2.00
2	Propionate	0.95	- 2.96	- 3.02
3	Butyrate	0.86	- 0.38[a]	- 1.26[a]
4	Valerate	0.88	0.81	0.81

[a] Very broad signals.
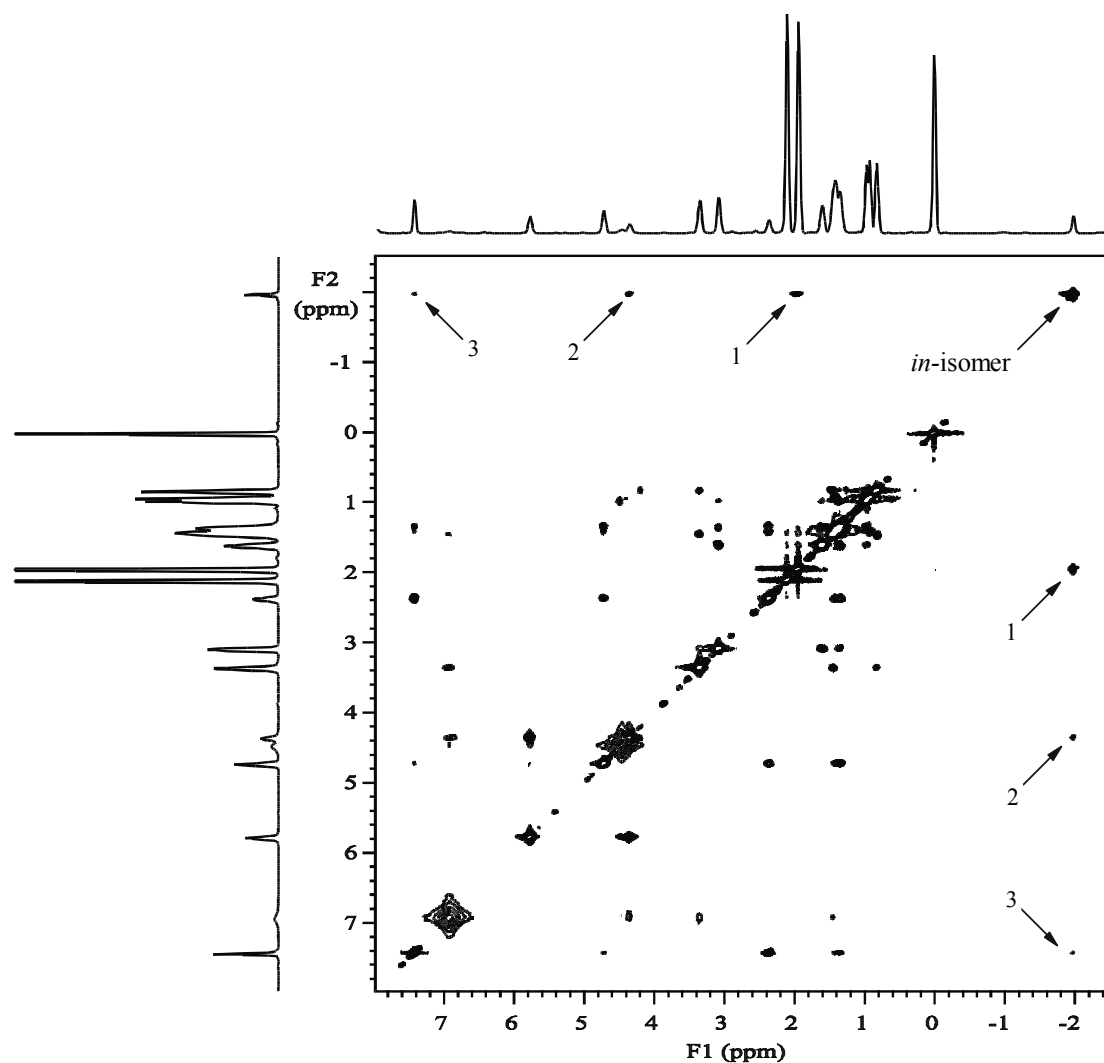
Figure 1. NOESY (mixing time = 0.4 s) 2D ^{1}H NMR spectrum of complex **2@OAc** in acetonitrile-d_3: 1 is the cross peak between *in-* and *out*-isomers, 2 and 3 are the cross peaks of the CH$_3$ protons of the *in*-isomer and cavitand OC*H^i*HO or Ar*H* protons, respectively.

Because of the very high binding affinity, NMR spectroscopy cannot be used for the *K*-value determination. Therefore, microcalorimetric (ITC) studies were carried out. The different binding constants and heat effects upon complexation are summarized in Table 2. With ITC, in all cases a 1:1 stoichiometry was found for the complex formation. The complexation of organic anions by receptors **1** and **2** is an enthalpically driven process, while the entropy contribution is small. For a representative example of an ITC titration, see Fig. 2.

Table 2. K_a-values and thermodynamic data of the complexation of carboxylates

by hosts **1** and **2** determined by ITC[a].

Entry	Guest	Host **1**			
		K_a, M^{-1}	ΔG, kcal mol^{-1}	ΔH, kcal mol^{-1}	ΔS, cal mol^{-1} K^{-1}
1	Formate	9.6×10^4	-6.80	-4.19	8.72
2	Acetate	8.0×10^5	-8.04	-9.85	-6.03
3	Propionate	4.0×10^5	-7.64	-8.42	-2.61
4	Butyrate	3.4×10^5	-7.54	-6.90	2.14
5	Valerate	2.0×10^5	-7.22	-7.19	0.08
6	Benzoate	4.1×10^4	-6.29	-5.15	3.82
		Host **2**			
7	Formate	5.3×10^5	-7.81	-4.73	10.32
8	Acetate	9.4×10^6	-9.51	-8.95	1.89
9	Propionate	7.4×10^6	-9.37	-8.98	1.31
10	Butyrate	4.7×10^6	-9.10	-8.61	1.65
11	Valerate	2.2×10^6	-8.66	-8.72	-0.22
12	Benzoate	5.0×10^4	-6.41	-3.52	9.68
13	Lactate	8.5×10^5	-8.08	-8.61	-1.79

[a] The data are average values of two titrations; the error is < 10%.

The entire process consists of two parts, viz. endothermic dissociation of **1**@**1** or **2**@**2** capsules and the exothermic formation of complexes with the anions (Fig. 3a). Figure 3b shows the changes in the concentration of all the components upon ITC titration. In general, the K_a-values of the *in*-isomer complexes (e.g. acetate, propionate, butyrate) and the *out*-isomer complexes (e.g. valerate) are about two-four times higher, indicating the possible contribution of CH-π interactions in the former cases. Ureidocavitand **1** is about ten times weaker complexing agent than thioureidocavitand **2**, in line with the fact that urea (pK_a = 26.9) is a weaker acid than

thiourea (pK_a = 21.0).[21] The selectivity for acetate over benzoate, that can only give an *out*-isomer complex due to its size, is about 20 in the case of ureidocavitand **1**, while it increases to almost 180 in the case of thiourea analogue **2**. The thioureidocavitand receptor **2** has an excellent binding affinity to organic anions, which is, to the best of our knowledge, higher than those of known neutral anion receptors[22] and comparable with that of charged and organometallic anion receptors.[23]
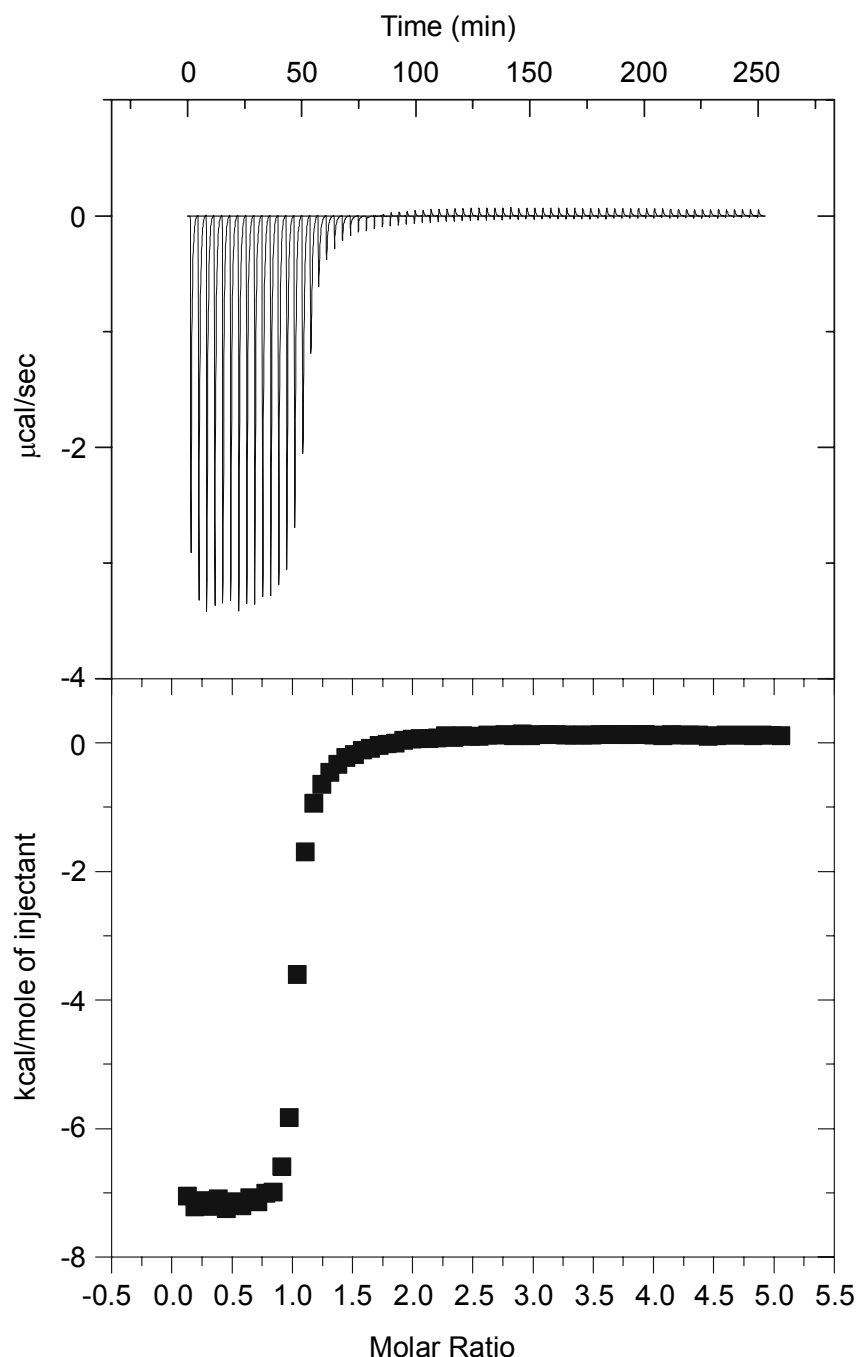
Figure 2. Example of an ITC titration curve: thioureidocavitand **2** (0.2 mM) with tetrabutylammonium valerate (4.5 mM).

a

b
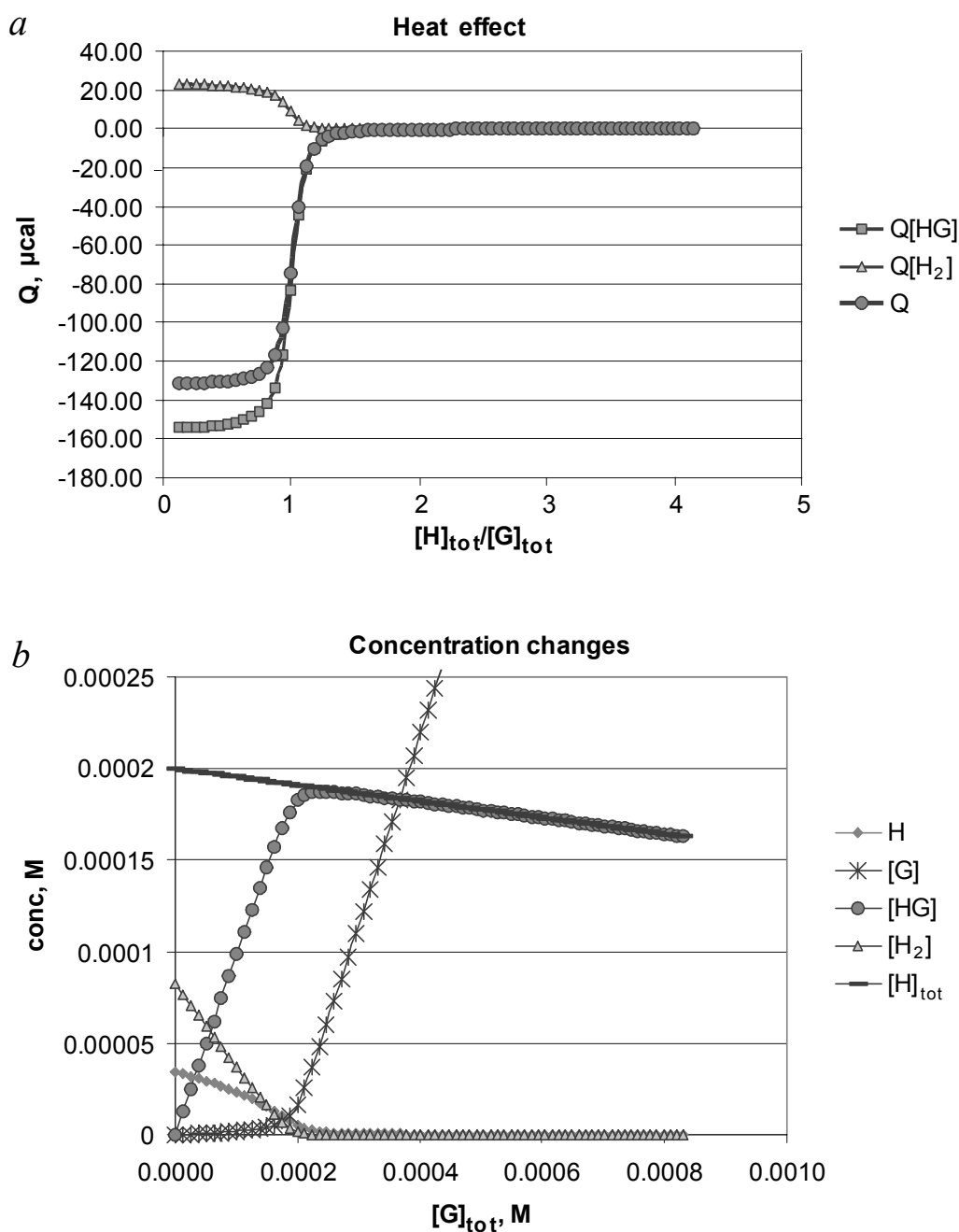
Figure 3. Changes of heat effects (a), and the concentration of the components (b) upon ITC titration of thioureidocavitand **2** (0.2 mM) with tetrabutylammonium valerate (4.5 mM) in acetonitrile; Q: heat effect monitored upon the titration, Q [H_2]: heat of the dissociation of the self-assembly, Q [HG]: heat of the complex formation, Q = Q [H_2] + Q [HG].

The complexation of ureidocavitand **1** with lactate shows a deviating behavior. By ITC, a 1:2 host/anion stoichiometry was found with K_{a1} = 4.5×10^5 M^{-1} and K_{a2} = 2.1×10^5 M^{-1}. ESI-MS measurements at a low cone voltage (16 V) revealed in the spectrum a small peak of the double-charged 1:2 complex.

The advantage of bringing together four (thio)urea binding sites on a molecular platform is clear from a comparison of the data of **1** and **2** with those of acyclic analogs, viz. 1-benzyl-3-propylurea (**3**) and 1-benzyl-3-propylthiourea (**4**): K_a (**3**@OAc) = 497 M^{-1}(ΔG = -3.67 kcal mol^{-1}, ΔH = -5.57 kcal mol^{-1}, ΔS = -6.37 cal mol^{-1} K^{-1}); K_a (**4**@OAc) = 3.5×10^3 M^{-1} (ΔG = -4.83 kcal mol^{-1}, ΔH = -4.52 kcal mol^{-1}, ΔS = 1.05 cal mol^{-1} K^{-1}). The corresponding cavitand-based receptors **1** and **2** bind about 1600 and 2700 times stronger, respectively. In general, binding with these cavitand-based ionophores is considerably stronger than with the structurally related, although more flexible, calix[4]arene counterparts. This may be caused by the fact that the rigid cavitand-based ionophores cannot form intramolecular hydrogen bonds.[15]

Acetate recognition in aqueous media. The complexation affinity of the corresponding glucose- and galactose-containing thioureidocavitands **5** and **6** (Chart 2) to acetate was studied by ITC in the more polar acetonitrile/water 1:1 mixture. In both cases, a K_a-value of 2.15 ± 0.4×10^3 M^{-1} (ΔG = -4.54 kcal mol^{-1}, ΔH = 0.69 kcal mol^{-1}, ΔS = 17.57 cal mol^{-1} K^{-1}) was obtained. Upon increasing the solvent polarity, the thermodynamic parameters change considerably – the process becomes endothermic and entropically driven, in contrast to the enthalphically driven complexation of acetate by hosts **1** and **2** in acetonitrile.
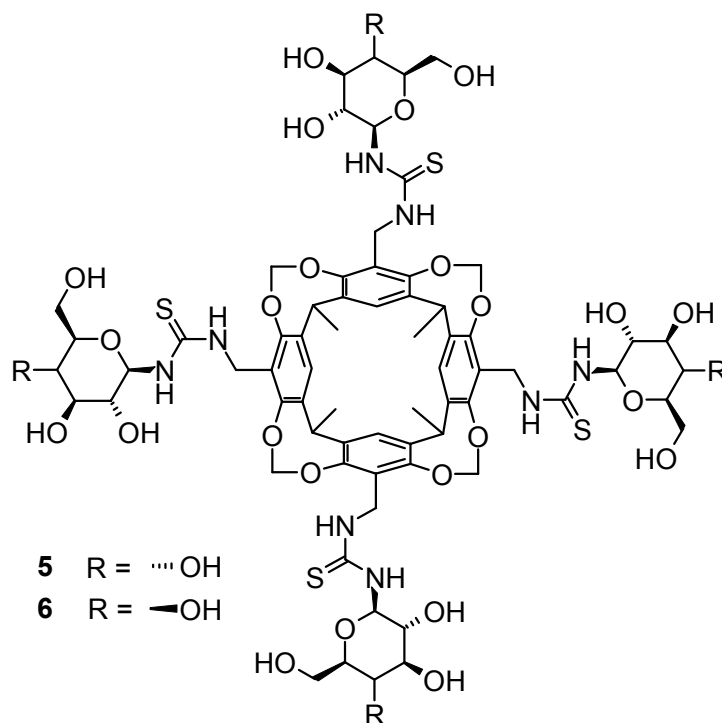

Chart 2. Glucose- and galactose-containing thioureidocavitands.

In conclusion, we have demonstrated that thioureidocavitands are among the strongest receptors for organic anion recognition with K_a values up to 9.4×10^6 M^{-1} in acetonitrile.

4.3 Experimental

^{1}H NMR spectra were recorded on a Varian Unity Inova (400 MHz) spectrometer. Tetramethylsilane (TMS) was used as internal standard. Acetonitrile-d_3 was purchased from Aldrich and stored for at least 2 days over molecular sieves before use. The ESI-MS experiments were carried out with a Micromass LST ESI-TOF instrument. The solutions were introduced at a flow rate of 20 μL/min for 2 min (120 scans). The standard spray conditions: negative ion mode, capillary voltage 2500 V, sample cone voltage 30-50 V, desolvation gas flow 250 L/h, source temperature 100 °C, desolvation temperature 100 °C.

(Thio)urea cavitands **1**,[24] **2**,[16] 1-benzyl-3-propylurea[25] **3**, 1-benzyl-3-propyl-thiourea[26] **4** and glycoside thiourea cavitand derivatives[16] **5**, **6** were prepared according to literature procedures. Tetrabutylammonium salts of organic acids were either purchased from Aldrich and Acros Organics or prepared from the corresponding acids and tetrabutylammonium hydroxide.[27] All the salts were dried in a freeze dryer for at least 3 days before use.

Determination of K_a-values of self-association of the hosts. The ^{1}H NMR titration curves were modeled using a non-linear regression analysis. Modeling of the ^{1}H NMR data was performed using an Excel program based on standard equations that consider self-association.[28]

Isothermal titration calorimetry experiments. The ITC titration experiments were performed using a Microcal VP-ITC microcalorimeter with a cell volume of 1.4115 mL [cell temperature 25 ˚C, reference power 16.3 μcal/s, stirring speed 310 RPM, auto ITC equilibration option, low feedback/mode gain, volume of injectant 4 μL (73 injections) or 5 μL (59 injections), duration of injection 20 s, spacing 210 s, filter period 5 s]. The host concentrations range from 0.04 mM to 7 mM, depending on the value of the binding constant. The guest (tetrabutylammonium salt) concentration is 15-25 times higher than the corresponding host concentration. Excel non-linear regression analysis models for the treatment of ITC data are based on equations that

include complexation and self-association equilibria, dilution of the solution upon injections, and the heat effect of the guest solution dilution.

The concentrations of all the components during an ITC titration were calculated by the iterative solution of the following set of equations that consider the self-association equilibrium, the 1:1 complexation equilibrium, and both of them.

$$H + H \rightleftharpoons H_2 \qquad\qquad 1$$

$$H + G \rightleftharpoons HG \qquad\qquad 2$$

a) Self-association:

$$[H_2] = K_s \times [H]^2 \qquad\qquad 3$$

$$[H] = \frac{[H]_{\text{tot}-i}}{1 + 2K_s \times [H]} \qquad\qquad 4$$

b) 1:1 complexation equilibria:

$$[H] = \frac{[H]_{\text{tot}-i}}{1 + K_a \times [G]} \qquad\qquad 5$$

$$[G] = \frac{[G]_{\text{tot}-i}}{1 + K_a \times [H]} \qquad\qquad 6$$

$$[HG] = K_a \times [H] \times [G] \qquad\qquad 7$$

c) Self-association and 1:1 complexation equilibria involve Eqs. 3, 6, 7, and 8.

$$[H] = \frac{[H]_{\text{tot}-i}}{1 + K_a \times [G] + 2K_s \times [H]} \qquad\qquad 8$$

where $[H]$, $[G]$, $[HG]$, $[H_2]$ are the concentrations of host, guest, host-guest complex, and self assembly, respectively; $[H]_{\text{tot-i}}$ and $[G]_{\text{tot-i}}$ are corrected for dilution total concentrations of host and guest following the i-th injection; K_s and K_a are the self-association and 1:1 binding constant. All the concentrations were corrected for the dilution during the ITC titration process.[29] The heat effect of complexation was calculated using the standard equation from the MicroCal VP-ITC manual. In the case of anion complexation by (thio)ureidocavitands, the sum of the heat effects of two

processes (Fig. 3a) was calculated. Subtraction of the residual heat effect caused by the heat of dilution and deaggregation of guests in acetonitrile or subtraction of the data of dilution of the guest solution in acetonitrile/water = 1:1 was carried out.

The fitting was carried out by varying K_s, K_a, ΔH, the residual heat effect, and the concentration of the solution of the guest added (concentration variations of < 10% relative to the 1:1 stoichiometry were accepted).

References and notes

1. *Coord. Chem. Rev.* **2003**, *240*, special issue on anion recognition; Beer, P. D.; Gale, P. A. *Angew. Chem., Int. Ed.* **2001**, *40*, 486-516.
2. Fan, E.; Vanarman, S. A.; Kincaid, S.; Hamilton, A. D. *J. Am. Chem. Soc.* **1993**, *115*, 369-370.
3. For a review, see: Fitzmaurice, R. J.; Kyne, G. M.; Douheret, D.; Kilburn, J. D. *J. Chem. Soc., Perkin Trans. 1* **2002**, 841-864.
4. Sansone, F.; Chierici, E.; Casnati, A.; Ungaro, R. *Org. Biomol. Chem.* **2003**, *1*, 1802-1809; Dudič, M.; Lhoták, P.; Stibor, I.; Lang, K.; Prošková, P. *Org. Lett.* **2003**, *5*, 149-152; Scheerder, J.; Engbersen, J. F. J.; Casnati, A.; Ungaro, R.; Reinhoudt, D. N. *J. Org. Chem.* **1995**, *60*, 6448-6454.
5. Pelizzi, N.; Casnati, A.; Friggeri, A.; Ungaro, R. *J. Chem. Soc., Perkin Trans. 2* **1998**, 1307-1311.
6. Jullian, V.; Shepherd, E.; Gelbrich, T.; Hursthouse, M. B.; Kilburn, J. D. *Tetrahedron Lett.* **2000**, *41*, 3963-3966.
7. Benito, J. M.; Gomez-Garcia, M.; Blanco, J. L. J.; Mellet, C. O.; Fernandez, J. M. G. *J. Org. Chem.* **2001**, *66*, 1366-1372.
8. Prevot-Halter, I.; Weiss, J. *New J. Chem.* **1998**, *22*, 869-874; Goodman, M. S.; Jubian, V.; Linton, B.; Hamilton, A. D. *J. Am. Chem. Soc.* **1995**, *117*, 11610-11611.
9. Jeong, K. S.; Park, T. Y. *Bull. Korean Chem. Soc.* **1999**, *20*, 129-131.
10. Kyne, G. M.; Light, M. E.; Hursthouse, M. B.; de Mendoza, J.; Kilburn, J. D. *J. Chem. Soc., Perkin Trans. 1* **2001**, 1258-1263.
11. Sasaki, S.; Mizuno, M.; Naemura, K.; Tobe, Y. *J. Org. Chem.* **2000**, *65*, 275-283.
12. Boas, U.; Karlsson, A. J.; de Waal, B. F. M.; Meijer, E. W. *J. Org. Chem.* **2001**, *66*, 2136-2145.
13. Budka, J.; Lhoták, P.; Michlová, V.; Stibor, I. *Tetrahedron Lett.* **2001**, *42*, 1583-1586.
14. Webber, P. R. A.; Beer, P. D. *Dalton Trans.* **2003**, 2249-2252.
15. Boerrigter, H.; Grave, L.; Nissink, J. W. M.; Chrisstoffels, L. A. J.; van der Maas, J. H.; Verboom, W.; de Jong, F.; Reinhoudt, D. N. *J. Org. Chem.* **1998**, *63*, 4174-4180.
16. Oshovsky, G. V.; Verboom, W.; Fokkens, R. H.; Reinhoudt, D. N. *Chem. Eur. J.* **2004**, *10*, 2739-2748.
17. For reviews, see: Rebek, J. *Chem. Commun.* **2000**, 637-643; Böhmer, V.; Mogck, O.; Pons, M.; Paulus, E. F., *Reversible Dimerization of Tetraureas Derived from Calix[4]arenes.* In *NMR in Supramolecular Chemistry;* Pons,

M., Ed. Kluwer Academic Publishers: New York, 1999; pp 45-60; Böhmer, V.; Vysotsky, M. O. *Aust. J. Chem.* **2001**, *54*, 671-677.

18. A K_a-value of $>10^5$ M^{-1} in CD$_2$Cl$_2$ has been reported for the 1:1 self-association of corresponding calix[4]arenes: Cho, Y. L.; Rudkevich, D. M.; Rebek, J. *J. Am. Chem. Soc.* **2000**, *122*, 9868-9869.

19. In C_3-symmetric metacyclophane-based anion receptors with three thiourea groups the involvement of six NH-protons has been demonstrated with molecular modeling: Lee, K. H.; Hong, J. I. *Tetrahedron Lett.* **2000**, *41*, 6083-6087.

20. For the corresponding *out*-isomer broad signals were not observed. This means that a scale of exchange between *in*- and *out*-isomers close to the NMR timescale can be excluded.

21. Bordwell, F. G.; Algrim, D. J.; Harrelson, J. A. *J. Am. Chem. Soc.* **1988**, *110*, 5903-5904.

22. Sessler, J. L.; An, D. Q.; Cho, W. S.; Lynch, V. *J. Am. Chem. Soc.* **2003**, *125*, 13646-13647; Sessler, J. L.; Pantos, G. D.; Katayev, E.; Lynch, V. M. *Org. Lett.* **2003**, *5*, 4141-4144; Sasaki, S.; Citterio, D.; Ozawa, S.; Suzuki, K. *J. Chem. Soc., Perkin Trans. 2* **2001**, 2309-2313; Kato, R.; Nishizawa, S.; Hayashita, T.; Teramae, N. *Tetrahedron Lett.* **2001**, *42*, 5053-5056; Albert, J. S.; Hamilton, A. D. *Tetrahedron Lett.* **1993**, *34*, 7363-7366.

23. Beer, P. D.; Cheetham, A. G.; Drew, M. G. B.; Fox, O. D.; Hayes, E. J.; Rolls, T. D. *Dalton Trans.* **2003**, 603-611; Kubo, Y.; Ishihara, S.; Tsukahara, M.; Tokita, S. *J. Chem. Soc., Perkin Trans. 2* **2002**, 1455-1460; Kubo, Y.; Tsukahara, M.; Ishihara, S.; Tokita, S. *Chem. Commun.* **2000**, 653-654.

24. Nissink, J. W. M.; Wink, T.; van der Maas, J. H. *J. Mol. Struct.* **1999**, *479*, 65-73.

25. Dimmock, J. R.; Vashishtha, S. C.; Stables, J. P. *Pharmazie* **2000**, *55*, 490-494.

26. Weller, L. E.; Ball, C. D.; Sell, H. M. *J. Am. Chem. Soc.* **1952**, *74*, 1104-1104.

27. Nakayama, H.; Torigata, S. *Bull. Chem. Soc. Jpn.* **1984**, *57*, 171-175; Skowronska-Ptasinska, M.; Telleman, P.; Aarts, V. M. L. J.; Grootenhuis, P. D. J.; Van Eerden, J.; Harkema, S.; Reinhoudt, D. N. *Tetrahedron Lett.* **1987**, *28*, 1937-1939.

28. Connors, K. A., *Binding Constants: The Measurement of Molecular Complex Stability;* Wiley-Interscience: New York, 1987; Fielding, L. *Tetrahedron* **2000**, *56*, 6151-6170.

29. Turnbull, W. B.; Daranas, A. H. *J. Am. Chem. Soc.* **2003**, *125*, 14859-14866.

TRIPLE ION INTERACTIONS FOR THE CONSTRUCTION OF SUPRAMOLECULAR CAPSULES[℘]

A novel type of [2+4] capsules based on triple ion interactions was obtained. Four monovalent anions (bromide, nitrate, acetate, or tosylate) bring together two tetrakis(pyridiniummethyl)tetramethyl cavitands by pyridinium-anion-pyridinium interactions. ESI-MS experiments have confirmed the capsule structure due to different fragmentation pathways of triple ions, cations, and ion-pairs. The capsules encapsulate one or two anions, depending on its size. The capsules exist in equilibrium with hemicapsules containing three walls. The latter form complexes with phenols and anilines to give new unsymmetrical capsules containing both pyridinium-anion-pyridinium and pyridinium-guest-pyridinium walls.

5.1 Introduction

Self-assembled architectures such as capsules,[1] cages,[2] rosettes,[3,4] guanosine quartets,[5] metallacycles,[6] etc are nowadays of interest in supramolecular chemistry.[3,7] Capsules are spherical molecules that are formed by specific interactions of two functionalized half-spheres. Due to multivalent interactions,[8] preferential formation of capsules takes place, while no polymerization is observed. The groups of Rebek and Böhmer systematically studied capsules based on hydrogen-bonding interactions and their host-guest complexes.[1,9] A number of capsules have been obtained using metal-ligand[10] or electrostatic interactions.[11,12] However, to the best of our knowledge, triple ion interactions have never been used to build capsules or any other type of supramolecular architectures.

The formation of triple ions, the result of the interaction of a singly charged anion A$^-$ or a cation C$^+$ with an ion-pair AC (Scheme 1), was proposed by Fuoss and Kraus more than 70 years ago.[13] Since that time a variety of triple ions based on inorganic and organic ions have been studied not only in non-competitive solvents (such as tetrahydrofuran, ethyl acetate, or chloroform),[14] but also in acetonitrile,[15] alcohols,[16] and even in supercritical water.[17] These transient ionic intermediates, that are present in conducting electrolyte solutions, have not only been studied by a variety of electrochemical methods,[13-16] but also by mass spectrometry.[18] Modern theories considering the properties of electrolyte solutions take into account the presence of triple ions and higher aggregates.[19]

$$A^- \ + \ C^+ \ \rightleftharpoons \ AC$$

$$A^- \ + \ AC \ \rightleftharpoons \ ACA^-$$

$$C^+ \ + \ AC \ \rightleftharpoons \ CAC^+$$
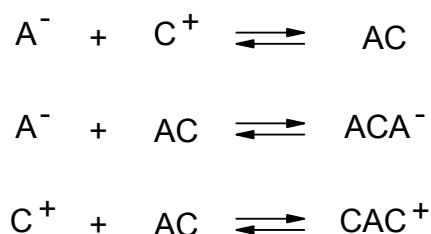
Scheme 1. The formation of triple ions (A$^-$ and C$^+$ are anion and cation, respectively).

Although the triple ion concept originally comes from electrochemistry, coordination chemistry gives another view on these associates: there are two

valencies, the charge of the ion and a secondary valence denoted by a "coordination number".[20] This has been realized in a variety of anion receptors,[21] in which the coordination number of a singly charged anion can be up to nine.[20] In the case of anions the secondary valence can be realized by electrostatic interactions,[22] anion-π interactions,[23] and hydrogen bonding.[20,21] These receptors can bind anions not only in non-competitive solvents, but also in polar competitive media and even in water.[21]

This chapter deals with the first example of the use of triple ion interactions for the construction of novel [2+4] cavitand-containing capsules in methanol and water. The capsules are based on pyridinium-anion-pyridinium interactions, in which the anion has the coordination number two. Strong evidence for the capsule structure was obtained by in-source voltage-induced dissociation ESI-MS experiments. The interaction of the capsules with different guests was also studied.

5. 2 Results and discussion

5.2.1 Synthesis

For our studies cavitands functionalized with four pyridiniummethyl substituents, containing different counterions, were used. Tetrakis(pyridinium-methyl)tetramethylcavitand tetrabromide **2** (X = Br)[24] was prepared by a slightly improved procedure starting from the corresponding tetrakis(bromomethyl)tetramethylcavitand **1**[25] (Scheme 2) using a mixture of chloroform/methanol instead of ethanol, giving less partially substituted compounds.

The known methanol-soluble cavitand **3**,[26] 1-(4-methylbenzyl)pyridinium salts **4**, and 1-(4-bromobenzyl)pyridinium bromide **5** were used as reference compounds (Chart 1). The nitrate, acetate, and tosylate salts of compounds **2** and **4** (X = NO$_3$, OAc, Tos) were prepared from the bromides **2** and **4**[27,28] (X = Br), respectively, using a column loaded with a Dowex anion exchange resin functionalized with the appropriate anion.
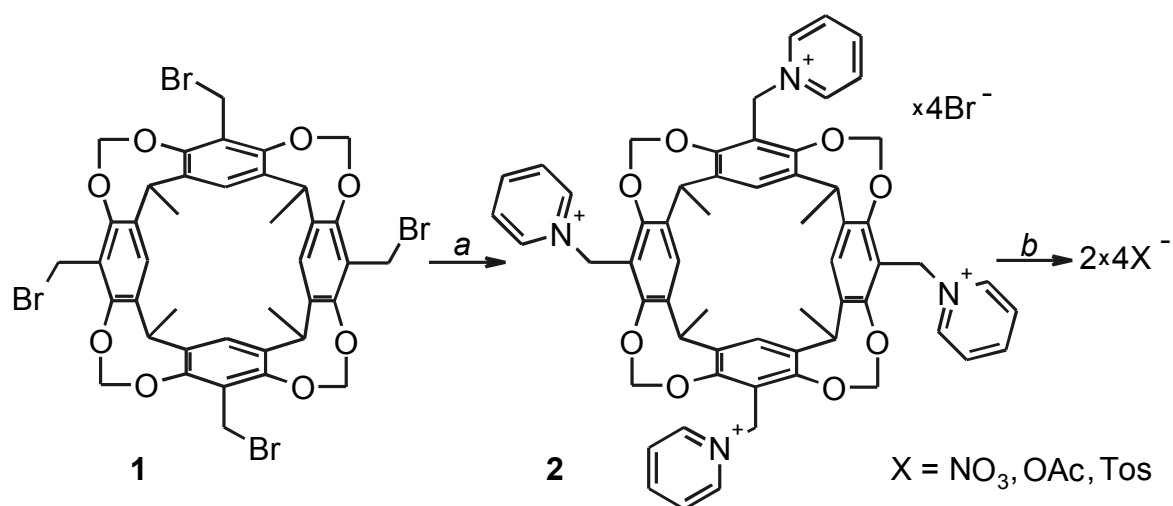
Scheme 2. Synthesis of cavitands **2**; a) pyridine, room temperature, in CHCl$_3$; after 12 hours, in CHCl$_3$:MeOH (1:1); b) Dowex X column.

R = CH$_2$CH$_2$CH$_2$OH   X = Br, NO$_3$, OAc, Tos

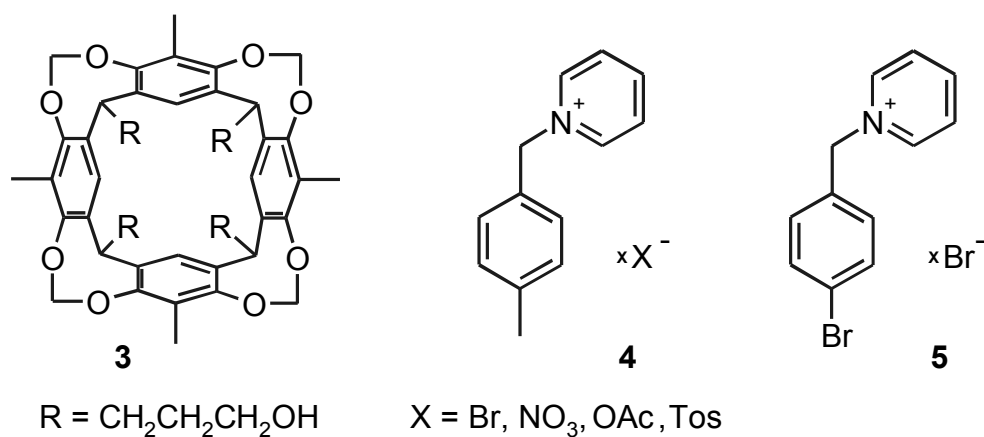**Chart 1.** Reference compounds.

5.2.2 ^{1}*H NMR spectroscopy*

^{1}H NMR dilution experiments of compounds **2** in methanol-d_4 show changes of shifts of almost all protons (up to ~ 0.4 ppm) upon varying the concentration from 0.1 to 50 mM (for example, see Figure 1). Since different types of protons experience shift changes upon dilution, different species and/or equilibria may be involved.
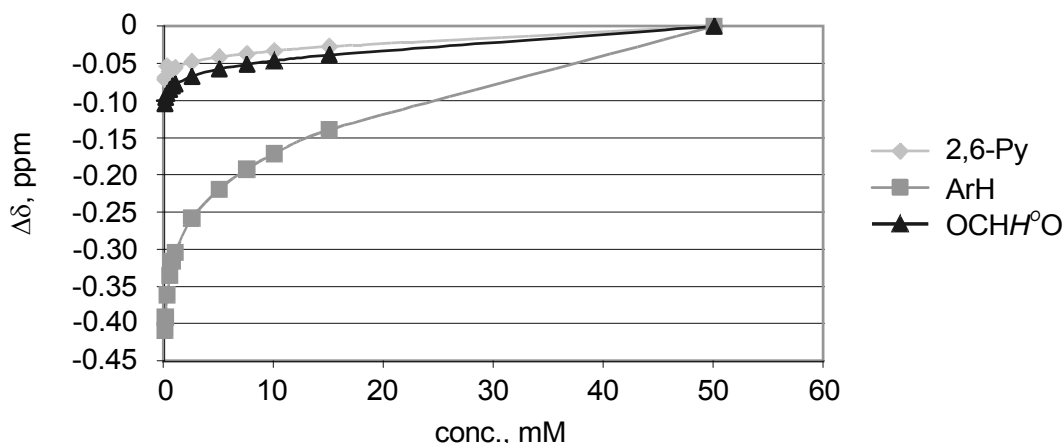
Figure 1. ^{1}H NMR shift differences observed upon dilution of **2**×4Br in methanol-d_4 (with respect to the shifts of **2**×4Br at 50 mM).

To understand this behavior ^{1}H NMR dilution experiments were carried out with the reference pyridinium salts **4** (for an example, see Figure 2). The largest shift differences were observed for the 2,6-pyridinium, 2,6-(4-methylbenzyl), and methylene protons. The dilution data in Figure 2 cannot be fitted with a 1+1 model and represent at least two consecutive processes: the first process with a K_a-value of ~ $10^{2\text{-}3}$ M^{-1} (the first part of the curve) is followed by one or several interactions that have a lower affinity. From the literature it is known that pyridinium salts experience ion-pairing in solution,[29] to which the first observed process can be attributed. Since anions form coordination compounds[20] with π-electron deficient aromatics including azaheterocycles (the coordination number is two to four)[23] and the formation of pyridinium-anion-pyridinium triple ions has been detected electrochemically,[15,30] the further shift changes in the ^{1}H NMR spectrum can be explained by the formation of triple ions, and, probably, higher aggregates.

To study the ability of the cavity of the cavitand to include an anion in methanol as a solvent, a ^{1}H NMR titration of reference cavitand **3** with Bu$_4$NBr was carried out. From the change of the shifts of the CH at the bottom rim and the inner proton of the OCH$_2$O-linker of the cavitand scaffold, a binding constant of 3-70 M^{-1} was determined by non-linear fitting (ion-pairing of 0-10^3 M^{-1} of Bu$_4$NBr was taken into account in the fitting model).
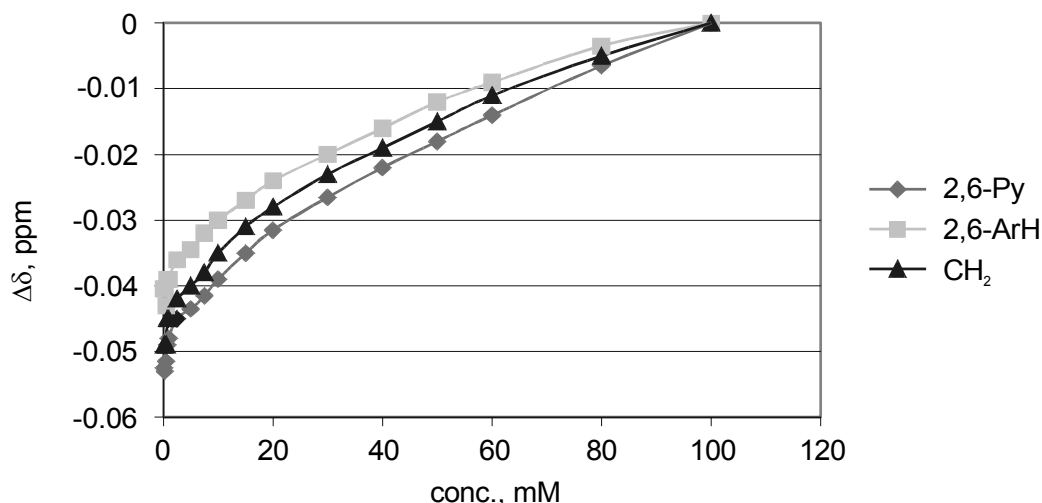
Figure 2. ^{1}H NMR shift differences observed upon dilution of **4**×Br in methanol-d_4 (with respect to the shifts of **4**×Br at 100 mM).

From the experiments with the reference compounds it can be concluded that the shifts observed upon dilution of compound **2** (Figure 1) are caused by several processes: inclusion of the anion into the cavity, ion-pairing of the anion with the pyridinium moiety, triple ion formation, and, probably, the formation of higher aggregates.

The position of the anions with respect to the pyridinium cation **2** was determined with NOESY NMR in the cases of **2**×4Tos and **2**×4OAc. Cross-peaks between the α- and β-pyridinium protons and the 2,6-protons of tosylate or the acetate methyl group show that the counterions form contact ion-pairs with the pyridiniums in solution (10 mM in methanol-d_4). The organic substituents at the sulphonic or carboxylic groups, respectively, are located close to the pyridinium rings. It allows the conclusion that, in addition to electrostatic interactions between the pyridinium nitrogens and anions, additional CH-π interactions of the hydrogens of the anions with the pyridinium rings takes place. The absence of cross-peaks between the α- and β-pyridinium protons and tosylate in **4**×Tos (40 mM in methanol-d_4) in the NOESY NMR spectrum recorded at the same conditions is an indication of the lower degree of association of this reference compound in solution.

Due to the complexity of the different processes, as well as the fast exchange between the species in solution, ^{1}H NMR spectroscopy cannot be used for a detailed study. Therefore ESI-MS was used, since it gives the opportunity to differentiate between the species present and to study the processes involved in more detail.

5.2.3 Basic ESI-MS experiments

ESI-MS spectra of a methanolic solution of **2**×4Br at different voltages are shown in Figure 3.[♣]
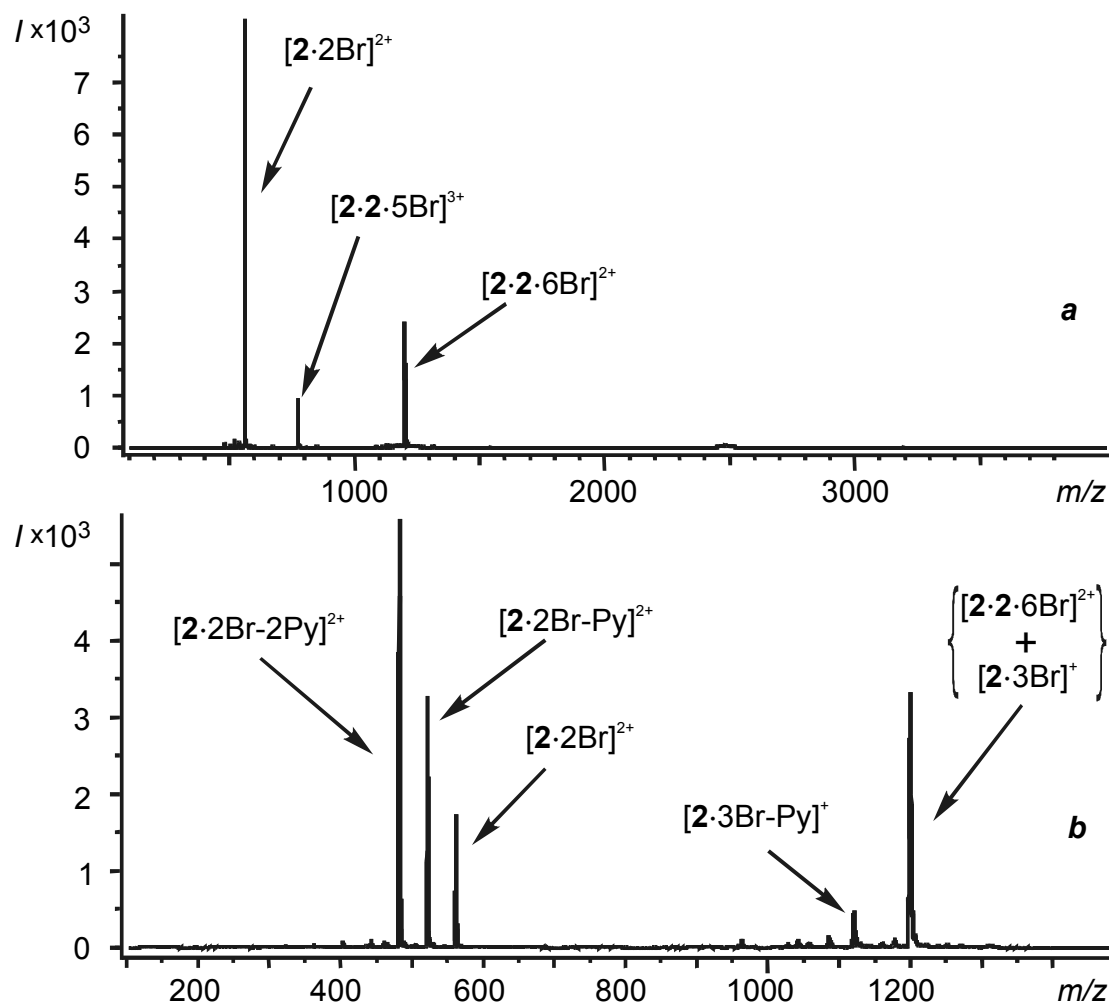
Figure 3. ESI-MS spectrum of a 0.5 mM solution of **2**×4Br in methanol (voltages: capillary = 2500 V, ring lens = 30 V, orifice 1 = 2 V, orifice 2 = 2 V (a) 15 V (b), flow rate 12.5 μL/min).

Three intensive signals that correspond to a complex of tetrakis(pyridiniummethyl)tetramethylcavitand **2** with two bromides ([**2**·2Br]$^{2+}$) and associates containing two molecules of **2** with 5 or 6 anions ([**2**·**2**·5Br]$^{3+}$ and [**2**·**2**·6Br]$^{2+}$, respectively) are present in the standard spectrum (Figure 3a). Upon increasing the concentration of **2**×4Br, the intensity of the signals of the associates

---

[♣] To keep a clear difference between compounds and ESI-MS signals, they are represented with the use of × and · symbols (for example, **2**×4Br and [**2**·2Br]$^{2+}$), respectively.

grows, and, after about 1.5 mM (at standard voltage settings) decreases due to suppression.[31] Using nano ESI-MS (continuous flow mode) diminishes the influence of the suppression,[32] and the increase of the intensity of the signal of the higher associates was observed till at least 5 mM **2×4Br**.

The associates $[\mathbf{2 \cdot 2 \cdot 5Br}]^{3+}$ and $[\mathbf{2 \cdot 2 \cdot 6Br}]^{2+}$ were also observed in the ESI-MS spectrum of a solution of **2×4Br** in water. However, the intensities of the signals of the complexes are about 5 times lower than in methanol (at the same concentrations) probably due to the competitive influence of water (see Chapter 2). It is striking that both in water and in methanol higher aggregates are not observed.
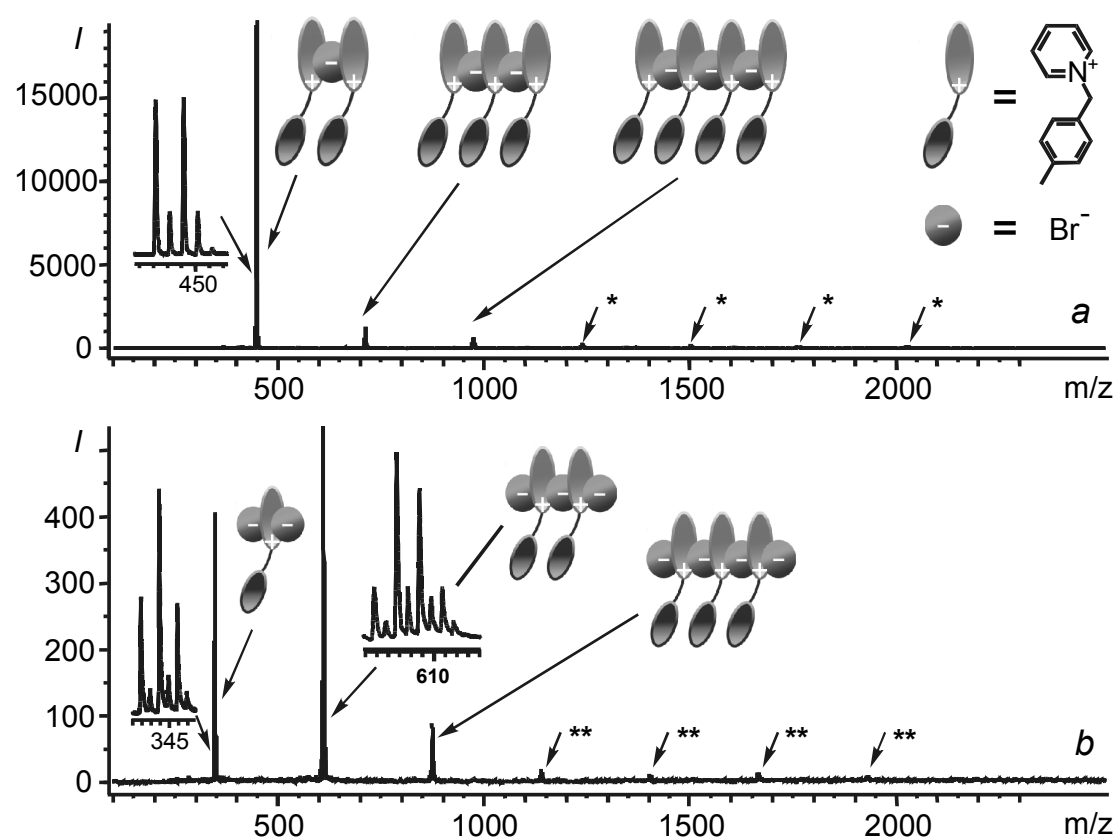
Figure 4. ESI-MS spectra in positive (**a**) and negative (**b**) modes of a 1 mM solution of **4×Br⁻** in methanol; * $[\mathbf{4 \cdot (Br \cdot 4)_n}]^+$, ** $[\mathbf{Br \cdot (4 \cdot Br)_n}]^-$, n = 3-6.

For a better understanding of the behavior of anion-pyridinium complexes in the gas phase, experiments were carried out with reference compounds **4**. Figures 4a and 4b show the ESI-MS spectra of 1 mM solutions of **4×Br⁻** in the positive and negative mode, respectively. Both spectra contain triple ions $[\mathbf{4 \cdot Br \cdot 4}]^+$ and $[\mathbf{Br \cdot 4 \cdot Br}]^-$, as well as the higher aggregates $[\mathbf{4 \cdot (Br \cdot 4)_n}]^+$ and $[\mathbf{Br \cdot (4 \cdot Br)_n}]^-$, n = 1-6.[33] A similar

aggregation behavior was observed for the other anions: nitrate, acetate, and tosylate. The coordination number of the anions[20] in the observed complexes is two. Higher coordination is not realized due to steric hindrance caused by the benzylic substituents and, probably, additional anion-π interaction with the benzene ring of the substituent.[23] The gas phase observations correspond with the aggregation behavior observed in solution.[34]

For the interpretation of the basic mass spectrometric data the preferential conformation of the tetrakis(pyridiniummethyl)tetramethyl cavitand **2** in the gas phase was determined with molecular modeling using Quanta/CHARMm (Figure 5). Cavitand **2** looks like an open flower in the gas phase, with the pyridinium moieties bended outwardly.[35]
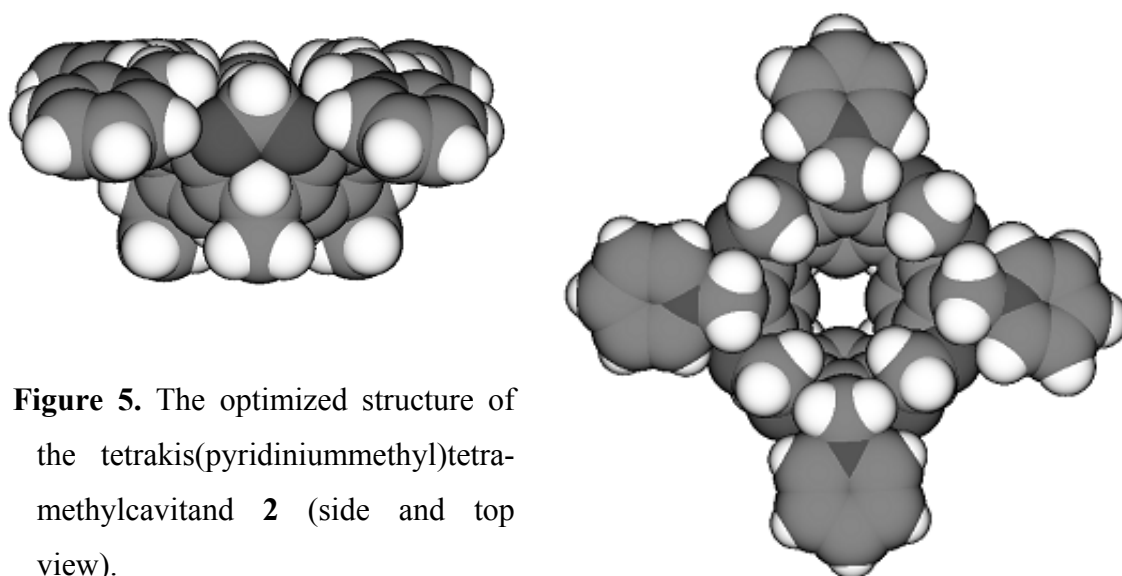
Figure 5. The optimized structure of the tetrakis(pyridiniummethyl)tetra-methylcavitand **2** (side and top view).

Theoretically, there are two possible ways for the association of anions with cavitand **2** in the complex represented by the [**2**·2Br]$^{2+}$ signal: either two anions are ion-paired with the pyridinium moieties or one anion is located inside the cavity and the second one is ion-paired. Steric hindrance and the position of two neighboring pyridinium groups in cavitand **2** do not allow intramolecular pyridinium-anion-pyridinium triple ion formation.

Similar to the simple pyridinium salts (Figure 4), triple ion interactions can bring together two cavitands **2**. There are three possible triple ion associates (**6-8**) that are not significantly sterically hindered (Figure 6). Two of them contain one or two

triple ion linkers and form associates **6** and **7**, respectively. In the third case, [2+4] capsule **8** is formed by four triple ion interactions.
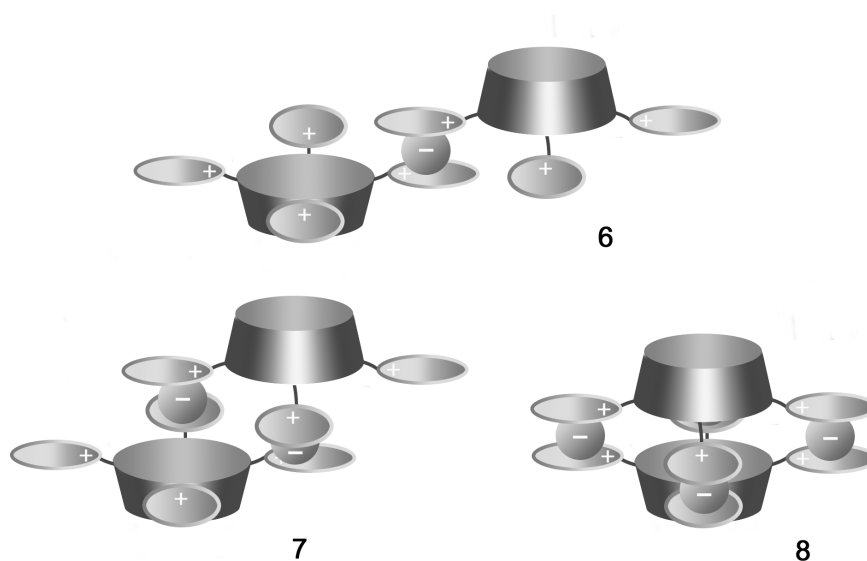
Figure 6. The possible ways of triple ion aggregation of cavitands **2** [tetrakis(pyridiniummethyl)tetramethylcavitand **2** is shown schematically].

The characteristic difference between the mass spectra of the bromides of cavitand **2** and reference compound **4** is the absence of significant signals of associates containing more than two organic molecules in the first case. It indicates that the formation of higher associates is very unfavorable or impossible. This points to the formation of capsule **8**, since its further triple ion association is impossible due to the absence of free pyridinium moieties (or pyridinium-anion ion-pairs). The formation of higher aggregates of **8** via cation-anion-cation-anion-cation interactions can be excluded for steric reasons. In the cases of the complexes **6** and **7** subsequent transformations into trimers, tetramers, etc will be possible via triple ion interactions in which free pyridinium moieties are involved.

The complexation of anions by reference cavitand **3** (vide supra) suggests the possible encapsulation of anions by capsule **8**. A complex of one or two bromides within the triple ion capsule $[\mathbf{2}\cdot\mathbf{2}\cdot4Br]^{4+}$ would explain the $[\mathbf{2}\cdot\mathbf{2}\cdot5Br]^{3+}$ and $[\mathbf{2}\cdot\mathbf{2}\cdot6Br]^{2+}$ signals. The structure of the complex represented by the $[\mathbf{2}\cdot\mathbf{2}\cdot5Br]^{3+}$ signal (Scheme 3) can correspond not only to a capsule containing one anion (anion@**8**) but also to hemicapsule **9**, which encapsulates two anions and exists in solution in equilibrium with a capsule containing two anions (2anions@**8**, $[\mathbf{2}\cdot\mathbf{2}\cdot6Br]^{2+}$). To distinguish the

isomers of [**2·2·5Br**]$^{3+}$ and to obtain more structural information about the [**2·2·6Br**]$^{2+}$ capsule, in-source voltage-induced dissociation experiments were carried out.
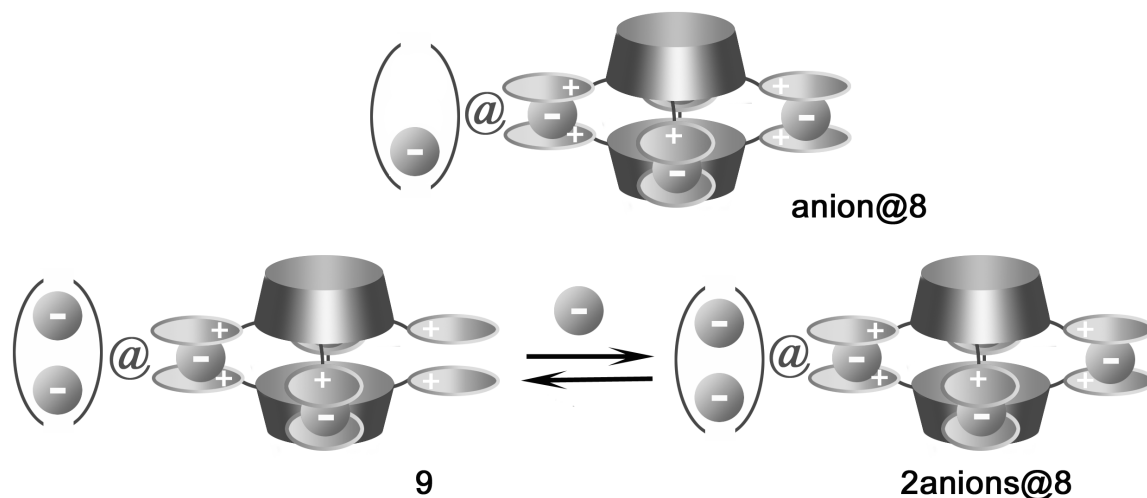
Scheme 3. Possible structures of anionic complexes of the capsule and hemicapsule (cavitand **2** is shown schematically).

5.2.4 In-source voltage-induced dissociation experiments

Mass spectrometry is a powerful tool not only for monitoring supramolecular interactions in solution,[36] but also for the elucidation of the structure of supramolecular aggregates due to a different stability and gas phase transformation of complexed and non-complexed species.[37,38] In-source voltage-induced fragmenta-tion/dissociation experiments,[38,39] realized by changes of the different voltages of an ESI mass spectrometer, were used to obtain evidence for the structure of the capsule and other complexes observed in the mass spectrum. In this study the influence of varying the orifice and ring lens voltages was studied.[40] It is known that the orifice voltage causes in-source collision-induced dissociation.[38,39] Less is known about the effect of the ring lens voltage. Hinderling et. al.[41] found in the case of organometallic complexes a different fragmentation compared to that caused by collision-induced dissociation.[42]

Complexes **6**, **7**, and capsule **8** have different types of (un)complexed pyridinium groups. Capsule **8** only contains triple ion pyridinium-anion-pyridinium moieties **10**. In the complexes **6** and **7**, in addition to the triple ion unit **10**, also methylenepyridinium cation **11** is present. The latter one is in equilibrium with contact ion-pair **12** (Scheme 4). Theoretically, in dimers of type **6** and **7** (complexed

with several anions), the presence of anion-pyridinium-anion triple ion **13** is also possible. However, this type of pyridinium triple ions is much weaker than the pyridinium-anion-pyridinium units **10**. For example, Hojo et al.[15,30] reported that in a conductometric study of pyridinium salts, the formation of pyridinium$^+$(X$^-$)$_2$ type species could not be observed at all, whereas, (pyridinium$^+$)$_2$X$^-$ species were easily found in acetonitrile (X$^-$ = Cl$^-$, Br$^-$).

Scheme 4. Possible pyridinium units present in complexes **6**, **7**, capsule **8**, and their associates with anions.

The different voltage-induced transformations of the complex fragments **10-13** in the gas phase were used to obtain additional evidence for the structure of the triple ion [2+4] capsule **8**.

In the case of the ESI-MS spectrum of **2×4Br**, increase of the orifice 2 voltage[43] from 2 to 15 V causes fragmentations, what is clearly visible by comparing Figures 3a and 3b.[44] The [**2·2Br**]$^{2+}$ complex at *m/z* 560 experiences loss of only one or two pyridines (Figure 3b) to give the [**2·2Br-Py**]$^{2+}$ and [**2·2Br-2Py**]$^{2+}$ complexes, respectively (Scheme 5). Ion-pairing stabilizes pyridinium cations.[37] For example, Schalley et al.[37] found that non-ion-paired substituted dibenzyl viologen is so unstable, that irrespective of the ionization conditions, the non-ion-paired cation was not detected in the mass spectrum. However, the viologen dication stabilized by ion-pairing is clearly observed in the spectrum as the most intensive signal. It is well known that the non ion-paired pyridinium cations **11** display the fragmentation shown

in Scheme 5,[27,37,45] but no cleavage of the pyridinium cations from the ion-pairs takes place.[46] Since loss of three pyridines from the $[\mathbf{2}\cdot2Br]^{2+}$ complex does not take place, both anions are ion-paired with pyridiniums (unit **12**). This means that the other possible structure, in which one anion is ion-paired and the second one is included inside the cavity can be excluded.
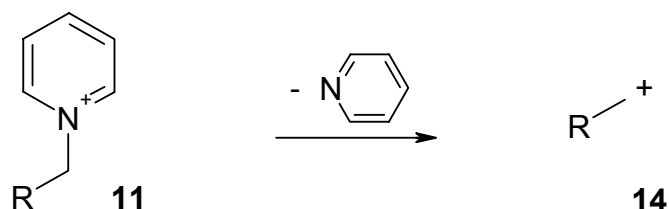
Scheme 5. Gas phase transformation of the methylene pyridinium cation: cleavage of the C-N bond.

The $[\mathbf{2}\cdot\mathbf{2}\cdot6Br]^{2+}$ signal at *m/z* 1201 (Figure 3b) shows a much higher stability, nevertheless, increase of an orifice voltage (for example, 20 V, Figure 7b) does cause fragmentation of the triple ion capsule $[\mathbf{2}\cdot\mathbf{2}\cdot6Br]^{2+}$ complex 2anions@**8**. It splits symmetrically to two $[\mathbf{2}\cdot3Br]^{+}$ cations.[47] The $[\mathbf{2}\cdot\mathbf{2}\cdot6Br]^{2+}$ and $[\mathbf{2}\cdot3Br]^{+}$ complexes have the same *m/z* but a different charge and isotopic contribution (due to the presence of six and three Br atoms, respectively), what allows easily distinguishing (Figure 7). The $[\mathbf{2}\cdot3Br]^{+}$ complex loses pyridine, resulting in the appearance of the $[\mathbf{2}\cdot3Br\text{-}Py]^{+}$ signal. This is in contrast to the $[\mathbf{2}\cdot\mathbf{2}\cdot6Br]^{2+}$ complex. The nonexistence of signals of $[\mathbf{2}\cdot\mathbf{2}\cdot6Br\text{-}nPy]^{2+}$ (n = 1, 2) indicates the absence of pyridinium cations of type **11** in the structure of the $[\mathbf{2}\cdot\mathbf{2}\cdot6Br]^{2+}$ complex, because *non-ion-paired* methylene-pyridinium cations should have been cleaved at these conditions (Scheme 5). This gives further evidence for the structure of the triple ion capsule **8**. The encapsulation of two anions into the capsule **8** (2anions@**8**) is confirmed by the high stability of the $[\mathbf{2}\cdot\mathbf{2}\cdot6Br]^{2+}$ signal, since no collision loss of one or two bromides is observed.
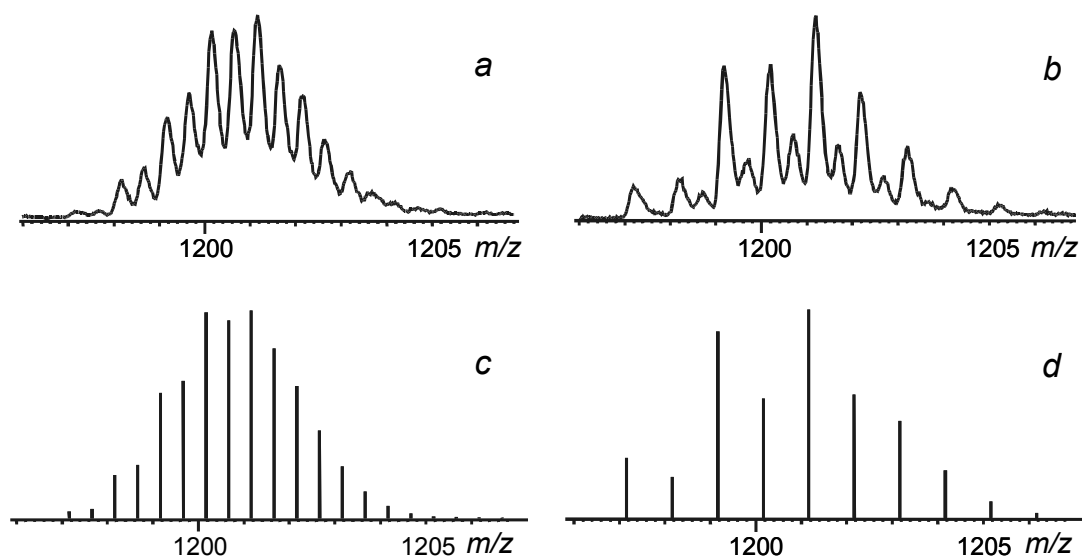
Figure 7. Example of the orifice voltage-induced fragmentation of capsule complex [**2·2·6Br**]$^{2+}$: initial complex (a); changes of the signal at increased orifice 2 voltage (20 V). Two complexes are present: [**2·2·6Br**]$^{2+}$ and [**2·3Br**]$^{+}$ (b); the calculated isotopic pattern of [**2·2·6Br**]$^{2+}$ (c) and [**2·3Br**]$^{+}$ (d), respectively.

The [**2·2·5Br**]$^{3+}$ signal disappears upon the increase of the orifice voltage. However, instead of the loss of pyridine giving [**2·2·5Br-Py**]$^{3+}$, the [**2·2·5Br**]$^{3+}$ complex breaks into the [**2·2Br**]$^{2+}$ and [**2·3Br**]$^{+}$ complexes. It allows the conclusion that its structure is very similar to that of the [**2·2·6Br**]$^{2+}$ capsule, but, due to its lower stability, it could rather correspond to hemicapsule **9** than to capsule anion@**8**.

Upon increase of the ring lens voltage, in the ESI-MS spectrum of **2×4Br** a significant decrease of the intensity of the [**2·2Br**]$^{2+}$ signal was observed, probably due to deprotonation[48] of the benzylic pyridinium cation **11**.[49] The intensity of the [**2·2·6Br**]$^{2+}$ and [**2·2·5Br**]$^{3+}$ signals is much less sensitive to ring lens voltage changes. Experiments with reference compound **5** were carried out to compare the sensitivity of the signals of the benzylic pyridinium cation **11** and triple ions **10** to changes of the ring lens voltage. At a very low ring lens voltage (5 V) the observed intensity of the signal of the cation **5**$^{+}$ is more than 15 times larger than that of the triple ion [**5·Br·5**]$^{+}$ (Figure 8a). Upon increase of the ring lens voltage (30 V), the intensity of the signal of **5**$^{+}$ drops more than 2 orders of magnitude, but the signal of the triple ion [**5·Br·5**]$^{+}$ decreases[47] only two times and becomes the most intensive signal in the spectrum (Figure 8b).[50] The higher stability of triple ion complexes **10** in comparison with

methylenepyridinium cations **11** is probably caused by the decreased acidity of the former due to the complexation.
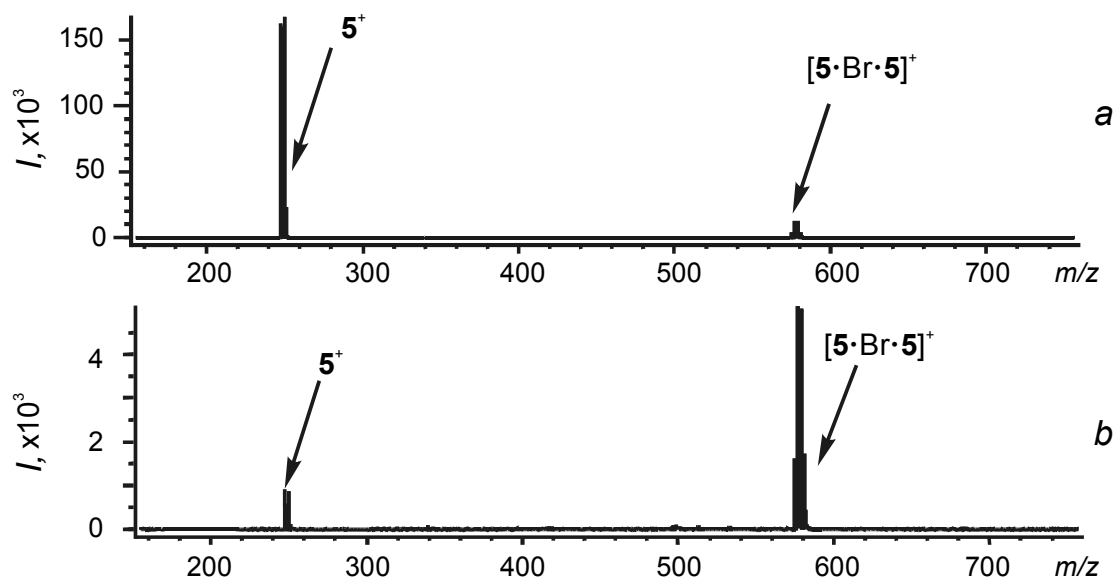

Figure 8. ESI-MS spectra of a 1 mM solution of **5** in methanol (flow rate 12.5 μL/min, voltages: capillary = 2500 V, orifice 1 and 2 = 2 V, ring lens = 5 V (a), 30 V (b)).

Methylenepyridinium cations **11** are much more sensitive to increase of the ring lens voltage than triple ions **10** (vide supra). Hence, a high voltage stability of the [**2·2·6Br**]$^{2+}$ capsule indicates the absence of benzylic pyridinium units **11** in its structure. The [**2·2·5Br**]$^{3+}$ signal could rather correspond to the hemicapsule **9** than to dimers of type **6** and **7** (complexed with several anions). Despite of the presence of pyridinium cations **11** in its structure, their deprotonation is less easy due to shielding of the protons by the second cavitand **2**.

Ring lens voltage experiments with **2×4NO$_3$** mainly exhibited a similar behavior. However, in the case of **2×4OAc**, a different behavior was observed. Figure 9a shows the continuous flow nano ESI-MS spectrum of a 5 mM solution of **2×4OAc** in methanol in the positive mode. The spectrum displays the signals of the [**2·2·6OAc**]$^{2+}$ capsule and the [**2·2·5OAc**]$^{3+}$ hemicapsule at *m/z* 1141 and 741, respectively. The signal of the complex of tetrapyridiniumcavitand **2** with two acetate anions ([**2·2OAc**]$^{2+}$) at *m/z* 540 is accompanied by two signals that are formed by cleavage of acetic acid from the ion-pairs of type **12**.[51] Upon increase of the voltage, only the signal of the [**2·2·6OAc**]$^{2+}$ capsule remains in the spectrum, and its intensity almost unchanged (Figure 9b). Such a high stability of the capsule is explained by the

absence of contact ion-pair moieties **12**, as well as due to effective shielding of the anions by pyridinium planes in the triple ions. A corresponding fragmentation of $[\mathbf{2}\cdot 2Br]^{2+}$ and $[\mathbf{2}\cdot 2NO_3]^{2+}$ is much less probable due to the much lower basicity of bromide and nitrate compared with acetate.
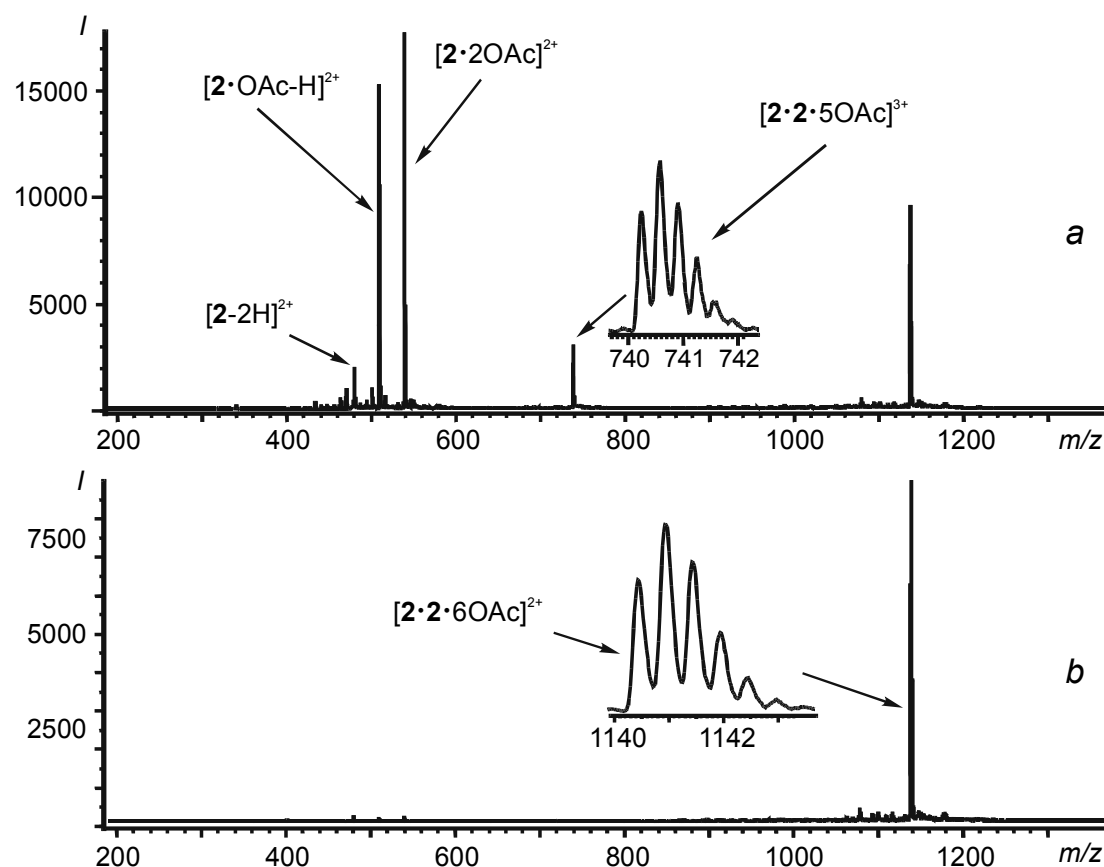
Figure 9. Nano ESI-MS (continuous flow) spectrum of a 5 mM **2×4OAc** solution in methanol (voltages: capillary 2500 V, orifices 1 and 2 = 5 V, ring lens = 20 V (a) and 30 V (b)).

In the cases of **2×4Br**, **2×4NO₃**, and **2×4OAc** the ESI-MS spectra exhibit a significant signal of a capsule containing two anions $[\mathbf{2}\cdot\mathbf{2}\cdot 6\text{Anion}]^{2+}$ (corresponding with 2anions@**8** in Scheme 3). As expected, in the case of **2×4Tos** the cavity of the capsule has not enough space to accommodate two large tosylate anions. As a result, in the ESI-MS spectrum the $[\mathbf{2}\cdot\mathbf{2}\cdot 5\text{Tos}]^{3+}$ signal, corresponding to a capsule with one guest molecule (as anion@**8** in Scheme 3), is intensive and voltage stable. The signal of the $[\mathbf{2}\cdot\mathbf{2}\cdot 6\text{Tos}]^{2+}$ capsule (2anions@**8**) containing two big guests has a very low intensity and displays voltage instability.

From the different ESI-MS experiments it can be concluded that the [2·2·6Anion]$^{2+}$ complex has a much higher stability than the other species present. The presence of methylene pyridinium cations and contact ion-pairs (11 and 12, respectively, in Scheme 4) can be excluded based on the results with the reference compounds and the different fragmentation behavior of the non-capsule species. Hence, all these data point to the formation of a triple ion [2+4] capsule with two anions (Br$^-$, NO$_3^-$, OAc$^-$) inside (2anions@8 in Scheme 3). In the case of tosylate, due to its size, the capsule 8 contains only one anion.

5.2.5 Host-guest complexation

Upon addition of phenols or anilines to a solution of **2×4X** in methanol the appearance of a new signal [guest·**2·2·**5X]$^{3+}$ (X$^-$ = Br$^-$, NO$_3^-$) was observed in the mass spectra (Figure 10). The intensity of the signal of the [**2·2·**5X]$^{3+}$ hemicapsules (**9**) decreases. In the continuous flow nano ESI-MS spectrum of a solution containing 5 mM **2×4Br** and 40 mM ethyl 4-aminobenzoate in methanol, the intensity of the two signals is almost the same (Figure 10b). In the case of 4-iodophenol, the [guest·**2·2·**5Br]$^{3+}$ signal becomes much more intensive, while the signal of the [**2·2·**5Br]$^{3+}$ hemicapsule (**9**) almost disappears (Figure 10c). A moderate decrease (about 30%)[52] of the intensity of the signal of capsule 2anions@**8** was also observed upon guest addition, which is, probably, the result of its participation in an equilibrium with hemicapsule **9** (Scheme 3). Attempts to substitute encapsulated anions for guests that could form complexes inside the cavity of the cavitand, such as acetone, ethyl acetate, benzene, toluene, acetonitrile, etc[53] were not successful. It indicates a much higher affinity of the cavitand capsule toward anions than to neutral molecules in the competitive solvent methanol. It is in agreement with ^{1}H NMR observations in methanol-d_4: cavitands form complexes with anions[54] (vide supra), but in the spectra expected shift changes have not been observed upon the addition of neutral organic guests.
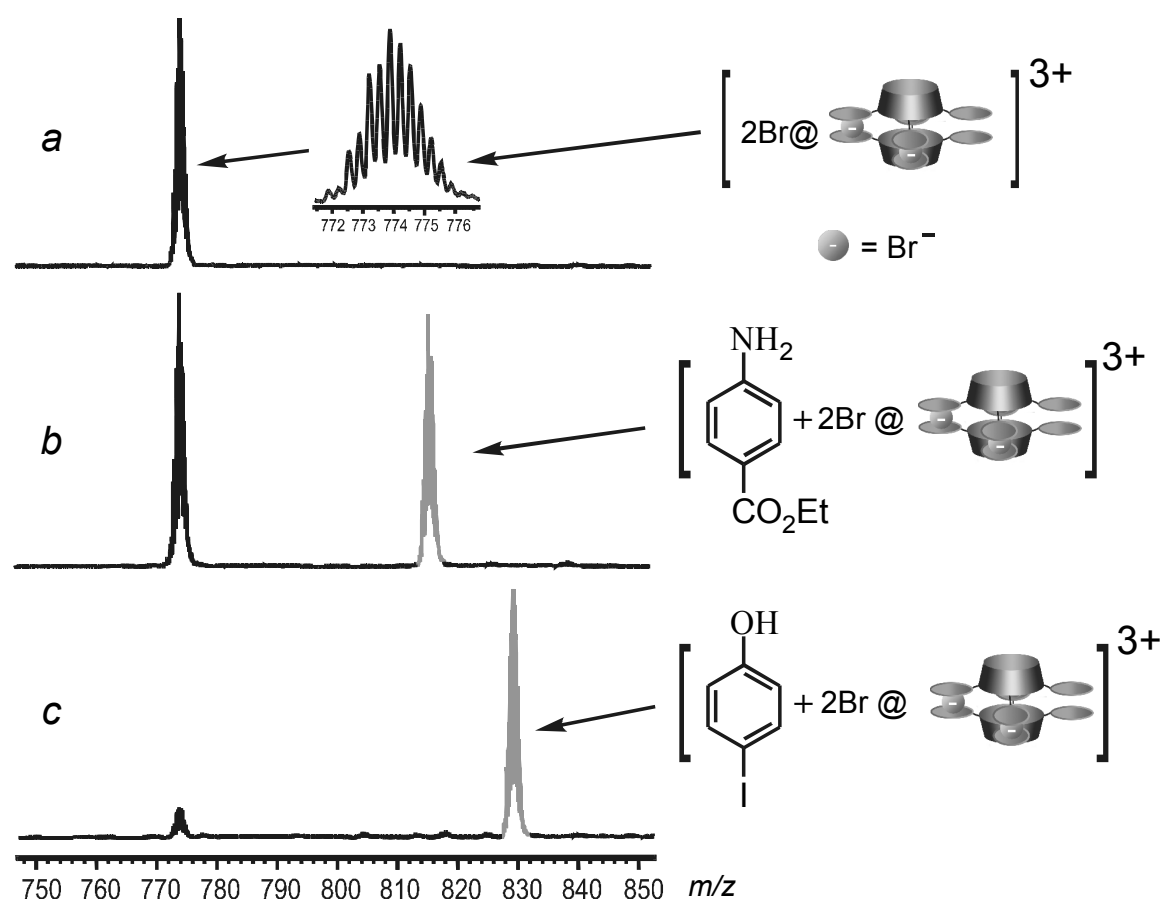
Figure 10. Continuous nano-flow ESI-MS spectra of a 5 mM solution of **2**×4Br in methanol (a); upon addition of ethyl 4-aminobenzoate (b); or 4-iodophenol (c). In both cases the resulting concentration of the guest is 40 mM.

The position of the guest was deduced from ^{1}H NMR titration experiments. Upon addition of 4-iodophenol to a solution of **2**×4Br in methanol-d_4 a shift of the 4-pyridinium proton of **2** up to 0.075 ppm was observed, while no significant changes of the OCH^iH^{o}O-protons pointing into the cavity of **2** took place. From that it can be concluded that the guest is not positioned in the cavity, but in between two pyridinium planes (Scheme 6).[55] In addition, molecular modeling showed that ethyl 4-aminobenzoate is too large to be accommodated within the capsule. The formation of the novel type of capsule-guest complex **15** can be explained by π-π and charge transfer interactions[56] between the electron-deficient pyridinium rings and the electron-rich phenols or anilines. This type of interactions, where pyridinium binding sites, realized in viologen cyclophanes, bind substituted phenols and naphthols, has widely been used by Stoddart c.s. to build catenanes, borromean rings, molecular machines, etc.[57] Upon further increase of the concentration of 4-iodophenol, the

appearance of the [guest·guest·**2**·**2**·4Br]$^{3+}$ signal that could corresponds to a capsule, in which nett two anions of the walls are substituted for the guest, was observed.[58]
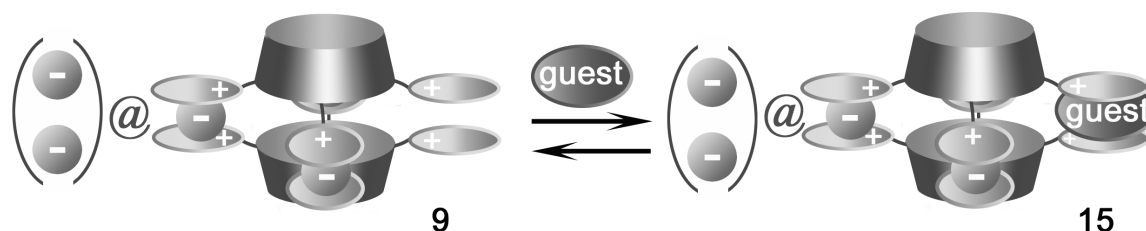
Scheme 6. Schematic representation of the host-guest complex formation.

Monitoring the decrease of the intensity of [**2**·**2**·5Br]$^{3+}$ as a reference signal upon guest addition allows an estimation[34] of the relative capsule-guest affinity[31,59] (Chart 2). In general, 4-iodo-substituted phenol and aniline are the best guests. This can be explained by an additional interaction of iodine with protons of the methylene linker connecting pyridinium and cavitand.[60]
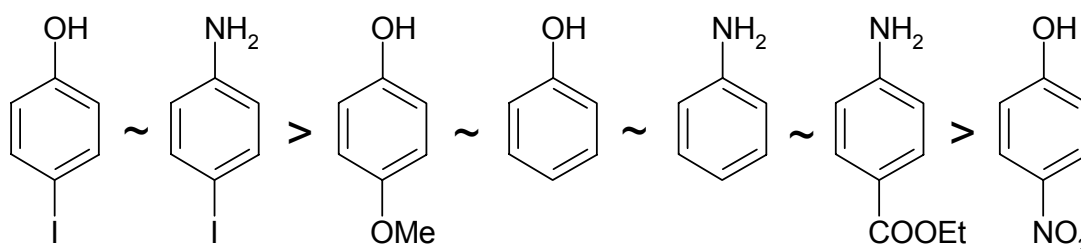
Chart 2. Relative guest affinity toward the [**2**·**2**·5Br]$^{3+}$ hemicapsule (**9**).

The complexes **15** represent a new type of unsymmetrical capsules, which has one pyridinium-guest-pyridinium wall and three pyridinium-anion-pyridinium ones.

5.3 Conclusions

For the first time triple ion interactions were used for the formation of capsules. The existence of the [2+4] cavitand-containing capsules, based on pyridinium-anion-pyridinium triple ion interactions, was proven in the gas phase by ESI-MS. In addition, indications of the presence of the capsules in solution were obtained. A novel type of capsules is introduced, in which one of the pyridinium-anion-pyridinium walls is replaced with a pyridinium-guest-pyridinium linker via equilibrium with the corresponding hemicapsule upon addition of a guest.

We feel that triple ion interactions can be used, alone or together with other interactions for the construction of different supramolecular architectures.

5.4 Experimental section

The reagents used were purchased from Aldrich or Acros Chimica and used without further purification. All the reactions were performed under a dry argon atmosphere. All solvents were freshly distilled before use. Dry pyridine was obtained by distillation over calcium hydride. Melting points were measured using a Sanyo Gellenkamp Melting Point Apparatus and are uncorrected. Proton and carbon NMR spectra were recorded on a Varian Unity Inova (300 MHz) spectrometer. Residual solvent protons were used as internal standard and chemical shifts are given relative to tetramethylsilane (TMS). Ion exchange resins were prepared from Dowex 550A OH anion exchange resin, 25-35 mesh. Compounds **3**[26], **4**×Br,[27,28] and **5**[27,61] were prepared similarly to the literature procedures (in the case of the compounds **4**×Br and **5** acetone was used as a solvent instead of methanol, nitrobenzene, or nitromethane). The presence of water in the analytical samples was proven by ^{1}H NMR spectroscopy.

Quanta/CHARMm calculations. The structural calculations were done using Quanta/CHARMm 2005 software. The tetrakis(pyridiniummethyl)tetramethylcavitand **2** preorganizes the pyridinium substituents in such a way that they are located in the corners of a square and point outside with angles of about 90º and 180º in the projection to the plane that is perpendicular to the C_4 axis of the molecule. The pyridinium rings are tilted only about 20° down from the plane. Due to steric hindrance caused by the oxygens of the cavitand scaffold and the protons of the CH_2N-linker, the rotation around the C-N bond is restricted.

Determination of binding constants. K_a-values (compound **3** with bromide) were determined by non-linear fitting of calculated values (equations 1-6) with experimental data obtained by ^{1}H NMR titration. The fitting program was based on Maple 8 software (Waterloo Maple Inc). The values of K_a, δ_{HG}, δ_H were varied till the best fitting of calculated with experimental data was obtained.

$$K_a = \frac{[HG]}{[H][G]} \tag{1}$$

$$K_{a,c} = \frac{[H_cG]}{[H][G_c]} \tag{2}$$

$$[G]_{tot} = [HG] + [H_cG] + [G] \tag{3}$$

$$[H]_{tot} = [HG] + [H] \tag{4}$$

$$[H_c]_{tot} = [H_cG] + [H_c] \tag{5}$$

$$\delta_{obs} = \chi_{HG}\delta_{HG} + \chi_H\delta_H \tag{6}$$

($[G]_{tot}$, $[H]_{tot}$, $[H_c]_{tot}$ − total concentration of the guest, host, and competitor (tetrabutylammonium cation), respectively; $K_{a,c}$ − binding constant of the anion with the competitor (several values varying from 0 to 10^3 M^{-1} were taken into the model); K_a − binding constant of host **3** with bromide; $[G]$, $[H]$, $[H_c]$, $[HG]$, $[H_cG]$ − concentrations of the guest, host **3**, competitor, the complexes of the host with the guest, and the complexes of the host with the competitor, respectively; χ_{HG} and χ_H − mole fractions of the host-guest complex and host; δ_{obs} − observed shift of the protons of the host; δ_{HG} and δ_H − shifts of protons of the host-guest complex and host, respectively).

ESI-MS: The ESI-MS experiments were carried out with a Jeol AccuTOF instrument. In the standard mode the solutions were introduced at a flow rate of 12.5 µL/min. In the continuous nanoflow mode, the solutions were introduced with pressure (the flow rate set in the syringe pump was up to 400 nL/min) into fused-silica PicoTip® emitters purchased from New Objective, Inc. The data were accumulated in the mass range 230 − 4000 *m/z* for 2 min. The standard spray conditions, unless otherwise specified are: capillary voltage 2500 V, ring lens voltage 30 V, orifice 1 voltage = 2 V, orifice 2 voltage = 2 V, orifice 1 temperature = 60 °C, temperature in the desolvation chamber 120 °C, drying gas flow 0.1 − 0.5 L/min, nebulizing gas flow = 0.5 L/min. For the characterization of compounds **2** and **4** the most intensive signals of the isotopic pattern observed are shown.

Tetrakis(pyridiniummethyl)tetramethylcavitand tetrabromide 2×4Br

To a solution of tetrakis(bromomethyl)tetramethylcavitand[25] **1** (1.0 g, 1.04 mM) in chloroform (50 mL), pyridine (0.51 mL, 6.22 mM) was added dropwise. The reaction mixture was stirred for 12 h. To the suspension formed, methanol (50 mL) was added and the clear reaction mixture obtained was stirred for an additional 24 h. The reaction

mixture was evaporated to dryness under vacuum. The product was purified twice by reprecipitation with diethyl ether from methanol. Yield: 1.2 g (94%); m.p. > 300 °C (dec); ^{1}H NMR (5 mM, CD$_3$OD) δ: 9.00 (d, 8 H, J = 6.2 Hz; α-pyridinium-H), 8.59 (t, 4 H, J = 7.7 Hz; γ-pyridinium-H), 8.11 (t, 8 H, J = 7.0 Hz; β-pyridinium-H), 7.89 (s, 4 H; cavArH), 6.30 (d, 4 H, J = 7.3 Hz; OCHH^OO), 5.81 (s, 8 H; ArCH$_2$Py), 4.97 (q, 4 H, J = 7.3 Hz; Ar$_2$CH), 4.77 + 4.75 (4 H + water; OCHH^iO), 1.89 (d, 12 H, J = 7.3 Hz; CH$_3$); ^{13}C NMR (50 mM, CD$_3$OD) δ: 154.8, 147.4, 146.4, 141.6, 129.8, 126.4, 121.5, 101.7, 56.6, 33.5, 17.2; nano ESI-MS (5 mM, CH$_3$OH): [**2**·2Br]$^{2+}$ 560.15 (calc: 560.12), [**2**·2·5Br]$^{3+}$ 773.85 (calc: 773.80), [**2**·2·6Br]$^{2+}$ 1201.19 (calc: 1201.16).

General procedure for ion exchange:

1. Column preparation

Dowex anion exchange resin (~ 150 mL) was washed with methanol (1 L) and placed into a column (d = 25 mL), which had a small piece of wool above the stopcock at the bottom of the column. The column was flushed under pressure by methanol (1 L) and Q-water (2 L). Subsequently, it was washed by an aqueous solution of NaOH (1 N, 400 mL, mainly without pressure) and Q-water (1.5 L, with pressure). It was followed by washing with an aqueous solution of the salt chosen (mainly without pressure; 0.5 L of 1 N solutions of sodium nitrate, sodium acetate, and sodium tosylate in water were used for the preparation of Dowex NO$_3$, Dowex OAc, and Dowex Tos, respectively). To remove the excess of the salt, the column was washed with Q-water (2.5 L) and flushing with MeOH (300 – 500 mL, with pressure).

2. Ion exchange

A solution of compound **2**×4Br or **4**×Br (400 mg) in methanol (20 mL) was flushed into the Dowex Anion column without pressure. The column was washed with methanol (200 mL). The methanol solution was evaporated to dryness under vacuum without heating to give the **2**×4Anions or **4**×Anions in quantitative yields.

Tetrakis(pyridiniummethyl)tetramethylcavitand tetranitrate 2×4NO$_3$

m.p. > 300 °C (dec); ^{1}H NMR (5 mM, CD$_3$OD) δ: 8.97 (d, 8 H, J = 6.5 Hz; α-pyridinium-H), 8.59 (t, 4 H, J = 7.5 Hz; γ-pyridinium-H), 8.10 (t, 8 H, J = 6.8 Hz; β-pyridinium-H), 7.74 (s, 4 H; cavArH), 6.27 (d, 4 H, J = 7.3 Hz; OCHH^OO), 5.76 (s, 8 H; ArCH$_2$Py), 4.98 (q, 4 H, J = 7.3 Hz; Ar$_2$CH), 4.67 (d, 4 H, J = 7.3 Hz; OCHH^iO), 1.83 (d, 12 H, J = 7.3 Hz; CH$_3$); ^{13}C NMR (10 mM, CD$_3$OD) δ: 154.9, 147.4, 146.4,

141.4, 129.7, 124.8, 121.8, 101.5, 56.3, 33.1, 24.2, 16.2; nano ESI-MS (5 mM, CH$_3$OH): [$\mathbf{2}$·2NO$_3$]$^{2+}$ 542.17 (calc: 542.19), [$\mathbf{2}$·$\mathbf{2}$·5NO$_3$]$^{3+}$ 743.90 (calc: 743.92), [$\mathbf{2}$·$\mathbf{2}$·6NO$_3$]$^{2+}$ 1146.83 (calc: 1146.87); elemental analysis calcd (%) for C$_{60}$H$_{56}$N$_8$O$_{20}$ + 3 H$_2$O (1263.2): C 57.05, H 4.95, N 8.87; found: C 57.21, H 4.72, N 8.75.

Tetrakis(pyridiniummethyl)tetramethylcavitand tetraacetate 2×4OAc

m.p. > 200 °C (dec); ^{1}H NMR (5 mM, CD$_3$OD) δ: 8.98 (d, 8 H, J = 5.9 Hz; α-pyridinium-H), 8.60 (t, 4 H, J = 7.5 Hz; γ-pyridinium-H), 8.11 (t, 8 H, J = 7.0 Hz; β-pyridinium-H), 7.68 (s, 4 H; cavArH), 6.29 (d, 4 H, J = 7.7 Hz; OCHH^OO), 5.77 (s, 8 H; ArCH$_2$Py), 4.98 (q, 4 H, J = 7.3 Hz; Ar$_2$CH), 4.74 (d, 4 H, J = 7.3 Hz; OCHH^iO), 1.80 + 1.82 (24 H; CH$_3$-cavitand + CH$_3$-acetate); ^{13}C NMR (25 mM, CD$_3$OD) δ: 179.9, 154.9, 147.5, 146.4, 141.3, 129.8, 124.8, 121.9, 101.5, 56.2, 33.0, 24.2, 16.2; nano ESI-MS (5 mM, CH$_3$OH): [$\mathbf{2}$·$\mathbf{2}$·6OAc]$^{2+}$ 1140.95 (calc: 1140.97); elemental analysis calcd (%) for C$_{68}$H$_{72}$N$_4$O$_{16}$ + 4.5 H$_2$O (1282.4): C 63.69, H 6.37, N 4.37; found: C 63.92, H 6.40, N 4.11.

Tetrakis(pyridiniummethyl)tetramethylcavitand tetratosylate 2×4Tos

m.p. 199–200 °C; ^{1}H NMR (5 mM, CD$_3$OD) δ: 8.96 (d, 8 H, J = 5.5 Hz; α-pyridinium-H), 8.55 (t, 4 H, J = 7.7 Hz; γ-pyridinium-H), 8.07 (t, 8 H, J = 7.0 Hz; β-pyridinium-H), 7.69 + 7.71 (12 H; cavArH + α-tosylate-H), 7.22 (d, 8 H, J = 7.7 Hz; β-tosylate-H), 6.32 (d, 4 H, J = 7.7 Hz; OCHH^OO), 5.79 (s, 8 H; ArCH$_2$Py), 4.98 (q, 4 H, J = 7.3 Hz; Ar$_2$CH), 4.74 + 4.77 (4 H + water; OCH^iO), 2.35 (s, 12 H; CH$_3$-tosylate), 1.82 (d, 12 H, J = 7.3 Hz; CH$_3$-cavitand); ^{13}C NMR (20 mM, CD$_3$OD) δ: 154.9, 147.3, 146.4, 143.9, 141.9, 141.3, 130.0, 129.7, 127.1, 124.9, 121.9, 101.7, 56.3, 33.0, 21.5, 16.3; nano ESI-MS (5 mM, CH$_3$OH): [$\mathbf{2}$·Tos]$^{3+}$ 377.16 (calc: 377.14), [$\mathbf{2}$·2Tos]$^{2+}$ 651.23 (calc: 651.22), [$\mathbf{2}$·$\mathbf{2}$·5Tos]$^{3+}$ 925.95 (calc: 925.96); elemental analysis calcd (%) for C$_{88}$H$_{84}$N$_4$O$_{20}$S$_4$ + H$_2$O (1663.9): C 63.52, H 5.21, N 3.37; found: C 63.55, H 5.33, N 3.18.

1-(4-Methylbenzyl)pyridinium nitrate 4×NO$_3$

Transparent oil; ^{1}H NMR (10 mM, CD$_3$OD) δ: 9.02 (d, 2 H, J = 5.5 Hz; α-pyridinium-H), 8.60 (t, 1 H, J = 7.7 Hz; γ-pyridinium-H), 8.10 (t, 2 H, J = 6.6 Hz; β-pyridinium-H), 7.38 (d, 2 H, J = 8.1 Hz; 2,6-benzyl-H), 7.29 (d, 2 H, J = 8.1 Hz; 3,5-benzyl-H), 5.79 (s, 2 H; ArCH$_2$Py), 2.36 (s, 6 H; CH$_3$); ESI-MS (1 mM, CH$_3$OH): [$\mathbf{4}$·NO$_3$·$\mathbf{4}$]$^+$ 430.24 (calc.: 430.21).

1-(4-Methylbenzyl)pyridinium acetate 4×OAc

Transparent slightly yellowish oil, which easily turns brown upon heating or influence of light; ^{1}H NMR (10 mM, CD$_3$OD) δ: 9.05 (d, 2 H, J = 5.4 Hz; α-pyridinium-H), 8.61 (t, 1 H, J = 7.5 Hz; γ-pyridinium-H), 8.12 (t, 2 H, J = 6.8 Hz; β-pyridinium-H), 7.40 (d, 2 H, J = 8.1 Hz; 2,6-benzyl-*H*), 7.30 (d, 2 H, J = 8.1 Hz; 3,5-benzyl-*H*), 5.80 (s, 2 H; ArCH$_2$Py), 1.90 (s, 3 H; CH$_3$-acetate); ESI-MS (1 mM, CH$_3$OH): [**4·OAc·4**]$^+$ 427.26 (calc.: 427.24).

1-(4-Methylbenzyl)pyridinium tosylate 4×Tos

Transparent oil; ^{1}H NMR (10 mM, CD$_3$OD) δ: 9.02 (d, 2 H, J = 5.6 Hz; α-pyridinium-H), 8.59 (t, 1 H, J = 7.6 Hz; γ-pyridinium-H), 8.10 (t, 2 H, J = 6.8 Hz; β-pyridinium-H), 7.70 (d, 2 H, J = 8.0 Hz; α-tosylate-H), 7.38 (d, 2 H, J = 8.4 Hz; 2,6-benzyl-*H*), 7.29 (d, 2 H, J = 8.4 Hz; 3,5-benzyl-*H*), 7.22 (d, 2 H, J = 8.0 Hz; β-tosylate-H), 5.78 (s, 2 H; ArCH$_2$Py), 2.36 (s, 6 H; 2×CH$_3$); ESI-MS (1 mM, CH$_3$OH): [**4·Tos·4**]$^+$ 539.23 (calc: 539.24).

References and notes

1. Rebek, J. *Angew. Chem., Int. Ed.* **2005**, *44*, 2068-2078.
2. Fujita, M.; Tominaga, M.; Hori, A.; Therrien, B. *Acc. Chem. Res.* **2005**, *38*, 369-378; Takeda, N.; Umemoto, K.; Yamaguchi, K.; Fujita, M. *Nature* **1999**, *398*, 794-796.
3. Reinhoudt, D. N.; Crego-Calama, M. *Science* **2002**, *295*, 2403-2407.
4. Prins, L. J.; de Jong, F.; Timmerman, P.; Reinhoudt, D. N. *Nature* **2000**, *408*, 181-184; Prins, L. J.; Huskens, J.; de Jong, F.; Timmerman, P.; Reinhoudt, D. N. *Nature* **1999**, *398*, 498-502.
5. Davis, J. T. *Angew. Chem., Int. Ed.* **2004**, *43*, 668-698.
6. Grote, Z.; Scopelliti, R.; Severin, K. *J. Am. Chem. Soc.* **2004**, *126*, 16959-16972.
7. Lehn, J.-M. *Science* **2002**, *295*, 2400-2403; Whitesides, G. M.; Grzybowski, B. *Science* **2002**, *295*, 2418-2421.
8. Badjić, J. D.; Nelson, A.; Cantrill, S. J.; Turnbull, W. B.; Stoddart, J. F. *Acc. Chem. Res.* **2005**, *38*, 723-732; Mammen, M.; Choi, S. K.; Whitesides, G. M. *Angew. Chem., Int. Ed.* **1998**, *37*, 2755-2794; Mulder, A.; Huskens, J.; Reinhoudt, D. N. *Org. Biomol. Chem.* **2004**, *2*, 3409-3424.
9. Böhmer, V.; Vysotsky, M. O. *Aust. J. Chem.* **2001**, *54*, 671-677.
10. Baldini, L.; Ballester, P.; Casnati, A.; Gomila, R. M.; Hunter, C. A.; Sansone, F.; Ungaro, R. *J. Am. Chem. Soc.* **2003**, *125*, 14181-14189; Haino, T.; Kobayashi, M.; Chikaraishi, M.; Fukazawa, Y. *Chem. Commun.* **2005**, 2321-2323; Pinalli, R.; Cristini, V.; Sottili, V.; Geremia, S.; Campagnolo, M.; Caneschi, A.; Dalcanale, E. *J. Am. Chem. Soc.* **2004**, *126*, 6516-6517;

Zuccaccia, D.; Pirondini, L.; Pinalli, R.; Dalcanale, E.; Macchioni, A. *J. Am. Chem. Soc.* **2005**, *127*, 7025-7032.

11. Corbellini, F.; Di Costanzo, L.; Crego-Calama, M.; Geremia, S.; Reinhoudt, D. N. *J. Am. Chem. Soc.* **2003**, *125*, 9946-9947; Corbellini, F.; Knegtel, R. M. A.; Grootenhuis, P. D. J.; Crego-Calama, M.; Reinhoudt, D. N. *Chem. Eur. J.* **2005**, *11*, 298-307; Zadmard, R.; Kraft, A.; Schrader, T.; Linne, U. *Chem. Eur. J.* **2004**, *10*, 4233-4239.

12. Zadmard, R.; Junkers, M.; Schrader, T.; Grawe, T.; Kraft, A. *J. Org. Chem.* **2003**, *68*, 6511-6521.

13. Fuoss, R. M.; Kraus, C. A. *J. Am. Chem. Soc.* **1933**, *55*, 2387-2399.

14. Chen, Z. D.; Hojo, M. *J. Phys. Chem. B* **1997**, *101*, 10896-10902; Reich, H. J.; Sikorski, W. H.; Gudmundsson, B. O.; Dykstra, R. R. *J. Am. Chem. Soc.* **1998**, *120*, 4035-4036.

15. Hojo, M.; Takiguchi, T.; Hagiwara, M.; Nagai, H.; Imai, Y. *J. Phys. Chem.* **1989**, *93*, 955-961.

16. Hojo, M.; Fujime, C.; Yoneda, H. *Chem. Lett.* **1993**, 37-40.

17. Oelkers, E. H.; Helgeson, H. C. *Science* **1993**, *261*, 888-891.

18. Jarek, R. L.; Denson, S. C.; Shin, S. K. *J. Chem. Phys.* **1998**, *109*, 4258-4266; Jarek, R. L.; Shin, S. K. *J. Am. Chem. Soc.* **1997**, *119*, 10501-10508.

19. Barthel, J.; Krienke, H.; Neueder, R.; Holovko, M. F. *Fluid Phase Equilib.* **2002**, *194*, 107-122; Weingartner, H.; Weiss, V. C.; Schroer, W. *J. Chem. Phys.* **2000**, *113*, 762-770.

20. Bowman-James, K. *Acc. Chem. Res.* **2005**, *38*, 671-678.

21. For reviews on anion receptors, see: Kubik, S.; Reyheller, C.; Stuwe, S. *J. Incl. Phenom. Macrocycl. Chem.* **2005**, *52*, 137-187; Gale, P. A. *Coord. Chem. Rev.* **2003**, *240*, 191-221, and other reviews in this issue; Fitzmaurice, R. J.; Kyne, G. M.; Douheret, D.; Kilburn, J. D. *J. Chem. Soc., Perkin Trans. 1* **2002**, 841-864; Beer, P. D.; Gale, P. A. *Angew. Chem., Int. Ed.* **2001**, *40*, 487-516; Antonisse, M. M. G.; Reinhoudt, D. N. *Chem. Commun.* **1998**, 443-448.

22. Worm, K.; Schmidtchen, F. P. *Angew. Chem., Int. Ed. Engl.* **1995**, *34*, 65-66.

23. Rosokha, Y. S.; Lindeman, S. V.; Rosokha, S. V.; Kochi, J. K. *Angew. Chem., Int. Ed.* **2004**, *43*, 4650-4652.

24. Grote Gansey, M. H. B.; Bakker, F. K. G.; Feiters, M. C.; Geurts, H. P. M.; Verboom, W.; Reinhoudt, D. N. *Tetrahedron Lett.* **1998**, *39*, 5447-5450; Middel, O.; Verboom, W.; Reinhoudt, D. N. *Eur. J. Org. Chem.* **2002**, 2587-2597.

25. Sorrell, T. N.; Pigge, F. C. *J. Org. Chem.* **1993**, *58*, 784-785.

26. Mezo, A. R.; Sherman, J. C. *J. Org. Chem.* **1998**, *63*, 6824-6829; Pirondini, L.; Bonifazi, D.; Menozzi, E.; Wegelius, E.; Rissanen, K.; Massera, C.; Dalcanale, E. *Eur. J. Org. Chem.* **2001**, 2311-2320.

27. Katritzky, A. R.; Watson, C. H.; Degaszafran, Z.; Eyler, J. R. *J. Am. Chem. Soc.* **1990**, *112*, 2471-2478.

28. Shpan'ko, I. V.; Korostylev, A. P.; Rusu, L. N. *J. Org. Chem. USSR (Engl. Transl.)* **1984**, *20*, 1715-1723.

29. Larsen, J. W.; Edwards, A. G.; Dobi, P. *J. Am. Chem. Soc.* **1980**, *102*, 6780-6783; Hemmes, P.; Costanzo, J. N.; Jordan, F. *J. Phys. Chem.* **1978**, *82*, 387-391; Chuck, R. J.; Randall, E. W. *Spectrochim. Acta* **1966**, *22*, 221-226.

30. Hojo, M.; Nagai, H.; Hagiwara, M.; Imai, Y. *Anal. Chem.* **1987**, *59*, 1770-1774.

31. Oshovsky, G. V.; Verboom, W.; Fokkens, R. H.; Reinhoudt, D. N. *Chem. Eur. J.* **2004**, *10*, 2739-2748.

32. Due to the formation of much smaller droplets in nano ESI-MS in comparison with standard ESI-MS, the way of large molecules from a solution to the gas phase is not more significantly diffusion limited. It causes a higher intensity of signals of large molecules in the nano mode, and gives a more realistic representation of the species in solution.

33. A similar aggregation of pyridinium salts was observed by: Yoneda, M.; Tanizaki, K.; Tsujimoto, K.; Ohashi, M. *Org. Mass Spec.* **1993**, *28*, 693-698; Alfassi, Z. B.; Huie, R. E.; Milman, B. L.; Neta, P. *Anal. Bioanal. Chem.* **2003**, *377*, 159-164.

34. Due to the different volatility and stability of the species observed in the mass spectrum, ESI-MS cannot be used for the quantification of the solution processes (see ref. 31 and Chapter 3).

35. The X-Ray crystal structures of **2×4Br** and **2×4NO₃** confirm the open flower structure of cation **2**. Nevertheless, due to packing forces and the domination of CH-anion above electrostatic interactions in the solid state, none of the interactions observed in solution and in the gas phase takes place in the solid state. Atwood, J. L.; Barbour, L. J.; Hardie, M. J.; Raston, C. L. *Coord. Chem. Rev.* **2001**, *222*, 3-32.

36. Daniel, J. M.; Friess, S. D.; Rajagopalan, S.; Wendt, S.; Zenobi, R. *Int. J. Mass. Spec.* **2002**, *216*, 1-27; Ganem, B.; Henion, J. D. *Bioorg. Med. Chem.* **2003**, *11*, 311-314; Schalley, C. A. *Int. J. Mass. Spec.* **2000**, *194*, 11-39.

37. Schalley, C. A.; Verhaelen, C.; Klarner, F. G.; Hahn, U.; Vogtle, F. *Angew. Chem., Int. Ed.* **2005**, *44*, 477-480.

38. Gabelica, V.; De Pauw, E. *Mass Spectrom. Rev.* **2005**, *24*, 566-587.

39. Bure, C.; Lange, C. *Curr. Org. Chem.* **2003**, *7*, 1613-1624.

40. For details about orifice and ring lens parts of an ESI mass spectrometer, see ref. 38.

41. Hinderling, C.; Feichtinger, D.; Plattner, D. A.; Chen, P. *J. Am. Chem. Soc.* **1997**, *119*, 10793-10804.

42. The difference might be caused by the different design of the orifice and ring lens parts of the mass spectrometer resulting in the release of the excessive energy of the ions via self-dissociation instead of collision-induced cleavage.

43. Orifice 1 and orifice 2 voltages have a similar influence on the fragmentation. Nevertheless, due to the proximity of the orifice 1 to the spray source, it also influences the movement of the species from droplets to the gas phase. It causes an increase of the intensity of the signals in the resulting spectrum, as well as the appearance of several additional signals that correspond to complexes of **2** with a different number of anions. To avoid the influence of this variable on the interpretation of the results, only the effect of orifice 2 voltage variations on the composition of the gas phase mixture is shown in this Chapter.

44. The influence of the gradual increase of the orifice 2 voltage is shown in attachment 1.

45. Gabelica, V.; De Pauw, E.; Karas, M. *Int. J. Mass. Spec.* **2004**, *231*, 189-195; Naban-Maillet, J.; Lesage, D.; Bossee, A.; Gimbert, Y.; Sztaray, J.; Vekey, K.; Tabet, J. C. *J. Mass. Spec.* **2005**, *40*, 1-8.

46. Recently, we have found that applying extremely drastic conditions gives cleavage of the pyridinium cation from the contact ion-pair in capsules based

on multivalent electrostatic interactions (Chapter 7). In the case of pyridinium cations, the almost complete cleavage of pyridine takes place already at 60 V (orifice 1 voltage). In the case of the pyridinium contact ion-pairs the cleavage only begins at 100 V and is even not complete at 225 V.

47.   A similar dissociation of triple ions to ions and ion-pairs has been reported in an ESI-MS CID study of solutions of pyridinium-containing salts: Milman, B. L. *Rapid Commun. Mass Spectrom.* **2003**, *17*, 1344-1349.

48.   Methylene-pyridinium cation **14** has a high CH-acidity due to the coulombic effect of the positive charge and the resonance delocalization effects of the aromatic ring. Zhang, X. M.; Bordwell, F. G.; Vanderpuy, M.; Fried, H. E. *J. Org. Chem.* **1993**, *58*, 3060-3066.

49.   At low ring lens voltage, 2^{4+} and $[2 \cdot Br]^{3+}$ signals are also present. But, due to lower stability of these cations, they experience easy deprotonation and, therefore, disappear upon increase of the voltage.

50.   Further increase of the ring lens voltage (45 V) leads to dissociation of $[5 \cdot Br \cdot 5]^{+}$ to 5^{+} and $[5 \cdot Br]^{0}$, what causes a relative increase of the intensity of the 5^{+} signal in comparison with that of the $[5 \cdot Br \cdot 5]^{+}$ signal. However, the absolute intensity of both signals decreases.

51.   A similar cleavage of pyridinium-containing ion-pairs, namely loss of an anion accompanied by deprotonation (in total, loss of an acid) is considered in ref. 47.

52.   A relative decrease in comparison with the sum of the intensities of the $[guest \cdot 2 \cdot 2 \cdot 5Br]^{3+}$ and $[2 \cdot 2 \cdot 5Br]^{3+}$ signals.

53.   Gui, X.; Sherman, J. C. *Chem. Commun.* **2001**, 2680-2681.

54.   Upon complexation of organic anions large ^{1}H NMR shifts (up to 5 ppm) have been observed: Oshovsky, G. V.; Verboom, W.; Reinhoudt, D. N. *Collect. Czech. Chem. Commun.* **2004**, *69*, 1137-1148, and Chapter 4.

55.   For a corresponding example with sulfate as a linker, see Chapter 6.

56.   Meyer, E. A.; Castellano, R. K.; Diederich, F. *Angew. Chem., Int. Ed.* **2003**, *42*, 1210-1250; Mori, T.; Inoue, Y. *Angew. Chem., Int. Ed.* **2005**, *44*, 2582-2585.

57.   Cantrill, S. J.; Chichak, K. S.; Peters, A. J.; Stoddart, J. F. *Acc. Chem. Res.* **2005**, *38*, 1-9; Liu, Y.; Bonvallet, P. A.; Vignon, S. A.; Khan, S. I.; Stoddart, J. F. *Angew. Chem., Int. Ed.* **2005**, *44*, 3050-3055; Rowan, S. J.; Cantrill, S. J.; Cousins, G. R. L.; Sanders, J. K. M.; Stoddart, J. F. *Angew. Chem., Int. Ed.* **2002**, *41*, 898-952.

58.   Complexation at the outside of the capsule, as was shown by Schrader c.s. in the case of 1:1 calix[4]arene capsules (see ref. 12), is of minor value due to the negligibly low intensity of the $[guest \cdot 2 \cdot 2 \cdot 6Br]^{2+}$ signals of complexes that could correspond to a complex of a guest with the capsule containing four anionic walls and two anions inside (structure 2anions@**8** in Scheme 3).

59.   Brady, P. A.; Sanders, J. K. M. *New J. Chem.* **1998**, *22*, 411-417.

60.   For examples of CH-I interactions, see: Kobayashi, K.; Ishii, K.; Yamanaka, M. *Chem. Eur. J.* **2005**, *11*, 4725-4734; Laughrey, Z. R.; Gibb, C. L. D.; Senechal, T.; Gibb, B. C. *Chem. Eur. J.* **2003**, *9*, 130-139; Gibb, C. L. D.; Stevens, E. D.; Gibb, B. C. *J. Am. Chem. Soc.* **2001**, *123*, 5849-5850.

61.   Kröhnke, F.; Vogt, I. *Chem. Ber.* **1952**, *85*, 368.

Appendix 1.

The influence of the gradual increase of the orifice 2 voltage

This appendix demonstrates the sensitivity of the methylene-pyridinium cations to the influence of an increase of the orifice voltage. The changes in the mass spectrum of a 0.5 mM solution of **2**×4Br upon increase of the orifice 2 voltage from 2 V (Figure 3, Chapter 5) till 10 V, 15 V and 20 V are shown in the Figure A1.1. The voltage increase significantly changes the picture on the left side of the spectrum. In the case of 10 V, two additional signals have appeared close to the $[\mathbf{2}\cdot2Br]^{2+}$ signal, corresponding to $[\mathbf{2}\cdot2Br\text{-}Py]^{2+}$ and $[\mathbf{2}\cdot2Br\text{-}2Py]^{2+}$. They have obviously been formed from $[\mathbf{2}\cdot2Br]^{2+}$ by the fragmentation considered in Scheme 5 (Chapter 5). The increase of the voltage till 15 V causes the $[\mathbf{2}\cdot2Br\text{-}2Py]^{2+}$ signal to be the most intensive in the spectrum, and further increase for 5 V gives rise to a very significant decrease of the $[\mathbf{2}\cdot2Br]^{2+}$ and $[\mathbf{2}\cdot2Br\text{-}Py]^{2+}$ signals. Decrease of the intensity of the two last mentioned signals is accompanied by an about equal increase of the intensity of the $[\mathbf{2}\cdot2Br\text{-}2Py]^{2+}$ signal. It should be noted that no further transformations of this signal were observed, what indicates the stability of the contact pyridinium ion-pairs at these conditions. The stability of the $[\mathbf{2}\cdot2Br\text{-}2Py]^{2+}$ signal indicates that two anions are ion-paired with the pyridinium groups, but not within the cavity, otherwise the third, in this case non-ion-paired, pyridinium group would have been cleaved off.
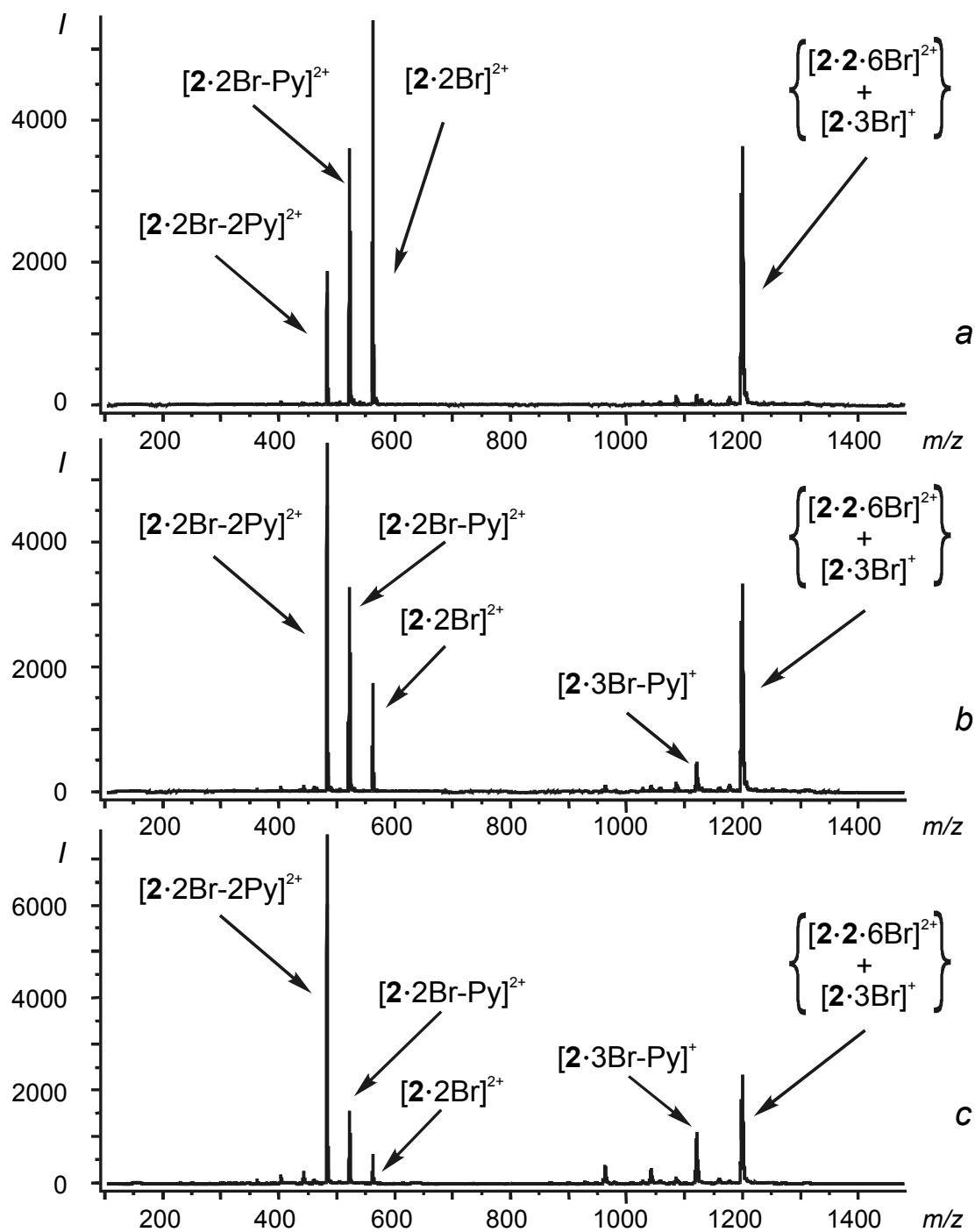
Figure A1.1. ESI-MS spectrum of a 0.5 mM solution of **2**×4Br in methanol (voltages: capillary = 2500 V, ring lens = 30 V, orifice 1 = 2 V, flow rate 12.5 μL/min), orifice 2 voltage = 10 V (a), 15 V (b), and 20 V (c).

ELECTROSTATIC ASSEMBLY OF TETRAKIS(PYRIDINIUMMETHYL)CAVITANDS AND DOUBLY CHARGED ANIONS IN POLAR MEDIA

Electrostatic self-assembly of tetrakis(pyridiniummethyl)cavitand hemispheres (H) *and doubly charged anions* (A) *in polar media gives rise to an equilibrium mixture that consists, as detected with ESI-MS, of capsule* H_2A_4, *hemicapsule* H_2A_3, *and other ion-pair associates. Fitting* [1]*H NMR data with a new model, which includes (hemi)capsules and ion-pair associates, gave an effective molarity (EM) for the intramolecular processes of 0.19 ± 0.02 M for assembly of the host* (H) *with sulphate* (A). *The model shows that in addition to capsules, comparable amounts of hemicapsules are present in solution together with substantial amounts of other ion-pair associates. For example, 5 mM and 25 mM solutions of the host* (H) *with sulphate as the anion* (A) *contain 14% and 33% of [2+4] capsule* H_2A_4, *as well as 10% and 14% of [2+3] hemicapsule* H_2A_3, *respectively. The [2+3] hemicapsules* H_2A_3 *built with sulphate linkers incorporate guests in between the closely positioned pyridinium planes.*

6.1 Introduction

Supramolecular chemistry aims at developing highly complex systems from components interacting through non-covalent intermolecular forces.[1] Self-assembly comprises the spontaneous generation of a well-defined, discrete supramolecular architecture from a given set of components under thermodynamic equilibrium.[2,3] Self-assembly processes driven by *strong* interactions and/or carried out in non-competitve media exclusively lead to the final product.[4,5] A high binding affinity between receptor and ligand, supported by multivalency,[6] excludes intermediates[4] and provides narcissistic self-sorting.[5] However, in the case of *weak* interactions, especially in the case of self-association in polar competitive media, it is expected that partial assemblies will be present in substantial amounts at equilibrium conditions.

Capsules are an example of complex assemblies.[7] Nowadays, in addition to [1+1] capsules[8] and hexameric resorcinarene capsule-like assemblies,[9] [2+4] capsules[10-13] attract substantial attention. These capsules contain half-spheres, which are brought together by four linkers (for example, **1**). For the construction of such capsules in solution quite strong interactions have been used (like metal-ligand[10,11] or hydrogen-bonding[12]).

In Chapter 5 evidence is described for the existence of (hemi)capsules formed by rather weak triple ion interactions (pyridinium-anion-pyridinium) of two tetrakis(pyridiniummethyl)tetramethylcavitands and singly charged anions in methanol. This chapter deals with the ion-pair interaction of these cavitands and doubly charged anions to give an equilibrium mixture of [2+4] capsules H_2A_4 **1**, [2+3] hemicapsules H_2A_3 **2**, and ion-pair associates (an equilibrium between **1** and **2** is shown in Scheme 1). With a model, based on ^{1}H NMR data, a quantitative description of the composition of the equilibrium mixture is presented.
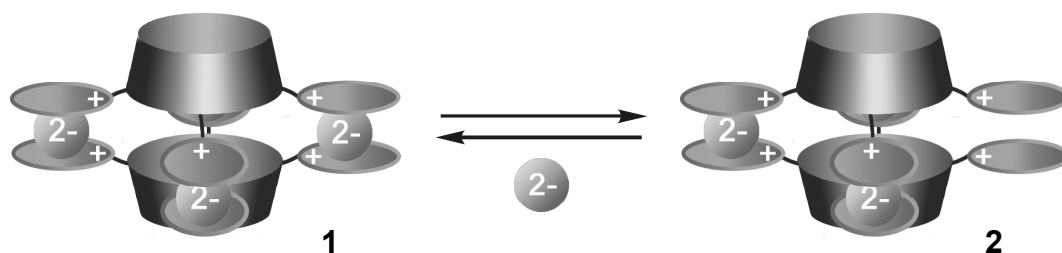
Scheme 1. Equilibrium between [2+4] capsule **1** and [2+3] hemicapsule **2**.

6.2 Results and discussion

6.2.1 *Synthesis*

Salts of tetrakis(pyridiniummethyl)cavitand tetracation **3** with doubly charged anions of different size (sulphate, oxalate, terephthalate, isophthalate, and phthalate) were prepared starting from the tetrabromide[14] **3**×4Br (Chart 1) using a column loaded with a Dowex anion exchange resin functionalized with the appropriate anion.[15] With this method all unwanted counterions are removed from the sample and, therefore, it avoids possible by-processes like contact ion-pair or triple ion formation with the initial counterion.[16]
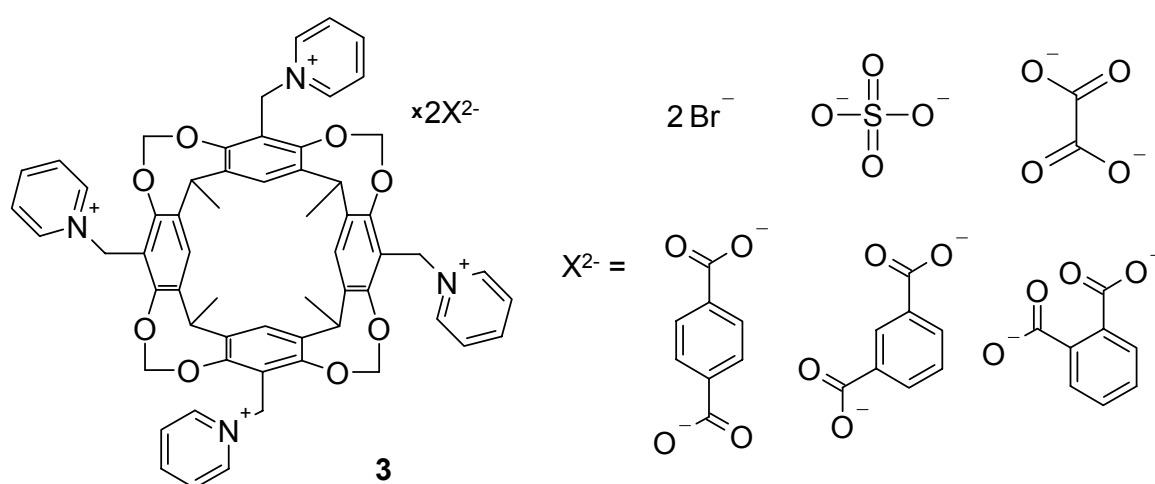
Chart 1. Tetrakis(pyridiniummethyl)tetramethylcavitand salts.

A column loaded with Dowex SO₄ was used to prepare *N*-(4-methylbenzyl)-pyridinium sulphate **4** as a model compound from the corresponding bromide.
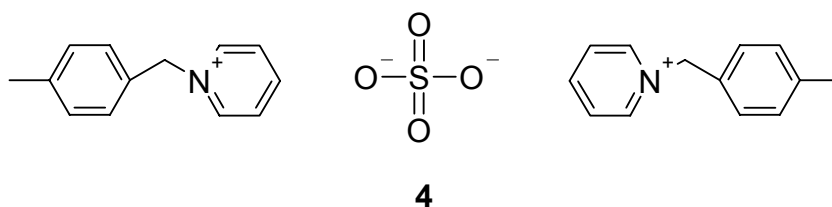
6.2.2 ^{1}H NMR and ESI-MS study

It is known that ion-pairing between a pyridinium cation and an anion in solution is accompanied by changes of the shifts of the pyridinium hydrogens in the ^{1}H NMR spectra.[17] Dilution experiments of compounds **3** and **4** in methanol-*d₄*

displayed changes of all the hydrogens in their ^{1}H NMR spectra. It is interesting to note that depending on the anion the hydrogens of the pyridinium ring experience different ^{1}H NMR shift differences. For example, in the case of **3**×2SO$_4$ the largest shift difference is observed for the α-pyridinium hydrogen (> 0.04 ppm, dilution 20 - 0.05 mM). However, in the case of isophthalate, the β-pyridinium hydrogen shows the larger relative shift difference (~ 0.02 ppm, the same concentration range), while the influence of the concentration changes on the shifts of the α-pyridinium hydrogens is negligible. The difference between the sulphate and isophthalate is probably caused by an additional specific influence of the ring currents of the substituted benzene[18] on the pyridinium protons in the ion-pairs. Relatively large ^{1}H NMR shifts, indicating the ion-pairing, are also observed for the protons of isophthalate (Figure 1).
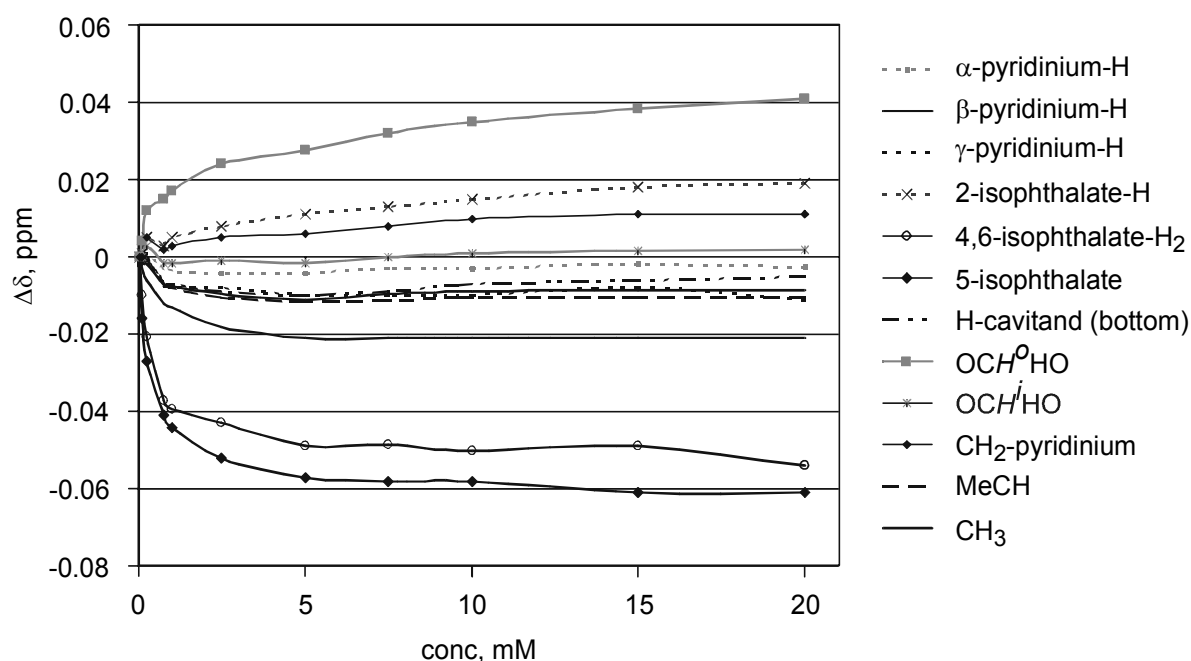
Figure 1. ^{1}H NMR shift differences observed upon dilution of **3**×2isophthalate in methanol-d_4 (with respect to the shifts of **3**×2isophthalate at 0.05 mM).

In the case of compounds **3** ion-pairing can lead to several species depending on the number of ion-paired anions viz. [**3**×A]$^{2+}$, [**3**×2A]^0, [**3**×3A]$^{2-}$, [**3**×4A]$^{4-}$ (A is doubly charged anion, sulphate, oxalate, terephthalate, isophthalate, and phthalate). These formulae indicate how many pyridinium substituents are ion-paired, but can represent several isomers. Complexes, containing two cavitands **3** should possess at least one pyridinium-A-pyridinium linker, and can be represented by the next formulae: [**3**$_2$×A]$^{6+}$, [**3**$_2$×2A]$^{4+}$, [**3**$_2$×3A]$^{2+}$, [**3**$_2$×4A]^0, [**3**$_2$×5A]$^{2-}$, etc. These species could present either linear aggregates or (hemi)capsules.

Electrospray ionization mass spectrometry (ESI-MS) allows the easy observation of charged species. A typical mass spectrum of **3**×2A salts only contains two main signals, viz. $[3 \cdot A]^{2+}$ and $[3_2 \cdot 3A]^{2+}$ (for example A = SO_4^{2-}, Figure 2).
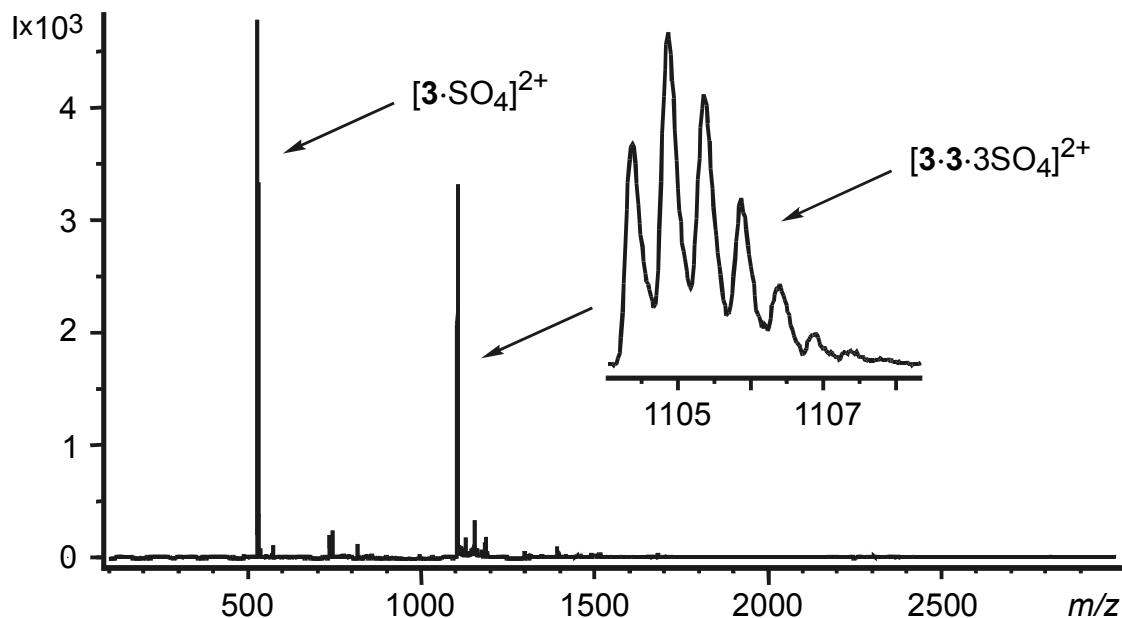
Figure 2. Nano ESI-MS continuous flow spectrum of a 5 mM solution of **3**×2SO$_4$ in methanol (voltages: capillary = 2500 V, orifice 1 and 2 = 1 V, ring lens = 30 V).[19]

The complex represented by the $[3 \cdot SO_4]^{2+}$ signal at *m/z* 528 is sensitive to changes of the ring lens voltage (for example, it completely disappears when the voltage is 40 V). Upon increase of the orifice voltage it can lose up to three pyridines. Similarly to the in-source voltage-induced fragmentation experiments described in Chapters 5 and 7, it indicates that a sulphate anion stabilizes one pyridinium moiety by ion-pairing, while the other, unstabilized, pyridiniums are cleaved off. The complex represented by the $[3_2 \cdot 3SO_4]^{2+}$ signal at *m/z* 1105 is more stable against ring lens voltage changes, similarly to the signals of the hemicapsules compared with simple ion-pair associates described in Chapter 5.

The signals of the negatively charged $[3 \cdot 3A]^{2-}$ complexes are observed in the negative ion mode ESI-MS spectra.

The expected species $[3 \cdot 2A]^0$ and $[3_2 \cdot 4A]^0$ are electrically neutral and, hence, are invisible in both positive and negative ion mode ESI-MS spectra. However, addition of a small amount of formic acid, allowed observing these species due to protonation. For example, in the spectrum of a 5 mM solution[19] of **3**×2SO$_4$ a new very

intensive signal appeared at *m/z* 1153 (Figure 3) corresponding to $[3 \cdot 2SO_4+H]^+$. It is superimposed with $[3_2 \cdot 4SO_4+2H^+]^{2+}$. A small signal of $[3_2 \cdot 4SO_4+H^+]^+$ at *m/z* 2307 is also present in the spectrum. Due to the different protonation efficiency of pyridinium-sulphonate and pyridinium-sulphonate-pyridinium contact ion-pairs (the first one contains an easily protonable O⁻), the relative intensity of the species cannot be used even for a qualitative estimation of the relative concentration of these species in solution.

ESI-MS (normal and nano) detects a number of associates viz. $[3 \times A]^{2+}$, $[3 \times 2A]^0$, $[3 \times 3A]^{2-}$, $[3_2 \times 3A]^{2+}$, and $[3_2 \times 4A]^0$ containing one or two tetrakis(pyridiniummethyl)tetramethyl cavitands with several anions. The $[3 \times A]^{2+}$, $[3 \times 2A]^0$, and $[3 \times 3A]^{2-}$ associates correspond to simple ion-paired species. In accordance with the stoichiometry, the $[3_2 \times 3A]^{2+}$, and $[3_2 \times 4A]^0$ associates could correspond to non-specific associates or (hemi)capsules. However, due to the higher voltage stability of $[3_2 \times 3A]^{2+}$, and the relatively low ability of $[3_2 \times 4A]^0$ to be protonated, it may be concluded that the main part of these species correspond to the (hemi)capsules *H₂A₃* and *H₂A₄*. To validate this conclusion and to obtain an impression of the composition of the equilibrium mixture in solution, the equilibrium was described with a model.

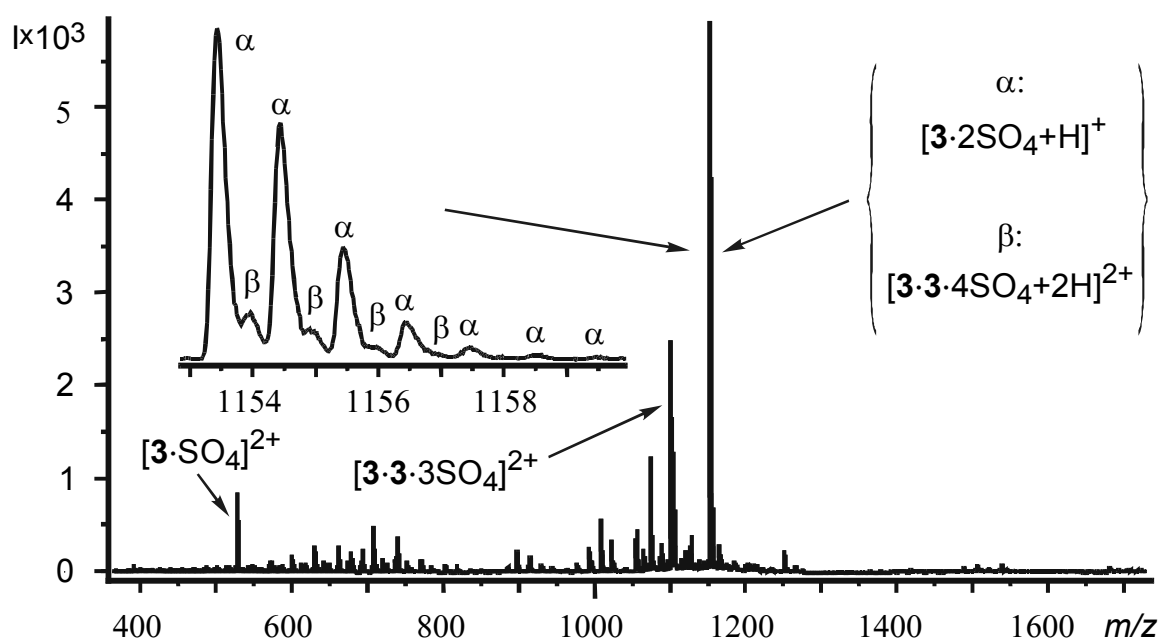**Figure 3.** Nano ESI-MS continuous flow spectrum of a 5 mM solution of **3**×2SO₄ in methanol containing small additives of formic acid (voltages: capillary = 2500 V, orifice 1 and 2 = 1 V, ring lens = 30 V).

6.2.3 Modeling of the composition of the equilibrium mixture

The association processes based on anion-pyridinium interactions are relatively weak, in comparison with metal-ligand self-assembly, and as a consequence give rise to the presence of a number of intermediates containing one or two tetrakis(pyridiniummethyl)tetramethylcavitands **3** with one or more anions. Since the species that could correspond to complexes containing more than two cavitands **3** have a negligibly low intensity in the ESI-MS spectrum, their value in the equilibrium will be unimportant at the concentrations studied. To quantify the extent to which the associates are present in the equilibrium at a given concentration, a model was developed as depicted in Schemes 2-5. Tetrakis(pyridiniummethyl)tetramethyl-cavitand **3** looks like an open flower in the most energetically favorable structure[20] and, therefore, is schematically represented as such. Non-specific dimers containing two tetrakis(pyridiniummethyl)tetramethylcavitands **3** with two or more anions (for example, $HA_2 \times HA_1$, Figure 4) are relatively weaker than the assemblies (for example, H_2A_3, Figure 4) and, hence, they are not included in the models (H – host, tetrakis(pyridiniummethyl)tetramethyl cavitand **3**; A – anion, sulphate). The validity of this approximation is described in section 6.2.4.

$HA_2 \times HA_1$ non-specific dimers
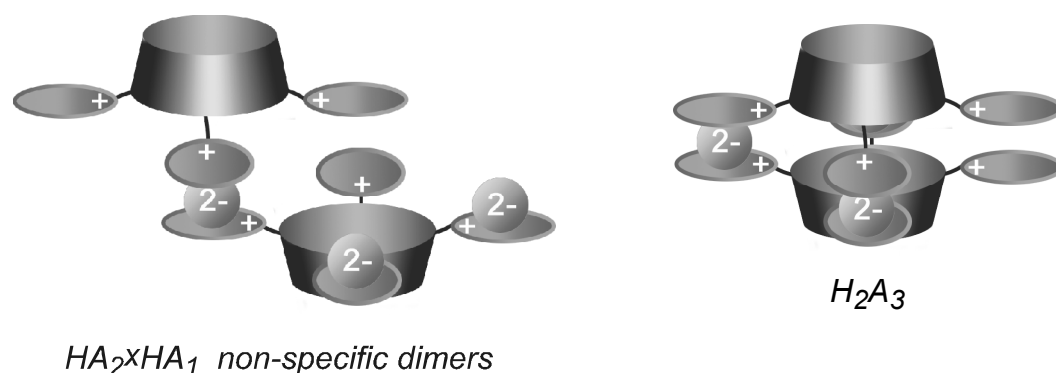
H_2A_3

Figure 4. An example of non-specific dimer $HA_2 \times HA_1$ in comparison with [2+3]hemicapsule H_2A_3

The intrinsic binding constants of the interaction of pyridinium with sulphate were determined using ^{1}H NMR dilution data of the reference compound **4** ($K_1 = 560$ M^{-1} and $K_2 = 20$ M^{-1}). The relationship between the binding constants and the intrinsic binding constants is shown in Scheme 2. K_{i1} and K_{i2} are the intrinsic binding constants

representing the interaction of pyridinium with a doubly charged anion and of the resulting contact ion-pair with another pyridinium, respectively. Using these equations,[21] $K_{i1} = 280$ M^{-1} and $K_{i2} = 40$ M^{-1}. The difference between the values for the 1:1 and 1:2 complexation process shows that the first ion-pairing strongly decreases the ability of the sulphate to form the second ion-pair pattern.
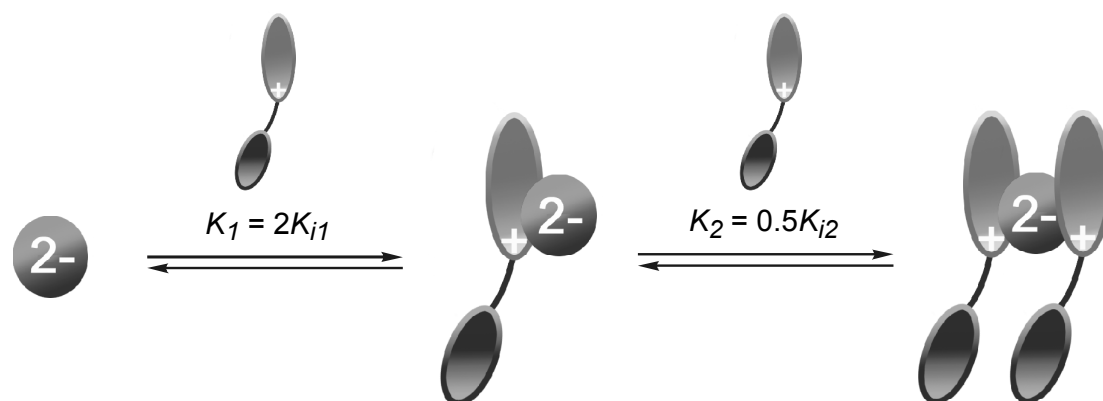
Scheme 2. Ion-pairing between a singly charged cation and a doubly charged anion.

The association constants of complexes of tetrakis(pyridiniummethyl)tetra-methyl cavitands **3** with one, two, three or four small anions contain the intrinsic binding constant between pyridinium and the anion and an additional statistic coefficient[21] (Scheme 3). As small anion, sulphate, was chosen to exclude intramolecular formation of pyridinium-anion-pyridinium associates. The HA_2 complex has two isomers z and e ($K = 16K_{i1}^2$ and $8K_{i1}^2$, respectively) depending on either the neighboring or opposite pyridinium substituents are ion-paired (the chosen nomenclature is arbitrary, related to z-zusammen and e-entgegen). The ion-pairing can take place on either side of the pyridinium plane, because the isomers can be transformed into one another by rotation around the CH$_2$-pyridinium bond; only one of the isomers (complexes above the pyridinium plane) is shown.
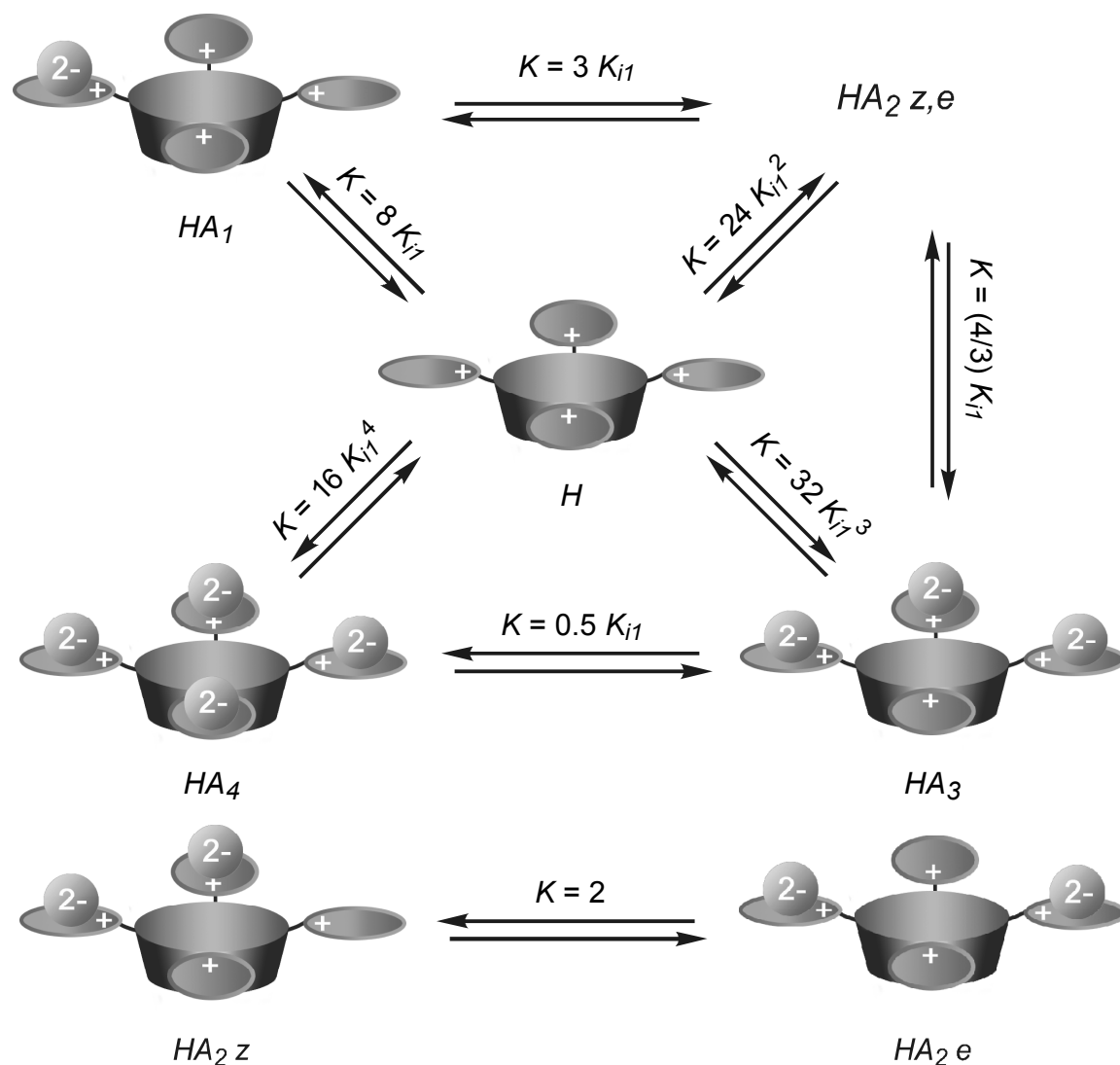
Scheme 3. The formation of multiple associates of tetrapyridinium cation **1** with a doubly charged small anion.

The formation of a complex, which contains two tetrakis(pyridiniummethyl)-cavitands **3** and one anion, is described by a binding constant that incorporates K_{i1} and K_{i2} (Scheme 4).

$$K = 16\, K_{i1}\, K_{i2}$$

$$2H + A \rightleftharpoons$$

H₂A
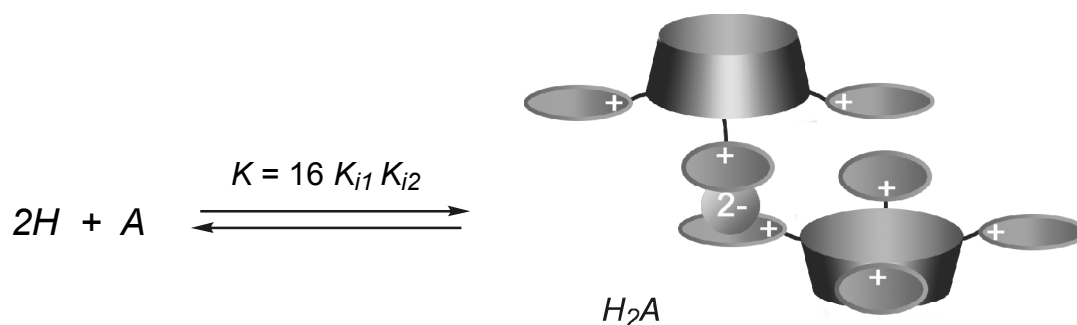
Scheme 4. Formation of *H₂A*.

The consideration of the binding constants of the formation of hemicapsules and capsules of **3**×2A in solution is based on the self-assembly model proposed by Ercolani (equation 1).[22,23] K_s is the constant of the assembly formation, σ_{sa} is the symmetry factor of the self-assembly equilibrium (equation 2), and K_i is the intrinsic binding constant. The number n represents the number of interactions, and m describes the number of independent intramolecular non-covalent 'loops' that give the self-assembly. The tendency to form intramolecular complexes is expressed in terms of effective molarity (EM) defined as K_{intra}/K_{inter}.[22-24] The averaged EM value is used to describe the formation of intramolecular 'loops'.[22] The coefficients σ_1, σ_2, and σ_s in equation 2 are symmetry numbers of the components of an assembly (1 and 2) and the assembly itself, respectively. The numbers *a* and *b* describe the number of components 1 and 2 in the assembly, respectively. The resulting equations, point groups, and symmetry numbers of the different assemblies are depicted in Scheme 5. The model was designed as non-cooperative, since the pyridinium substituents in tetrakis(pyridiniummethyl)tetramethyl cavitand **3** are located quite far away from each other and experience no intramolecular interaction.[23]

$$K_s = \sigma_{sa} K_i^{\,n} EM^{\,m} \tag{1}$$

$$\sigma_{sa} = \sigma_1^{\,a} \sigma_2^{\,b} / \sigma_s \tag{2}$$

$H_2A_2 z$

C_{2v}; sn = 2

$K = 32\ EM\ K_{i1}^2 K_{i2}^2$

$K = 16\ EM\ K_{i1}^2 K_{i2}^2$

$H_2A_2 e$

D_{2h}; sn = 4

H

C_{4v}; sn=4

$SO_4^{2-}\ G\ C_{2v}$; sn=2

$K = 64\ EM^2 K_{i1}^3 K_{i2}^3$

$K = 32\ EM^3\ K_{i1}^4 K_{i2}^4$

H_2A_3

C_{2v}; sn = 2

H_2A_4

D_{4h}; sn = 8
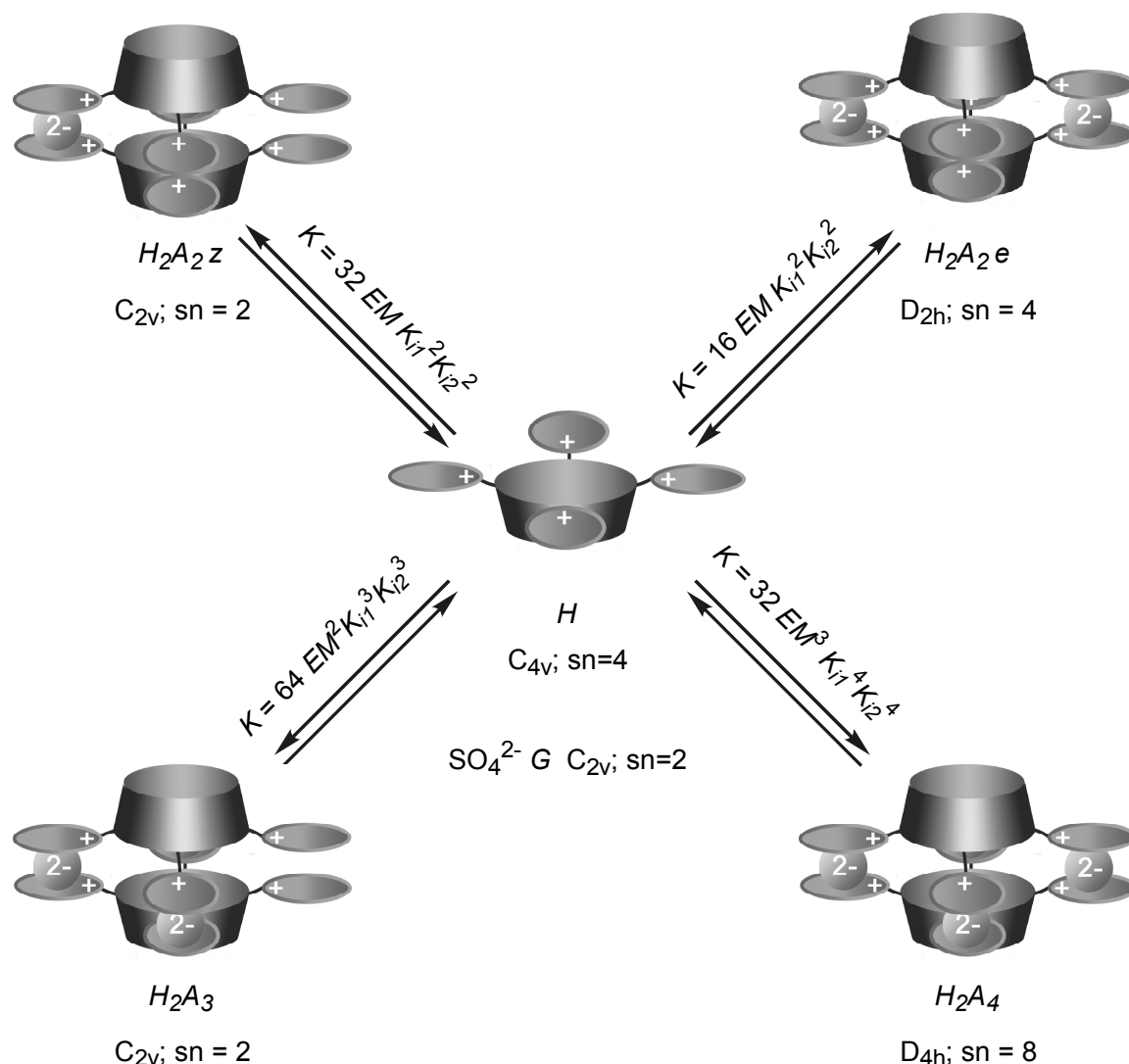
Scheme 5. Association processes, which lead to hemicapsules and capsules, based on pyridinium cavitands **3**×2A and small doubly charged anions.

Maple™ software provides a solution of the set of equations, which describes the composition of the equilibrium mixture at different concentrations. The values for the intrinsic binding constant were taken from experiments with reference compound **4**: $K_{i1} = 280\ M^{-1}$ and $K_{i2} = 40\ M^{-1}$. Fitting the calculated values (Figure 5) with the results of the ^1H NMR dilution experiments of **3**×2SO$_4$ yielded an EM value of 0.19 ± 0.02 M. The binding constants for the species considered in the model are summarized in Table 1.

The composition of the equilibrium mixture with a set of concentrations between 0.1 mM and 25 mM is described in Table 1. The data show that substantial amounts of (hemi)capsules and ion-pair associates are present in the equilibrium. For example, [2+3] hemicapsule H_2A_3 is present in larger amounts than [2+4] capsule

H_2A_4 till at least 2.5 mM. At higher concentrations, there is more [2+4] capsule H_2A_4 than [2+3] hemicapsule H_2A_3. The concentration of HA_1 is quite substantial at each concentration. Therefore, it is not surprising that the signal, which corresponds to the HA_1 complex, is always present in the ESI-MS spectrum (unless destroyed by the voltage). Analysis of the composition of the equilibrium mixture at a 5 mM concentration reveals that it contains 14% of the [2+4] capsule H_2A_4 and 10% of [2+3] hemicapsule H_2A_3. Other types of structures, containing supramolecular 'loops', H_2A_2 *z* and H_2A_2 *e* are present in smaller amounts (1.6% and 0.8%, respectively).
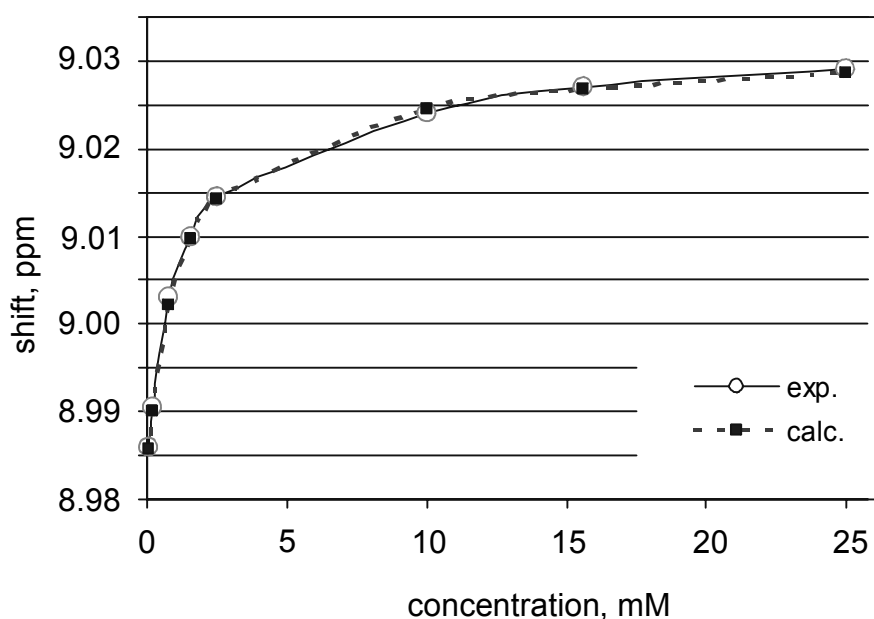
Figure 5. Fitting ^{1}H NMR dilution data of **3**×2SO$_4$ in methanol-d_4 to the model.

Simple ion-paired species represent about 43% of the mixture, among which 1:1 complex HA_1 (15%), which is followed by HA_2 *z*, HA_3, HA_2 *e*, and HA_4 with 11, 9, 6, and 2%, respectively. About 5% of tetrakis(pyridiniummethyl)tetramethyl cavitand **3** (*H*) and 27% of sulphate are uncomplexed at this concentration. H_2A_1 is present only at 0.3%, what is expected due to the relatively low K_{i2} value of the interaction of sulphate with pyridinium.

Table 1. Equilibrium concentrations (M/L) of the capsules, hemicapsules and ion-paired associates depending on the concentration of the initial salt calculated using the model (EM = 0.19 M, K_{i1} = 280 M^{-1}, K_{i2} = 40 M^{-1})

#	$[H]_{tot}$	$[A]_{tot}$	$[H]$	$[A]$	$[HA_1]$	$[HA_2 z]$	$[HA_2 e]$
1*	-	-	-	-	2.24×10^3 M^{-1}	1.25×10^6 M^{-2}	6.27×10^5 M^{-2}
2	1.00×10^{-4}	2.00×10^{-4}	6.96×10^{-5}	1.66×10^{-4}	2.58×10^{-5}	2.39×10^{-6}	1.20×10^{-6}
3	5.00×10^{-4}	1.00×10^{-3}	1.59×10^{-4}	5.21×10^{-4}	1.86×10^{-4}	5.42×10^{-5}	2.71×10^{-5}
4	1.00×10^{-3}	2.00×10^{-3}	1.91×10^{-4}	7.44×10^{-4}	3.18×10^{-4}	1.33×10^{-4}	6.63×10^{-5}
5	2.50×10^{-3}	5.00×10^{-3}	2.21×10^{-4}	1.08×10^{-3}	5.37×10^{-4}	3.26×10^{-4}	1.63×10^{-4}
6	5.00×10^{-3}	1.00×10^{-2}	2.38×10^{-4}	1.38×10^{-3}	7.36×10^{-4}	5.67×10^{-4}	2.84×10^{-4}
7	7.50×10^{-3}	1.50×10^{-2}	2.48×10^{-4}	1.56×10^{-3}	8.68×10^{-4}	7.60×10^{-4}	3.80×10^{-4}
8	1.00×10^{-2}	2.00×10^{-2}	2.54×10^{-4}	1.70×10^{-3}	9.70×10^{-4}	9.25×10^{-4}	4.62×10^{-4}
9	1.50×10^{-2}	3.00×10^{-2}	2.64×10^{-4}	1.91×10^{-3}	1.13×10^{-3}	1.21×10^{-3}	6.03×10^{-4}
10	2.00×10^{-2}	4.00×10^{-2}	2.72×10^{-4}	2.06×10^{-3}	1.25×10^{-3}	1.45×10^{-3}	7.23×10^{-4}
11	2.50×10^{-2}	5.00×10^{-2}	2.78×10^{-4}	2.18×10^{-3}	1.36×10^{-3}	1.66×10^{-3}	8.30×10^{-4}

#	$[HA_3]$	$[HA_4]$	$[H_2A_1]$	$[H_2A_2 z]$	$[H_2A_2 e]$	$[H_2A_3]$	$[H_2A_4]$
1*	7.02×10^8 M^{-3}	9.83×10^{10} M^{-4}	1.79×10^5 M^{-2}	7.63×10^8 M^{-3}	3.81×10^8 M^{-3}	3.25×10^{12} M^{-4}	3.45×10^{15} M^{-5}
2	2.22×10^{-7}	5.15×10^{-9}	1.44×10^{-7}	1.01×10^{-7}	5.07×10^{-8}	7.14×10^{-8}	1.26×10^{-8}
3	1.58×10^{-5}	1.15×10^{-6}	2.37×10^{-6}	5.25×10^{-6}	2.62×10^{-6}	1.16×10^{-5}	6.45×10^{-6}
4	5.52×10^{-5}	5.75×10^{-6}	4.87×10^{-6}	1.54×10^{-5}	7.70×10^{-6}	4.88×10^{-5}	3.86×10^{-5}
5	1.98×10^{-4}	3.01×10^{-5}	9.51×10^{-6}	4.39×10^{-5}	2.20×10^{-5}	2.03×10^{-4}	2.34×10^{-4}
6	4.38×10^{-4}	8.44×10^{-5}	1.40×10^{-5}	8.23×10^{-5}	4.11×10^{-5}	4.82×10^{-4}	7.07×10^{-4}
7	6.65×10^{-4}	1.46×10^{-4}	1.72×10^{-5}	1.14×10^{-4}	5.72×10^{-5}	7.62×10^{-4}	1.27×10^{-3}
8	8.82×10^{-4}	2.10×10^{-4}	1.97×10^{-5}	1.43×10^{-4}	7.15×10^{-5}	1.04×10^{-3}	1.88×10^{-3}
9	1.29×10^{-3}	3.44×10^{-4}	2.39×10^{-5}	1.94×10^{-4}	9.69×10^{-5}	1.57×10^{-3}	3.19×10^{-3}
10	1.67×10^{-3}	4.81×10^{-4}	2.73×10^{-5}	2.39×10^{-4}	1.20×10^{-4}	2.10×10^{-3}	4.59×10^{-3}
11	2.03×10^{-3}	6.20×10^{-4}	3.02×10^{-5}	2.81×10^{-4}	1.40×10^{-4}	2.61×10^{-3}	6.05×10^{-3}

* Binding constants are shown in row 1.

At a 25 mM concentration of the tetrakis(pyridiniummethyl)cavitand sulphate, the equilibrium contains 33% of [2+4] capsule H_2A_4 and 14% of [2+3] hemicapsule H_2A_3. The amount of other associates is higher than 50% at this quite high concentration, what is explained by the relative weakness of the capsule association process. This is reflected in the binding constants, for example, the K_a value of [2+4] capsule formation is 3.45×10^{15} M^{-5} (Table 1), which is 18 orders of magnitude lower

than that reported for calix[4]arene [2+4] capsules based on Zn-porphyrin + DABCO interactions (6.3×10^{33} M^{-5}).[11]

The different species, HA_1, H_2A_3, HA_2 *(z+e)*, HA_3, and H_2A_4, which are present in the equilibrium mixture in reasonable amounts according to the model, were also detected by ESI-MS spectrometry (vide supra). However, due to a different volatility, charge, protonation ability, stability, etc. of the species, the intensity of the signals in the mass spectra is dependent on many unknowns, and consequently only gives qualitative information.

6.2.4 Non-specific dimers

The model neglects the formation of non-specific dimers $HA_n \times HA_m$ (n + m = 2...7). As an example, one of the isomers of non-specific dimers $HA_2 \times HA_1$ is shown in Figure 4. The binding constant of the dimers $HA_2 \times HA_1$ (as a mixture of isomers) can be treated as a product of the interaction of HA_1 ($K = 8\ K_{i1}$) with HA_2 z, e ($K = 24\ K_{i1}^2$). This interaction is characterized by $K = 0.5\ K_{i2}$ (0.5 is the statistic coefficient): $K_{HA2 \times HA1} = 96\ K_{i1}^3 K_{i2}$. The binding constant K_{H2A3} of the formation of the [2+3] hemicapsule H_2A_3 is $64\ EM^2\ K_{i1}^3 K_{i2}^3$ (vide supra). It allows determining the equilibrium constant for the process shown in Scheme 6 ($K = K_{H2A3}\ /K_{HA2 \times HA1}$).

$$HA_2 \times HA_1 \ \text{non-specific dimers} \quad \underset{\xrightarrow{\hspace{2cm}}}{\overset{K = (2/3)\ EM^2\ K_{i2}^2}{\rightleftharpoons}} \quad H_2A_3$$

Scheme 6. Equilibrium between the non-specific dimers $HA_2 \times HA_1$ and the [2+3] hemicapsule H_2A_3 (the schematic structures are shown in Figure 4).

In the case of the association of compounds $3 \times 2SO_4$ in solution, $K_{i2} = 40$ M^{-1} and EM = 0.19 M, hence the equilibrium constant K of the process described in Scheme 6 is 38.5. It means that the concentration of the [2+3] hemicapsule H_2A_3 is 38.5 times higher than that of the unspecific dimers $HA_2 \times HA_1$, what allows to neglect them to give a realistic representation of the dynamic equilibrium. In general this approach works excellently, if the equilibria modeled in section 6.2.3 are characterized by similar and higher binding constants and EM (namely, $K_{i2} \geq 40$ M^{-1} and EM ≥ 0.19 M). In addition, this approach can give useful information for even

weaker interactions. For example, in the case of a hypothetic process, characterized by $K_{i2} = 20$ M^{-1} and EM = 0.19 M, the concentration of the [2+3] hemicapsule is an order of magnitude higher than that of non-specific dimers. But, in the case of $K_{i2} = 10$ M^{-1} and EM = 0.19 M, the ratio [2+3] hemicapsule/non-specific dimers is only 2.5 and consequently these non-capsule associates become important participants of the equilibrium mixture.

6.2.5 Host-guest studies

Hemicapsules based on pyridinium-anion-pyridinium triple ion interactions can form complexes with electron-rich aromatic compounds (Chapter 5). A similar behavior was observed for the capsules built with doubly charged anions. Upon addition of the methyl- and ethyl esters of 4-aminobenzoic acid, 4-iodophenol, and 4-iodoaniline to a methanolic solution of $3 \times 2SO_4$ changes of the shifts of the α,β,γ-pyridinium protons were observed (up to 0.3 ppm) in the ^{1}H NMR spectra. In the ESI-MS spectrum of a solution of $3 \times 2SO_4$ significant changes took place upon guest addition (Figure 6). For example, an intensive signal at *m/z* 1187 corresponding to $[3_2 \cdot 3SO_4 + \text{ethyl 4-aminobenzoate}]^{2+}$ has appeared, while the intensity of the $[3_2 \cdot 3SO_4]^{2+}$ signal at *m/z* 1105 was significantly decreased. Several multiple charged signals corresponding to *two* tetrakis(pyridiniummethyl)tetramethyl cavitands **3**, 1…3 SO_4^{2-}, and 1…3 guest molecules are also present. It should be noted that no complexes of the guests with a *single* molecule of **3** (and n×SO$_4^{2-}$ n = 0…4) are observed. These results indicate that the complexation of the guests takes place in between the two pyridiniums of the hemicapsule $[3_2 \cdot 3SO_4]^{2+}$, analogous to the triple-ion-based hemicapsules described in Chapter 5. It is notorious, that in the case of large anions, such as iso- and terephthalate, no such guest complexation was observed either by ^{1}H NMR spectroscopy or ESI-MS. Apparently, in this case the distance between the pyridiniums is already too large to provide an effective complexation.

Complexation of the guest within the [2+4]capsule can be excluded in methanol due to the absence of (large) ^{1}H NMR shifts of the methyl protons of methyl and ethyl 4-aminobenzoate guests. For a comparison, see the complexation in water (vide infra) and Chapter 4.[25]
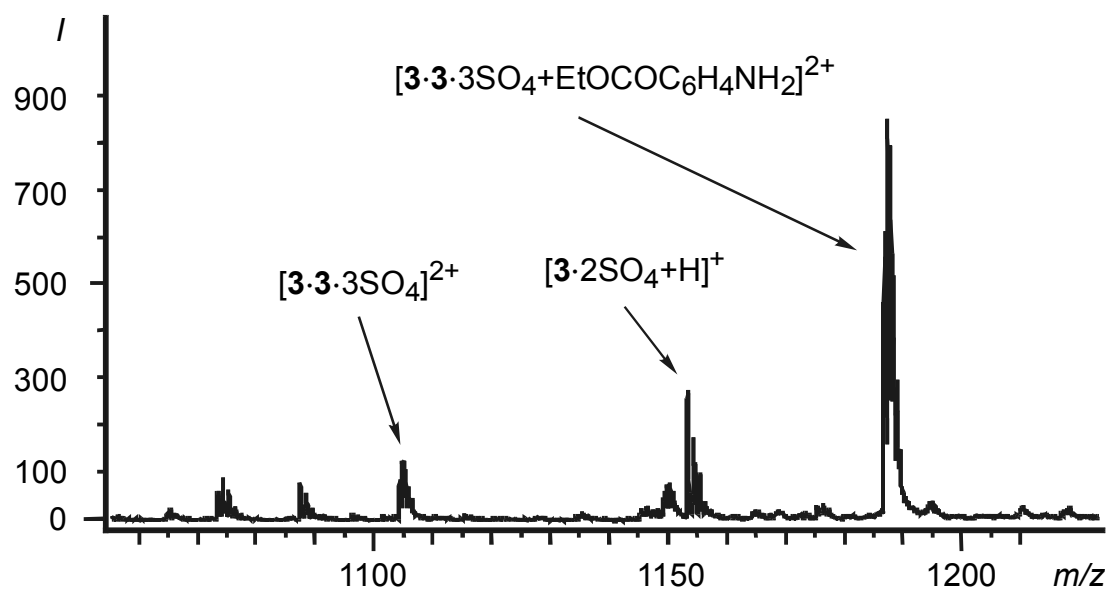
Figure 6. Nano ESI-MS continuous flow spectrum of a 5 mM[19] of $3\times2SO_4$ and 15 mM of ethyl 4-aminobenzoate solution in methanol (voltages: capillary = 2500 V, orifice 1 and 2 = 1 V, ring lens = 10 V).

In water the formation of self-assemblies based on electrostatic interactions is strongly suppressed. However, cavitands have a hydrophobic cavity, in which organic molecules can be complexed, driven by hydrophobic interactions. Sherman c.s. have reported the recognition of small organic molecules, such as ethyl acetate, acetone, benzene, and acetonitrile in water by a cavitand solubilized with four phosphoric acid groups at the bottom rim.[26] Middel et al. described the complexation of phenol, cresol, and benzene by water-soluble cavitands.[27]

Only cavitands $3\times4Br$, $3\times2SO_4$, and $3\times2Oxalate$ show a moderate solubility in water (> 5 mM/L). Titration of aqueous solutions of organic molecules by $3\times4Br$, $3\times2SO_4$, and $3\times2Oxalate$ indicates a general trend pointing out the similarity of the host-guest behavior between the previously studied cavitands and the new ones. Acetone, acetonitrile, and ethyl acetate are complexed by host $3\times4Br$ with binding constants of 30, 60, and 420 M^{-1} in neutral aqueous solution. Compounds $3\times2SO_4$ and $3\times2Oxalate$ show a similar binding affinity. The methyl- and ethyl esters of 4-aminobenzoic acid form complexes with $3\times2SO_4$ with K_a-values of 680 and 640 M^{-1}, respectively. The complexation is accompanied by a large ^{1}H NMR shift of the methyl group of the esters (more than 1 ppm).

6.3 Conclusions

In the case of tetrakis(pyridiniummethyl)cavitands **3** weak electrostatic interactions between the pyridinium rings and doubly charged anions lead to a mixture of ion-paired associates, hemicapsules, and capsules in polar competitive media. ESI-MS gives qualitative information about the composition of the equilibrium mixture. A new model, which describes the equilibrium, is proposed. It quantifies the composition of the mixture at different concentrations based on ^{1}H NMR dilution data of **3**×2SO$_4$ and provides an effective molarity (EM) of the intramolecular processes (0.19 ± 0.02 M). The models show that the equilibrium mixture at a 5 mM concentration of **3**×2SO$_4$ contains 14% of the [2+4] capsule H_2A_4, 10% of the [2+3] hemicapsule H_2A_3 and about 43% of simple ion-paired species, while 5% of the cavitand and 27% of sulphate are present as uncomplexed. Increase of the concentration till 25 mM gives rise to higher percentages of the [2+4] capsule H_2A_4 and the [2+3] hemicapsule H_2A_3 (33 and 14%, respectively). The [2+3] hemicapsules H_2A_3 built with small sulphate linkers incorporate guests in between the closely positioned pyridinium planes.

6.4 Experimental section

The reagents used were purchased from Aldrich or Acros Chimica and used without further purification. Melting points were measured using a Sanyo Gellenkamp melting point apparatus and are uncorrected. Proton and carbon NMR spectra were recorded on a Varian Unity Inova (300 MHz) spectrometer. Residual solvent protons were used as internal standard and chemical shifts are given relative to tetramethylsilane (TMS). Ion exchange resins were prepared from Dowex 550A OH anion exchange resin, 25-35 mesh. Compound **3**×4Br[14,27] was prepared similarly to the literature procedures.[20] The presence of water in the analytical samples was proven by ^{1}H NMR spectroscopy.

Determination of binding constants: *EM*-values of the capsule formation (compound **3** with sulphate) were determined by non-linear fitting of experimental data obtained by ^{1}H NMR titration experiments with calculated values (equations 3-16; $[H]_{tot}$ and $[A]_{tot}$ are total concentrations of the cation and doubly charged anions, respectively; K_{i1} and K_{i2} are intrinsic binding constants of pyridinium with sulphate

determined using reference compound **4**; [H] and [A] are concentrations of the unbound cation and anion, respectively; $[HA_1]$, $[HA_2z]$, $[HA_2e]$, $[HA_3]$, $[HA_4]$, $[H_2A_1]$, $[H_2A_2z]$, $[H_2A_2e]$, $[H_2A_3]$, $[H_2A_4]$ are the equilibrium concentrations of different complexes in solution; δ_{obs} = calculated shift of the α-pyridinium protons in the equilibrium; δ_H and δ_{HA} are the shifts of the α-pyridinium protons of unbound pyridinium cation and ion-paired pyridinium, respectively). The numerical solution of the system of equations 1-14 was calculated using Maple 8 software (Waterloo Maple Inc). The non-linear fitting of calculated to experimental data (EM, δ_H and δ_{HA}) was carried out by the grid method.[28]

$$[A]_{tot} = 2[H]_{tot} \tag{3}$$

$$[HA_1] = 8K_{i1}[H][A] \tag{4}$$

$$[HA_2z] = 16K_{i1}^{\;2}[H][A]^2 \tag{5}$$

$$[HA_2e] = 8K_{i1}^{\;2}[H][A]^2 \tag{6}$$

$$[HA_3] = 32K_{i1}^{\;3}[H][A]^3 \tag{7}$$

$$[HA_4] = 16K_{i1}^{\;4}[H][A]^4 \tag{8}$$

$$[H_2A_1] = 16K_{i1}K_{i2}[H]^2[A] \tag{9}$$

$$[H_2A_2z] = 32K_{i1}^{\;2}K_{i2}^{\;2}EM[H]^2[A]^2 \tag{10}$$

$$[H_2A_2e] = 16K_{i1}^{\;2}K_{i2}^{\;2}EM[H]^2[A]^2 \tag{11}$$

$$[H_2A_3] = 64K_{i1}^{\;3}K_{i2}^{\;3}EM^2[H]^2[A]^3 \tag{12}$$

$$[H_2A_4] = 32K_{i1}^{\;4}K_{i2}^{\;4}EM^3[H]^2[A]^4 \tag{13}$$

$$
\begin{aligned}
[H]_{tot} &= [H]+[HA_1]+[HA_2z]+[HA_2e]+[HA_3]+[HA_4]+ \\
&+ 2([H_2A_1]+[H_2A_2z]+[H_2A_2e]+[H_2A_3]+[H_2A_4])
\end{aligned}
\tag{14}
$$

$$
\begin{aligned}
[A]_{tot} &= [A]+[HA_1]+[H_2A_1]+2([HA_2z]+[HA_2e]+[H_2A_2z]+ \\
&+ [H_2A_2e])+3([HA_3]+[H_2A_3])+4([HA_4]+[H_2A_4])
\end{aligned}
\tag{15}
$$

$$
\begin{aligned}
\delta_{obs} &= \delta_H \frac{4([H]+[H_2A_2z]+[H_2A_2e])+2([HA_2z]+[HA_2e]+[H_2A_3])}{4[H]_{tot}} + \\
&+ \delta_H \frac{[HA_3]+3[HA_1]+6[H_2A]}{4[H]_{tot}} + \delta_{HG}\frac{[HA_1]+3[HA_3]+6[H_2A_3]+8[H_2A_4]}{4[H]_{tot}} + \\
&+ \delta_{HG}\frac{2([HA_2z]+[HA_2e]+[H_2A_1])+4([HA_4]+[H_2A_2z]+[H_2A_2e])}{4[H]_{tot}}
\end{aligned}
\tag{16}
$$

ESI-MS: The ESI-MS experiments were carried out with a Jeol AccuTOF instrument. In the standard mode the solutions were introduced at a flow rate of 12.5 µL/min. In the continuous nanoflow mode, the solutions were introduced with pressure (the flow rate set in the syringe pump was up to 400 nL/min) into fused-silica PicoTip® emitters purchased from New Objective, Inc. The data were accumulated in the mass range 230 – 4000 *m/z* for 2 min. The standard spray conditions, unless otherwise specified are: capillary voltage 2500 V, ring lens voltage 30 V, orifice 1 voltage = 2 V, orifice 2 voltage = 2 V, orifice 1 temperature = 60 °C, temperature in the desolvation chamber 120 °C, drying gas flow 0.1 – 0.5 L/min, nebulizing gas flow = 0.5 L/min. For the characterization of compounds **3** the most intensive signals of the isotopic pattern observed are shown.

General procedure for ion exchange:

1. Column preparation

Dowex anion exchange resin (~ 150 mL) was washed with methanol (1 L) and placed into a column (d = 25 mL), which had a small piece of wool above the stopcock at the bottom of the column. The column was flushed under pressure by methanol (1 L) and Q-water (2 L). Subsequently, it was washed by an aqueous solution of NaOH (1 N, 400 mL, mainly without pressure) and Q-water (1.5 L, with pressure). It was followed by washing with an aqueous solution of the salt chosen (mainly without pressure; 2 L of 0.2 N solutions of sodium sulphate, sodium oxalate, sodium phthalate, sodium isophthalate, and sodium terephthalate in water were used for the preparation of Dowex SO$_4$, Dowex Oxalate, Dowex Phthalate, Dowex Isophthalate, and Dowex Terephthalate, respectively). To remove the excess of the salt, the column was washed with Q-water (2.5 L) and flushing with MeOH (300 – 500 mL, with pressure).

2. Ion exchange

A solution of compound **1**×4Br (400 mg) in methanol (20 mL) was flushed into the Dowex Anion column without pressure. The column was washed with methanol (200 mL). The methanol solution was evaporated to dryness under vacuum *without heating* to give the **1**×2Anions in quantitative yields.

Tetrakis(pyridiniummethyl)tetramethylcavitand disulphate 3×2SO$_4$

m.p. > 100 °C (dec); ^{1}H NMR (5 mM, CD$_3$OD) δ: 9.02 (d, 8 H, J = 5.5 Hz; α-pyridinium-H), 8.57 (t, 4 H, J = 7.7 Hz; γ-pyridinium-H), 8.11 (t, 8 H, J = 6.6 Hz; β-pyridinium-H), 7.67 (s, 4 H; cavArH), 6.20 (d, 4 H, J = 7.3 Hz; OCHH^OO), 5.83 (s, 8 H; ArCH$_2$Py), 4.96 (q, 4 H, J = 7.7 Hz; Ar$_2$CH), 4.73 (d, 4 H, J = 7.7 Hz; OCHH^iO), 1.81 (d, 12 H, J = 7.0 Hz; CH$_3$); ^{13}C NMR (CD$_3$OD) δ: 155.0, 146.5, 141.1, 129.6, 122.1; ESI-MS (0.2 mM, CH$_3$OH) m/z: [**3**·SO$_4$]$^{2+}$ 528.16 (calc.: 528.18); elemental analysis calc.(%) for C$_{60}$H$_{56}$N$_4$O$_{16}$S$_2$ + 4.5 H$_2$O (1234.3): C 58.38, H 5.31, N 4.54; found: C 58.50, H 5.25, N 4.48.

Tetrakis(pyridiniummethyl)tetramethylcavitand dioxalate 3×2Ox

m.p. ~ 60 °C (dec); ^{1}H NMR (5 mM, CD$_3$OD) δ: 9.01 (d, 8 H, J = 5.5 Hz; α-pyridinium-H), 8.57 (t, 4 H, J = 7.7 Hz; γ-pyridinium-H), 8.10 (t, 8 H, J = 6.6 Hz; β-pyridinium-H), 7.65 (s, 4 H; cavArH), 6.20 (d, 4 H, J = 4.0 Hz; OCHH^OO), 5.81 (s, 8 H; ArCH$_2$Py), 4.96 (q, 4 H, J = 7.3 Hz; Ar$_2$CH), 4.71 (d, 4 H, J = 4.0 Hz; OCHH^iO), 1.80 (d, 12 H, J = 7.3 Hz; CH$_3$); ^{13}C NMR (CD$_3$OD) δ: 155.0, 141.1, 129.5; ESI-MS (0.2 mM, CH$_3$OH) m/z: [**3**·Oxalate]$^{2+}$ 524.15 (calc.: 524.19); elemental analysis calc.(%) for C$_{64}$H$_{56}$N$_4$O$_{16}$ + 3 H$_2$O (1191.2): C 64.53, H 5.25, N 4.70; found: C 64.63, H 5.11, N 4.55.

Tetrakis(pyridiniummethyl)tetramethylcavitand diterephthalate 3×2Tph

m.p. > 300 °C (dec); ^{1}H NMR (5 mM, CD$_3$OD) δ: 8.96 (d, 8 H, J = 5.9 Hz; α-pyridinium-H), 8.58 (t, 4 H, J = 7.3 Hz; γ-pyridinium-H), 8.09 (t, 8 H, J = 7.3 Hz; β-pyridinium-H), 7.92 (s, 8 H; terephthalate-H), 7.63 (s, 4 H; cavArH), 6.22 (d, 4 H, J = 7.3 Hz; OCHH^OO), 5.63 (s, 8 H; ArCH$_2$Py), 4.92 (q, 4 H, J = 7.7 Hz; Ar$_2$CH), 4.52 (d, 4 H, J = 7.3 Hz; OCHH^iO), 1.77 (d, 12 H, J = 7.3 Hz; CH$_3$); ^{13}C NMR (CD$_3$OD) δ: 154.8, 146.4, 141.2, 130.0, 129.7, 121.7; ESI-MS (0.2 mM, CH$_3$OH) m/z: [**3**·Terephthalate]$^{2+}$ 562.22 (calc.: 562.21); elemental analysis calc.(%) for C$_{76}$H$_{64}$N$_4$O$_{16}$ + 3.5 H$_2$O (1352.4): C 67.50, H 5.29, N 4.14; found: C 67.56, H 5.35, N 4.06.

Tetrakis(pyridiniummethyl)tetramethylcavitand diisophthalate 3×2Iph

m.p. > 300 °C (dec); ^{1}H NMR (5 mM, CD$_3$OD) δ: 8.97 (d, 8 H, J = 6.2 Hz; α-pyridinium-H), 8.56 (t, 4 H, J = 7.7 Hz; γ-pyridinium-H), 8.45 (s, 2 H; 2-isophthalate-H), 8.08 (t, 8 H, J = 7.0 Hz; β-pyridinium-H), 8.01 (d, 4 H, J = 7.7 Hz; 4,6-isophthalate-H), 7.63 (s, 4 H; cavArH), 7.36 (t, 2 H, J = 7.7 Hz; 5-isophthalate-H),

6.20 (d, 4 H, J = 7.3 Hz; OCHH^OO), 5.69 (s, 8 H; ArCH$_2$Py), 4.93 (q, 4 H, J = 7.3 Hz; Ar$_2$CH), 4.65 (d, 4 H, J = 7.3 Hz; OCHH^iO), 1.78 (d, 12 H, J = 7.3 Hz; CH$_3$); ^{13}C NMR (CD$_3$OD) δ: 154.9, 146.4, 141.1, 129.6, 128.5, 122.0; ESI-MS (0.2 mM, CH$_3$OH) *m/z*: [**3**·Isophthalate]$^{2+}$ 562.22 (calc.: 562.21); elemental analysis calc.(%) for C$_{76}$H$_{64}$N$_4$O$_{16}$ + 3 H$_2$O (1343.4): C 67.95, H 5.25, N 4.17; found: C 68.22, H 5.15, N 4.10.

Tetrakis(pyridiniummethyl)tetramethylcavitand diphthalate 3×2Ph

m.p. ~ 65 °C (dec); ^{1}H NMR (5 mM, CD$_3$OD) δ: 9.07 (d, 8 H, J = 5.5 Hz; α-pyridinium-H), 8.53 (t, 4 H, J = 7.7 Hz; γ-pyridinium-H), 8.07 (t, 8 H, J = 7.0 Hz; β-pyridinium-H), 7.64 (s, 4 H; cavArH), 7.59 (m, 4 H; phthalate-H), 7.27 (m, 4 H; phthalate-H), 6.33 (d, 4 H, J = 7.7 Hz; OCHH^OO), 5.84 (s, 8 H; ArCH$_2$Py), 4.97 (q, 4 H, J = 7.7 Hz; Ar$_2$CH), 4.81 (d, 4 H, J = 7.7 Hz; OCHH^iO), 1.80 (d, 12 H, J = 7.3 Hz; CH$_3$); ^{13}C NMR (CD$_3$OD) δ: 155.0, 146.7, 141.1, 129.5, 129.3, 124.4; ESI-MS (0.2 mM, CH$_3$OH) *m/z*: [**3**·Phthalate]$^{2+}$ 562.21 (calc.: 562.21); elemental analysis calc.(%) for C$_{76}$H$_{64}$N$_4$O$_{16}$ + 3.5 H$_2$O (1352.4): C 67.50, H 5.29, N 4.14; found: C 67.64, H 5.25, N 4.07.

References and notes

1. Lehn, J.-M. *Science* **2002**, *295*, 2400-2403.
2. Whitesides, G. M.; Grzybowski, B. *Science* **2002**, *295*, 2418-2421.
3. For reviews on self-assembly, see: Yu, S. Y.; Li, S. H.; Huang, H. P.; Zhang, Z. X.; Jiao, Q.; Shen, H.; Hu, X. X.; Huang, H. *Curr. Org. Chem.* **2005**, *9*, 555-563; Keizer, H. M.; Sijbesma, R. P. *Chem. Soc. Rev.* **2005**, *34*, 226-234; Davis, J. T. *Angew. Chem., Int. Ed.* **2004**, *43*, 668-698; Johnson, D. W.; Raymond, K. N. *Supramol. Chem.* **2001**, *13*, 639-659; Sherrington, D. C.; Taskinen, K. A. *Chem. Soc. Rev.* **2001**, *30*, 83-93; Albrecht, M. *Chem. Rev.* **2001**, *101*, 3457-3497; Leininger, S.; Olenyuk, B.; Stang, P. J. *Chem. Rev.* **2000**, *100*, 853-907; Fujita, M. *Chem. Soc. Rev.* **1998**, *27*, 417-425; Linton, B.; Hamilton, A. D. *Chem. Rev.* **1997**, *97*, 1669-1680.
4. Pfeil, A.; Lehn, J.-M. *J. Chem. Soc. Chem. Commun.* **1992**, 838-840; ten Cate, M. G. J.; Huskens, J.; Crego-Calama, M.; Reinhoudt, D. N. *Chem. Eur. J.* **2004**, *10*, 3632-3639.
5. Taylor, P. N.; Anderson, H. L. *J. Am. Chem. Soc.* **1999**, *121*, 11538-11545.
6. Badjić, J. D.; Nelson, A.; Cantrill, S. J.; Turnbull, W. B.; Stoddart, J. F. *Acc. Chem. Res.* **2005**, *38*, 723-732; Mulder, A.; Huskens, J.; Reinhoudt, D. N. *Org. Biomol. Chem.* **2004**, *2*, 3409-3424; Mammen, M.; Choi, S. K.; Whitesides, G. M. *Angew. Chem., Int. Ed.* **1998**, *37*, 2755-2794.
7. Rebek, J. *Angew. Chem., Int. Ed.* **2005**, *44*, 2068-2078; Hof, F.; Craig, S. L.; Nuckolls, C.; Rebek, J. *Angew. Chem., Int. Ed.* **2002**, *41*, 1488-1508; Rudkevich, D. M. *Bull. Chem. Soc. Jpn.* **2002**, *75*, 393-413.

8. For recent examples of [1+1] capsules studies, see: Corbellini, F.; Knegtel, R. M. A.; Grootenhuis, P. D. J.; Crego-Calama, M.; Reinhoudt, D. N. *Chem. Eur. J.* **2005**, *11*, 298-307; Corbellini, F.; van Leeuwen, F. W. B.; Beijleveld, H.; Kooijman, H.; Spek, A. L.; Verboom, W.; Crego-Calama, M.; Reinhoudt, D. N. *New J. Chem.* **2005**, *29*, 243-248; Zadmard, R.; Kraft, A.; Schrader, T.; Linne, U. *Chem. Eur. J.* **2004**, *10*, 4233-4239; Shivanyuk, A.; Saadioui, M.; Broda, F.; Thondorf, I.; Vysotsky, M. O.; Rissanen, K.; Kolehmainen, E.; Böhmer, V. *Chem. Eur. J.* **2004**, *10*, 2138-2148; Letzel, M. C.; Decker, B.; Rozhenko, A. B.; Schoeller, W. W.; Mattay, J. *J. Am. Chem. Soc.* **2004**, *126*, 9669-9674; Moon, K.; Kaifer, A. E. *J. Am. Chem. Soc.* **2004**, *126*, 15016-15017.

9. Dalgarno, S. J.; Tucker, S. A.; Bassil, D. B.; Atwood, J. L. *Science* **2005**, *309*, 2037-2039; Yamanaka, M.; Shivanyuk, A.; Rebek, J. *J. Am. Chem. Soc.* **2004**, *126*, 2939-2943.

10. Zuccaccia, D.; Pirondini, L.; Pinalli, R.; Dalcanale, E.; Macchioni, A. *J. Am. Chem. Soc.* **2005**, *127*, 7025-7032; Pinalli, R.; Cristini, V.; Sottili, V.; Geremia, S.; Campagnolo, M.; Caneschi, A.; Dalcanale, E. *J. Am. Chem. Soc.* **2004**, *126*, 6516-6517.

11. Baldini, L.; Ballester, P.; Casnati, A.; Gomila, R. M.; Hunter, C. A.; Sansone, F.; Ungaro, R. *J. Am. Chem. Soc.* **2003**, *125*, 14181-14189.

12. Kobayashi, K.; Shirasaka, T.; Yamaguchi, K.; Sakamoto, S.; Horn, E.; Furukawa, N. *Chem. Commun.* **2000**, 41-42.

13. Harrison, R. G.; Burrows, J. L.; Hansen, L. D. *Chem. Eur. J.* **2005**, *11*, 5881-5888; Harrison, R. G.; Dalley, N. K.; Nazarenko, A. Y. *Chem. Commun.* **2000**, 1387-1388.

14. Grote Gansey, M. H. B.; Bakker, F. K. G.; Feiters, M. C.; Geurts, H. P. M.; Verboom, W.; Reinhoudt, D. N. *Tetrahedron Lett.* **1998**, *39*, 5447-5450.

15. Attempts to prepare salts **1** with doubly charged anions by precipitation from an aqueous solution of **1**×4Br upon addition of excess of disodium sulphate, oxalate, terephthalate, isophthalate, or phthalate led to only partial substitution of bromide. The precipitated salts kept up to two bromide anions.

16. About the importance of ion-pairing with initial counterions in electrostatic self-assembly, see Chapter 7.

17. Chuck, R. J.; Randall, E. W. *Spectrochim. Acta* **1966**, *22*, 221-226.

18. Wannere, C. S.; Schleyer, P. V. R. *Org. Lett.* **2003**, *5*, 605-608.

19. Nano ESI-MS continuous flow experiments of a 25 mM solution of **3**x2SO$_4$ were practically impossible due to the very easy stoppering of the nano needle.

20. Chapter 5.

21. Connors, K. A., *Binding Constants: The Measurement of Molecular Complex Stability;* Wiley-Interscience: New York, 1987.

22. Ercolani, G. *J. Phys. Chem. B* **2003**, *107*, 5052-5057.

23. Ercolani, G. *J. Am. Chem. Soc.* **2003**, *125*, 16097-16103.

24. Galli, C.; Mandolini, L. *Eur. J. Org. Chem.* **2000**, 3117-3125.

25. Oshovsky, G. V.; Verboom, W.; Reinhoudt, D. N. *Collect. Czech. Chem. Commun.* **2004**, *69*, 1137-1148, and Chapter 4.

26. Gui, X.; Sherman, J. C. *Chem. Commun.* **2001**, 2680-2681.

27. Middel, O.; Verboom, W.; Reinhoudt, D. N. *Eur. J. Org. Chem.* **2002**, 2587-2597.

28. Isotani, S.; Fujii, A. T. *Comput. Phys. Commun.* **2003**, *151*, 1-7.

THE UNDERESTIMATED ROLE OF COUNTER-IONS IN ELECTROSTATIC SELF-ASSEMBLY

[1+1] CAVITAND-CALIX[4]ARENE CAPSULES BASED ON AZINIUM-SULPHONATE INTERACTIONS[℘]

The apparent K_a-values of the formation of [1+1] cavitand-calix[4]arene capsules, based on azinium-sulphonate electrostatic interactions, obtained by direct titration experiments are concentration dependent due to the influence of the interaction of the charged capsule components with their initial counterions. ^1H NMR and UV dilution experiments, in which this ion-pairing is excluded, gave K_a-values of $> 2 \times 10^6 M^1$ in methanol and methanol/water (1:1) for the capsule formation. The capsule encapsulates small guests such as methanol, ethanol, etc, as proven by ESI-MS.

7.1 Introduction

A large number of supramolecular architectures is based on the assembly of different components making use of electrostatic interactions.[1] In nearly all studies the interaction between cations and anions in the initial, charged components is neglected. The same holds for host-guest complexation studies[2] (unless an ion-pair recognition is involved[3]). It is assumed that the process of ion-pairing, or the formation of higher ionic aggregates, is weak and, hence, negligible. However, Smith c.s.[4] reported that anion binding by neutral hosts in organic solvents can be inhibited by the presence of alkali metal cations due to ion-pairing. Gibson c.s.[5] found that the apparent K_a-values of pseudorotaxane formation between dibenzylammonium salts or paraquat and dibenzo-24-crown-8 are strongly concentration dependent. This was explained by ion-pairing of the charged guests with their anion. Anions influence cation recognition not only in non-competitive solvents like chloroform,[6] but also *in water*. Electrolytes (buffers or added salts) tend to depress apparent binding constants orders of magnitude (in the case of n-alkylpyridinium-containing receptor-guest systems).[7]

In this Chapter it is demonstrated that for the determination of the binding strength of capsules based on electrostatic interactions it is essential to take into account the ion-pairing of the initial components. Capsules are spherical molecules that are formed by multiple interactions of two polyfunctionalized half-spheres.[8-10] Capsules based on multivalent electrostatic interactions have recently attracted much attention due to the good solubility and stability in polar competitive media like alcohols[11,12] or even water.[13] For this study capsules **1×2**, based on azinium-anion interactions were selected, since ion-pairing of azinium salts can be studied by UV-vis spectroscopy due to the presence of (a) charge-transfer band(s) that correspond to a contact ion-pair.
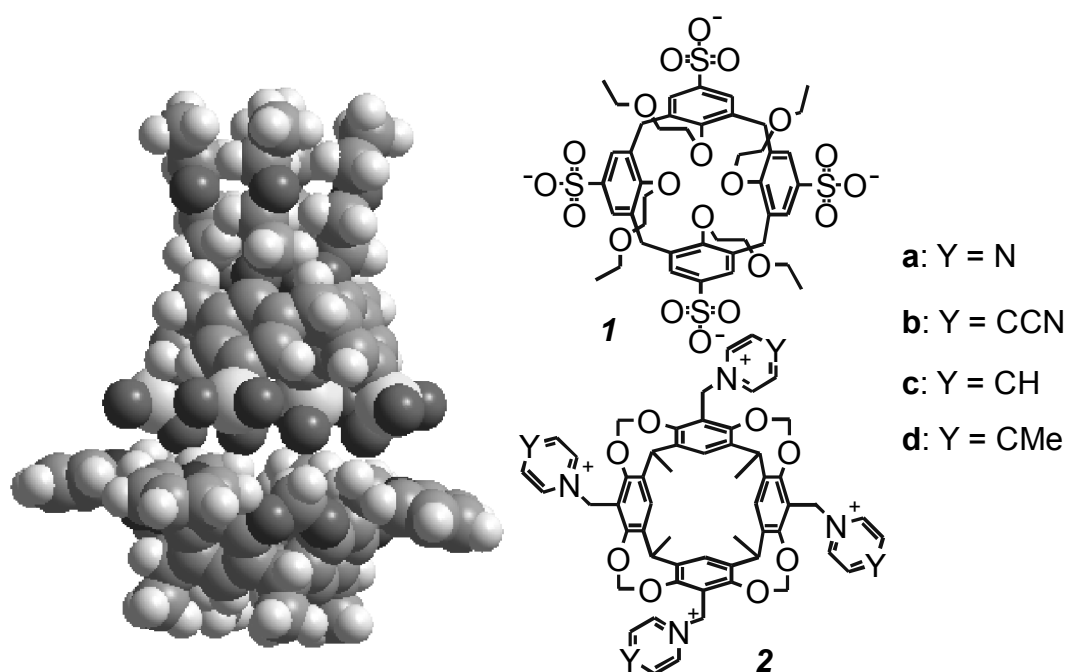
Chart 1. Molecular model representing capsule **1×2c** and structures of the capsule components **1** and **2a-d**.

7.2 Results and discussion

7.2.1 Synthesis and confirmation of the capsule structure

The capsules **1×2** are based on two halfspheres: a cavitand **2** functionalized with four azinium substituents and calix[4]arene **1** containing four sulphonate substituents. Four pyridinium-sulphonate interactions bring the two halfspheres together to form a capsule (Chart 1). Capsules **1×2a-d** were prepared in 89–97% yield by mixing aqueous solutions of equimolar amounts of azinium salts **2a-d**×4Br⁻ with the known tetrasodium calix[4]arene tetrasulphonate **1**×4Na⁺.[12,14]

Capsule components **2a**,[15] **2b**, **2c**,[16] and **2d**, as tetrabromide salts, were prepared by reaction of tetrakis(bromomethyl)tetramethylcavitand **3**[17] with the appropriate azine (Scheme 1). Heating of tetrabromide **3** in a 4-cyanopyridine melt furnished **2b** in 79% yield. The synthesis of **2d** (yield 83%) was carried out in solution due to the much higher reactivity of 4-picoline compared with pyrazine.[18]

The capsules **1×2** are very badly soluble in water. Their solubility in methanol is < 2 mM, which is much lower than the solubility of the initial capsule components **2a-d** (> 100 mM).

Y = N (**a**), CCN (**b**), CH (**c**), CMe (**d**)
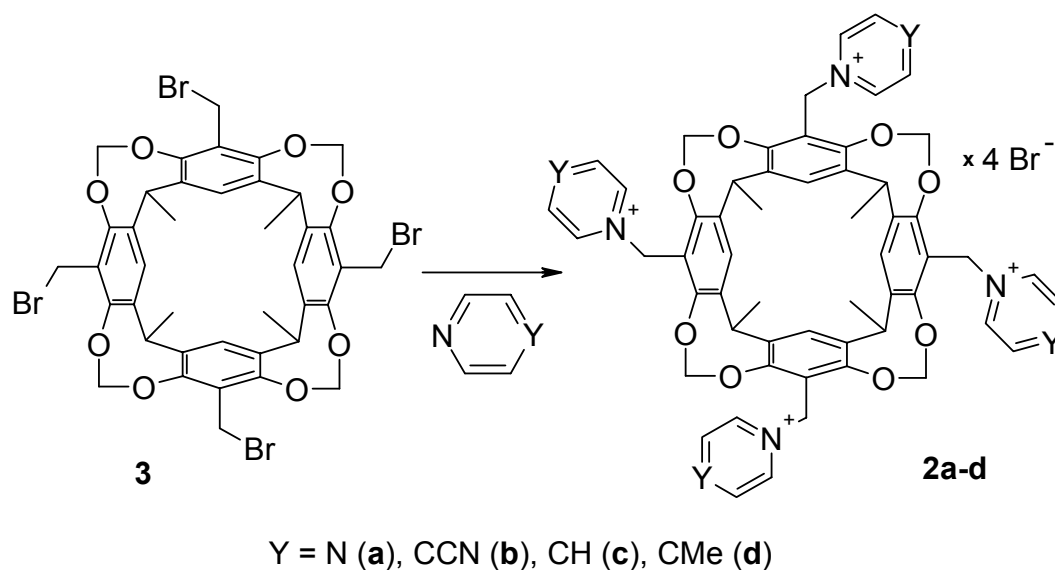
Scheme 1. Synthesis of tetrakis(aziniummethyl)tetramethylcavitands **2a-d**.

Electrospray ionization mass spectrometry (ESI-MS) confirms the formation of the capsules **1×2**. For example, in the case of capsule **1×2a** the mass spectrum exclusively contains signals of the capsule (with one or two sodium cations) (Figure 1). In some cases, also signals of the capsule containing one or two solvent molecules are present (vide infra). Since no significant influence of suppression takes place at these concentrations,[19] it can be concluded that the absence of signals of the capsule components **1** and **2** is a strong indication of the almost complete association of the capsule at this low concentration (50 μM).
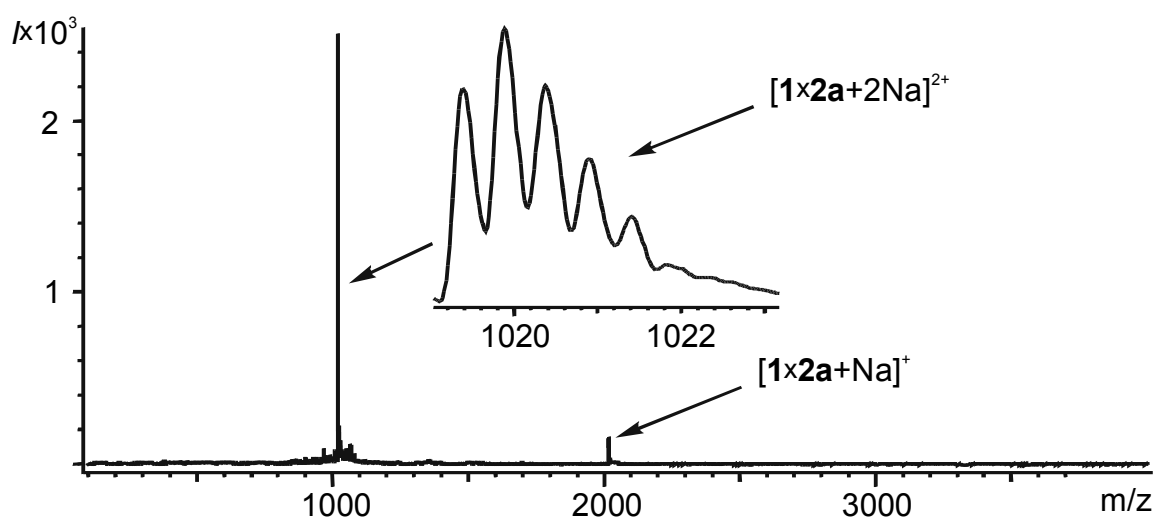

Figure 1. ESI-MS spectrum of a 50 μM solution of capsule **1×2a** in methanol (voltages: ring lens = 30 V, orifice 1 = 2 V, orifice 2 = 2 V).

The absence of signals of trimers, tetramers, etc. indicates that the signals correspond to a capsule and not to associates, in which only one or two azinium moieties are ion-paired and others are not complexed.[20]

Upon mixing the capsule half-spheres $1 \times 4Na^+$ and $2 \times 4Br^-$ significant changes in the ^1H NMR spectra are observed (for an example, see Figure 2), which is a clear indication of significant structural changes upon capsule formation. In the case of $1 \times 2c$, the largest shift changes were observed for the γ- (~ 1 ppm) and β-pyridinium hydrogens (~ 0.5 ppm).
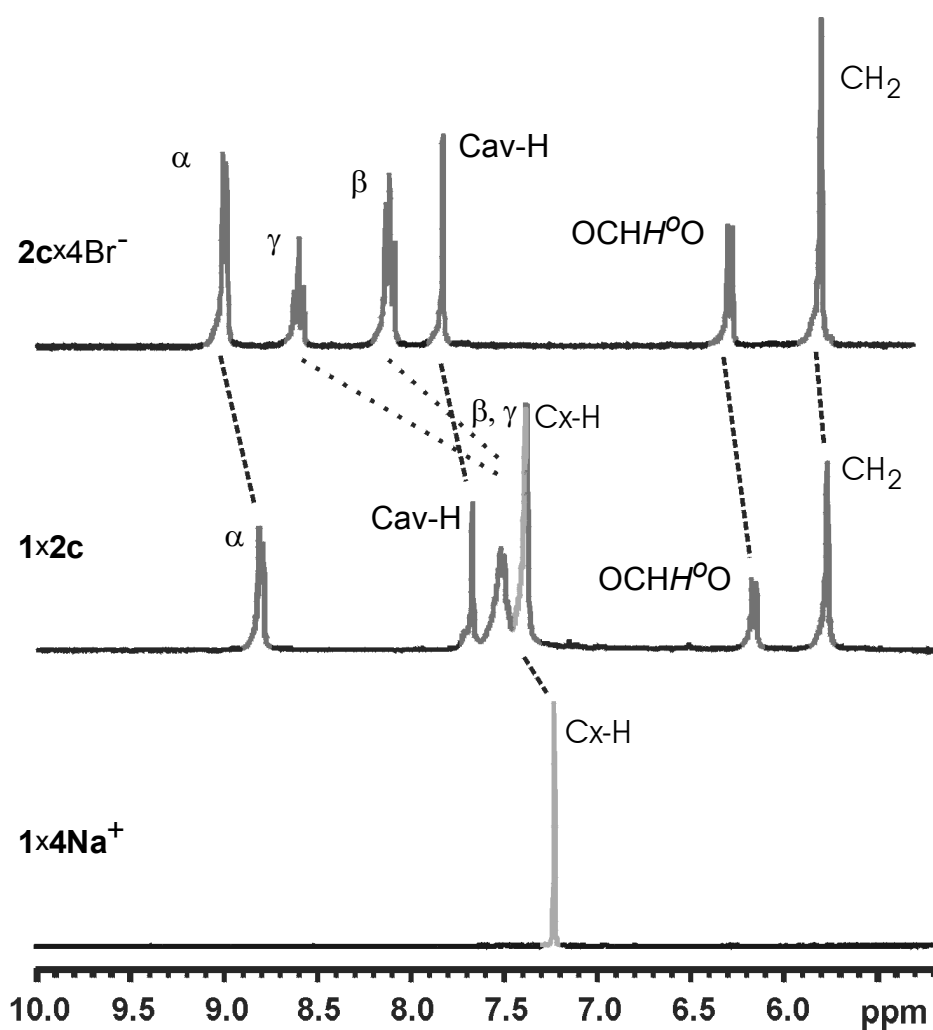

Figure 2. Spectra of 1 mM solutions of the initial compounds ($1 \times 4Na^+$ and $2c \times 4Br^-$) and capsule $1 \times 2c$ in methanol-d_4. The dashed lines indicate the changes in the ^1H NMR spectra upon capsule formation.

The α-pyridinium protons experience a smaller shift change (~ 0.2 ppm). The considerable difference in shift changes between the pyridinium hydrogens can be explained by the structural difference between the initial compound **2c** and capsule

137

1×2c. In compounds **2**, all the pyridinium protons are influenced by electrostatic interactions (ion-pairing[21] and higher association[18]). In pyridinium-anion contact ion-pairs, the anion is located above the pyridinium plane.[22] In the case of capsules **1×2**, the rigidity of the calix[4]arene skeleton prevents the sulphonate substituent to be located above the pyridinium ring (Chart 1). Instead the sulphonate groups are positioned as such that they can only interact with the positively charged nitrogen center, and not with the whole pyridinium ring. Therefore the α-pyridinium hydrogens experience only a slight change, caused by the different influence of bromide and sulphonate. Protons in the β- and, especially, the γ-position of the pyridinium ring are located far away from the sulphonate group (Chart 1) and, consequently, a larger shift difference is observed for these protons upon capsule formation.

A small difference was also observed for the aryl hydrogens of the cavitand scaffold (~ 0.1 ppm). Since cavitands form complexes with anions,[23] which can be monitored by ^{1}H NMR spectroscopy (vide infra), decomplexation of bromide from **2c** during the capsule formation leads to the shift change.

An ^{1}H NMR titration of calix[4]arene tetrasulphonate **1×4Na$^+$** with tetrakis-(pyridiniummethyl)tetramethyl cavitand **2c×4Br$^-$** shows that till a 1:1 ratio is attained, all **2c** is bound. This is concluded from the negligible changes in the shift of the pyridinium protons; only addition of an excess of **2c** gives shift changes. This is a strong indication for a 1:1 binding stoichiometry.[24]

^{1}H NMR titration experiments of compound **2c×4Br$^-$** with calix[4]arene tetrasulphonate **1×4Na$^+$** in methanol-d_4 revealed that the apparent association constant is concentration dependent. K_a-values of 7×10^4 M^{-1} – $>2 \times 10^5$ M^{-1} were obtained varying the initial concentration of **2c×4Br$^-$** from 0.5 mM to 0.05 mM. A plot of the ^{1}H NMR shift changes of the α-pyridinium protons during a titration of **2c×4Br$^-$** with **1×4Na$^+$** showed a systematic deviation from the best-fit data (Figure 3) indicating the presence of (an) additional process(es). This led us to study the influence of the ion-pairing of the initial components.
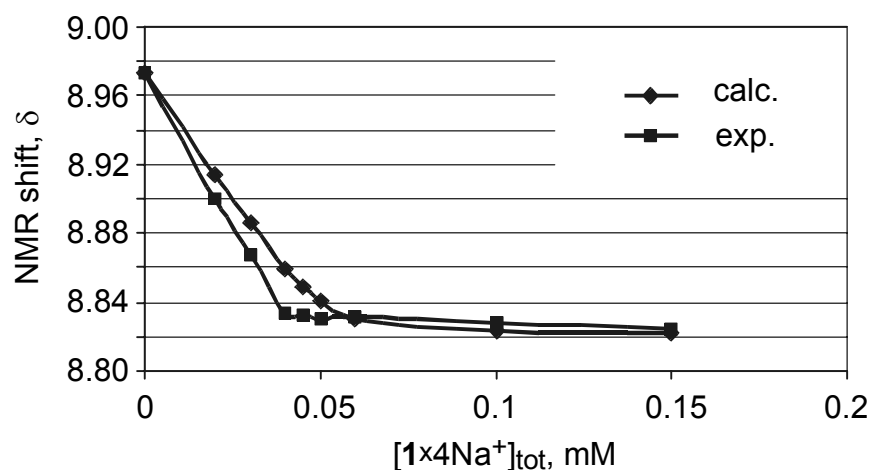
Figure 3. Plot of the shift of the α-pyridinium protons versus the concentration of $1 \times 4Na^+$ upon ^{1}H NMR titration of $2c \times 4Br^-$ (0.05 mM) with $1 \times 4Na^+$ in methanol-d_4:D_2O = 7:3 (v:v).

7.2.2 Ion-pairing of the initial components

It is known that ion-pairing of pyridinium cations with anions causes concentration dependent ^{1}H NMR shifts of the pyridinium hydrogens.[21] ^{1}H NMR dilution experiments of the tetrakis(aziniummethyl)tetramethylcavitands **2a-d** exhibited changes of the shifts of the azinium protons, indicating ion-pairing of the pyridinium rings with bromide (for an example, see Figure 4). A large shift difference was also observed for the protons of the cavitand scaffold due to inclusion of the anion into the cavity (K_a-value > 30 M^{-1} in methanol[3]).

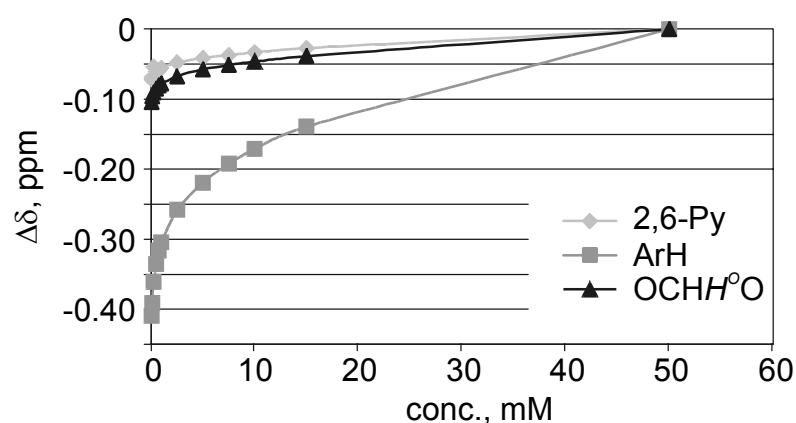**Figure 4.** ^{1}H NMR shift changes upon dilution of $2c \times 4Br^-$ in methanol-d_4.

---

[3] This value was obtained assuming that all bromide is available for complexation. The real value should be > 30 M^{-1}, because the anion participates in the ion-pairing.

ESI-MS also shows ion-pair association of the azinium cavitands **2**×4Br$^-$. For example, the ESI-MS spectrum of a 100 μM solution of **2c**×4Br$^-$ in methanol contains signals of ion-pairs and triple ion capsules[18] (Figure 5).

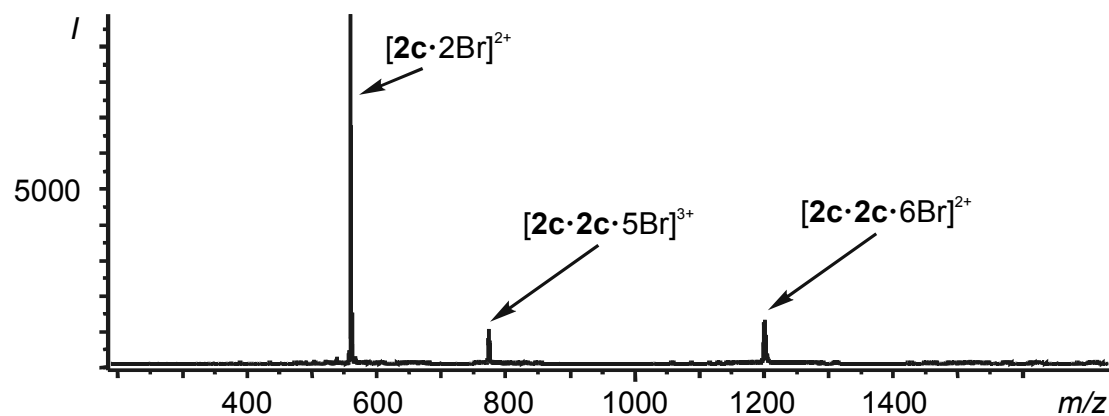**Figure 5.** ESI-MS spectrum of a 100 μM solution of **2c**×4Br$^-$ in methanol.

From the literature it is known that UV-vis spectroscopy allows the monitoring of the formation of contact ion-pairs from azinium cations with counterions in solution.[25-28] In the case of pyridinium salts, containing electron-withdrawing groups, such as cyano- or 4-pyridinium (viologen derivatives), the formation of ion-pairs can be easily followed by the appearance of (a) charge-transfer band(s) above 300 nm in the UV-vis spectra.[28] The appearance of charge-transfer bands upon contact ion-pair formation has been observed for a variety of anions, such as iodide,[25,26,28] bromide,[29] sulphite,[29] sulphate,[30] hexacyanoferrate,[30,31] etc.

A methanolic solution (26 μM) of freshly prepared tetrakis(pyrazinium-methyl)tetramethylcavitand tetrabromide **2a**×4Br$^-$ shows two maxima in its UV-spectrum: 276 nm and 317 nm (Figure 6). The high intensity of the charge-transfer band at 317 nm at such a low concentration indicates a significant ion-pairing of pyrazinium with bromide. The charge transfer band can represent multiple equilibria, i.e. not only ion-pairs but also higher aggregates.[32] Upon addition of tetrasulphonate **1**×4Na$^+$, the intensity of the band at 317 nm was decreased, leaving a 'pyrazinium shoulder'[33] covering the area of 300 - 350 nm (Figure 6). This change involves the replacement of a pyrazinium-bromide for a pyrazinium-sulphonate ion-pair. The absorption in the 300 - 350 nm area is not changed upon the addition of a larger amount of **1**×4Na$^+$ (Figure 6), indicating the complete replacement of bromide in the previous complex. Calix[4]arene tetrasulphonate **1**×4Na$^+$ has a band below 300 nm in the UV-spectrum (Figure 6) that does not interfere with the charge-transfer band.
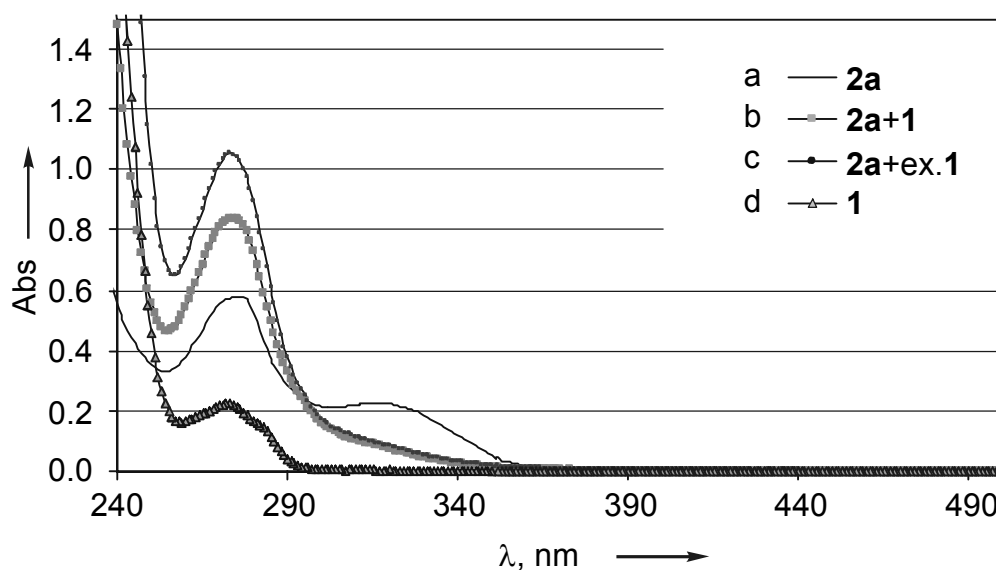
Figure 6. UV-vis spectra of a) a solution of **2a** in methanol, b) solution a + **1**, c) solution a + excess of **1**, d) a solution of **1** in methanol.

7.2.3 K_a-value determination of the capsules 1×2

The K_a-values of capsule **1×2** formation were determined with dilution experiments. Upon dilution of capsules **1×2** in methanol-d_4 from 1 mM to 5 μM in the ^{1}H NMR spectrum a very small shift was observed for the α-azinium protons (up to ~ 0.005 ppm) due to some dissociation of the capsule at low concentrations. Attempts to fit the NMR dilution data resulted in K_a-values $> 10^6$ M^{-1}.

Upon dilution of methanolic solutions of the capsules **1×2** a systematic deviation from the Lambert-Beer law was observed in the UV-spectra. For example, in the case of capsule **1×2a** (Figure 7), an increase of the molar absorptivity of about 40-70 L mol^{-1} cm^{-1} was observed at 300 nm. This deviation is caused by the presence of a charge-transfer band between sulphonate and pyridinium (~ 290 − 320 nm).[30] Non-linear fitting of the data yielded K_a-values of $> 2×10^6$ M^{-1} for the capsules **1×2** in methanol and **1×2a,b** in methanol/water = 1:1 (band at 260 − 280 nm).[34]

The K_a-values are higher than those obtained via ^{1}H NMR titration experiments (vide supra). This is caused by the significant influence of ion-pairing on the titration data, which is excluded in the case of the dilution experiments.

The capsule is resistant to addition of an excess of bromide or iodide (as tetrabutylammonium salts). However, addition of tetrabutylammonium iodide to a

solution of the capsule **1×2a** in methanol results in the appearance of a new charge transfer band at 340 nm. This charge-transfer band does not disappear even upon addition of triphenylphosphine to remove traces of iodine and triiodide.[25] It could be caused by the formation of a complex of iodide with the pyrazinium-sulphonate contact ion-pair at the outside of the capsule to give an iodide-pyrazinium-sulphonate triple ion.[35]
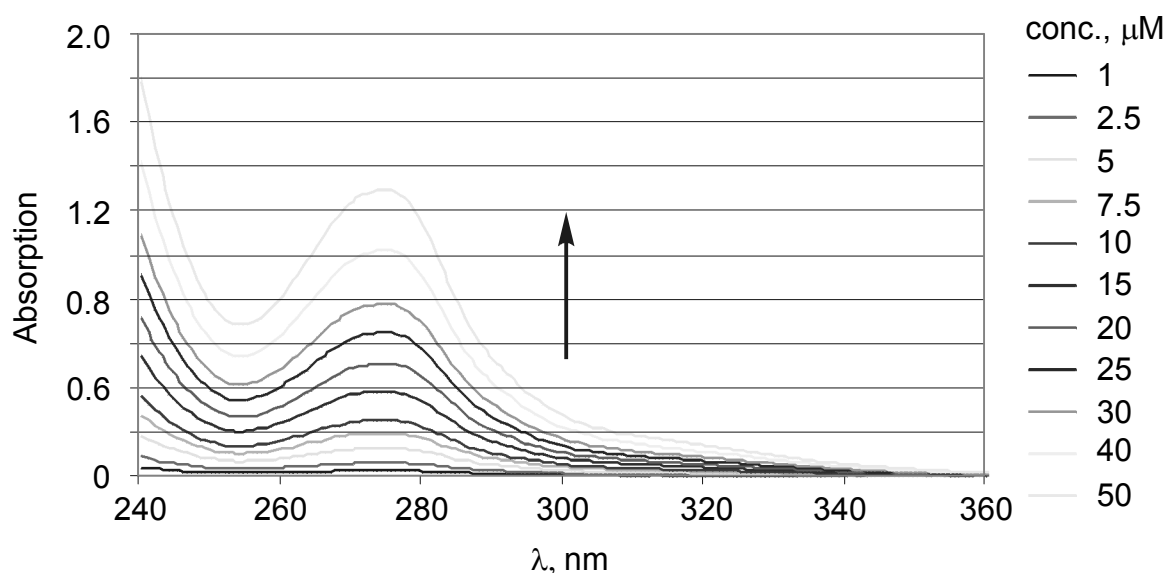

Figure 7. UV-dilution of **1×2a** in methanol.

7.2.4 Behavior of the capsule in the gas phase (ESI-MS)

The high stability of capsules **1×2** allows studying both its gas-phase fragmentation and the behavior of ion-pairs at a high voltage. As examples, parts of the voltage-induced dissociation spectra of capsules **1×2a,c** are shown in Figure 8. It is striking, that the fragmentation begins with the loss of an ion-paired wall of the capsule: SO_3×pyrazine. Due to the loss of the wall, the capsule becomes very destabilized, and loses subsequently the other pyrazines (Figure 8a). It is the reason of the simultaneous presence in the spectrum of a high capsule signal and intensive signals of fragmentation products (Figure 8a). The other fragmentation pathway, the loss of azinium rings (without SO_3) from an ion-pair, is observed at higher voltages and is concluded from the appearance of the [**1×2c**+Na-3pyridine]$^+$ signal (Figure 8b). Qualitatively, the same fragmentation behavior is observed for all capsules **1×2**. The ratio of the intensities of the signals of the fragmentation products and those of the capsules is higher in the case of capsules based on ion-pairs of pyrazinium and 4-cyanopyridinium (**1×2a** and **1×2b**). The relative voltage stability of the $-SO_3$×CH_2-

azinium contact ion-pairs, which form the walls of the capsules, follows the order 4-methylpyridinium > pyridinium > 4-cyanopyridinium > pyrazinium. Electron-accepting substituents are supposed to destabilize the CH_2-N bond within the -$SO_3 \times CH_2$-azinium contact ion-pairs.
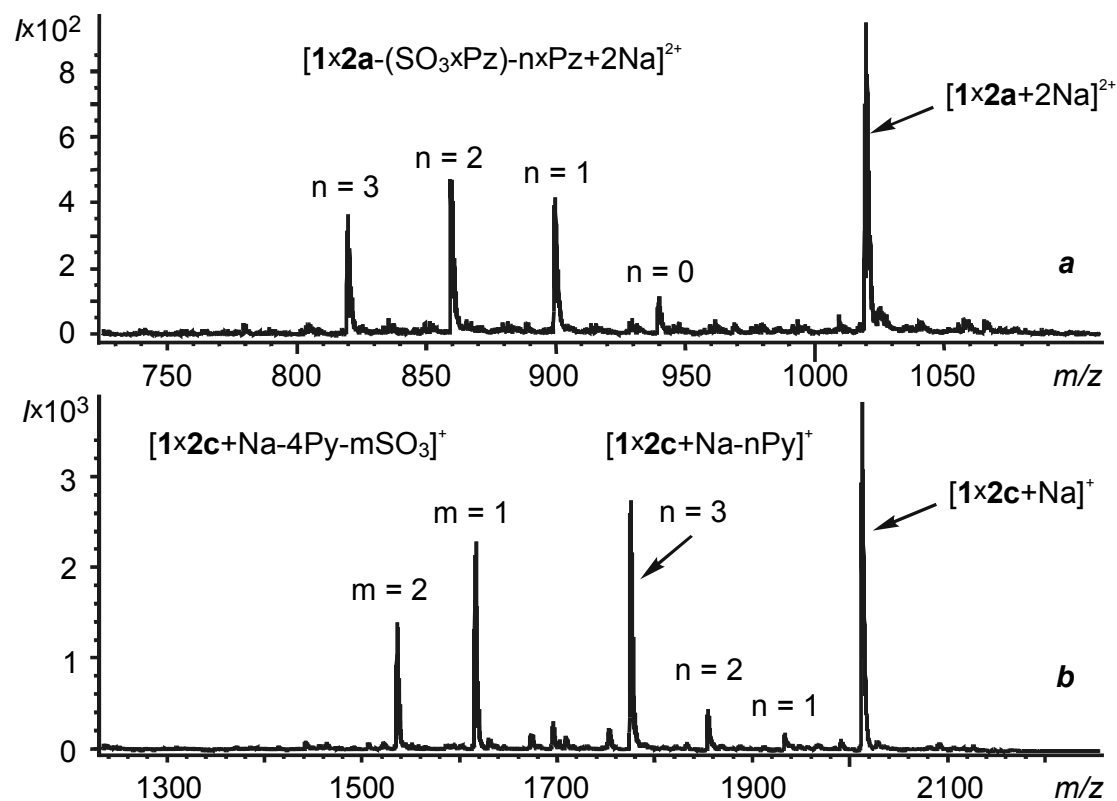
Figure 8. Parts of the ESI-MS spectra of 50 μM methanolic solutions of capsules **1×2a** (*a*: voltages: ring lens = 2 V, orifice 1 = 75 V, orifice 2 = 25 V), and **1×2c** (*b*: voltages: ring lens = 30 V, orifice 1 = 200 V, orifice 2 = 25 V); Pz = pyrazine, Py = pyridine.

7.2.4 Gas-phase guest inclusion complexes within the capsules

Under low voltage conditions the ESI-MS spectra of **1×2a-d** in methanol exhibit, in addition to the signal of the capsule, also peaks corresponding to the capsule and one or two methanol molecules. It should be noted that under these conditions desolvation takes place quite efficiently; the capsule components **1**×4Na[+] and **2a**×4Br[−] do not show solvated species in the ESI-MS spectra. Therefore it can be concluded that in the case of the capsules **1×2** methanol is encapsulated. Using higher voltages, as in Figure 1, methanol encapsulation is not observed. The exception is capsule **1×2b**, which keeps methanol till a very high voltage.

The influence of the size of the guest was studied by recording the ESI-MS spectra of 25 μM solutions of capsule in **1**×**2a** in a 1:1 mixture of methanol and $CH_3(CH_2)_nOH$ (n = 1…5). In the case of ethanol, in addition to the complexes with either methanol or ethanol, also a capsule containing both alcohols is present (Figure 9). n-Propanol, n-butanol, and n-amyl alcohol form 1:1 complexes with the capsule. These complexes have a higher voltage stability than those with methanol. In the case of n-hexanol (n = 5), a peak corresponding with the encapsulated guest in the capsule was not observed. This indicates that this alcohol is already too large to be accommodated within the cavity.
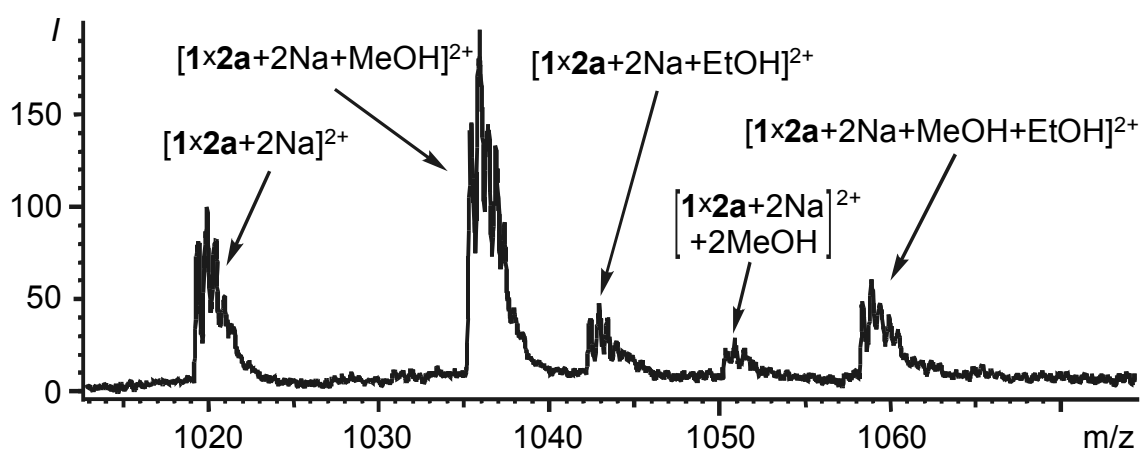
Figure 9. ESI-MS spectrum of a 25 μM solution of capsule **1**×**2a** in a 1:1 mixture of methanol/ethanol (v/v); voltages: ring lens = 20 V, orifice 1 = 5 V, orifice 2 = 5 V.

The capsule can also accommodate nitromethane, but experiments with ethyl acetate, toluene, and pyrazine in methanol showed no encapsulation. The inner volume of the capsule is smaller than that of the capsules of Rebek[9] and Böhmer,[10] nevertheless smaller molecules can be located inside as clearly shown by mass spectrometry.

7.3 Conclusions

In this Chapter it is clearly shown that it is essential to be aware of the presence of ion-pairing of the initial components in the formation of assemblies based on electrostatic interactions in polar media.

In the case of the formation of [1+1] cavitand-calix[4]arene capsules, based on azinium-anion interactions, ^{1}H NMR titration experiment resulted in concentration-dependent apparent K_a-values ranging from 7×10^4 M^{-1} to $>2 \times 10^5$ M[-1] in methanol-d_4.

However, ^{1}H NMR and UV-vis dilution experiments, in which the influence of ion-pairing is excluded, in the latter case making use of the sulphonate-azinium contact ion-pair charge transfer band gave K_a-values of $> 2 \times 10^6$ M^{-1} in methanol.

In many supramolecular studies the effect of the ion-pairing of charged starting components has probably been overlooked. Therefore, in those studies where titration experiments have been used for K_a-value determination, it should be realized that the obtained data might be concentration dependent.

7.4 Experimental section

The reagents were purchased from Aldrich or Acros Chimica and used without further purification. All the reactions were performed under a dry argon atmosphere. All solvents were freshly distilled before use. Dry pyridine was obtained by distillation over calcium hydride. Melting points were measured using a Sanyo Gellenkamp Melting Point Apparatus and are uncorrected. Proton and carbon NMR spectra were recorded on a Varian Unity Inova (300 MHz or 400 MHz for ^{1}H; 400 MHz for ^{13}C) spectrometer. Residual solvent protons were used as internal standard and chemical shifts are given relative to tetramethylsilane (TMS). UV-vis spectra were measured on a Varian Cary 3E UV-spectrophotometer in 10 mm cuvettes. Compounds **1**,[12,14] **2a**,[15] **2c**,[16] and, **3**[17] were prepared in accordance with the literature procedures. The presence of water in the analytical samples was proven by ^{1}H NMR spectroscopy.

ESI-MS: The ESI-MS experiments were carried out with a Jeol AccuTOF instrument. In the standard mode the solutions were introduced at a flow rate of 6 µL/min. The data were accumulated in the mass range 230 – 4000 *m/z* for 2 min. The standard spray conditions, unless otherwise specified are: capillary voltage 2500 V, ring lens voltage 30 V, orifice 1 voltage = 2 V (for compounds **2b,d**) and 100 V (for capsules **1×2**), orifice 2 voltage = 2 V, orifice 1 temperature = 60 °C, temperature in the desolvation chamber 120 °C, drying gas flow 0.5 L/min, nebulizing gas flow = 0.5 L/min. For the characterization of compounds **2b,d** and capsules **1×2** the most intensive signals of the isotopic pattern are shown.

Tetrakis(4-cyanopyridiniummethyl)tetramethylcavitand tetrabromide 2b:

Tetrakis(bromomethyl)tetramethyl cavitand **3**[17] (300 mg, 0.31 mmol) was added to a melt of 4-cyanopyridine (1.2 g, 11.5 mmol). The reaction mixture was stirred at 100 ºC for 20 h. After cooling down the reaction mixture, diethyl ether (50 mL) was added and the reaction mixture was stirred for 1 h. The precipitate was filtered off and recrystallized from methanol/dichloromethane to give **2b** as a yellow powder. Yield: 79%; m.p. > 300 °C; ^{1}H NMR (5 mM, CD_3OD, 300 MHz) δ: 9.24 (d, 8 H, J = 6.6 Hz; α-pyridinium-H), 8.49 (d, 8 H, J = 6.2 Hz; β-pyridinium-H), 7.95 (s, 4 H; CavArH), 6.32 (d, 4 H, J = 7.3 Hz; O_2CHH^O), 5.90 (s, 8 H; $ArCH_2Py$), 4.96 (q, 4 H, J = 7.7 Hz; Ar_2CH), 4.80 – 4.73 (bs; water + O_2CHH^i), 1.89 (d, 12 H, J = 7.3 Hz; CH_3-Cav); UV-vis (CH_3OH) ν: 278 nm; ESI-MS (200 μM, CH_3OH) *m/z*: $[2b+2Br]^{2+}$ 610.14 (calc.: 610.11); elemental analysis calc.(%) for $C_{64}H_{52}Br_4N_8O_8$ + 3 H_2O (1434.8): C 53.57, H 4.07, Br 22.28, N 7.81; found: C 53.44, H 3.96, Br 21.95, N 7.60.

Tetrakis(4-methylpyridiniummethyl)tetramethylcavitand tetrabromide 2d:

To a stirred solution of tetrakis(bromomethyl)tetramethylcavitand **3** (1.0 g, 1.04 mmol) in chloroform (50 mL), 4-picoline (0.61 mL, 6.24 mmol) was added dropwise. The reaction mixture was stirred for 24 h. To the suspension formed, methanol (50 mL) was added and the resulting clear reaction mixture was stirred for an additional 24 h. The reaction mixture was evaporated to dryness under vacuum. The product was purified twice by reprecipitation with diethyl ether from methanol. Yield: 1.15 g (83%); m.p. > 300 °C; ^{1}H NMR (5mM, CD_3OD, 300 MHz) δ: 8.78 (d, 8 H, J = 6.6 Hz; α-pyridinium-H), 7.91 (d, 8 H, J = 6.2 Hz; β-pyridinium-H), 7.86 (s, 4 H; CavArH), 6.28 (d, 4 H, J = 7.3 Hz; O_2CHH^O), 5.70 (s, 8 H; $ArCH_2Py$), 4.95 (q, 4 H, J = 7.7 Hz; Ar_2CH), 4.73 (d, 4 H, J = 7.3 Hz; O_2CHH^i), 2.67 (s, 12 H; CH_3-Py), 1.87 (d, 12 H, J = 7.3 Hz; CH_3-Cav); UV-vis (CH_3OH) ν: 281 nm; ESI-MS (200 μM, CH_3OH) *m/z*: $[2d+2Br]^{2+}$ 588.17 (calc.: 588.15), $[2d+2d+5Br]^{3+}$ 811.22 (calc.: 811.18), $[2d+2d+6Br]^{2+}$ 1257.28 (calc.: 1257.23); elemental analysis calc.(%) for $C_{64}H_{64}Br_4N_4O_8$ + 4.5 H_2O (1417.9): C 54.21, H 5.19, Br 22.54, N 3.95; found: C 54.20, H 5.10, Br 22.25, N 4.01.

General procedure for the synthesis of capsules 1×2:

An aqueous solution (6 mL) of **1** (15.7 mg, 14 μM) was added dropwise to an aqueous solution (6 mL) of **2** (14 μM). The suspension formed was stirred for 1 h and

allowed to stay for an additional 1 h. The product was filtered, washed with water, diethyl ether and dried in vacuum.

Tetrakis(1-pyraziniummethyl)tetramethylcavitand tetrakis(ethoxyethyl)-calix[4]arenetetrasulphonate 1×2a: Yield 89%; m.p. > 250 °C; ^{1}H NMR (CD$_3$OD, 400 MHz) δ: 9.33 (bs, 8 H; α-pyrazinium-H), 9.02 (d, 8 H, J = 4.4 Hz; β-pyrazinium-H), 7.66 (s, 4 H; cavArH), 7.45 (s, 8 H; calixArH), 6.17 (d, 4 H, J = 7.7 Hz; OCHH^OO), 5.91 (s, 8 H; ArCH$_2$Py), 4.96 (q, 4 H, J = 7.3 Hz; Ar$_2$CH), 4.73 (d, 4 H, J = 7.7 Hz; OCHH^iO), 4.72 (d, 4 H, J = 12.8 Hz; ArCH$^{eq}H^{ax}$Ar), 4.27 (t, 8 H, J = 5.5 Hz; ArOCH$_2$), 3.91 (t, 8 H, J = 5.5 Hz; ArOCH$_2$CH_2), 3.54 (q, 8 H, J = 7.3 Hz; CH_2CH$_3$), 3.29-3.38 (m; CHD$_2$OD+ArCH^{eq}H^{ax}Ar), 1.81 (d, 12 H, J = 7.3 Hz; CH$_3$), 1.22 (t, 12 H, J = 7.3 Hz; CH$_2$CH_3); ^{13}C NMR (CD$_3$OD) δ: 159.1, 155.2, 152.5, 141.0, 140.8, 138.5, 136.0, 128.0, 124.9, 121.1, 101.9, 75.1, 70.9, 67.6, 57.5, 32.9, 32.7, 16.2, 15.9; UV-vis (CH$_3$OH) ν: 275 nm; ESI-MS (50 μM, CH$_3$OH) *m/z*: [**1×2a**+2Na]$^{2+}$ 1019.82 (calc.: 1019.78), [**1×2a**+Na]$^+$ 2016.61 (calc.: 2016.57); elemental analysis calc.(%) for C$_{100}$H$_{104}$N$_8$O$_{28}$S$_4$ + 6 H$_2$O (2102.3): C 57.13, H 5.56, N 5.33; found: C 56.98, H 5.50, N 5.14.

Tetrakis(1-(4-cyanopyridinium)methyl)tetramethylcavitand tetrakis(etho-xyethyl)calix[4]arenetetrasulphonate 1×2b: Yield 97%; m.p. > 250 °C; ^{1}H NMR (CD$_3$OD, 300 MHz) δ: 9.24 (d, 8 H, J = 7.0 Hz; α-pyridinium-H), 8.46 (d, 8 H, J = 7.0 Hz; β-pyridinium-H), 7.59 (s, 4 H; cavArH), 7.45 (s, 8 H; calixArH), 6.18 (d, 4 H, J = 7.5 Hz; OCHH^OO), 5.92 (s, 8 H; ArCH$_2$Py), 4.93 (q, 4 H, J = 7.3 Hz; Ar$_2$CH), 4.65-4.84 (water + ArCH$^{eq}H^{ax}$Ar + OCHH^iO), 4.26 (t, 8 H, J = 5.5 Hz; ArOCH$_2$), 3.89 (t, 8 H, J = 5.5 Hz; ArOCH$_2$CH_2), 3.55 (q, 8 H, J = 7.0 Hz; CH_2CH$_3$), 3.29-3.33 (CHD$_2$OH + ArCH^{eq}H^{ax}Ar), 1.78 (d, 12 H, J = 7.7 Hz; CH$_3$), 1.21 (t, 12 H, J = 7.0 Hz; CH$_2$CH_3); UV-vis (CH$_3$OH) ν: 278 nm; ESI-MS (50 μM, CH$_3$OH) *m/z*: [**1×2b**+2Na]$^{2+}$ 1067.79 (calc.: 1067.78), [**1×2b**+2Na+CH$_3$OH]$^{2+}$ 1083.91 (calc.: 1083.80), [**1×2b**+Na]$^+$ 2112.65 (calc.: 2112.57), [**1×2b**+Na+CH$_3$OH]$^+$ 2144.71 (calc.: 2144.60); elemental analysis calc.(%) for C$_{108}$H$_{104}$N$_8$O$_{28}$S$_4$ + 5.5 H$_2$O (2189.4): C 59.25, H 5.29, N 5.12; found: C 59.32, H 5.12, N 5.15.

Tetrakis(pyridiniummethyl)tetramethylcavitand tetrakis(ethoxyethyl)-calix[4]arenetetrasulphonate 1×2c: Yield 92%; m.p. > 250 °C; ^{1}H NMR (CD$_3$OD, 300 MHz) δ: 8.82 (d, 8 H, J = 5.5 Hz; α-pyridinium-H), 7.5-7.7 (m, 16 H; β,γ-pyridinium-H and cavArH), 7.47 (s, 8 H; calixArH), 6.14 (d, 4 H, J = 7.7 Hz;

OCHH^OO), 5.79 (s, 8 H; ArCH$_2$Py), 4.96 (q, 4 H, *J* = 7.3 Hz; Ar$_2$CH), 4.7-4.87 (water + ArCH$^{eq}H^{ax}$Ar), 4.60 (d, 4 H, *J* = 7.7 Hz; OCHH^iO), 4.31 (t, 8 H, *J* = 5.3 Hz; ArOCH$_2$), 3.93 (t, 8 H, *J* = 5.3 Hz; ArOCH$_2$CH_2), 3.58 (q, 8 H, *J* = 7.0 Hz; CH_2CH$_3$), 3.37 (d, 4 H, *J* = 12.1 Hz; ArCH^{eq}H^{ax}Ar), 1.80 (d, 12 H, *J* = 7.3 Hz; CH$_3$), 1.23 (t, 12 H, *J* = 7.0 Hz; CH$_2$CH_3); ^{13}C NMR (CD$_3$OD) δ: 159.2, 155.2, 140.9, 136.2, 128.1, 75.3, 70.8, 32.9; UV-vis (CH$_3$OH) ν: 279 nm; ESI-MS (50 μM, CH$_3$OH) *m/z*: [**1**×**2c**+2Na]$^{2+}$ 1017.84 (calc.: 1017.79), [**1**×**2c**+Na]$^+$ 2012.67 (calc.: 2012.60); elemental analysis calc.(%) for C$_{104}$H$_{108}$N$_4$O$_{28}$S$_4$ + 7 H$_2$O (2116.4): C 59.02, H 5.81, N 2.65; found: C 59.09, H 5.78, N 2.54.

Tetrakis(4-methylpyridiniummethyl)tetramethylcavitand tetrakis(ethoxy-ethyl)calix[4]arenetetrasulphonate 1×2d: Yield 93%; m.p. > 250 °C; ^{1}H NMR (CD$_3$OD, 300 MHz) δ: 8.65 (d, 8 H, *J* = 5.1 Hz; α-pyridinium-H), 7.62 (s, 4 H; cavArH), 7.54, 7.50 (s, 12 H; β-pyridinium-H, calixArH), 6.07 (d, 4 H, *J* = 7.7 Hz; OCHH^OO), 5.72 (s, 8 H; ArCH$_2$Py), 4.95 (q, 4 H, *J* = 7.3 Hz; Ar$_2$CH), 4.65-4.85 (water + ArCH$^{eq}H^{ax}$Ar), 4.61 (d, 4 H, *J* = 7.7 Hz; OCHH^iO), 4.30 (t, 8 H, *J* = 5.5 Hz; ArOCH$_2$), 3.91 (t, 8 H, *J* = 5.5 Hz; ArOCH$_2$CH_2), 3.58 (q, 8 H, *J* = 7.3 Hz; CH_2CH$_3$), 3.38 (d, 4 H, *J* = 12.8 Hz; ArCH^{eq}H^{ax}Ar), 1.90 (s, 12 H; CH$_3$-Py), 1.80 (d, 12 H, *J* = 7.3 Hz; CH$_3$), 1.23 (t, 12 H, *J* = 7.0 Hz; CH$_2$CH_3); ^{13}C NMR (CD$_3$OD) δ: 158.8, 155.2, 146.1, 141.5, 140.9, 136.6, 129.3, 128.0, 124.5, 121.8, 101.9, 75.3, 70.8, 67.6, 56.4, 32.9, 16.3, 15.8; UV-vis (CH$_3$OH) ν: 280 nm; ESI-MS (50 μM, CH$_3$OH) *m/z*: [**1**×**2d**+2Na]$^{2+}$ 1045.82 (calc.: 1045.82), [**1**×**2d**+Na]$^+$ 2068.70 (calc.: 2068.66); elemental analysis calc.(%) for C$_{108}$H$_{116}$N$_4$O$_{28}$S$_4$ + 8 H$_2$O (2190.5): C 59.22, H 6.07, N 2.56; found: C 59.26, H 6.07, N 2.40.

K_a-value determination: K_a-values were determined from ^{1}H NMR and UV-titration and dilution data by non-linear fitting. Capsule formation was described by standard equations for 1+1 stoichiometry.[36] For the fitting of the NMR titration and dilution data standard relationships between the shift of the α-pyridinium protons and the concentrations of the capsule and capsule components were used.[37] For the fitting of the UV dilution data, the K_a-value of the capsule formation and the molar absorptivity of the scaffold (ε$_c$) and the charge-transfer band (ε$_{c-t}$) were varied to obtain a minimal difference between calculated and experimental data using the least square method (an approximate maximal value of ε'$_{obs}$ was initially determined at a

higher concentration to limit the sum of ε_c and $\varepsilon_{c\text{-}t}$). The observed molar absorptivity ε'_{obs} at the wavelength, where a charge-transfer band is appearing, includes the molar absorptivity of the scaffold ε_c and that of the second component $\varepsilon'_{c\text{-}t}$, which is proportional to the degree of association of the capsule (equations 1 and 2).

$$\varepsilon'_{obs} = \varepsilon_c + \varepsilon'_{c\text{-}t} \qquad (1)$$

$$\varepsilon'_{c\text{-}t} = \varepsilon_{c\text{-}t} \left([\mathbf{1} \times \mathbf{2}] / [\mathbf{1} \times \mathbf{2}]_{max} \right) \qquad (2)$$

References and notes

1.   Takemura, H. *Curr. Org. Chem.* **2005**, *9*, 521-533.
2.   For reviews on synthetic anion and cation receptors, see: Kubik, S.; Reyheller, C.; Stuwe, S. *J. Incl. Phenom. Macrocycl. Chem.* **2005**, *52*, 137-187; Gale, P. A. *Coord. Chem. Rev.* **2003**, *240*, 191-221, and other reviews in this issue; Fitzmaurice, R. J.; Kyne, G. M.; Douheret, D.; Kilburn, J. D. *J. Chem. Soc., Perkin Trans. 1* **2002**, 841-864; Beer, P. D.; Gale, P. A. *Angew. Chem., Int. Ed.* **2001**, *40*, 486-516; Hartley, J. H.; James, T. D.; Ward, C. J. *J. Chem. Soc., Perkin Trans. 1* **2000**, 3155-3184; Snowden, T. S.; Anslyn, E. V. *Curr. Opin. Chem. Biol.* **1999**, *3*, 740-746; Antonisse, M. M. G.; Reinhoudt, D. N. *Chem. Commun.* **1998**, 443-448.
3.   For recent examples, see: Garozzo, D.; Gattuso, G.; Notti, A.; Pappalardo, A.; Pappalardo, S.; Parisi, M. F.; Perez, M.; Pisagatti, F. *Angew. Chem., Int. Ed.* **2005**, *44*, 4892-4896; Cametti, M.; Nissinen, M.; Cort, A. D.; Mandolini, L.; Rissanen, K. *J. Am. Chem. Soc.* **2005**, *127*, 3831-3837; Mahoney, J. M.; Davis, J. P.; Beatty, A. M.; Smith, B. D. *J. Org. Chem.* **2003**, *68*, 9819-9820; Kim, Y. H.; Hong, J. I. *Chem. Commun.* **2002**, 512-513.
4.   Shukla, R.; Kida, T.; Smith, B. D. *Org. Lett.* **2000**, *2*, 3099-3102.
5.   Huang, F. H.; Jones, J. W.; Slebodnick, C.; Gibson, H. W. *J. Am. Chem. Soc.* **2003**, *125*, 14458-14464; Jones, J. W.; Gibson, H. W. *J. Am. Chem. Soc.* **2003**, *125*, 7001-7004.
6.   Böhmer, V.; Dalla Cort, A.; Mandolini, L. *J. Org. Chem.* **2001**, *66*, 1900-1902; Bartoli, S.; Roelens, S. *J. Am. Chem. Soc.* **1999**, *121*, 11908-11909.
7.   Sirish, M.; Schneider, H. J. *Chem. Commun.* **2000**, 23-24; Ong, W.; Kaifer, A. E. *J. Org. Chem.* **2004**, *69*, 1383-1385.
8.   Kobayashi, K.; Ishii, K.; Yamanaka, M. *Chem. Eur. J.* **2005**, *11*, 4725-4734; Rudkevich, D. M. *Bull. Chem. Soc. Jpn.* **2002**, *75*, 393-413.
9.   Rebek, J. *Angew. Chem., Int. Ed.* **2005**, *44*, 2068-2078.
10.   Böhmer, V.; Vysotsky, M. O. *Aust. J. Chem.* **2001**, *54*, 671-677.
11.   Corbellini, F.; van Leeuwen, F. W. B.; Beijleveld, H.; Kooijman, H.; Spek, A. L.; Verboom, W.; Crego-Calama, M.; Reinhoudt, D. N. *New J. Chem.* **2005**, *29*, 243-248; Zadmard, R.; Junkers, M.; Schrader, T.; Grawe, T.; Kraft, A. *J. Org. Chem.* **2003**, *68*, 6511-6521; Zadmard, R.; Kraft, A.; Schrader, T.; Linne, U. *Chem. Eur. J.* **2004**, *10*, 4233-4239.
12.   Fiammengo, R.; Timmerman, P.; Huskens, J.; Versluis, K.; Heck, A. J. R.; Reinhoudt, D. N. *Tetrahedron* **2002**, *58*, 757-764; Fiammengo, R.; Timmerman, P.; de Jong, F.; Reinhoudt, D. N. *Chem. Commun.* **2000**, 2313-2314.

13. Corbellini, F.; Di Costanzo, L.; Crego-Calama, M.; Geremia, S.; Reinhoudt, D. N. *J. Am. Chem. Soc.* **2003**, *125*, 9946-9947; Corbellini, F.; Knegtel, R. M. A.; Grootenhuis, P. D. J.; Crego-Calama, M.; Reinhoudt, D. N. *Chem. Eur. J.* **2004**, *11*, 298-307; Jullien, L.; Cottet, H.; Hamelin, B.; Jardy, A. *J. Phys. Chem. B* **1999**, *103*, 10866-10875.

14. Casnati, A.; Ting, Y. H.; Berti, D.; Fabbi, M.; Pochini, A.; Ungaro, R.; Sciotto, D.; Lombardo, G. G. *Tetrahedron* **1993**, *49*, 9815-9822.

15. Middel, O.; Verboom, W.; Reinhoudt, D. N. *Eur. J. Org. Chem.* **2002**, 2587-2597.

16. Grote Gansey, M. H. B.; Bakker, F. K. G.; Feiters, M. C.; Geurts, H. P. M.; Verboom, W.; Reinhoudt, D. N. *Tetrahedron Lett.* **1998**, *39*, 5447-5450.

17. Sorrell, T. N.; Pigge, F. C. *J. Org. Chem.* **1993**, *58*, 784-785.

18. For details, see Chapter 5.

19. Oshovsky, G. V.; Verboom, W.; Fokkens, R. H.; Reinhoudt, D. N. *Chem. Eur. J.* **2004**, *10*, 2739-2748, and Chapter 3.

20. The absence of non-ion-paired azinium moieties was confirmed by in-source voltage-induced dissociation experiments (Gabelica, V.; De Pauw, E. *Mass Spectrom. Rev.* **2005**, *24*, 566-587); for details see Appendix 1.

21. Chuck, R. J.; Randall, E. W. *Spectrochim. Acta* **1966**, *22*, 221-226.

22. Larsen, J. W.; Edwards, A. G.; Dobi, P. *J. Am. Chem. Soc.* **1980**, *102*, 6780-6783.

23. See, for example, Chapter 5.

24. Corbellini, F.; Fiammengo, R.; Timmerman, P.; Crego-Calama, M.; Versluis, K.; Heck, A. J. R.; Luyten, I.; Reinhoudt, D. N. *J. Am. Chem. Soc.* **2002**, *124*, 6569-6575.

25. Binder, D. A.; Kreevoy, M. M. *J. Phys. Chem. A* **1997**, *101*, 1774-1781; Hemmes, P.; Costanzo, J. N.; Jordan, F. *J. Phys. Chem.* **1978**, *82*, 387-391.

26. Kosower, E. M. *J. Am. Chem. Soc.* **1955**, *77*, 3883-3885; Kosower, E. M.; Skorcz, J. A. *J. Am. Chem. Soc.* **1960**, *82*, 2195-2203; Mackay, R. A.; Poziomek, E. J. *J. Am. Chem. Soc.* **1970**, *92*, 2432-2439.

27. Foucher, D. A.; Macartney, D. H.; Warrack, L. J.; Wilson, J. P. *Inorg. Chem.* **1993**, *32*, 3425-3432.

28. Mackay, R. A.; Landolph, J. R.; Poziomek, E. J. *J. Am. Chem. Soc.* **1971**, *93*, 5026-5030.

29. Ray, A.; Mukerjee, P. *J. Phys. Chem.* **1966**, *70*, 2138-2143.

30. Monk, P. M. S.; Hodgkinson, N. M.; Partridge, R. D. *Dyes Pigm.* **1999**, *43*, 241-251.

31. Nakahara, A.; Wang, J. H. *J. Phys. Chem.* **1963**, *67*, 496-498.

32. The solutions of **2a**×4Br and **2b**×4Br show a strong time-dependent UV-response: within 12 hours a new small band at 370 nm appears, the intensity of the band at 317 nm decreases, the maximum at 276 nm shifts to the left for 5 nm, and the absorption in the area 240 - 280 nm increases. This may correspond to the setting of an equilibrium between free cations, contact ion-pairs and triple ions. Upon standing of diluted methanolic solution of **2a**×4Br and **2b**×4Br for longer time, a solvolysis of these compounds takes place, leading to changes in the ^{1}H NMR spectra of these compounds.

33. Rosokha, Y. S.; Lindeman, S. V.; Rosokha, S. V.; Kochi, J. K. *Angew. Chem., Int. Ed.* **2004**, *43*, 4650-4652.

34. Due to the low molar absorptivity value (<300 L mol^{-1} cm^{-1}) of the charge-transfer band, no experiments at lower concentrations are possible to determine a more precise K_a-value.

35. Hojo, M.; Hasegawa, H.; Morimoto, Y. *J. Phys. Chem.* **1995**, *99*, 6715-6720; The charge transfer band of **2a** and iodide appears at 360 nm.

36. Connors, K. A., *Binding Constants: The Measurement of Molecular Complex Stability;* Wiley-Interscience: New York, 1987; Hirose, K. *J. Incl. Phenom. Macrocycl. Chem.* **2001**, *39*, 193-209.

37. Fielding, L. *Tetrahedron* **2000**, *56*, 6151-6170.

Appendix 1

Differentiation between ion-paired and free azinium cations using ESI mass spectrometry

To determine whether the assemblies between **1** and **2** are real capsules, or associates based on only one or two pyridinium-sulphonate interactions, in-source voltage-induced dissociation experiments[1] were carried out. The capsule signal [**1**×**2**+ nNa]$^{n+}$ (n = 1, 2) shows a very high stability that is much higher than that of the tetrakis(aziniummethyl)tetramethylcavitand tetrabromides **2**. For example, in Figure A1a a part of the ESI-MS spectrum of a 0.1 mM solution of compound **2c** in methanol is shown. The signal at *m/z* 560.1 corresponds to tetrakis(pyridiniummethyl)tetra-methylcavitand [**2c**×2Br]$^{2+}$ in which two pyridiniums are ion-paired with bromides and two exist as free cations.[2] Upon a moderate increase of the orifice 1 voltage (from 20 to 60 V), the initial signal almost disappears. It is accompanied by the appearance of a new intensive signal of species in which both non-ion-paired pyridinium moieties are split off (Figure A1b) in accordance with scheme A (X = CH).
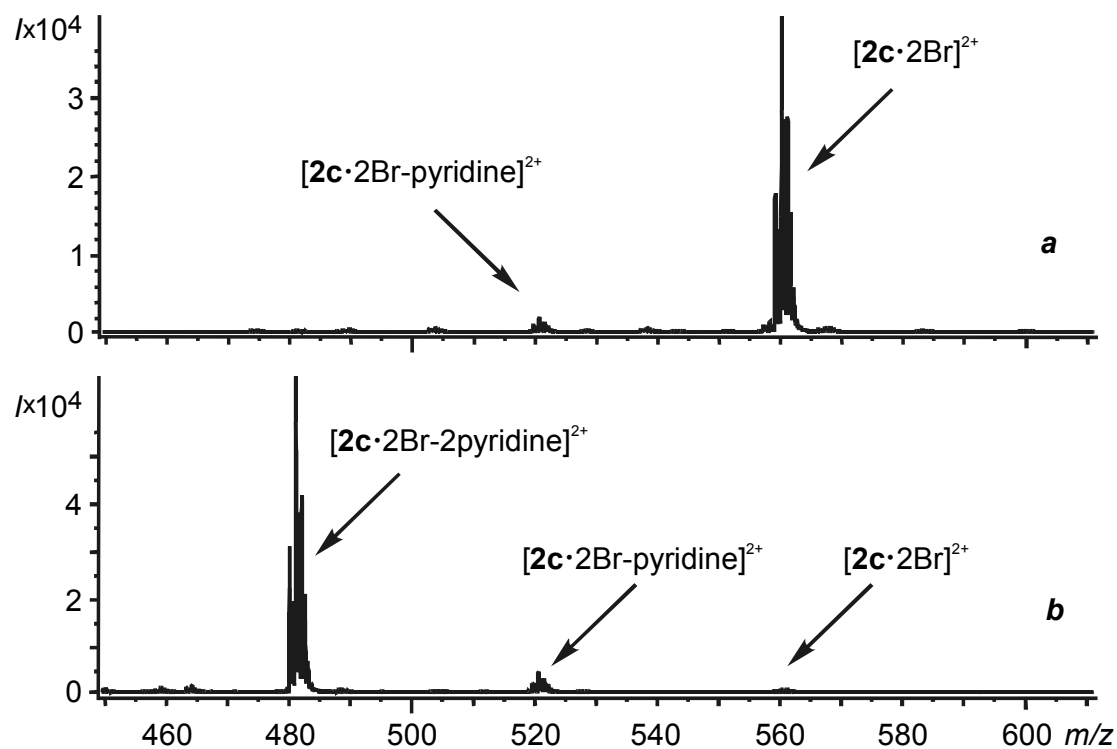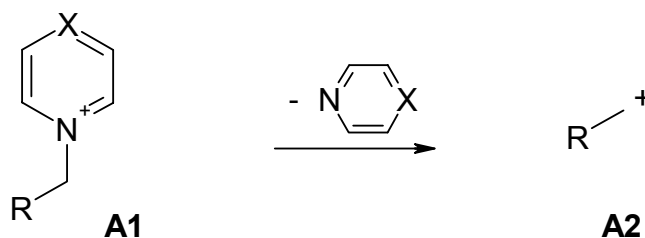
Figure A1. Voltage induced cleavage of the pyridinium cation from $[2c \cdot 2Br]^{2+}$ voltages: ring lens = 30 V; orifice 1 = 20 V (a), 60 V (b) , orifice 2 = 2 V.

Scheme A1. Gas phase transformation of the methylene azinium cations: cleavage of the C-N bond.[3]

Although in the case of non-ion-paired pyridiniums complete cleavage is observed at an orifice 1 voltage of 60 V (vide supra), in the case of the capsules 1×2, no significant fragmentations take place even at higher voltage (100 V). For example, in the case of $1 \times 2c$ the major signals in the spectra correspond to non-fragmented species $[1 \times 2c + 2Na]^{2+}$ and $[1 \times 2c + Na]^+$ (Figure A2).[4] The transformations shown in scheme A1 are negligibly small, indicating that ion-pairing stabilizes all four pyridinium cations.
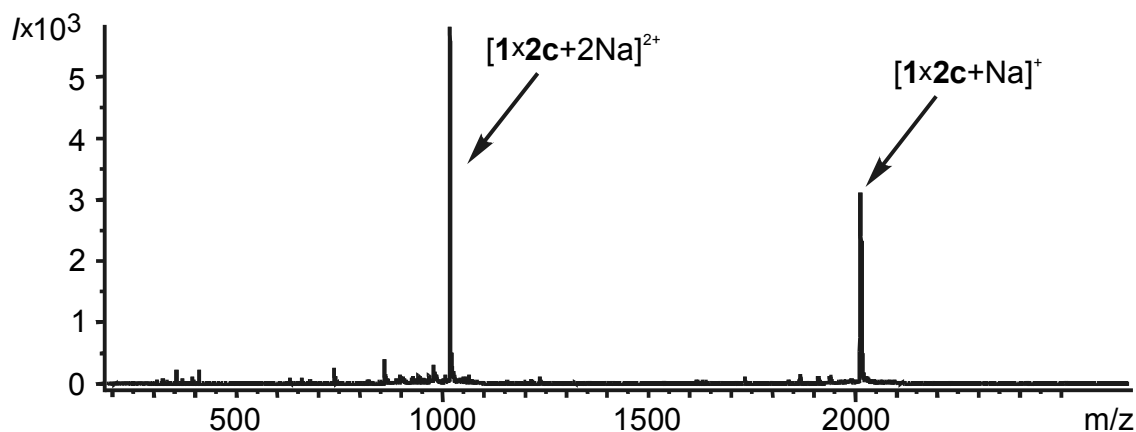
Figure A2. ESI-MS spectrum of a 50 µM solution of capsule **1×2c** in methanol, voltages: ring lens = 30 V, orifice 1 = 100 V, orifice 2 = 2 V.

These experiments demonstrate that compounds **1×2** contain no easily cleavable pyridinium cations, i.e. all the pyridinium or pyrazinium cations are ion-paired with the anionic sulphonate group, what unequivocally corresponds to the capsule structure.

1. Gabelica, V.; De Pauw, E. *Mass Spectrom. Rev.* **2005**, *24*, 566-587; Bure, C.; Lange, C. *Curr. Org. Chem.* **2003**, *7*, 1613-1624.
2. For details, see Chapter 5.
3. Katritzky, A. R.; Watson, C. H.; Degaszafran, Z.; Eyler, J. R. *J. Am. Chem. Soc.* **1990**, *112*, 2471-2478; Gabelica, V.; De Pauw, E.; Karas, M. *Int. J. Mass. Spec.* **2004**, *231*, 189-195; Naban-Maillet, J.; Lesage, D.; Bossee, A.; Gimbert, Y.; Sztaray, J.; Vekey, K.; Tabet, J. C. *J. Mass. Spec.* **2005**, *40*, 1-8; Schalley, C. A.; Verhaelen, C.; Klarner, F. G.; Hahn, U.; Vogtle, F. *Angew. Chem., Int. Ed.* **2005**, *44*, 477-480.
4. Only partial loss of complexed sodium from [**1×2c**+2Na]$^{2+}$ takes place, inducing an increase of the [**1×2c**+2Na]$^{2+}$/[**1×2c**+Na]$^{+}$ intensities ratio.

SUMMARY

This thesis is focused on a study of two basic supramolecular phenomena, viz. recognition and self-assembly in polar competitive media using appropriately functionalized cavitands.

Chapter 1 gives a general introduction to supramolecular chemistry in solution and describes the influence of solvents on the interaction of molecules.

Chapter 2 offers an overview of recent advances in the area of water-soluble synthetic receptors and assemblies, with consideration of the functionalities that are used to increase the water solubility, as well as the supramolecular interactions and approaches used for effective guest recognition in water.

Chapter 3 describes cavitand-based (thio)urea-functionalized glycoclusters and their recognition properties toward inorganic anions in polar (a)protic media (acetonitrile and a mixture of acetonitrile and water). With ESI-MS a relationship was found between the intensity of the signals of the host-guest complexes and the concentration of the host-guest species in solution. In a titration experiment, first the intensity follows the so-called 'square root rule', while at higher guest concentrations the intensity decreases due to suppression. This finding allowed the elaboration of several direct and competitive ESI mass spectrometric methods for the determination of binding constants. The calculated data are in agreement with those obtained with microcalorimetry.

Chapter 4 deals with an investigation of organic anion complexation in polar media by (thio)ureido cavitands, which are among the strongest organic anions binders reported up to now with K_a-values up to 9.4×10^6 M^{-1} in acetonitrile. These compounds exist in solution in equilibrium with the corresponding 1:1 capsules with a K_a-value of 6.86×10^4 M^{-1} in acetonitrile for the thiourea derivative. The anion

complexation is a strongly enthalpy driven process and leads to the formation of isomeric host-guest complexes (in and out). The binding of small organic anions like acetate and propionate leads to the appearance of guest signals at a very high field (up to $\delta = -3.02$ ppm) in the ^{1}H NMR spectra due to insertion of the alkyl substituents of the guest into the cavity (formation of in-isomers). Long alkyl chain-containing carboxylates, as e.g. valerate, are too large to be accommodated in the cavity and, consequently form out-isomers, where the complexation exclusively takes place by the (thio)urea moieties.

Chapter 5 shows the first example of the use of triple ions to build supramolecular architectures. [2+4] Capsules are formed from two tetrakis(pyridiniummethyl)tetramethyl cavitands, which have an 'open flower'-like structure, and four singly charged anions (bromide, nitrate, acetate, and tosylate). The pyridinium-anion-pyridinium binding motif is realized by the ability of the singly charged anions to form coordination complexes, which extends the valency of the anions. ESI-MS allowed the determination of the structure of the [2+4] capsules due to the different fragmentation motifs of pyridinium cations, pyridinium-anion contact ion-pairs, and the triple ions. The [2+4] capsules encapsulate one or two anions, depending on its size. They exist in equilibrium with [2+3] hemicapsules containing only three walls. The latter form complexes with phenols and anilines to give new unsymmetrical capsules containing both pyridinium-anion-pyridinium and pyridinium-guest-pyridinium walls.

Chapter 6 presents a study of electrostatic self-assembly of tetrakis(pyridiniummethyl)cavitand and doubly charged anions in polar media using classical ion-pair interactions, realized, for example, by the pyridinium-sulphate-pyridinium motif. ^{1}H NMR spectroscopy indicates the formation of the ion-pair associates and ESI-MS reveals the presence of different ion-paired species in the equilibrium mixture. A model that considers an equilibrium, which includes (hemi)capsules and ion-pair associates, was developed and an effective molarity (EM) of 0.19 ± 0.02 M was found for the intramolecular association. The model showed that in addition to the capsules reasonable amounts of hemicapsules and simple ion-paired species are present in solution dependent on the concentration. For example, in a 5 mM solution of the sulphate, the composition is 10% of the [2+3] hemicapsule, 15% of 1:1 complex, 17% of 1:2 complexes, and 14% of the [2+4] capsule. The hemicapsule forms complexes with electron-rich guests (like 4-iodophenol and -

aniline) in methanol by intercalation in between two 'free' pyridinium rings. In water the starting cavitand forms inclusion complexes with different guests due to hydrophobic interactions between the alkyl chain of a guest and the cavity.

Chapter 7 stresses the importance of electrostatic interactions between the initial components of an assembly with its counterions, in a study of [1+1] capsules based on tetrakis(aziniummethyl)cavitands and calix[4]arene tetrasulphonate. Not taking into account the initial azinium-anion association causes a decrease of the apparent association constants by more than two orders of magnitude. The [1+1] capsules have binding affinities of $> 2 \times 10^6$ M^{-1} in methanol and can encapsulate one or two small molecules (as methanol and ethanol) depending on their size.

SAMENVATTING

Het hoofdthema van dit proefschrift omvat twee belangrijke supramoleculaire fenomenen, namelijk herkenning en zelfassemblage in polaire oplosmiddelen van gefunctionaliseerde cavitanden.

Hoofdstuk 1 geeft een algemene inleiding over supramoleculaire chemie in oplossing en beschrijft de invloed van oplosmiddelen op moleculaire interacties.

Hoofdstuk 2 biedt een overzicht van de laatste ontwikkelingen op het gebied van in water oplosbare synthetische receptoren en assemblages, gericht op de functionaliteiten die gebruikt worden om de wateroplosbaarheid te vergroten, alsook supramoleculaire interacties en benaderingen die voor effectieve gast-herkenning gebruikt worden.

Hoofdstuk 3 beschrijft op cavitanden gebaseerde thioureum-gefunctionaliseerde glycoclusters en hun eigenschapen om anorganische anionen te herkennen in polair (a)protisch medium (acetonitril of een mengsel van acetonitril en water). Met ESI-MS werd een relatie gevonden tussen de intensiteit van de signalen van de gastheer-gast complexen en de concentratie van de overeenkomstige species in oplossing. In een titratie-experiment, volgt de intensiteit eerst de zogenaamde 'wortel regel', terwijl, als de gastconcentratie toeneemt, de intensiteit vermindert door suppressie. De gevonden relatie maakt het mogelijk om bindingsconstanten te bepalen met behulp van verschillende 'directe' en ESI massa-spectrometrische competitie methoden. De berekende data zijn in overeenstemming met die bepaald met microcalorimetrie.

Hoofdstuk 4 behandelt het onderzoek naar de complexering in polair medium van organische anionen door (thio)ureidocavitanden. Deze behoren tot de sterkste binders van organische anionen ooit gepubliceerd, met K_a-waarden tot 9.4×10^6 M^{-1}

in acetonitril. De (thio)ureidocavitanden zijn in oplossing in evenwicht met de overeenkomstige 1:1 capsules, met een K_a-waarde van 6.86×10^4 M^{-1} voor het thioureumderivaat in acetonitril. De complexering van anionen is een sterk enthalpie-gestuurd proces en leidt tot vorming van isomere gastheer-gast complexen (endo en exo). De binding van kleine organische anionen als acetaat en propionaat resulteert in gastsignalen bij erg hoog veld (tot δ = –3.02 ppm) in de ^{1}H NMR spectra, door de complexering van de alkylsubstituenten van de gast in de holte (vorming van endo-isomeren). Langere carboxylaten, zoals b.v. valereaat, zijn te groot om in de holte te passen en vormen daarom exo-isomeren. Daarbij vindt de complexering exclusief bij het (thio)ureum gedeelte van het molecuul plaats.

Hoofdstuk 5 laat het eerste voorbeeld zien van het gebruik van 'triplet ionen' om supramoleculaire structuren te construeren. [2+4] Capsules worden gevormd door twee tetrakis(pyridiniummethyl)tetramethylcavitanden, die een 'open bloem'-achtige structuur hebben, en vier enkel geladen anionen (bromide, nitraat, acetaat of tosylaat). Het pyridinium-anion-pyridinium bindingspatroon wordt gerealiseerd door de mogelijkheid van enkel geladen ionen om coördinatiecomplexen te vormen, hetgeen de valentie van de anionen vergroot. ESI-MS maakte de structuurbepaling van de [2+4] capsules mogelijk, gebruikmakend van de verschillende fragmentatiepatronen van pyridiniumcationen, pyridinium-anionen contact ionenparen en de 'triplet ionen'. De [2+4] capsules bevatten één of twee anionen, afhankelijk van de grootte. Ze zijn in evenwicht met [2+3] hemicapsules, die slechts drie wanden hebben. Deze laatste complexeren fenolen en anilines onder vorming van nieuwe asymmetrische capsules, die zowel pyridinium-anion-pyridinium als pyridinium-gast-pyridinium wanden bevatten.

Hoofdstuk 6 omvat een studie naar de elektrostatische zelfassemblage van een tetrakis(pyridiniummethyl)cavitand en dubbel geladen anionen in polair medium met behulp van klassieke ionenpaar-interacties, bijvoorbeeld het pyridinium-sulfaat-pyridinium bindingspatroon. ^{1}H NMR spectroscopie wijst op de vorming van ionenpaar-verbindingen en ESI-MS laat de aanwezigheid van verschillende ionenpaar-species in het evenwichtsmengsel zien. Een model dat uitgaat van een evenwicht, dat zowel (hemi)capsules als ionenpaar-verbindingen bevat, is ontwikkeld. Voor de intramoleculaire interactie werd een effectieve molariteit (EM) van 0.19 ± 0.02 M gevonden. Het model liet zien dat naast de capsules, redelijke hoeveelheden van hemicapsules en eenvoudige ionenparen in de oplossing aanwezig zijn,

afhankelijk van de concentratie. Bijvoorbeeld in een 5 mM oplossing van tetrakis(pyridiniummethyl)cavitand sulfaat, is de samenstelling 10% [2+3] hemicapsule, 15% 1:1 complexen, 17% 1:2 complexen en 14% [2+4] capsules. De hemicapsules vormen complexen met elektronenrijke gasten (zoals 4-jodofenol en – aniline) in methanol door intercalatie tussen twee 'vrije' pyridiniumringen. In water vormt de cavitand insluitingscomplexen met verschillende gasten door hydrofobe interacties tussen de alkylketen van een gast en de holte van de cavitand.

Hoofdstuk 7 illustreert het belang van electrostatische interacties tussen de componenten van een zelfassemblage met zijn tegenionen aan de hand van een studie van [1+1] capsules gebaseerd op tetrakis(aziniummethyl)cavitand en calix[4]areen tetrasulfonaat. Wanneer met de initiële azinium-anion binding geen rekening wordt gehouden, geeft dat een vermindering van de schijnbare associatieconstante van meer dan twee ordesvergrote. De [1+1] capsules hebben bindingsconstanten van meer dan 2×10^6 M^{-1} in methanol en kunnen één of twee kleine moleculen (zoals methanol en ethanol) inkapselen, afhankelijk van de grootte.

ACKNOWLEDGEMENTS

First of all I would like to thank my promotor Prof. Dr. Ir. David N. Reinhoudt for the honor and the excellent opportunity to make my second Ph. D. in his group. From you I have learned that good management of scientific activity is as important and fruitful as doing scientific research itself. Inspiration and scientific enthusiasm are flourishing in our group under your leadership.

I am very grateful to my assistent promotor Dr. Wim Verboom for all the freedom I have received during the work on my Ph. D. project. I have learned a lot, working with you. It was a great pleasure to study a lot of different methods and approaches and to collect comprehensive experience in the field I really intended to work in, namely, supramolecular and physical organic chemistry. Your talent to represent our scientific results in a clear and attractive way always impresses me. I wish I would ever be able to write as excellent as you do.

With pleasure I am recalling the day, about 5 years ago, when Prof. Dr. Vitaly I. Kalchenko informed me about the open research position in Twente. Thank you very much, Vitaly Ivanovich, for the advice to apply for this position. At that time, I could not imagine how it would change my life totally.

Due to the challenging subject of the project, this thesis includes only about 20-30% of the physicochemical and synthetic experiments carried out. It appeared that the biggest part of successful results is connected with mass spectrometry. Before, I could not even imagine how much information can be obtained by mass-spectrometric study. For this I would like to express gratitude to Roel H. Fokkens, who has opened for me the marvelous world of modern mass spectrometry.

I am very thankful to Richard Egberink, who was not only always helping with chemical questions and software and hardware computer problems, but also saving in really crucial situations, such as when my 10 L 270 ºC reaction mixture seemed to go out of control!

I would like to express gratitude to Kenneth A. Connors for his excellent book "Binding Constants. The Measurement of Molecular Complex Stability" that was a very good help and inspiration in my research.

I would also like to thank my lab mates and people from our group for the pleasant stay in SMCT: Mattijs, Tsutomu, Xue-Mei, Bart Jan, Mercedes, Jurriaan, Frank, Thieme, Ben, Marcel, Monica, Emiel, Luca, Alart, Siva, Fernando, Lourdes, Olga, Alessio, Andrea, Oscar, Christian, Pascale, Miguel, Jessica, Kazu, Paolo, Wiljan, Leon, Venkat, Amela, Francesca, Roberto, Socco, Becky, Mirko, Christiaan, Manon, Nuria, Carmela(s), Dominik, Dorota, Hans, Henk, Xuexin, Veera, and many others.

I am very grateful to Mercedes, Bart Jan, and Richard for reading my concept thesis and for your helpful advises to make this book better.

A special word of thanks I address to the promotor of my first Ph. D. defense, Prof. Dr. Alexander M. Pinchuk. Thank you very much, Alexander Mikhailovich, for all experience and knowledge, obtained during my work in your group. They were very helpful in solving new research problems here, in the Netherlands.

Jeroen, Mariëlle, Yme-Jelle, Marit, Marc, Robin, Marjolein, Steven, Saron, Lucas, Ola, Douwe, Sybren, Vera, Erwin, and Olga. It is great pleasure to have friends like you. Thank you very much for the nice time together.

Misha, thank you for your friendship and nice conversations about almost everything, with a glass of beer. I am also grateful for your advice to use Maple for solving my 'binding constants' problems that eventually allowed working out tasks, which at first looked unsolvable.

Yura, I am very happy that our friendship continues for already almost 15 years. Thank you for our often hours-long weekly telephone conversations, without which I could not imagine even a single Sunday.

Lisette, you have appeared in my life like the sun and are my friend and wife about whom men could only dream. You brought new dimensions and colors to my life and are a continuous inspiration in everything I do. Dank je wel voor alle passie en liefde.

Gena Oshovsky-Harting

CURRICULUM VITAE

Gennady V. Oshovsky was born on April 10, 1974 in Kiev (USSR, now Ukraine).

Simultaneously to school, he was involved in research activity of the Small Academy of Sciences of Ukraine 'Doslidnyik' (the research organization of young scientists) in 1989-1991. He carried out the project '*Photometric determination of traces of iron in copper alloys*' in the National Taras Shevchenko University of Kiev together with Eugeniy V. Voronenko (under supervision of Dr. Valery Soloshonok).

He studied chemistry at the National Taras Shevchenko University of Kiev (1991-1996). In addition to these studies, he carried out the following research: in 1992 '*Crown complexes of Pb*' (under supervision of Prof. Dr. Aleksander Y. Nazarenko), in 1993-1994 '*Synthesis of condensed imidazole-containing heterocycles*' (under supervision of Dr. Gennady P. Kutrov), and in 1995-1996 '*C-phosphorylation of π-electron saturated heteroaromatic systems*" (master thesis under supervision of Prof. Dr. Alexander M. Pinchuk). He graduated *cum laude* from the University (June, 1996) with a specialisation in Organic Chemistry (research and teaching).

Starting from June 1996, he worked in the Institute of Organic Chemistry of the National Academy of Sciences of Ukraine on a research devoted to the investigation of hetarylformamidines. On September 1999, he successfully defended his Ph. D. dissertation '*C-Phosphorylated N-azolylformamidines*' (under supervision of Prof. Dr. Alexander M. Pinchuk). The work was awarded by two grants from the International Soros Foundation and the International Renaissance Foundation.

From September 1999 until April 2001, he worked as a researcher in the same institute on the projects '*Nucleophilic amidine heterocyclizations*' and '*Synthesis of functionalized phosphorus and heterocyclic compounds as potential pesticides*'.

In May 2001, he started a second Ph. D. project in the group of Prof. Dr. Ir. David N. Reinhoudt at the University of Twente (SMCT group, MESA$^+$ Research Institute for Nanotechnology, Enschede, The Netherlands), because it was an excellent opportunity to acquire comprehensive experience in a variety of methods that can be used for studying and understanding properties of organic molecules. The project entitled '*Cavitand-based anion receptors and self-assembled (hemi)capsules in polar competitive media*' was carried out under supervision of Dr. W. Verboom.

Starting from January 2006, he is working as a research associate in the 'Laboratoire de Chimie de Coordination du CNRS' (Toulouse, France) in the group of Prof. Dr. Jean-Pierre Majoral on the project '*Functionalized phosphorus compounds and their metal complexes for catalysis and self-assembly in water.*'